



UNIL | Université de Lausanne

Unicentre

CH-1015 Lausanne

<http://serval.unil.ch>

Year : 2021

Regulation and function study of Acid-Sensing Ion Channels

Peng Zhong

Peng Zhong, 2021, Regulation and function study of Acid-Sensing Ion Channels

Originally published at : Thesis, University of Lausanne

Posted at the University of Lausanne Open Archive <http://serval.unil.ch>

Document URN : urn:nbn:ch:serval-BIB_8EB1188539D26

Droits d'auteur

L'Université de Lausanne attire expressément l'attention des utilisateurs sur le fait que tous les documents publiés dans l'Archive SERVAL sont protégés par le droit d'auteur, conformément à la loi fédérale sur le droit d'auteur et les droits voisins (LDA). A ce titre, il est indispensable d'obtenir le consentement préalable de l'auteur et/ou de l'éditeur avant toute utilisation d'une oeuvre ou d'une partie d'une oeuvre ne relevant pas d'une utilisation à des fins personnelles au sens de la LDA (art. 19, al. 1 lettre a). A défaut, tout contrevenant s'expose aux sanctions prévues par cette loi. Nous déclinons toute responsabilité en la matière.

Copyright

The University of Lausanne expressly draws the attention of users to the fact that all documents published in the SERVAL Archive are protected by copyright in accordance with federal law on copyright and similar rights (LDA). Accordingly it is indispensable to obtain prior consent from the author and/or publisher before any use of a work or part of a work for purposes other than personal use within the meaning of LDA (art. 19, para. 1 letter a). Failure to do so will expose offenders to the sanctions laid down by this law. We accept no liability in this respect.



UNIL | Université de Lausanne

Faculté de biologie
et de médecine

Département des sciences biomédicales

Regulation and function study of Acid-Sensing Ion Channels

Thèse de doctorat en Neurosciences

présentée à la

Faculté de biologie et de médecine
de l'Université de Lausanne

par

Zhong PENG

Master of Science in Neuroscience
Shanghai Jiao Tong University, China

Jury

Prof. Nicole DEGLON, Président
Dr. Stephan KELLENBERGER, Directeur de thèse
Dr. Marie-Christine BROILLET, Expert
Dr. Alexandre BOURON, Expert

Thèse n° 320

Lausanne
(2021)

***Programme doctoral interuniversitaire en Neurosciences
des Universités de Lausanne et Genève***



**UNIVERSITÉ
DE GENÈVE**



Imprimatur

Vu le rapport présenté par le jury d'examen, composé de

Président-e	Madame	Prof.	Nicole	Deglon
Directeur-trice de thèse	Monsieur	Dr	Stephan	Kellenberger
Expert-e-s	Madame	Dre	Marie-Christine	Broillet
	Monsieur	Dr	Alexandre	Bouron

le Conseil de Faculté autorise l'impression de la thèse de

Monsieur Zhong Peng

Master of Sciences, Shanghai Jiao Tong University, CN

intitulée

Regulation and function study of Acid-Sensing Ion Channels

Lausanne, le 15 octobre 2021

pour Le Doyen
de la Faculté de Biologie et de Médecine


Prof. Nicole Deglon

Table of Contents

<i>Acknowledgments</i>	V
<i>Abstract</i>	VI
<i>Résumé</i>	VII
<i>Résumé à un large public</i>	IX
<i>List of abbreviations</i>	X
1. Introduction	1
1.1 Acid-sensing ion channels (ASICs)	1
1.1.1 <i>Expression and distribution of ASICs</i>	1
1.1.2 <i>ASICs structure and regulation</i>	2
1.1.3 <i>Physiological and pathological functions of ASICs</i>	4
1.2 Hydrogen Sulfide (H₂S)	7
1.2.1 <i>H₂S biogenesis, clearance, donors and measurement</i>	7
1.2.2 <i>Ion channel regulation by H₂S</i>	11
1.2.3 <i>Physiological and pathological roles of ion channel regulation by H₂S</i>	13
1.3 Circadian rhythm	16
1.3.1 <i>Physiological basis of circadian rhythm</i>	17
1.3.2 <i>Regulation of the circadian rhythm</i>	20
1.3.3 <i>Circadian rhythm and body temperature</i>	22
1.3.4 <i>Circadian rhythm and disease</i>	25
2. Specific research aims of this thesis	28
2.1 Regulation of ASICs by H₂S	28
2.2 Circadian expression of ASIC1a in hypothalamus	28
3. Results	29
3.1 Project 1: Regulation of ASICs by H₂S	29
3.2 Project 2: Circadian expression of ASIC1a in hypothalamus	51
4. General Discussion	99
4.1 Mechanism and function of ASIC regulation by H₂S	99
4.1.1 <i>H₂S potentiates ASIC currents in CHO cell</i>	99
4.1.2 <i>H₂S regulates ASICs in a biphasic manner</i>	99
4.1.3 <i>H₂S may modulate ASICs directly</i>	100
4.1.4 <i>Physiological and pathological function of ASICs regulated by H₂S</i>	100
4.2 Circadian expression of ASIC1a regulates the body temperature	101
4.2.1 <i>Circadian rhythm of body temperature</i>	101
4.2.2 <i>Regulation of circadian rhythm by the pineal gland</i>	102
4.2.3 <i>Circadian rhythm of hormone synthesis</i>	102
4.2.4 <i>Signalling pathway of ASIC1a regulates Trh and Prl</i>	103
5. Perspectives	104
5.1 Regulation of ASICs by H₂S	104
5.2 Circadian expression of ASIC1a in hypothalamus	105
6. References	107

Acknowledgments

I would like to express my sincere thanks and best wishes to my supervisor, colleagues, family members and friends who have cared, helped and supported me in this thesis study.

First and foremost, I would like to thank my supervisor, Dr. Stephan Kellenberger, during the five years of my doctoral degree. In the research project, Dr. Kellenberger always guided and encouraged me to develop freely, expand gradually, and innovate continuously; Dr. Kellenberger also provided an open and free communication environment and platform for us. Dr. Kellenberger created such a good working environment and academic atmosphere for us that I get good training and growth. Here, I would like to express my highest respect and heartfelt thanks to Dr. Kellenberger.

I wish to thank my committee members: Prof. Deglon Nicole, Dr. Marie-Christine Broillet and Dr. Alexandre Bouron, for their time and for contributing to my thesis; you are very appreciated. The completion of this thesis is inseparable from the care, help and support of many colleagues and friends. I would like to thank members in the lab: Sophie Roy, Ivan Gautschi, Dr. Olivier Bignucolo, Dr. Omar Alijevic, Dr. Sabrina Vullo, Dr. Anand Vaithia, Ophélie Molton and Nicolas Ambrosio, for their help in project design and experimental techniques. I would like to express my sincere gratitude to them for their constructive comments on my project.

I thank Tomaz Martini and Prof. Urs Albrecht at the University of Fribourg for their help in circadian rhythm behavioral analysis. I also thank Panos Ziros and Dr. Gerasimos Sykiotis at CHUV for their help in mouse hormone analysis. I also thank Prof. Ron Stoop group for their help in brain slice recording.

I would like to acknowledge and thank all the members of the Department of Biomedical Sciences and Ivan Gautschi for their technical and scientific suggestions, and all people I had the pleasure to know during these years.

Finally, I would like to thank my parents and family for their moral motivation and concern for my life and their strong support that enabled me to focus on my thesis study.

Abstract

Acid-sensing ion channels (ASICs) are voltage-insensitive Na^+ channels activated by extracellular protons. ASICs belong to the degenerin/epithelial sodium channel (DEG/ENaC) family. Four genes (ASIC 1-4) encoding at least six subtypes (1a, 1b, 2a, 2b, 3, 4). ASICs are widely distributed in the central and peripheral nervous systems. ASICs are involved in many physiological and pathological processes, such as fear conditioning, pain sensation, and seizures. Hydrogen sulfide (H_2S) has emerged as a new gasotransmitter and has been shown to exert cellular effects by interacting with proteins, including many ion channels. Endogenous H_2S is widely biosynthesized in the nervous system, cardiovascular system and endocrine system. We found that the H_2S donor NaHS potentiated the acid-induced ASIC1a peak currents in a time- and concentration-dependent manner. Similarly, NaHS potentiated also the acid-induced currents of ASIC1b, ASIC2a, and ASIC3. The endogenous ASIC currents of cultured hypothalamus neurons were also increased by the H_2S donors. We also found that the total and plasma membrane expression of ASIC1a was increased by H_2S donors, as determined in cultured cortical neurons. H_2S also enhanced the activation of the extracellular signal-regulated kinase (pErk1/2), and pharmacological blockade of the MAPK-Erk1/2 signaling pathway prevented the H_2S donor-induced increase of ASIC function and expression.

Circadian rhythm is the result of natural selection in the long-term evolution of organisms. The various physiological behaviors and functions of the body show obvious circadian rhythms, such as sleep/wake, feeding and body temperature. The body temperature is mainly regulated by the Hypothalamic-Pituitary-Thyroid (HPT) axis. We found that the expression of ASIC1a in the hypothalamus has a diurnal rhythm in WT mice under a normal light/dark cycle. Global deletion of ASIC1a changed the body temperature at night, and this change depended on the HPT axis. Activation of ASIC1a upregulates the expression of *Trh* through the Akt-mTOR pathway in hypothalamus to regulate the HPT axis.

Our study demonstrated the expression and function of ASICs in the hypothalamus, and identified the signaling mechanism involved. Since ASICs are involved in many physiological and pathological processes, our studies can help to better understand the regulation of physiological and pathological processes, as well as the inhibition of disease progression.

Résumé

Les canaux sensibles aux protons (ASICs) sont des canaux sodiques non voltage dépendants activés par une acidification extracellulaire. Les ASICs appartiennent à la famille des dégénérines/canaux sodiques épithéliaux (DEG/ENaC) et quatre gènes codant pour six sous-unités (1a, 1b, 2a, 2b, 3, 4) ont été identifiés. Les ASICs sont largement distribués dans le système nerveux central et périphérique. Ils sont impliqués dans de nombreux processus physiologiques et pathologiques, tels que le conditionnement de peur, la sensation de douleur et les convulsions. Le sulfure d'hydrogène (H₂S) est récemment apparu comme un nouveau gazotransmetteur et il a été démontré qu'il exerce des effets cellulaires en interagissant avec des protéines, parmi lesquelles de nombreux canaux ioniques. Le H₂S endogène est biosynthétisé dans le système nerveux, le système cardiovasculaire et le système endocrinien. Nous avons constaté que le donneur de H₂S, le NaHS, augmentait les courants de pointe induits par l'acide d'une manière dépendante du temps et de la concentration. De même, NaHS a également potentialisé les courants induits par l'acide d'ASIC1b, ASIC2a et ASIC3. Les courants ASIC endogènes des neurones de l'hypothalamus en culture ont également été potentialisés par les donneurs de H₂S. Nous avons également constaté une augmentation de l'expression totale et membranaire plasmique d'ASIC1a par le donneur de H₂S, comme déterminé dans les neurones corticaux en culture. Le H₂S a également augmenté l'activation de la kinase Erk1/2, et le blocage pharmacologique de la voie de signalisation MAPK-Erk1/2 a empêché l'augmentation de la fonction et de l'expression des ASICs induite par le donneur de H₂S.

Le rythme circadien est le résultat de la sélection naturelle dans l'évolution à long terme des organismes. Les divers comportements et fonctions physiologiques du corps montrent des rythmes circadiens évidents, tels que le sommeil/l'éveil, l'alimentation et la température corporelle. La température corporelle est principalement régulée par l'axe hypothalamo-hypophysio-thyroïdien (HPT). Nous avons constaté que l'expression d'ASIC1a dans l'hypothalamus a un rythme circadien chez les souris wild-type sous un cycle lumière/obscurité normal. La suppression globale d'ASIC1a a modifié le rythme de la température corporelle, et ce changement dépendait de l'axe HPT. L'activation d'ASIC1a régule positivement l'expression de Trh via la voie Akt-mTOR dans l'hypothalamus pour réguler l'axe HPT.

Nos études ont examiné l'expression et la fonction des canaux ASIC dans l'hypothalamus, et ont identifié le mécanisme de signalisation impliqué. Puisque les ASICs sont impliqués dans de nombreux processus physiologiques et pathologiques, nos études peuvent nous aider à mieux comprendre la régulation des processus physiologiques et pathologiques, ainsi que l'inhibition de la progression de maladies.

Étude de la régulation et de la fonction des canaux ioniques à détection d'acide

Zhong Peng

Département des sciences biomédicales, Faculté de biologie et de médecine, UNIL

En 1980, les scientifiques ont enregistré des courants induits par l'acide provenant des neurones sensoriels, mais le premier gène des canaux ioniques à détection d'acide (ASIC) n'a été cloné qu'en 1997. Les ASIC sont largement distribués dans le système nerveux central et périphérique. Dans le système nerveux périphérique, l'acidose tissulaire est une caractéristique commune de nombreuses conditions de nociception. Des protons sont libérés par les tissus blessés et activent les canaux ASIC pour induire une sensation de douleur. Dans le système nerveux central, des conditions telles qu'une consommation d'énergie élevée, un métabolisme anormal, une inflammation, un accident vasculaire cérébral ischémique et une excitation neuronale excessive peuvent provoquer une acidification du système nerveux central.

Depuis plusieurs centaines d'années, le H₂S est connu comme un gaz incolore toxique qui sent les œufs pourris. Les fonctions physiologiques et pathologiques importantes du H₂S produit de manière endogène n'ont pas été étudiées. Ici, nous avons constaté que le H₂S augmentait les courants ASIC d'une manière dépendante du temps et de la concentration. Nous avons également constaté que l'expression totale et membranaire d'ASIC1a était augmentée par le H₂S, et cette augmentation dépendait de la voie de signalisation MAPK-Erk1/2. La compréhension du mécanisme de régulation des ASICs par H₂S est très utile pour des maladies telles que la mort neuronale induite par un AVC ischémique.

Le rythme circadien est le résultat de la sélection naturelle dans l'évolution à long terme des organismes. Ce rythme circadien permet aux organismes de mieux prévoir les changements et d'ajuster leur état pour s'adapter aux changements de l'environnement extérieur. La température corporelle des mammifères a un rythme circadien qui est principalement régulé par l'axe hypothalamo-hypophyse-thyroïdien (HPT). Nous caractérisons ici la régulation de la température corporelle par ASIC1a. Chez les souris soumises à un cycle lumière/obscurité normal, l'expression d'ASIC1a dans l'hypothalamus a un rythme circadien. La suppression globale d'ASIC1a a modifié le rythme de la température corporelle, et ce changement dépendait de l'axe HPT.

List of abbreviations

3MST: 3-mercaptopyruvate sulfur transferase	Fshb: follicle-stimulating hormone beta subunit
5-HT: serotonin	GC: guanylate cyclase
AP-1: activator protein-1	GC-FPD: gas chromatography with flame photometric detector
AR: β 3-adrenergic receptor	GH: growth hormone
ASICs: acid-sensing ion channels	GMQ: 2-guainidine-4-methylquinazoline
AVP: arginine vasopressin	GPX2: glutathione peroxidase 2
BAT: brown adipose tissue	GSH: glutathione
BK: bradykinin	H ₂ S: hydrogen sulfide
BK _{Ca} : large-conductance Ca ²⁺ - and voltage activated K ⁺	HPT: Hypothalamic-Pituitary-Thyroid
BMAL1: brain and muscle ARNT-like protein 1	IC: ion chromatography
CaMKII: Ca ²⁺ /calmodulin-dependent protein kinase II	IC ₅₀ : half maximal inhibitory concentration
CAT: cysteine aminotransferase	iGluR: ionotropic glutamate receptor
CBS: cystathionine- β -synthase	IL-1: interleukin-1
CFA: complete Freund's adjuvant	ISEs: sulfide-specific ion-selective electrodes
cGMP: cyclic guanosine monophosphate	JNK: c-Jun aminoterminal kinases
CHO: Chinese hamster ovary	K _{ATP} : ATP-sensitive potassium channel
CLOCK: circadian locomotor output cycle kaput	KO: knockout
CREB: cAMP-response element-binding protein	LD: light-dark cycle
CSE: cystathionine- γ -lyase	LH: lateral hypothalamus,
Cys: cysteine residues	LTP: long-term potentiation
DEG/ENaC: degenerin/epithelial sodium channel	LTS: low-threshold spike
DMH: dorsomedial nucleus of the hypothalamus	MAPKs: mitogen-activated protein kinases
DRG: dorsal root ganglion	mBB: monobromobimane
DTNB: 5,5'-dithio-bis-(2-nitrobenzoic acid)	MES: 2-(N-morpholino)-ethanesulfonic acid
DTT: DL-dithiothreitol	MitTx: Mit-Toxin- α/β
EC ₅₀ : half maximal effective concentration	mpd: medial parvocellular division
ERG: early response genes	MPO: medial preoptic region
Erk1/2: extracellular signal-regulated kinase 1/2	NE: norepinephrine
FAS: fatty acid synthase	NGF: nerve growth factor
FBS: fetal bovine serum	NMDA: N-methyl-D-aspartate
FMRF-NH ₂ : Phe-Met- Arg-Phe-NH ₂	NO: nitric oxide
	NOS: nitric oxide synthase
	NSAIDs: non-steroidal anti-inflammatory drugs
	PARP1: ADP-Ribose polymerase 1
	PcTx-1: psalmotoxin-1
	PI ₃ K: phosphoinositide 3-kinase
	PKA: protein kinase A

PKC: protein kinase C	WAT: white adipose tissue
PKG: cGMP-dependent protein kinase G	WT: wild-type
PLC: phospholipase C	
PO/AH: preoptic area of the anterior hypothalamus	
Pomc: pro-opiomelanocortin	
Prl: prolactin	
PVN: paraventricular nucleus,	
qRT-PCR: quantitative real-time polymerase chain reaction	
RHT: retino-hypothalamic tract	
RIP1: serine/threonine kinase receptor interaction protein 1	
ROS: reactive oxygen species	
SCN: suprachiasmatic nucleus	
SDH: spinal dorsal horn	
SERCA: sarcoplasmic reticulum Ca ²⁺ -ATPase	
SFR: spontaneous firing rate	
SNS: sympathetic nervous system	
SOX: sulfite oxidase	
sPVz: subparaventricular zone	
SQR: sulfide quinone oxidoreductase	
SSFD: sulfide-sensitive fluorescent dyes	
SSH: covalent persulfide	
T3: 3,5,3'-triiodothyronine	
T4: 3,5,3',5'-tetraiodothyronine	
TH: thyroid hormones	
TM: transmembrane domains	
TRH: thyrotropin-releasing hormone	
TRP: transient receptor potential	
TRPA1: ankyrin-repeat TRP1	
TSH: thyroid-stimulating hormone	
Tshb: thyroid-stimulating hormone beta subunit	
TSM: tracheal smooth muscle	
VD: vas deferens	
VIP: vasoactive intestinal polypeptide	
VLPO: ventrolateral preoptic nucleus,	
VMH: ventromedial nucleus of the hypothalamus	
VSMCs: vascular smooth muscle cells	

1. Introduction

1.1 Acid-sensing ion channels (ASICs)

1.1.1 Expression and distribution of ASICs

In 1980, scientists recorded acid-induced currents from sensory neurons ¹, but ASICs' first gene was not cloned until 1997 ². ASICs belong to the degenerin/epithelial sodium channel (DEG/ENaC) family. Mammalian ASICs are encoded by four genes (*ASIC 1-4*) and a total of six subtypes (1a, 1b, 2a, 2b, 3, 4). ASIC2b homomers do not form functional homomeric channels and could only be expressed in the plasma membrane as part of functional heterotrimers with other ASICs ^{1,3}. ASICs are widely distributed in the central and peripheral nervous systems. ASIC1a, ASIC1b, ASIC2a, ASIC2b and ASIC3 are expressed in the peripheral nervous system, where ASIC3 is the highest expressed ASIC isoform ⁴⁻⁹. Acid-induced currents in mouse peripheral sensory neurons are mediated by heteromers composed of ASIC1a, ASIC2, and ASIC3 subunits ⁶. ASICs mainly distribute to the cell body and sensory terminals in peripheral sensory neurons, and play a role of nociceptive sensors ¹⁰. In the central nervous system, neurons express ASIC1a, ASIC2a, ASIC2b, and ASIC4. ASICs mainly distribute in the cell body, dendrites, and dendritic spines. They mainly contribute to synaptic transmission, learning and memory, and cell death after ischemic stroke ^{7,11,12}. The currents induced by protons recorded from cultured brain neurons are a mixture of ASIC1a, ASIC2a, and ASIC2b ¹³⁻¹⁵. Interestingly, ASICs are not expressed in glial cells ¹⁶. In addition to the nervous system, ASICs also express in non-neural tissues such as vascular smooth muscle cells and bone cells ¹⁷⁻¹⁹.

Functional ASICs are homotrimers or heterotrimers; channel properties of different subtypes are different. Homomeric ASIC1a can conduct Ca^{2+} , while the heteromeric ASIC1a is not Ca^{2+} permeable ²⁰. After being activated by protons, ASICs can quickly open to induce a peak current and then quickly desensitize into a desensitization (non-conducting) state ^{1,2}. ASICs cannot be activated by additional extracellular acidification during the desensitized state. This property of ASICs may help to prevent neuronal death under the conditions of continuous acidification ²¹⁻

²³. However, ASIC3 is able to generate a biphasic current containing a transient component followed by a non-desensitizing sustained current in response to acidic stimulation. This property of ASIC3 may be related to its physiological function, such as ASIC3-mediated chronic and inflammatory pain ²⁴⁻²⁷.

1.1.2 ASICs structure and regulation

The crystal structure of ASIC1 provides an additional understanding of the effect that ligand binding has on ion permeation and gating of ASIC1 channels (**Figure 1**). ASICs have a large extracellular loop, and the extracellular loop contains many conserved cysteine residues, which can form disulfide bonds within subunits. The N- and C- terminal of ASICs are intracellular ^{2,28,29}. A single subunit's overall structure resembles an upheld arm with a loosely clenched fist, the large extracellular loop is similar to a clenched "fist", and the transmembrane area is similar to the "arm". According to different parts of the fist, the extracellular loop can be divided into "palm", "knuckle", "finger", "thumb", and " β ball" part ²⁰. The study of ASIC1a structure found an "acidic pocket" in the extracellular region supposed to be conducts the ASIC activation, but our group found that proton sensing in the "acidic pocket" is not required for channel function³⁰. Many ASICs regulators also bind at this domain to regulate the opening of the channel³¹.

Like other DEG/ENaC family members, each subunit of ASICs contains two transmembrane domains (TM1 and -2), and the transmembrane domain is mainly responsible for the function of ion permeability ^{20,31,32}. TM2 is involved in forming ion inflow paths near the extracellular side, while TM1 interacts with the lipid bilayer. In addition, studies had found that some amino acid residues before TM1 contributed to the ion selectivity of the ASICs channel ^{20,31,33,34}. The TM2 domain predominantly lines the pore to mediate ion permeation and form the selectivity filter. ASICs can activate by extracellular acidification, but the specific mechanism of acidification leading to ASICs' opening is still unclear ²⁰.

ASIC1a is distinguished from other ASICs by a reduced response to successive acid stimulations, and this process is called Tachyphylaxis. This effect may be due to the fact that

ASIC1a can also permeate protons to increase the intracellular proton concentration, thereby inhibiting the opening of channel^{35,36}. Extracellular Ca^{2+} as an allosteric modulator and channel blocker of ASICs. The apparent affinity for the proton of ASIC1a and 1b is modulated by extracellular Ca^{2+} through a competition between Ca^{2+} and proton; the recovery process of ASIC1a from the desensitized state is also affected by the Ca^{2+} concentration^{2,14}.

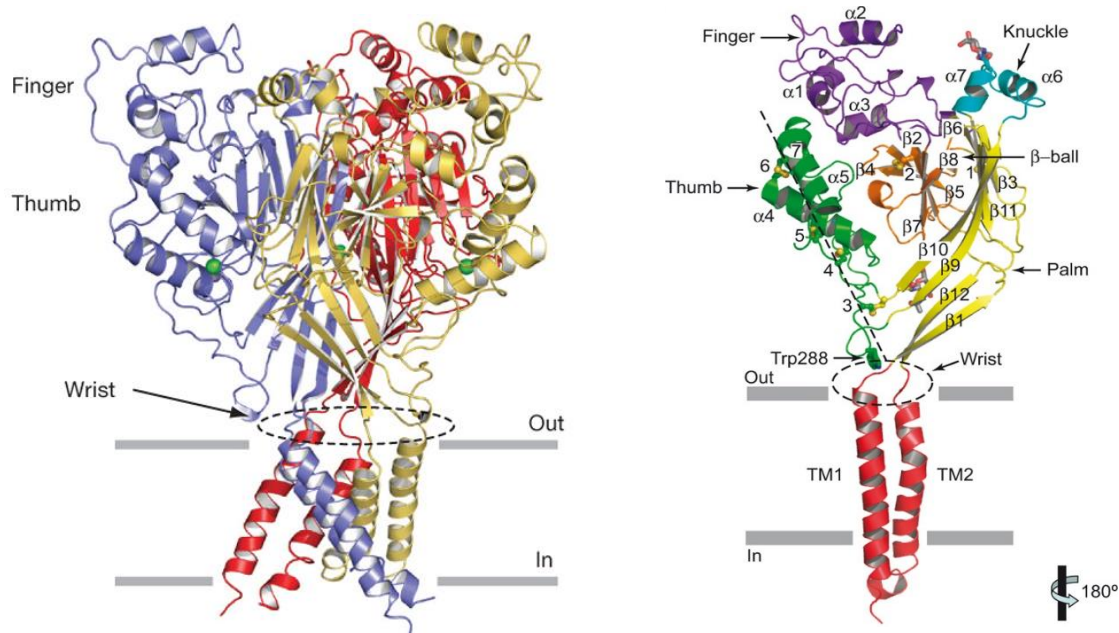


Figure 1. Structure of chicken ASIC 1^{20,31}.

Left: Crystal structure of ASIC1 homotrimer. The green ball in the picture represents chloride ion, the "thumb", "finger" area are marked in the picture, and the gray bars represent the boundaries of the outer (out) and inner (in) leaflets of the membrane bilayer. **Right:** The crystal structure analysis of a single subunit. The black dash line in the picture indicates the disulfide bond formed (labeled 1–7).

There are many molecules that can regulate ASICs, but only few are subtype-selective inhibitors or agonists. The most commonly used inhibitor of ASICs is Amiloride, widely used for the DEG/ENaC family^{37,38}. Recently it was found that Psalmotoxin-1 (PcTx-1), a toxin secreted by tarantulas, can specifically inhibit ASIC1a, but does not affect other subtypes³⁹. There is also a specific inhibitor of ASIC3, APETx2 is a peptide isolated from the sea anemone, it can specifically inhibit ASIC3⁴⁰. The Mambalgins, a toxin from black mamba venom, inhibit homomeric rodent and human ASIC1a channels, homomeric rodent ASIC1b channels as well as other heteromeric ASIC1a-containing and ASIC1b-containing channels.

In addition to regulating the activation of channels, the researchers also found that a class of peptides can bind on the acidic pocket in the extracellular domain to regulate ASICs'

desensitization without directly activating ASICs ⁴¹⁻⁴⁴. These peptides have a common structural basis, the last amino acid at the C-terminus is phenylalanine, and the penultimate amino acid is arginine. The first discovered peptide was FMRF-NH₂ (Phe-Met- Arg-Phe-NH₂), called FMRFamide ⁴¹.

1.1.3 Physiological and pathological functions of ASICs

In the peripheral nervous system, ASICs play a role in pain and itch sensation ^{45,46}. Tissue acidosis is a common feature of many nociception conditions, and protons are released by injured tissues and activates ASIC to induce pain sensation. The acid-induced currents on medium-sized dorsal root ganglion (DRG) neurons are the same as heteromers composed of ASIC1, ASIC2, and ASIC3, while medium and small DRG neurons are mainly responsible for nociceptive sensations ⁴⁷. This finding suggests that ASICs may play an important role in nociceptive sensation ^{6,48}. The expression of ASIC subunits in DRG increases under inflammatory conditions ⁴⁹; expression of ASIC1a in the spinal cord increased in the inflammatory pain model induced by complete freund's adjuvant (CFA). In addition, some pro-inflammatory modulators such as nerve growth factor (NGF) ⁵⁰, serotonin (5-HT) ⁵¹, Interleukin-1 (IL-1) ⁵¹, Bradykinin (BK) ⁵², and brain-derived neurotrophic factor (BDNF) ⁵³ can also increase ASIC transcription. Some non-steroidal anti-inflammatory drugs (NSAIDs), such as flurbiprofen and ibuprofen can inhibit ASIC current and the increase of ASIC expression induced by inflammatory modulators under high concentration condition^{49,51,54,55}.

It was found that ASICs, especially ASIC3, play an important role in pain sensation ⁵⁶⁻⁵⁹, and ASIC3 is mainly expressed on peripheral sensory neurons. On the DRG and nodose ganglia, ASIC3 mainly forms heteromeric channels with other ASICs subtypes ^{6,60,61}. ASIC3 is particularly sensitive to acid and can be activated to generate steady-state current at pH 7.0. Local acidification will occur during peripheral tissue damage, inflammation, ischemia, hematoma, and physical exercise, and the lowest pH that can be reached is 6.7 ⁶². The tissue acidification leads to a decrease of pH, and it can activate ASIC3 and induce pain ⁶³⁻⁶⁵. In addition, administration of the ASIC3 agonist GMQ on wild-type (WT) mice can induce pain-

related behaviors, while GMQ cannot induce pain on ASIC3 knockout (KO) mice ⁶⁶. The endogenous agonist of ASIC3 agmatine, a bioactive metabolite of arginine, has the same binding site as GMQ on ASIC3, and agmatine can also induce pain-related behavior. More interesting is that agmatine can also have a synergistic effect with other inflammatory factors, thus that agmatine increases the acid-induced current and pain behavior dependent on ASIC3 ⁶⁶. Correspondingly, pharmacologically blocking the ASIC3 channel with the selective inhibitor of ASIC3, APETx2, can reduce pain-related behavior ^{58,67}. However, since APETx2 inhibits also several voltage-gated ion channels (Nav1.2, Nav1.8 and hERG) ⁶⁸⁻⁷⁰, the analgesic effect of APETx2 may be not only due to ASIC inhibition ⁷¹.

Subcutaneous injection of acidic solution can induce long-term mechanical allodynia in WT mice, not in ASIC3 KO mice. ASIC3 expression are increased in inflamed tissues, and ASIC3 may contribute to inflammation-induced mechanical allodynia and thermal hyperalgesia⁷². Although ASIC1a is also expressed on DRG neurons, there is no difference in mechanoreception and pain perception between WT and ASIC1a KO mice ^{73,74}.

In the splanchnic colonic and vagal gastro-oesophageal, knockout ASIC1a will increase the mechanical sensitivity ⁷⁵. Knockout of ASIC2 increases the response to mechanical stimulation, while knocking out AISC3 will weaken sensitivity to mechanical stimuli ⁷⁴⁻⁷⁷. ASIC2 also plays a very important role in blood pressure sensation, and it was shown that ASIC2 KO mice exhibited hypertension symptoms ⁷⁸.

In the central nervous system, ASICs play an important role in synaptic transmission, learning and memory, pain, cell death after ischemic stroke, and fear conditioning ^{11,23,53,54,79-81}. ASIC1a modulates the synaptic transmission. Knock out ASIC1a increased the miniature excitatory postsynaptic currents frequencies ⁸², impaired long-term depression and ong-term potentiation (LTP) ^{11,83}, and potentiated neuromuscular transmission ⁸². Conditions such as high energy consumption, abnormal metabolism, inflammation, ischemic stroke, and excessive neuronal excitement can cause acidification of the central nervous system. The acidification of the central nervous system can activate ASICs to produce certain physiological functions ⁸⁴⁻⁸⁶.

ASIC1a is the most abundantly expressed subtype of ASICs in the central nervous system. In cultured cortical neurons of ASIC1a KO mice, the pH6.0-induced current almost completely disappears, which shows that the main ASIC subunit in the cortex is ASIC1a^{7,80,87}.

In the central nervous system local acidification may also occur under normal physiological conditions. For example, in the synapses of the retinal ganglia, the release of neurotransmitters can reduce the synaptic cleft's pH and is sufficient to inhibit the opening of calcium channels in the presynaptic membrane. This indicates that the pH of synapses significantly decreases during the release of neurotransmitters^{88,89}. The pH value of synaptic vesicles is about 5.2-5.7. The protons will enter the synaptic cleft together with the release of synaptic vesicles, and it will cause local acidification of the synaptic cleft and activate ASICs expressed in postsynaptic membrane⁹⁰.

In the brain, ASIC1a is most abundantly expressed in the amygdala. In ASIC1a KO mice, behaviors related to the amygdala, such as fear-conditioning, are significantly decreased^{23,91,92}. Overexpression of ASIC1a in the amygdala increased the current induced by acid and enhanced the response of conditioned fear⁹³. Meanwhile, the response of conditioned fear to cue and situational dependence in mice overexpressing ASIC1a increased, and the learning ability was slightly decreased^{11,12,23,93}. These findings indicate that ASIC1a plays an important role in fear learning and memory. In hippocampus brain slices of mice, the induced LTP was decreased in ASIC1a KO mice, and the acid-induced dendritic spines Ca^{2+} influx was also reduced. The number of dendritic spines in the hippocampus declined, and the release of vesicles increased in cultured hippocampus neurons of ASIC1a KO mice^{7,94,95}. ASIC1a KO mice showed abnormalities in hippocampus-dependent learning and memory, but the hippocampal-dependent spatial learning ability was normal.

ASIC1a also affects the death of neurons in the case of the neurological disease. An intense or prolonged acid treatment can induce neuronal death. Inhibiting ASIC1a can reduce acid-induced neuronal death^{80,81}. In mouse stroke models, inhibition or knockout of ASIC1a reduced the area of cerebral infarction caused by ischemia^{80,96-98}. ASIC1a-mediated acid-induced

neurotoxicity is due to homomeric ASIC1a that has a small conduction for Ca^{2+} . Therefore, extracellular Ca^{2+} can flow into the neuron when ASIC1a is activated leading to calcium overload and ultimately to neuron death^{80,81,94}. Some studies found that ASIC1a plays a role in multiple sclerosis, Huntington's disease, Parkinson's disease, and spinal cord injury⁹⁸⁻¹⁰¹.

In the central nervous system, ASIC1a also plays an important role in nociception. Intrathecal injection of the ASIC1a inhibitor PcTx-1 attenuated pain relative behaviors^{54,102}. Under the condition of inflammatory pain, the expression of ASIC1a on the cell surface will increase⁵⁴. BDNF can activate the Akt1 signaling pathway to promote the transfer of ASIC1a from the cytoplasm to the plasma membrane. With this the expression of ASIC1a on the cell membrane is up-regulated and inflammatory pain is enhanced^{53,54,103}. Several signaling pathways are known to participate in the regulation of ASIC trafficking and expression, such as protein kinase A (PKA)^{104,105}, protein kinase C (PKC)¹⁰⁶, the phosphoinositide 3-kinase-protein kinase B (PI₃K-AKT), and extracellular signal-regulated kinase 1/2 (Erk1/2)⁵³.

1.2 Hydrogen Sulfide (H₂S)

1.2.1 H₂S biogenesis, clearance, donors and measurement

For several hundred years, H₂S has been known as a toxic colorless gas smelling of rotten eggs. The significant physiological and pathological functions of endogenously produced H₂S were ignored. Recently, H₂S emerged as the third gasotransmitter, beside the nitric oxide (NO) and carbon monoxide, that exerts sensory and metabolic control by interacting with different targets. Endogenous H₂S is widely biosynthesized in the nervous system¹⁰⁷, cardiovascular system¹⁰⁸ and endocrine system¹⁰⁹. H₂S regulates ion channels, similarly to other gasotransmitters, through the modulation of specific cysteine residues (Cys) to form covalent persulfide (-SSH) bonds; this modification is termed protein S-sulfuration¹¹⁰.

Neurotransmitters are generally stored in vesicles; the intracellular pool is partially released upon activation. Gasotransmitters can't be stored and must be quickly generated and released to nearby targets. Therefore, the biosynthetic enzymes which synthesize H₂S must be closely

regulated and have high-performance synthesis ability. Endogenous H₂S in mammals is the product of three pyridoxal-5'-phosphate (PLP)-dependent enzymes. H₂S is directly produced by cystathionine-β-synthase (CBS, EC 4.2.1.22) and cystathionine-γ-lyase (CSE, EC 4.4.1.1) ¹¹¹⁻¹¹³, and indirectly by 3-mercaptopyruvate sulfur transferase (3MST, EC 2.8.1.2) ^{114,115}. In mammals, the enzymes of H₂S biosynthesis have a tissue-specific expression with CBS predominantly in the brain and CSE and 3MST in peripheral organs ¹¹⁶⁻¹¹⁸.

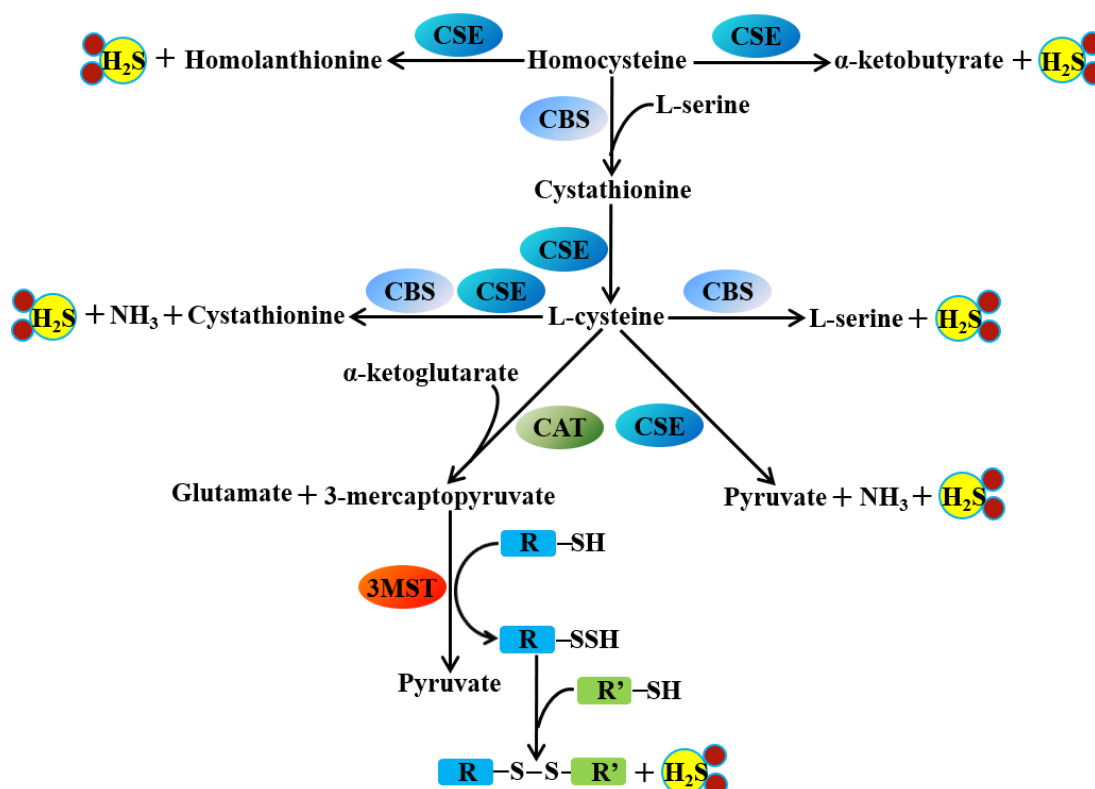


Figure 2. Endogenous pathways involved in enzymatic biogenesis of H₂S

The transsulfuration pathway in mammalian consisting of three enzymes: produced directly by cystathionine-β-synthase (CBS) and cystathionine-γ-lyase (CSE), and indirectly by 3-mercaptopyruvate sulfur transferase (3MST).

CBS and CSE are predominantly located in the cytoplasm ¹¹⁹, and 3MST is in both the cytoplasm and mitochondria ¹²⁰. CBS, CSE and 3MST generate H₂S by a multitude of reactions and substrate combinations (**Figure 2**). The primary function of CSE in the biosynthesis of H₂S is the conversion of L-cysteine to H₂S, pyruvate, and ammonia (NH₃). CSE also uses homocysteine as a substrate to generate H₂S, α-ketobutyrate and homolanthionine; alternatively it uses cystathionine to generate Cys. CBS also uses Cys as a substrate to generate H₂S and L-serine, or it uses homocysteine and L-Ser as substrates to generate cystathionine. Cysteine aminotransferase (CAT) catalyzes the generation of 3-mercaptopyruvate and glutamate out

of Cys and α -ketoglutarate. The enzyme 3MST transfers the sulfane sulfur to an acceptor and releases H_2S in the presence of reductants ¹²¹.

The most commonly used experimental H_2S donors are NaHS and Na_2S . As a gas, H_2S is difficult to dissolve in aqueous solution and its concentration is difficult to control. But both NaHS and Na_2S , as solid agents, are easy to dissolve in solution and hydrolyze to generate S^{2-} , HS^- and H_2S . HS^- is the main product and is the reaction component to forms $-\text{SSH}$ ¹²². As a non-physiological agent, NaHS is toxic at high concentrations. H_2S induced neuronal death through ionotropic glutamate receptors, which recruits apoptosis to ensure cellular demise and employs calpains and lysosomal rupture ^{123,124}. Recently, a novel H_2S donor, GYY4137 was developed to replace NaHS to apply to physiological experiments ¹²⁵. The slow-release H_2S donor GYY4137 can better reflects endogenous physiological release. GYY4137 concentration-dependently decreased the spontaneous contraction of pregnant rat and human myometrium. It also reduced oxytocin-stimulated and high- K^+ depolarized contraction significantly; these effects are similar as NaHS ¹²⁶. Other H_2S donors, such as AP67/AP72 (slow-releasing), AP39 (mitochondria-targeted), Diallyl disulfide (organosulfur compound), ADT-OH (H_2S -aspirin hybrid molecule), ZYZ-803 (H_2S -NO hybrid molecule) and ZYZ-802 (S-Propargyl-cysteine) were developed for disease treatment, such as hypertension, myocardial infarction, adrenergic overload and Hyperglycemia¹²⁷. Until now, no H_2S donors are available for clinical applications. Therefore, new agents, especially membrane-permeable compounds, that can release H_2S , are still needed.

As a potentially toxic gasotransmitter, H_2S must be rapidly cleared after synthesis by CBS and CSE in vivo. An uncontrolled production of H_2S would disturb normal physiological functions ¹²⁸. The main metabolic pathway of H_2S is oxidation by sulfite oxidase (SOX) to thiosulfate ($\text{S}_2\text{O}_3^{2-}$), sulfite (SO_3^{2-}) and sulfate (SO_4^{2-}) ¹²⁹ (**Figure 3**). In murine tissues, the catabolism of H_2S occurs *via* a mitochondrial sulfide oxidation pathway. Firstly, H_2S is oxidized by sulfide quinone oxidoreductase (SQR) to form protein-bond persulfide, while the electrons are transferred to ubiquinone, and then sulfur dioxygenase (ETHE1) oxidizes SQR-bond sulfane sulfur to sulfite ¹³⁰. The clearance of H_2S is rapid under aerobic conditions because the

degradation of H₂S is coupled to electron transfer, and it is easy to transfer the electron to ubiquinone in the presence of oxygen. In mammals, H₂S also binds to haem proteins, such as neuroglobin and cytochrome *c* oxidase, and these proteins may play a role of “buffer” to attenuate the damage done by H₂S^{108,131}.

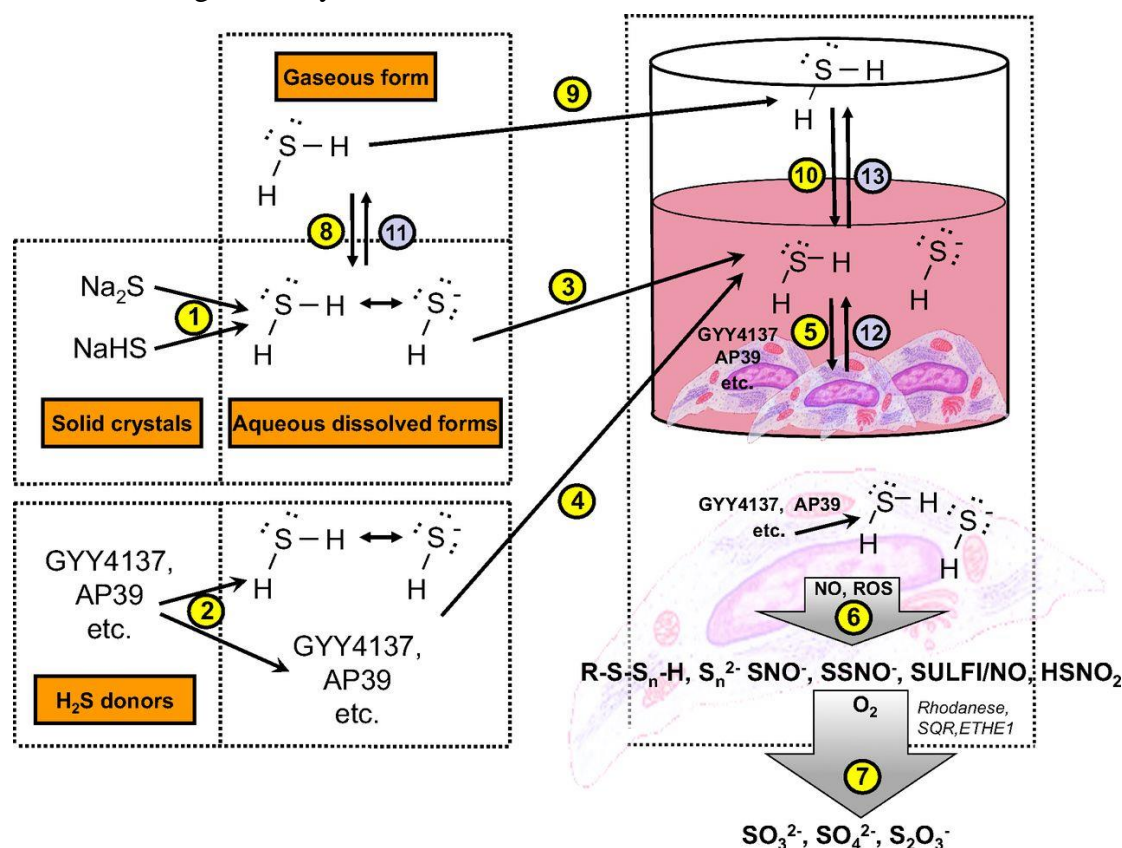


Figure 3. H₂S donor delivery to cells and their clearance¹³²

H₂S and HS⁻ are generated when H₂S donors (NaHS, Na₂S, GYY4137, AP39 *etc.*) are dissolved in aqueous solutions. Intracellularly, H₂S will react with various molecules (proteins, thiols, nitric oxide, reactive oxygen species) to create a mixture of biologically active species (polysulfides, persulfides, hybrid S/N compounds). H₂S decomposition products (SO₃²⁻, SO₄²⁻, S₂O₃²⁻) are also produced *via* enzymatic and nonenzymatic processes.

The measured concentration of total H₂S is around 10-100 μM or higher in blood¹³³⁻¹³⁵, but the accurate concentration of H₂S, especially the free H₂S, remains to be determined by improving the measurement method. The methylene blue method is the most common method to measure the concentration of total H₂S based on the reaction of H₂S with N,N-dimethyl-*p*-phenylenediamine sulfate in aqueous solution¹³⁶. However, with the reaction of methylene blue it is difficult to distinguish the free H₂S from acid-labile sulfide under acidic conditions; this property restricted the application of this method of H₂S measurement^{137,138}. Sulfide-specific ion-selective electrodes (ISEs) were also developed to measure S²⁻ in biological samples. The

measurement requires strong alkaline solution (pH>11), so it has the same defect as the methylene blue method and can't be applied to continuous or real-time measurement¹³⁹. The most common method to measure low concentration of H₂S is the monobromobimane (mBBBr) method, which is sensitive to nanomolar concentrations of H₂S^{140,141}. The GC-FPD (gas chromatography with flame photometric detector) and IC (ion chromatography) are also sensitive to nanomolar concentrations of H₂S, but these methods can't be applied to real-time measurement^{142,143}. Sulfide-sensitive fluorescent dyes (SSFD) were developed to detect local H₂S production, but these dyes show a delayed response time (>20 min) toward hydrogen sulfide^{144,145}. Recently, novel polarographic H₂S sensor has been developed for monitoring and directly measure the concentration of H₂S in real-time; the polarography sensor can detect micromoles concentration of H₂S¹⁴⁶⁻¹⁴⁸.

1.2.2 Ion channel regulation by H₂S

The first report on ion channel regulation by H₂S showed that injection of H₂S gas-saturated solution into the rat vein decreased the blood pressure; this effect was antagonized by prior blockade of ATP-sensitive potassium channel (K_{ATP}) channels¹⁴⁹. In primary cultured rat mesenteric artery vascular smooth muscle cells (VSMCs), H₂S interacts with Cys6 and Cys26 residues of the extracellular N terminal of rvSUR1 subunit of K_{ATP} channel complex (EC₅₀= 116±8.3 μM) and hyperpolarizes the membrane, implying that H₂S might be a co-activator candidate of K_{ATP}. In VSMCs, H₂S can enhance the whole-cell K_{ATP} current and increase the single K_{ATP} channel's open probability. Inhibition of the endogenous H₂S generation will decrease the K_{ATP} current. These results indicate that extracellular and intracellular H₂S can activate the K_{ATP} channel; these effects on both sides of the plasma membrane might be attributed to the fact that H₂S is membrane-permeable. With heterologously expressed rvKir6.1 and rvSUR1 subunits of K_{ATP} channel in HEK293 cells, H₂S could activate the co-expressed K_{ATP} channel but did not affect the K_{ATP} current generated by expression of rvKir6.1 alone. Selective point-mutations of cysteine residues of the extracellular loop of rvSUR1 (C6S and C26S) subunit led to a loss of the stimulatory effects of H₂S on the rvKir6.1/rvSUR1 K_{ATP} current¹⁵⁰. This implies that the sites of the K_{ATP} channel that are modified by H₂S are Cys6

and Cys26 in the rvSUR1 subunit.

The large-conductance Ca^{2+} - and voltage-activated K^+ (BK_{Ca}) channels are activated by both elevated $[\text{Ca}^{2+}]_i$ and membrane depolarization¹⁵¹⁻¹⁵³. H_2S modifies BK_{Ca} channel activity by acting on sulfhydryl groups of the channel¹⁵⁴. In primary cultured mouse tracheal smooth muscle (TSM) cells, NaHS decreased the calcium-activated potassium outward current of single BK_{Ca} channels in a concentration-dependent manner ($\text{EC}_{50}=174\mu\text{M}$)¹⁵⁵. NaHS induced voltage-dependently and calcium-independently a reversible decrease of channel open probability; this effect was blocked by pretreatment with DL-dithiothreitol (DTT)¹⁵⁶. H_2S enhanced the sensory response to hypoxia in carotid body type I cells through inhibition of the TASK channels leading to membrane depolarization and voltage-gated Ca^{2+} entry¹⁵⁷. H_2S also inhibited mitochondrial function *via* an action on TASK channels; cyanide inhibited TASK channels to a similar extent to H_2S ¹⁵⁷.

The T-type Ca^{2+} channels are low voltage-activated calcium channels. Intracolonic administration of NaHS, evoked visceral pain-like nociceptive behavior and referred hyperalgesia in mice, an effect abolished by NNC 55-0396, a selective T-type Ca^{2+} -channel blocker¹⁵⁸. NaHS also activated Erk1/2 in the spinal dorsal horn in the colitis rat model, and facilitated T-type Ca^{2+} channel-dependent membrane currents¹⁵⁹. H_2S increased $[\text{Ca}^{2+}]_i$ *via* both PKA and phospholipase C (PLC)/PKC pathways. Inhibition of PKA and PLC/PKC reversed the H_2S -induced elevation of $[\text{Ca}^{2+}]_i$. In isolated cardiomyocytes, NaHS inhibit the peak amplitude of L-type calcium current ($I_{\text{Ca,L}}$) in a concentration-dependent manner, an effect that was reversed by pretreatment with DTT^{160,161}.

Transient receptor potential (TRP) channels are polymodal cellular sensors involved in a wide variety of cellular processes. In HEK293 cells heterologously expressing the ankyrin-repeat TRP1 (TRPA1) channel, NaHS activated TRPA1 to induce calcium responses. This effect was inhibited by DTT pretreatment. Mutations of two cysteine residues (Cys422 and Cys622) located in the N-terminal internal domain of TRPA1 channel led to a loss of H_2S -induced activation¹⁶². In sensory neurons, H_2S increases the intracellular $[\text{Ca}^{2+}]_i$ in DRG neurons, this

effect was prevented by ruthenium red (a nonselective TRP channel blocker), HC-030031 (a TRPA1 blocker), or removal of extracellular Ca^{2+} ^{163,164}. In sensory neurons from TRPV1^{-/-} mice, the $[\text{Ca}^{2+}]_i$ increase by H_2S was conserved; it was however lost in neurons from TRPA1^{-/-} mice.

The N-methyl-D-aspartate (NMDA) receptor is a member of the ionotropic glutamate receptor (iGluR) family that has high permeability to Ca^{2+} ¹⁶⁵. In SH-SY5Y neuronal cells, NaHS increased $[\text{Ca}^{2+}]_i$ in a concentration-dependent manner. This potentiation was reversed by EGTA (a chelating agent) and NMDA receptor blockers (MK-801, AP-5, and ifenprodil).

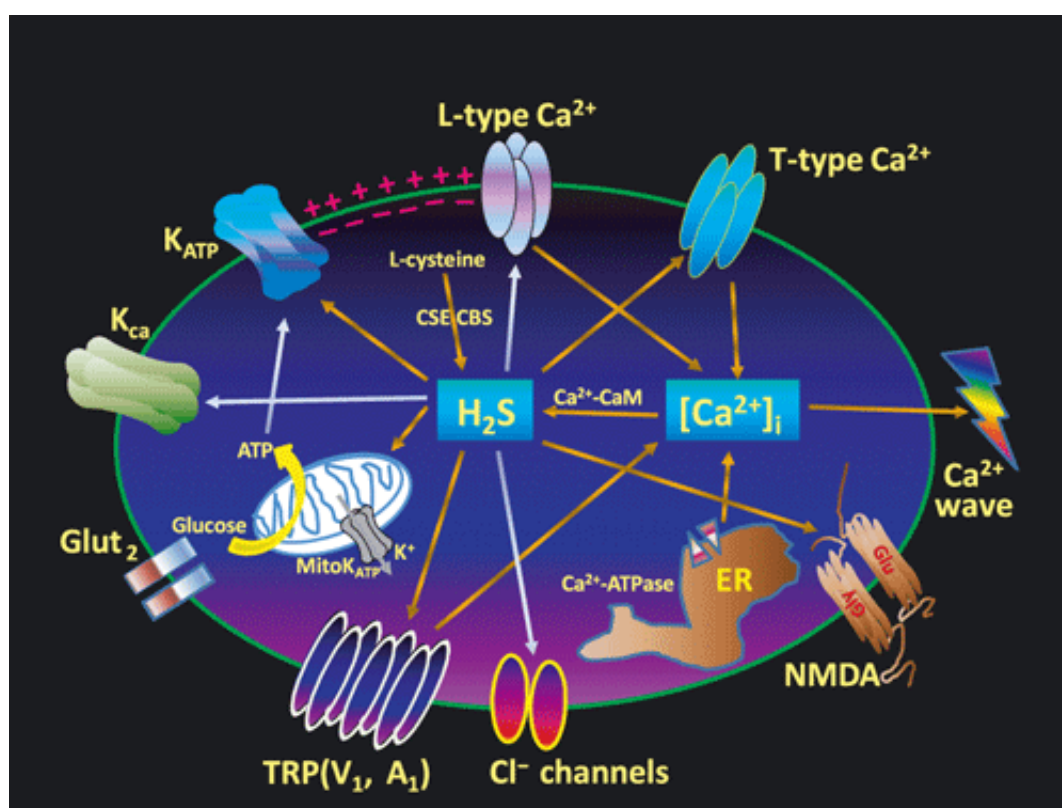


Figure 4. Interaction of H_2S with ion channels ¹⁶⁶

The stimulatory effects of H_2S on K_{ATP} channels, T-type Ca^{2+} channels, $\text{Nav}1.5$ channels, TRP channels and NMDA receptors and its inhibitory effect on Cl^- channels and L-type Ca^{2+} channels.

1.2.3 Physiological and pathological roles of ion channel regulation by H_2S

H_2S acts as a gasotransmitter to regulate various ion channels in the endocrine, respiratory, cardiovascular, muscle and nervous systems.

In the endocrine system, endogenous H_2S significantly affects insulin secretion by stimulation of K_{ATP} channels *in vivo* ¹⁶⁷. An increase of the glucose concentration in the culture medium of

INS-1E cells (rat insulinoma cell line) significantly decreased the endogenous production of H₂S, increase insulin secretion, and reduced the basal K_{ATP} channel current. Overexpression of CSE in INS-1E cells abolished the high glucose-stimulated insulin secretion. The insulin secretion changes were not ATP- or redox-dependent because H₂S did not change intracellular ATP and glutathione (GSH) levels. In pancreatic β-cells, NaHS decreased the L-type Ca²⁺ current density in a concentration-dependent manner (IC₅₀= 65.4 ± 5.6 μM); this effect was inhibited by nifedipine (calcium channel blocker)¹⁶⁰. The pancreatic β-cells of CSE-KO mice had higher L-type Ca²⁺ current densities than those of WT mice, and the insulin secretion was also elevated in CSE-KO mice compared with WT mice. NaHS inhibited glucose-stimulated insulin secretion in a dose-dependent manner; this stimulation was reversed by nifedipine.

In the respiratory system, H₂S plays a critical role in carotid body chemoreceptors' response to hypoxia *via* modulating the BK_{Ca} channels. In the isolated mouse carotid body/sinus nerve preparations, NaHS excited the chemoreceptor afferent nerves in a concentration-dependent manner¹⁶⁸⁻¹⁷⁰. The NaHS-evoked excitation was abolished by removing extracellular Ca²⁺, application of Cd²⁺, and hexamethonium (a nicotinic (nAChR) receptor antagonist), suggesting that NaHS evokes the release of ATP/ACh from type I glomus cells in carotid body¹¹⁹. The BK_{Ca} current was inhibited by hypoxia and the diminished of BK_{Ca} current *via* inhibit CBS lead mice to hyperventilate in response to hypoxia¹¹⁹. Inhibition of the CBS, not CSE, can decrease the chemoreceptor afferent activation.

CBS and CSE are also functionally expressed in vas deferens (VD), and H₂S was shown to mediate VD smooth muscle relaxation¹⁷¹. H₂S relaxes the VD smooth muscle by targeting BK_{Ca} channels *via* a redox-mediated mechanism. The K_{ATP} channels are not involved in the NaHS-induced relaxant effect in VD smooth muscle, since pretreatment with glibenclamide (an K_{ATP} channel blocker) did not affect the response of VD to NaHS. However, inhibition of BK_{Ca} channels with iberiotoxin or tetraethylammonium was shown to reverse the relaxant effect¹⁷². In guinea pig papillary muscles, NaHS decreased the maximal velocity of depolarization at phase 0, the overshoot, the amplitude of the action potential and the action potential duration in the normal papillary muscles in a concentration-dependent manner¹⁷³.

In the cardiovascular system, exogenous H₂S can protect regional myocardial ischemia-reperfusion (I/R) injury^{174,175}. The cardioprotection effect of exogenous and endogenous H₂S is mediated by K_{ATP} channels. Pretreatment with NaHS decreased myocardial infarct size and improved heart contractile function in the isolated rat hearts; inhibition of the ERK1/2 or PI₃K/Akt pathway significantly attenuated the cardioprotection¹⁷⁶. BK_{Ca} channel inhibition by hydrogen sulfide also contributes to I/R protective effects. Neutrophils play an essential role in I/R-induced mucosal mitochondrial dysfunction, and NaHS prevents postischemic mitochondrial dysfunction by a BK_{Ca} channel-dependent mechanism. Coincident treatment with BK_{Ca} channels blockers, paxilline and penitrem A, completely reversed the protective effect of NaHS or NS-1619 on postischemic mitochondrial function¹⁷⁷.

In the peripheral nervous system, NaHS potentiates hyperalgesia through the effect on Cav3.2 T-type Ca²⁺ and TRP channels¹⁷⁸. In rat, treatment with NaHS rapidly decreased the nociceptive threshold. This effect was prevented by co-administration of the T-type Ca²⁺ channel inhibitor mibefradil, and it was also suppressed by pretreatment with zinc chloride (ZnCl₂), which preferentially inhibits Cav3.2 but not K_{ATP} channels or L-type Ca²⁺ channels. In the rat, knockdown the Cav3.2 was shown to attenuate the hyperalgesia induced by NaHS¹⁷⁸. After spinal nerve injury, Cav3.2 channels were upregulated and sensitized by H₂S in sensory neurons. It was shown that the upregulation of Cav3.2 expression was due to the activation of Erk1/2 by H₂S¹⁷⁹. In cyclophosphamide-induced cystitis-related bladder pain in mice, endogenous H₂S can activate Cav3.2 channels to induce bladder pain. The NaHS also prompts the activation of Erk1/2 in SDH bladder pain mice; this effect was inhibited by T-type Ca²⁺ channel blockers (Mibefradil and NNC 55-0396,)¹⁸⁰. In mice, the intraplantar administration of NaHS induced neuropathic pain. This effect was blocked by AP18 (reversible TRPA1 channel blocker) or silencing of TRPA1 channels in the sensory neurons¹⁸⁰. In the capsaicin-sensitive primary afferent neurons of rat isolated urinary bladder, NaHS induced contractile responses in a dose-dependent manner, which was blocked by TRPV1 antagonists. The non-selective blocker of TRP channels ruthenium red also blocked the contraction induced by NaHS or capsaicin¹⁸¹. NaHS also prompted ERK phosphorylation in the spinal dorsal horn

through activation of TRPV1 ¹⁷⁹.

In the central nervous system, H₂S might act a novel inducer of neuronal differentiation, as characterized by neuritogenesis and expression of high-voltage-activated currents *via* activation of Cav3.2 channels ^{182,183}. Pretreatment with BAPTA (a Ca²⁺ chelator) or selective Cav3.2 channel inhibitors, but not the inhibitors of Cav3.1 or Cav3.3, fully reverse the neuritogenesis induced by NaHS, ¹⁸². H₂S induced neuronal death through ionotropic glutamate receptors. The NaHS enhanced cell death in mature neuron was inhibited by the glutamate receptor antagonists MK801 and APV (NMDA receptor antagonists), and CNQX (kainate and AMPA receptor antagonist) ¹²⁴. In immature non-glutamate receptor-expressing mouse cortical neurons, treatment with NaHS can inhibit cell death induced by high glutamate concentrations ¹⁸⁴. H₂S potentiates NMDA receptor-mediated current by enhancing the sensitivity to glutamate at low concentration in the hippocampus and facilitating LTP ¹⁸⁵⁻¹⁸⁸.

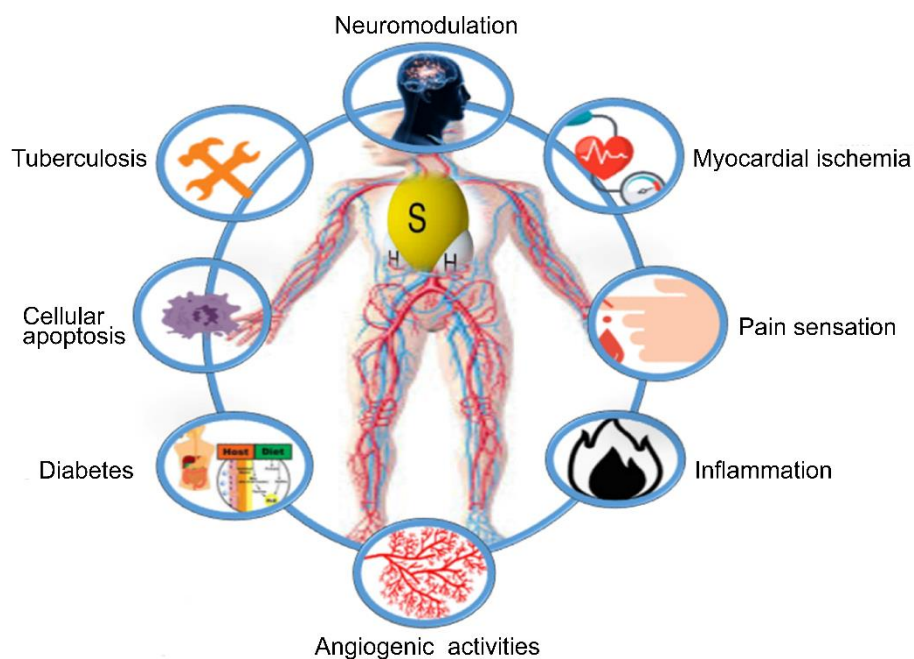


Figure 5. physiological and pathological roles of H₂S ¹⁸⁹

H₂S is formed throughout the body and moderates signaling processes in various tissues, including neuromodulation, myocardial ischemia, pain sensation, inflammation, angiogenesis, diabetes, cellular apoptosis and tuberculosis.

1.3 Circadian rhythm

The circadian rhythm is the result of natural selection in the long-term evolution of organisms.

This circadian rhythm enables organisms to predict changes better and adjust their state to adapt to changes in the external environment. The body's various behaviors and physiological functions show obvious circadian rhythms, such as sleep/wake, feeding, and autonomous activities, such as blood pressure, coagulation-fibrinolysis balance, heart rate, body temperature, hormone levels, cell metabolism, cell proliferation, immune regulation *etc.* ¹⁹⁰. The generation, maintenance and regulation of the circadian rhythm is constituted by three conceptual components, the intrinsic pacemaker, and the input and the output pathways ¹⁹¹. The circadian rhythm depends on the precise regulation of the endogenous clock gene network at the cellular level. Abnormalities of the clock gene network can lead to disturbances in the circadian rhythm ^{192,193}.

1.3.1 Physiological basis for the generation and maintenance of a circadian rhythm

The physiological basis for the generation and maintenance of the circadian rhythm includes the input to and output from the central and peripheral circadian rhythm systems. The rhythm input system transmits environmental synchronization of light signals to the central circadian rhythm system. The central circadian rhythm system acts as the circadian rhythm master pacemaker, transmits the generated rhythm signals to the periphery through the output system, and communicates with the endogenous circadian of the peripheral organs ¹⁹⁴⁻¹⁹⁶. These systems work together to maintain physiological activities (**Figure 6**). The period length of the endogenous human circadian rhythm is not exactly 24 hours. Studies have found that the spontaneous human circadian rhythm is between 24-25 hours, and it is slightly different between different individuals ^{197,198}. The main circadian rhythm pacemaker that regulates the circadian rhythm of mammals is located in the suprachiasmatic nucleus (SCN) of the hypothalamus, which contains approximately 20,000 neurons, with most of the cells showing self-sustained circadian oscillations ¹⁹⁹.

The SCN neurons express a variety of topologically specific neuropeptides. Vasoactive intestinal polypeptide (VIP) in the core region and arginine vasopressin (AVP) in the shell region are the two major neuropeptides that mediate the networking in the SCN²⁰⁰⁻²⁰². To

maintain synchronization between the internal and external environments, external environmental stimuli, which are named zeitgeber, are required and the main zeitgeber is transmitted to the SCN through the retino-hypothalamic tract (RHT) ²⁰³. The SCN can output nerve and humoral signals to the brain and peripheral organs to synchronize its internal rhythm with the external rhythm ²⁰⁴. Each organ's circadian rhythm is not necessarily synchronized; organs and tissues may be in different rhythms but must coordinate to maintain the organism's internal homeostasis ^{205,206}.

Studies have found that the rhythmic oscillation signals generated by the neurons in the SCN are not completely synchronized; there is complex diversity in time and space, which may be related to the physiological and anatomical positions of the neurons ²⁰⁷⁻²⁰⁹. Moreover, there are some neurons in the SCN without obvious endogenous circadian rhythms. These neurons receive direct projections from retinal ganglion cells, and affect other neurons in the SCN. In addition to the SCN, the amygdala, hippocampus, olfactory bulb, and other brain nuclei also have a circadian rhythm, which plays an important regulatory role in maintaining the neural activity in their respective regions ²¹⁰⁻²¹³. The peripheral clock genes are expressed in the heart, kidney, liver, spleen and other organs ^{214,215}. As the secondary pacemaker of the circadian rhythm system, these clock genes are directly or indirectly regulated by various nerves, humoral, and other signal factors under the central circadian rhythm's control.

The SCN can be stimulated by light or non-light signal transduction, trigger the SCN rhythm oscillator and then output signals through neural or humoral pathways to control the circadian rhythm in the body. The output projection pathway of the SCN is mainly composed of the hypothalamus, thalamus and brainstem. A study using retrograde tracing showed that the dorsolateral area of the SCN is composed of sympathetic and parasympathetic nerves ²¹⁶. The SCN output pathways are responsible for proper timing of diverse physiological functions, including hormone release, sleep-wake cycle, feeding behavior, and thermoregulation²¹⁷. The SCN output to the subparaventricular zone (sPVz) is through the medial preoptic region (MPO) to control circadian rhythms of body temperature. Single synaptic projections of SCN are connected to the hypothalamic paraventricular nucleus (PVN). Part of the nerve fibers of the

PVN connect to the dorsomedial hypothalamus (DMH), and then the fibers emitted by DMH to control daily hormone secretion. The other output pathway is projected to the lateral hypothalamus (LH) and ventrolateral preoptic nucleus (VLPO) to control sleep-wake cycles. The output nerve fibers of SCN can also project to the arcuate nucleus, stria terminalis nucleus and amygdala ²¹⁸. All of these brain nuclei also have the characteristics of circadian rhythm oscillations. However, in the absence of an SCN signal input, the synchronization of these cell oscillation rhythms is not maintained ²¹⁵.

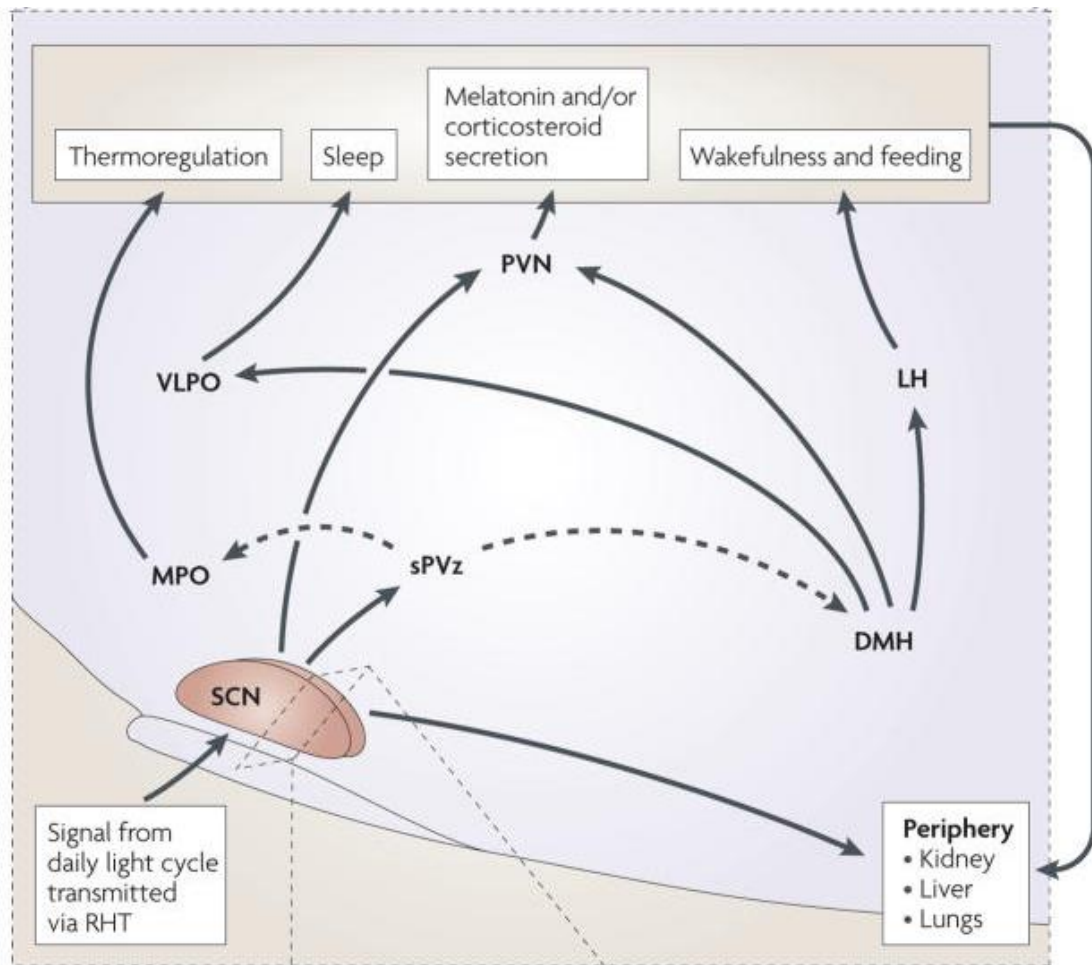


Figure 6. Input and output pathways of SCN ²¹⁷

The SCN receives light signaling *via* the retinohypothalamic tract (RHT). The SCN output to the subparaventricular zone (sPVz) is relayed to the medial preoptic region (MPO) to control circadian rhythms of body temperature; and a separate projection through the dorsomedial nucleus of the hypothalamus (DMH) controls daily hormone secretion (*via* paraventricular nucleus, PVN) and sleep-wake cycles (*via* lateral hypothalamus, LH, and ventrolateral preoptic nucleus, VLPO).

Clock genes regulate the generation and maintenance of circadian rhythm in the brain and peripheral organs. Studies found that the expression of about 10% of genes in cells has a

circadian rhythm ²¹⁹. The periodic oscillation of the circadian rhythm relies on the precise regulation of the clock genes and the clock-controlled gene regulatory network, including the feedback inhibition oscillation at the transcription, translation, and post-translational modification level.

The regulation mechanism of the circadian rhythm is conserved in the central and peripheral tissues of multicellular animals. The clock genes in mammals include *Bmal1*, *Clock*, *Per1*, *Pert*, *Per3*, *Cry1*, *Cry2*, etc. First, *Bmal1* and *Clock* form a heterodimer, which binds to the E-BOX element in the *PER* and *CRY* genes' promoter region to promote this transcription ²²⁰. As the negative feedback regulation, *PER* and *CRY* can form dimer. When *PER/CRY* dimer aggregate to a certain concentration in the cytoplasm, the dimer enters the nucleus to inhibits the transcriptional activity of the *Bmal1/Clock* dimer ²²¹. This negative feedback inhibits the transcription of *Per* and *Cry* genes ²²¹. In addition, the nuclear receptor REV-ERB can bind to the ROR element in the *Bmal1* promoter region to inhibit *Bmal1* transcription while the nuclear receptors ROR and PPAR can bind to the ROP and PPRE binding elements in the *Bmal1* promoter region to promote the transcription of *Bmal1* ²²².

1.3.2 Regulation of the circadian rhythm

Light is the most critical zeitgeber of the circadian rhythm system, it acts on the central clock to cause the time phase to be delayed or advanced. Studies found that light is transmitted to SCN through RHT, which releases the neurotransmitter glutamate and activates glutamate receptors on SCN neurons leading to depolarization of the membrane potential and induction of Ca^{2+} influx. The intracellular Ca^{2+} increase will activate nitric oxide synthase (NOS) and promote NO synthesis ²²³. NO activates guanylate cyclase (GC), which increases the concentration of cyclic guanosine monophosphate (cGMP) in the cell, thereby activating cGMP-dependent protein kinase G (PKG). PKG promotes the phosphorylation of cAMP-response element-binding protein (CREB), which binds to cAMP response elements in promoters, resulting in the transcription of clock genes such as *Per1* and *Per2*.

Changes of the light time (such as exposure to light at night) cause phase shifts based on the

ways by which the rhythmic pacemaker responds to light pulses. Exposure to light pulses in the early or late night can lead to delay or advancement of sleep phase, suggesting that light exposure before night delay the sleep cycle of animal²²⁴. This effect is related to the rapid activation of a large number of early light-induced genes in SCN by light exposure, such as early growth response protein-1, growth arrest and DNA damage-inducing protein β , poly ADP-Ribose polymerase 1 (PARP1) to regulates the clock gene expression^{225,226}. Moreover, some of early light-induced genes in SCN were also shown to reduce cell activity and prevent cell apoptosis, suggesting that organisms can reduce the sensitivity of the SCN to light exposure by changing the phase shift of the circadian rhythm²²⁷.

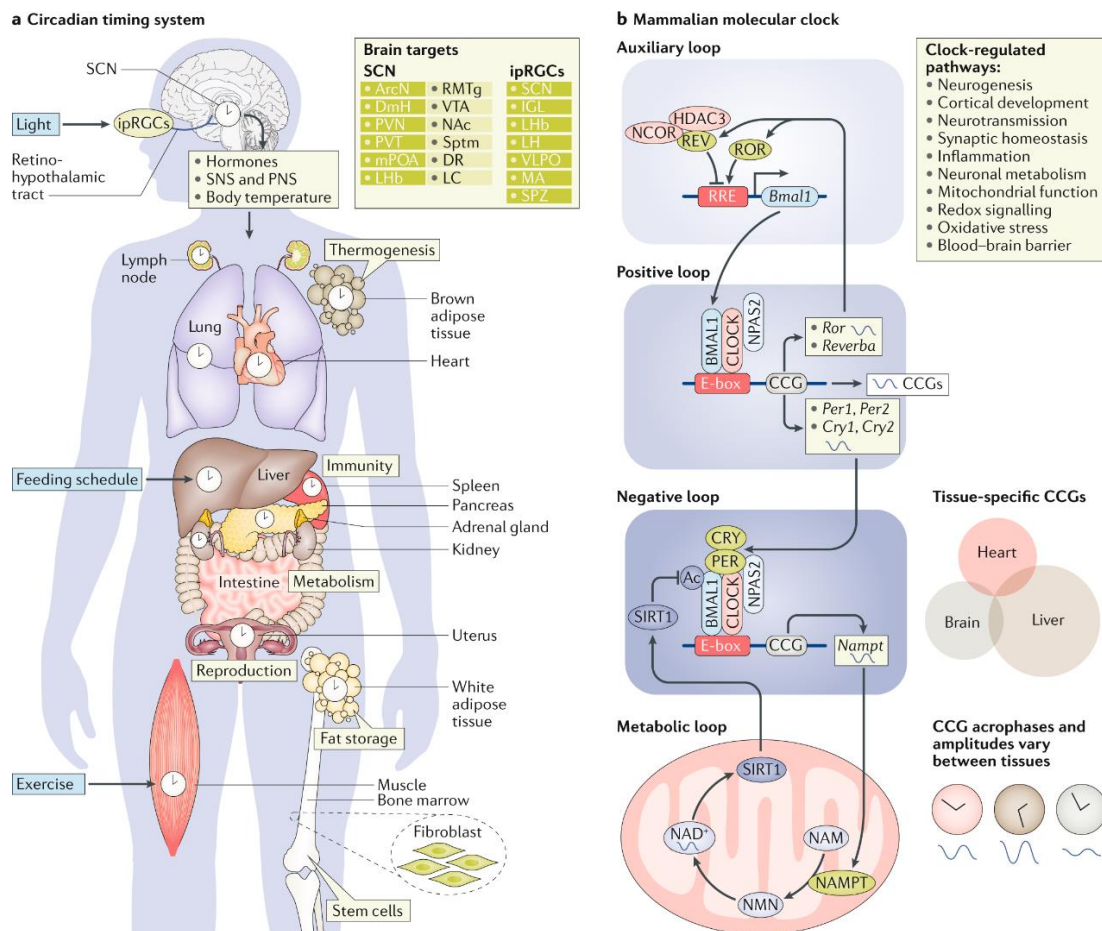


Figure 7. Overview of the circadian rhythm system²²⁸

a, circadian rhythm system synchronizes clocks across the entire body to adapt and optimize physiology to changes in external environment. **b**, The mammalian molecular clock is composed of transcriptional and translational feedback loops.

Food is the second most effective circadian rhythm signal in the environment, after light. This signal mainly affects the peripheral circadian rhythm and can reset the phase of various organs

and tissues. Restricted feeding (food is provided daily at a fixed time of day) induced food anticipatory activity before feeding time (such as increase in body temperature, corticosterone secretion), and induced the expression of clock genes (such as *Per1*, *Per2*) in peripheral organs (liver, kidney, heart, lung *etc.*) and brain nuclei (cerebral cortex, hippocampus and striatum). These effects are out of the control of the SCN and form a relatively independent peripheral clock rhythm caused by food signals ^{229,230}.

The circadian rhythm and energy balance system play a critical role in maintaining the normal operation of various functions of the organism. The disconnection between dietary habits and daily activity patterns will cause the separation of metabolic processes from SCN-based time signals, leading to energy metabolism and substrate consumption changes. The secretion of hormones related to energy metabolism such as cortisol, insulin, leptin, and ghrelin is closely related to the circadian rhythm ²³¹. In addition to feeding schedule, the food type will also affect the daily rhythm. A study found that high-salt diet can impair the normal oscillation of circadian rhythm ²³². A study showed that the sleep rhythm of the elderly is less affected by high-salt diet and that the mechanism may be related to the dopaminergic system ²³³.

1.3.3 Circadian rhythm and body temperature

The biological clock drives all circadian rhythms in mammals, body temperature is the most obvious rhythm in timing across individuals. The circadian rhythm of body temperature is a relatively complicated process and is affected by many factors. Central thermoregulatory neurons are mainly distributed in the preoptic area of the anterior hypothalamus (PO/AH). Temperature changes in peripheral organs and brain can be transmitted to the hypothalamus through temperature-sensitive neurons in this area, causing related changes in nervous system to maintain a relatively constant body temperature ²³⁴. The hypothalamus senses the temperature of blood flowing through it and controls the balancing of heat production and of heat loss.

Heat production depends on the Hypothalamic-Pituitary-Thyroid axis (HPT axis, **Figure 8**): thyrotropin-releasing hormone (TRH) release from PVN stimulates the release of thyrotropin

(TSH) from the anterior pituitary, which in turn stimulates the synthesis and release of thyroid hormones (TH), 3,5,3',5'-tetraiodothyronine (T₄) and 3,5,3'-triiodothyronine (T₃). T₃ is the main biologically active form because of its greater affinity for thyroid hormone receptors²³⁵. T₃ increases fatty acid synthase (FAS) activity and promotes fatty acid synthesis in the ventromedial nucleus of the hypothalamus (VMH).

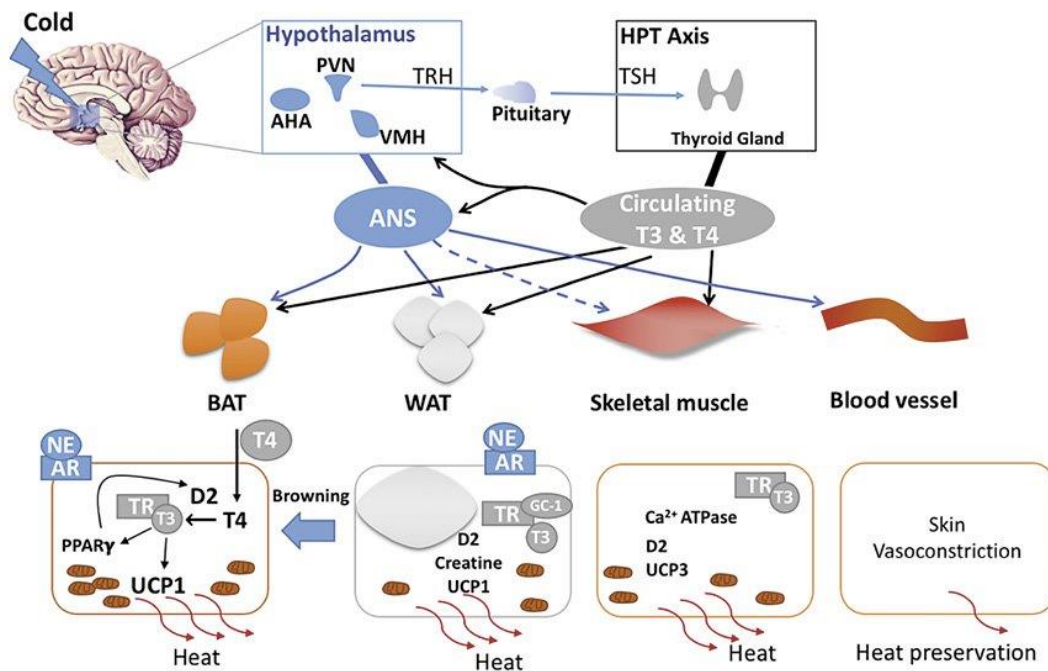


Figure 8. Central and systemic regulation of thermogenesis²³⁶

Thermogenesis regulated by Hypothalamic-Pituitary-Thyroid axis (HPT axis). HPT axis regulates the release of thyroid hormones and norepinephrine, which promote thermogenesis in adipose tissue and skeletal muscle.

The hypothalamic lipid synthesis increases the activity of the sympathetic nervous system (SNS) and stimulates brown adipose tissue (BAT) to promote thermogenesis^{237,238}. Norepinephrine (NE) activates β₃-adrenergic receptor (AR) in BAT to promote *UCP1* gene expression, stimulates 5'-deiodinase type 2 (D2) activity, which stimulates BAT lipolysis to promote thermogenesis^{237,239}. In the white adipose tissue (WAT), SNS signals promote norepinephrine release to activate β₁- and β₂-AR in WAT, which increases the lipolysis and thermogenesis²⁴⁰. In the skeletal muscle, T₃ promotes expression of T₃-target gene such as myoD, myosin heavy chain and sarcoplasmic reticulum Ca²⁺-ATPase (SERCA)^{241,242}. In addition to HPT axis regulation by TH feedback, there is central modulation by nutritional signals, such as leptin. Leptin promotes the STAT3 phosphorylation to stimulate TRH

expression in PVN²⁴³. Heat loss depends on the through of blood to skin capillaries, and cutaneous vasoconstriction mediated by the noradrenergic vasoconstrictor neurons of SNS²⁴⁴.

The HPT axis is also under the regulation of the circadian rhythm. SCN neurons project to PVN and regulate *Trh* expression, and SCN lesions disrupted the rhythm of TSH and TH^{245,246}. The concentration of TSH, total T₃ and free T₃ in blood exhibit a clear circadian rhythm in mammals^{247,248}. Studies found that neurotransmitters, including 5-HT, acetylcholine and NE participate in the regulation of hypothalamic body temperature and circadian rhythm²⁴⁹.

The light has a significant effect on the circadian rhythm of body temperature. Diurnal animal body temperature increases at daytime, while nocturnal animals are opposite^{250,251}. In addition, if the animal's light-dark cycle is disturbed, advancing or delaying the light time of the normal light-dark cycle can make the animal's body temperature adapt a new circadian rhythm and gradually synchronize with the new light-dark cycle²⁵². These findings suggest that the change of the light-dark cycle can change the time phase, and the change of periodic light participates in the formation of the circadian rhythm of body temperature.

When the ambient temperature was continuously lower or higher than the neutral temperature of environment, no effect on the circadian rhythm of body temperature was found²⁵³. However, it is found that a cold environment can increase the amplitude of the body temperature rhythm oscillation, accompanied by a decrease in the median temperature amplitude²⁵⁴.

Feeding induces the body temperature to rise, and most animals are feeding at a fixed time each day. Experiments found that the circadian rhythmic changes in humans' and mammal's body temperature are related to regular daily feeding²⁵⁵. Appropriate restriction of feeding can induce a decrease of the metabolic rate and body temperature in many animals.

Circadian changes in animal activities are similar to the circadian rhythm of body temperature. Diurnal animals increase activities in daytime and their body temperature also rises, while activities decrease at night time at which the body temperature is decreased²⁵⁶. Nocturnal animals are just the opposite. Humans and rodents have a slow increase in body temperature before waking up. Once they wake up their body temperature rises rapidly^{257,258}. Since the

circadian rhythm of activity is very similar to that of the body temperature, the increase in body temperature seems to result from increased activity ^{259,260}. Although activity can affect the amplitude of the circadian rhythm of body temperature, but the circadian rhythm of body temperature is not dependent on the activity ^{204,261}.

Generally, the basal body temperature of male mammals is lower than that of female. This is also the case in humans. The body temperature of men is lower than that of women ²⁶². The main factor affecting female body temperature changes in mammals is the menstrual cycle. The body temperature rhythm amplitude was changed when female animals are in estrus ²⁶³.

The SCN partly regulates body temperature rhythm, and damage of the SCN can result in complete loss of the circadian rhythm of body temperature ²⁶³. Under the conditions of the regular (12/12) light-dark cycle (LD), it was found that a few months after a complete SCN damage in rats, the circadian rhythm of body temperature gradually recovered and the body temperature rhythm became obvious over time ²⁶³. These findings suggest that the light-dark cycle can restore the circadian rhythm of body temperature, and that the SCN play as a relay station of light signals in this process.

Animals usually choose environmental temperature that is exactly the opposite of the body temperature in that period of the circadian rhythm. Nocturnal animals have a high body temperature at night, but they choose a lower ambient temperature, and have a low body temperature during the day but choose a higher ambient temperature; the choice of diurnal animals is the opposite of that of nocturnal animals ²⁶⁴.

1.3.4 Circadian rhythm and disease

Since the circadian rhythm provides a time reference for the activities of multiple systems, it can be speculated that its abnormalities will cause changes in the physiological activities of other systems, such as changes in metabolism, endocrine, reproduction, cardiovascular, and immune systems.

The circadian clock participates in the regulation of the sleep-wake system. Disorders of the sleep-wake system are common symptoms of neurodegenerative diseases. There is evidence

that the irregular sleep-wake rhythm disorder, long periods of wakefulness during the night, and sleep throughout the day, can accelerate the development of neurodegenerative diseases^{265,266}. Such as the changes in the rhythm of clock genes *Bmal1*, *Per1*, *Cry* in Alzheimer's patients lead to a change in sleep-wake homeostasis, and are related to the decline and loss of learning and memory ability²⁶⁷. Parkinson's disease is another common neurodegenerative disease. Its neuropathological characteristics are the progressive loss of dopaminergic neurons in the substantia nigra compact area and the decrease of dopamine content in the striatum. Dopamine is an important factor in regulating the biological clock system, and the dopamine metabolism disorders are often accompanied by circadian clock disorders²⁶⁸.

The circadian clock regulates the body's metabolic processes, and clinical evidence shows that metabolic diseases such as metabolic syndrome, obesity, and diabetes are all related to circadian rhythm disorders^{269,270}. Many rate-limiting enzymes and nuclear receptors in the process of metabolic reactions are directly or indirectly regulated by clock genes, such as element involved in glycolysis, gluconeogenesis, bile acid synthesis and metabolism^{271,272}. Gene mutations animal models provide the most direct evidence of the clock gene function in metabolic diseases. The C57 homozygous mice with a mutation in the *Clock* gene exhibit a phenotype of hyperphagia, obesity and hyperlipidemia²⁷³, and *Per* gene knockout mice are obese²⁷⁴. Human genomic studies have found a certain relationship between *Clock* and *Bmal1* gene polymorphisms and metabolic syndrome^{275,276}.

Processes of the cardiovascular system function and cardiovascular disease pathogenesis such as blood pressure, heart rate, vascular endothelial function, and platelet aggregation have circadian rhythms. Regarding disease states, myocardial infarction, sudden cardiac death and cerebral thrombosis often occur in the early morning, while cerebral hemorrhagic stroke occurs in the afternoon^{277,278}. This suggests that cardiovascular physiological functions, cardiovascular diseases and circadian rhythm are closely related.

Many human trial and animal experiments have found that circadian clock disorders are closely related to tumorigenesis^{279,280}. Due to the clock system's disorder among night shift workers or

flight attendants, the cancer rate is higher than that of ordinary people, especially the incidence of breast cancer in female flight attendants is significantly higher than that of ordinary people²⁸¹. Compared with normal breast tissue, the expression of genes *Per1* and *Per2* decreased in female flight attendants²⁸². The use of drugs for chronotherapy at the right time can significantly improve the therapeutic effect, and reduce side effects²⁸³.

2. Specific research aims of this thesis

It is a well-known fact that ASICs play an important role in many physiological and pathological processes. However, the structure and regulation mechanism of ASICs in these processes is far from clear, and it is worth exploring. These expression, structures and functions and their related regulated pathways may be promising targets for many diseases.

2.1 Regulation of ASICs by H₂S

The regulation of ASIC expression is still unclear, and only a few signaling pathways that regulate ASIC expression are known. The aim of this project was to determine whether H₂S regulates the expression of ASICs and their function. To this end, I determined the H₂S donors affect ASIC function and expression, and identified the signaling pathway involved. The understanding of the mechanism of ASIC regulation by H₂S is very helpful for diseases such as ischemic stroke-induced neuronal death. Given the critical role of ASICs in physiological and pathological conditions, we hope to explore the mechanism of ASICs expression regulated by H₂S. This study can provide new targets and ideas for the development of neuronal disease treatment.

2.2 Circadian expression of ASIC1a in hypothalamus

ASIC1a is highly expressed in the hypothalamus, but the physiological role of ASICs in this brain area is not fully understood. Thus, characterizing the circadian expression of ASIC is important for understanding their physiological and pathological functions. The aim of this project was to determine whether ASIC expression in hypothalamus has a circadian rhythm, whether and how ASIC expression affects the circadian behavior, and the mechanism. This project was done using *in vivo* and *in vitro* electrophysiological recording, biochemical assay, animal behavioral assay and RNA sequencing technique to study the circadian expression of ASIC1a in mouse hypothalamus. To determine the circadian expression of ASIC in the hypothalamus will improve our knowledge about the physiological function of ASICs.

3. Results

3.1 Project 1: Regulation of ASICs by H₂S

Article: Hydrogen Sulfide Upregulates Acid-sensing Ion Channels *via* the MAPK-Erk1/2 Signaling Pathway

Authors: Zhong Peng, Stephan Kellenberger

Abstract: Hydrogen sulfide (H₂S) emerged recently as a new gasotransmitter and was shown to exert cellular effects by interacting with proteins, among them many ion channels. Acid-sensing ion channels (ASICs) are neuronal voltage-insensitive Na⁺ channels activated by extracellular protons. ASICs are involved in many physiological and pathological processes, such as fear conditioning, pain sensation, and seizures. We characterize here the regulation of ASICs by H₂S. In transfected mammalian cells, the H₂S donor NaHS increased the acid-induced ASIC1a peak currents in a time- and concentration-dependent manner. Similarly, NaHS potentiated also the acid-induced currents of ASIC1b, ASIC2a, and ASIC3. An upregulation induced by the H₂S donors NaHS and GYY4137 was also observed with the endogenous ASIC currents of cultured hypothalamus neurons. In parallel with the effect on function, the total and plasma membrane expression of ASIC1a was increased by GYY4137, as determined in cultured cortical neurons. H₂S also enhanced the phosphorylation of the extracellular signal-regulated kinase (pErk1/2), which belongs to the family of mitogen-activated protein kinases (MAPKs). Pharmacological blockade of the MAPK signaling pathway prevented the GYY4137-induced increase of ASIC function and expression, indicating that this pathway is required for ASIC regulation by H₂S. Our study demonstrates that H₂S regulates ASIC expression, and identifies the involved signaling mechanism. Since H₂S shares several roles with ASICs, as for example facilitation of learning and memory, protection during seizure activity, and modulation of nociception, it may be possible that H₂S exerts some of these effects via a regulation of ASIC function.

My contribution to this manuscript:

I performed and analyzed all of the experiments, and contributed to the writing of the manuscript.

ORIGINAL RESEARCH ARTICLE

Hydrogen Sulfide Upregulates Acid-sensing Ion Channels via the MAPK-Erk1/2 Signaling Pathway

Zhong Peng and Stephan Kellenberger  *

Department of Biomedical Sciences, University of Lausanne, Rue du Bugnon 27, 1011 Lausanne, Switzerland

*Address correspondence to S.K. (e-mail: stephan.kellenberger@unil.ch)

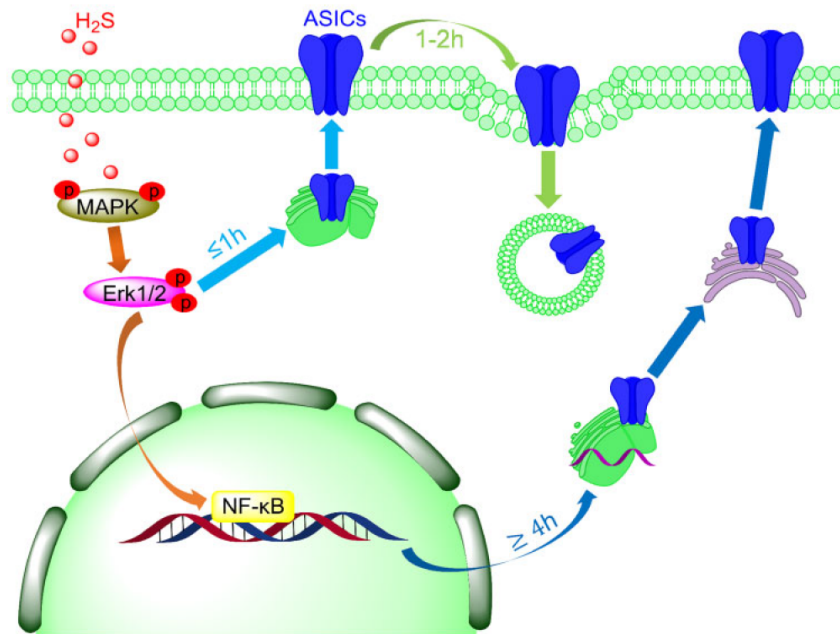
Abstract

Hydrogen sulfide (H₂S) emerged recently as a new gasotransmitter and was shown to exert cellular effects by interacting with proteins, among them many ion channels. Acid-sensing ion channels (ASICs) are neuronal voltage-insensitive Na⁺ channels activated by extracellular protons. ASICs are involved in many physiological and pathological processes, such as fear conditioning, pain sensation, and seizures. We characterize here the regulation of ASICs by H₂S. In transfected mammalian cells, the H₂S donor NaHS increased the acid-induced ASIC1a peak currents in a time- and concentration-dependent manner. Similarly, NaHS potentiated also the acid-induced currents of ASIC1b, ASIC2a, and ASIC3. An upregulation induced by the H₂S donors NaHS and GYY4137 was also observed with the endogenous ASIC currents of cultured hypothalamus neurons. In parallel with the effect on function, the total and plasma membrane expression of ASIC1a was increased by GYY4137, as determined in cultured cortical neurons. H₂S also enhanced the phosphorylation of the extracellular signal-regulated kinase (pErk1/2), which belongs to the family of mitogen-activated protein kinases (MAPKs). Pharmacological blockade of the MAPK signaling pathway prevented the GYY4137-induced increase of ASIC function and expression, indicating that this pathway is required for ASIC regulation by H₂S. Our study demonstrates that H₂S regulates ASIC expression and function, and identifies the involved signaling mechanism. Since H₂S shares several roles with ASICs, as for example facilitation of learning and memory, protection during seizure activity, and modulation of nociception, it may be possible that H₂S exerts some of these effects via a regulation of ASIC function.

Submitted: 25 January 2021; Revised: 12 February 2021; Accepted: 15 February 2021

© The Author(s) 2021. Published by Oxford University Press on behalf of American Physiological Society.

This is an Open Access article distributed under the terms of the Creative Commons Attribution License (<http://creativecommons.org/licenses/by/4.0/>), which permits unrestricted reuse, distribution, and reproduction in any medium, provided the original work is properly cited.



Key words: hydrogen sulfide; ASIC; MAPK; p-Erk1/2; regulation; patch-clamp

Introduction

Acid-sensing ion channels^{1,2} (ASICs) are part of the epithelial sodium channel/degnerin (ENaC/DEG) family.^{2,3} Four genes encode at least six ASIC subunits (ASIC1a, -1b, -2a, -2b, -3, and -4), which form homotrimeric or heterotrimeric channel complexes. Tissue-dependent differences in ASIC subunit composition due to the different expression patterns of the subunits contribute to a multi-modality of ASIC functions. ASICs are Na⁺-selective⁴ and have in addition a small Ca²⁺ permeability.^{1,5,6} Their activation leads therefore generally to excitation of neurons.⁷⁻⁹ ASIC1a is distributed throughout the central and peripheral nervous systems, participating in synaptic transmission and plasticity.¹⁰⁻¹² Dysfunction of ASIC1a is associated with the development of diverse neurological diseases, including neurodegeneration after ischemic stroke,¹³⁻¹⁶ epileptic seizures,¹⁷ and neurodegenerative diseases.^{18,19} ASIC3 is widely expressed in peripheral sensory neurons and to some extent in non-neuronal tissues. It is implicated in multimodal sensory perception,^{2,20} including nociception,²¹⁻²³ mechanosensation,²⁴ and chemosensation.^{25,26}

Exposure of ASICs to an acidic pH induces rapid channel opening, followed by desensitization. ASIC3 and some heterotrimeric ASICs display a sustained current component that follows the transient component. The Texas coral snake toxin MitTx- α / β activates ASIC channels.²⁷ The synthetic compound 2-guainidine 4-methylquinazoline (GMQ) causes persistent activation of ASIC3 at pH 7.4,²⁸ while it modulates the activity of other

ASICs.²⁹ ASIC activity is regulated by many modulators, such as ions, neuropeptides, and animal toxins (reviewed in Wemmie et al.² and Kellenberger and Schild³⁰). Reducing reagents potentiate ASIC currents of GNS neurons reversibly and increase acid-induced membrane depolarization, while oxidizing reagents inhibit ASIC currents and reduce acid-induced membrane depolarization.^{31,32} The endogenous gasotransmitter nitric oxide (NO) also has a direct potentiation effect on ASICs through oxidation of Cys residues.³³

Recently, hydrogen sulfide (H₂S) has emerged as the third gasotransmitter after NO and carbon monoxide. H₂S had long been known as a toxic agent. Several studies have shown that H₂S is produced in several organs/tissues of our body, as in the nervous,³⁴ digestive,³⁵ and endocrine system.³⁶ Endogenous H₂S is produced by three pyridoxal-5'-phosphate-dependent enzymes: (1) cystathionine- β -synthase (CBS, EC 4.2.1.22) and (2) cystathionine- γ -lyase (CSE, EC 4.4.1.1)³⁷⁻³⁹—which both produce H₂S directly, and (3) 3-mercaptopyruvate sulfurtransferase (3MST, EC 2.8.1.2),⁴⁰ which produces H₂S indirectly. In mammals, CBS is predominantly expressed in the brain, while CSE and 3MST are found mostly outside the brain.⁴¹⁻⁴³ Physiological concentrations of H₂S, generated by CBS and CSE, of 10–100 μ M in the blood were reported,^{44,45} but the accurate concentration of free H₂S remains difficult to determine. H₂S regulates ion channels, similarly to other gasotransmitters, through modulation of Cys residues by the formation of persulfide (-SSH) bonds.

This modification has been termed protein S-sulfuration.⁴⁶ H₂S was shown to potentiate or activate glutamate receptors and ATP-sensitive K⁺ channels,^{47–49} and inhibit Ca²⁺ currents in native pancreatic β-cells,⁵⁰ leading to reduced glucose-stimulated insulin secretion.

Here, we report that H₂S enhances ASIC currents as well as total and cell surface expression in cultured brain neurons, and we provide evidence that this regulation involves the mitogen-activated protein kinase (MAPK)–extracellular signal-regulated kinase (Erk)1/2 signaling pathway.

Materials and Methods

Ethical Approval

All animal handling procedures were done in accordance with institutional and Swiss guidelines and approved by the authorities of the Canton de Vaud. All animal experiments respected the Swiss Animal Welfare legislation and were reviewed by the Veterinary Service of the Canton de Vaud (Animal Welfare Act 2019; Project License N° 1750.4 licensed to Dr. Stephan Kellenberger).

Recombinant Expression of ASICs in CHO Cells

The cDNAs used for heterologous expression of ASIC channels were as follows: human ASIC1a, GenBank ID: U78181; rat ASIC1b, GenBank ID: 3445467; human ASIC2a, GenBank ID: U57352; rat ASIC3, GenBank ID: 27465600. The ASIC1a-C466A-C471A-C497A-C528stop cDNA construct⁵¹ was kindly provided by Miguel van Bemmelen (University of Lausanne, Switzerland). The experiments with recombinant human ASIC1a in the present study were carried out with the ASIC1a clone containing the mutation G212D, whose main effect is an acceleration of the desensitization kinetics.⁵² All constructs were expressed in Chinese hamster ovary (CHO) cells. The transient transfection of CHO cells was performed as reported previously.⁵² In brief, CHO cells were cultured at 37°C in a humidified atmosphere with 5% (v/v) CO₂, and passaged twice a week. CHO cells were transiently co-transfected with ASIC and EGFP cDNA, using Rotifect transfection reagent (Carl Roth, D-Karlsruhe). CHO cells were cultured in Ham's F-12K (Kaighn's) medium (ThermoFisher Scientific) supplemented with 10% (w/v) fetal bovine serum (FBS, ThermoFisher Scientific) and 1% penicillin–streptomycin (5000 U·mL⁻¹, ThermoFisher Scientific). Electrophysiological measurements were performed 24–48 h after transfection.

Embryonic Mouse Cerebral Cortex and Hypothalamus Neuron Culture

Twenty-four pregnant mice and 144 mouse embryos were used in these experiments to obtain cells for culture; ASIC1a^{-/-} mice (C57BL/6 background) were provided by Dr. John Wemmie (University of Iowa). Mice used in the experiments were kept in the departmental animal house and maintained on a 12 h light/dark cycle with food and water *ad libitum*. Neuron culture was performed as previously described.⁵³ Briefly, Days 14–15 pregnant mice were sacrificed by exposure to CO₂, the embryos were killed, and the cortex and hypothalamus of the E14–15 embryos were dissected in ice-cold HBSS medium (ThermoFisher). Brain tissues were chopped into small pieces (~1 mm) and incubated at 37°C for 18 min in 0.05% Trypsin-EDTA (ThermoFisher), then washed 3 times in Neurobasal medium (ThermoFisher) containing 10% FBS, and dissociated into single cells. After a 5-min centrifugation at 1000 rpm, neurons were resuspended in

Neurobasal/FBS medium. For the biochemical assay, neurons were seeded at 300 000 cells/dish on 60-mm Petri dishes previously coated with poly-L-lysine. For electrophysiological recording, neurons were seeded at 50 000 cells/dish on 35-mm Petri dishes containing three 15-mm diameter glass coverslips previously coated with poly-L-lysine. For both 60-mm dishes and coverslips, the medium was replaced after 12 h by Neurobasal Medium Electro (ThermoFisher) containing the B27 serum-free supplement, the GlutaMAX supplement (ThermoFisher), and Gentamicin (10 µg·mL⁻¹ final concentration, ThermoFisher). Neuronal cultures were maintained at 37°C in a humidified atmosphere with 5% (v/v) CO₂, and every 2–3 days, half of the medium was replaced with fresh plating medium. Patch-clamp experiments of hypothalamus neurons were carried out after at least 12 days after seeding. Biochemical experiments of cortical neurons were done after at least 9 days after seeding.

Electrophysiological Recording

Electrophysiological recordings were done using the whole-cell patch-clamp technique in voltage-clamp mode with an EPC10 patch-clamp amplifier (HEKA Elektronik-Harvard Bioscience) as previously described.⁵³ The solution exchange was carried out using computer-controlled electrovalves (cF-8VS) and the MPRE8 perfusion head (Cell MicroControls, Norfolk, VA). Data were acquired with Patchmaster software and analysis of the currents was carried out with Fitmaster (HEKA Elektronik-Harvard Bioscience). The sampling interval and the low-pass filtering were set to 50 µs and to 3 kHz, respectively.

The pipette solution contained, in mM, 120 KCl, 30 NaCl, 10 HEPES, 5 EGTA, 2 MgATP, 1 MgCl₂ and 0.5 CaCl₂, adjusted to pH 7.2 with Tris-base. The osmolarity of the pipette solution was 280–300 mOsm (Advanced Instrument Osmometer, Norwood, MA, USA). The extracellular Tyrode solution contained, in mM, 140 NaCl, 5 KCl, 10 glucose, 2 CaCl₂, and 1 MgCl₂, buffered to various pH values with either 10 mM HEPES (pH > 6.0) or 10 mM 2-(N-morpholino)-ethanesulfonic acid (MES; pH ≤ 6.0). The osmolarity of the extracellular solution was 310–320 mOsm. The pH of the solutions was controlled on the day of the experiment and adjusted if necessary. All recordings were performed at room temperature (23 ± 2°C).

Plasma Membrane Protein Extraction

Plasma membrane protein extraction was carried out as previously described.⁵⁴ Briefly, the cultured cortical neurons were washed 3 times with ice-cold PBS, and the neurons were harvested with a cell scraper. After centrifugation at 500g for 5 min at 4°C, the pellet was resuspended in ice-cold homogenization buffer (250 mM sucrose, 1 mM EDTA, 10 mM Tris-HCl buffer, pH 7.2, containing 1:100 diluted protease and phosphatase inhibitor cocktail, Sigma Aldrich). The neurons were then sonicated 15 s using a probe sonicator (Bandelin SONOPULS HD 2200), centrifuged at 10 000g for 10 min at 4°C, and the supernatant was collected. The sonication and supernatant extraction was done twice. The supernatant was centrifuged at 25 000g in an Optima MAX-XP benchtop ultracentrifuge with an MLA-55 rotor (Beckman Coulter Inc., Brea, CA) for 1 h at 4°C and the pellet was collected and resuspended in starting buffer (225 mM mannitol, 75 mM sucrose, and 30 mM Tris-HCl, pH 7.4). The suspension was centrifuged for 20 min at 25 000g, and the pellet was collected and lysed with 1× sample loading buffer (0.3 M sucrose, 2% SDS, 2.5 mM EDTA, 60 mM Tris, pH 8.8, 0.05% (w/v)

bromophenol blue, 25 mM DTT), followed by heating at 95°C for 10 min.

Biochemical Assay

Western blot analysis was carried out as previously described.⁵² Briefly, 10 μ L protein samples were separated on 10% SDS-PAGE gels for 2 h electrophoresis at 100 V, then transferred to 0.2 μ M nitrocellulose membranes (Amersham Biosciences) at 4°C, 100 V for 2 h. After the transfer, the blot was blocked with 5% milk (in TBST buffer, Tris-buffered saline with 0.1% Tween 20 solution) for 1 h at room temperature, followed by 2% BSA in TBST buffer at room temperature. The blot was incubated at 4°C overnight with the primary antibodies, followed, after washing, by the HRP-labeled secondary antibody for 2 h at room temperature. The signals were detected using the Fusion SOLO chemiluminescence system (Vilber Lourmat, Marne-la-Vallée, France) using SuperSignal™ West Femto Maximum Sensitivity Substrate (Thermo Scientific). The following antibodies were used: anti-ASIC1 (1:1000, rabbit,¹⁰ kindly provided by Dr John Wemmie), Anti-Actin (1:1000, rabbit; A2066, Sigma Aldrich), anti-Na⁺/K⁺ ATPase α 1 (1:10000, rabbit,⁵⁵ kindly provided Dr Käthi Geering), anti-Erk1/2 (1:500, rabbit; 4695S, Cell Signaling), anti-phosphor-ERK1/2 (1:200, mouse; 9106S, Cell Signaling), anti-JNK (1:500, rabbit; 9252S, Cell Signaling), anti-phosphor-JNK (1:500, rabbit; 4668s, Cell Signaling), anti-p38 (1:500, rabbit; 9211s, Cell Signaling), anti-phosphor-p38 (1:500, rabbit; 9212s, Cell Signaling), donkey anti-rabbit IgG (1:2000; NA934VS, GE Healthcare), and rabbit anti-mouse IgG (1:2000; 06-371, Sigma Aldrich). p38 and JNK expression levels were determined using the anti-p38 or anti-JNK antibody after stripping of the p-p38 or p-JNK membrane. The blot membrane was incubated in stripping buffer (0.15% glycine, w/v; 0.1% SDS, w/v; 1% Tween 20, v/v; pH adjusted to 2.2 with HCl) at RT for 2 times 5 min, and washed 2 times for 5 min in TBST. Afterward, the membrane was re-blocked. Quantification was done using ImageJ. β -actin was used as the total protein control, and Na⁺/K⁺ ATPase α 1 as plasma membrane protein control, to which the band signals were normalized.

Reagents

All drugs were purchased from Sigma-Aldrich (Buchs, Switzerland) unless otherwise mentioned.

Data Analysis and Statistics

Results are expressed as the mean \pm SEM. Statistical comparisons were performed using Student's *t*-test for comparison between two groups or for paired comparisons, and one-way ANOVA followed by Dunnett's *post hoc* test when more than two groups were involved. For the analysis of the (time or concentration) series of the biochemical experiments (non-Gaussian distribution), Multiple Mann-Whitney tests were used. Statistical tests were carried out with Graphpad Prism8 (GraphPad, San Diego). The sustained ASIC3 currents were measured during the last 2 s of the acidic pH application.

Results

H₂S Potentiates ASIC1a Currents in a Concentration- and Time-dependent Way

Currents of ASIC1a, heterologously expressed in CHO cells, were recorded by whole-cell patch-clamp. Since the gas H₂S is

difficult to dissolve in aqueous solutions, and its concentration would be hard to control, the H₂S donor NaHS was used, which releases H₂S rapidly.⁵⁶ ASIC1a was activated every 3 min by a 10-s acidification from pH 7.4 to 6.7. The acidification induced a rapidly developing transient inward current (Figure 1A). When applied alone, 1 mM NaHS did not generate any current in ASIC1a-expressing CHO cells (Figure 1A). However, the pH 6.7-induced ASIC1a current amplitude increased after a 40-s incubation with 1 mM NaHS. One hour after the short NaHS exposure, without any additional administration of NaHS, the ASIC1a current was increased by 4.4 ± 1.3 -fold (mean \pm SEM, $n = 6$; Figure 1A and B). To further characterize the effects of H₂S on acid-induced ASIC1a activation, the changes in ASIC1a current amplitudes over time were also determined after a 40 s exposure to other concentrations of NaHS (Figure 1B). With concentrations of 30 μ M to 3 mM NaHS, the increase in ASIC1a current was statistically significant if analyzed for the duration of the experiment. A concentration of 30 μ M H₂S can be attained under multiple physiological and pathological conditions.^{57,58} Although no gradual concentration dependence of the NaHS effect was observed, it is obvious from the time course and from the comparison after 30 and 60 min (Figure 1C and D) that the current activation with 3 mM NaHS was smaller than that observed with 1 mM ($P = 0.0026$ at 60 min). With 3 mM NaHS, a tendency of a maximal potentiation in the time window of 12–30 min was observed, before it gradually decreased (Figure 1B). At the physiological pH 7.4 and a temperature of 20°C, approximately 70% of the total sulfide exists as the HS⁻, which, via prior formation of intermediate species such as polysulfides, can form covalent persulfide bonds with Cys.⁵⁹

NaHS Potentiates the Current of all Tested ASIC Isoforms

Next, it was tested whether NaHS modulates other ASIC isoforms. The measurements of ASICs transiently expressed in CHO cells were carried out by repetitive stimulation at a pH that induced approximately 20% of the maximal peak current amplitude (pH 6.3 for ASIC1b, pH 5.0 for ASIC2a, pH 6.8 for ASIC3). To test whether NaHS can regulate ASICs, NaHS was applied at a concentration of 1 mM once during 40 s, as described for ASIC1a. After 60 min, the NaHS-induced current increase amounted to ~ 2 -fold with ASIC1b, and ~ 3 -fold with ASIC2a (Figure 2A–D). Furthermore, NaHS enhanced the ASIC3 peak current by ~ 3 -fold, and its sustained current by ~ 4 -fold (Figure 2E–G). These results indicate that H₂S potentiates all functional homomeric ASICs. The analysis of two selected time points, 0 min (thus directly after NaHS exposure) and 60 min, showed a significant potentiation for all isoforms except ASIC2a at 0 min, and for ASIC1a and ASIC3 at 60 min (Supplementary Figure S1A and B, multiple Mann-Whitney tests between the 1 mM NaHS condition and the respective control experiment).

The ASIC1a Current Potentiation by NaHS is Not Due to a Change in pH Dependence

To determine whether the observed potentiation of pH 6.7-induced currents by NaHS is due to a shift in the pH dependence, the pH dependence of ASIC1a activation was determined in ASIC1a-expressing CHO cells 15 min after a 40-s exposure to NaHS or control solution (Figure 3A). NaHS treatment did not affect the pH of half-maximal activation (pH_{50} ; 6.51 ± 0.14 for control, 6.52 ± 0.04 for NaHS treatment, $n = 5-9$; Figure 3B–D). Consistent with Figures 1A–B and 3B–C, the pH 6.7-induced

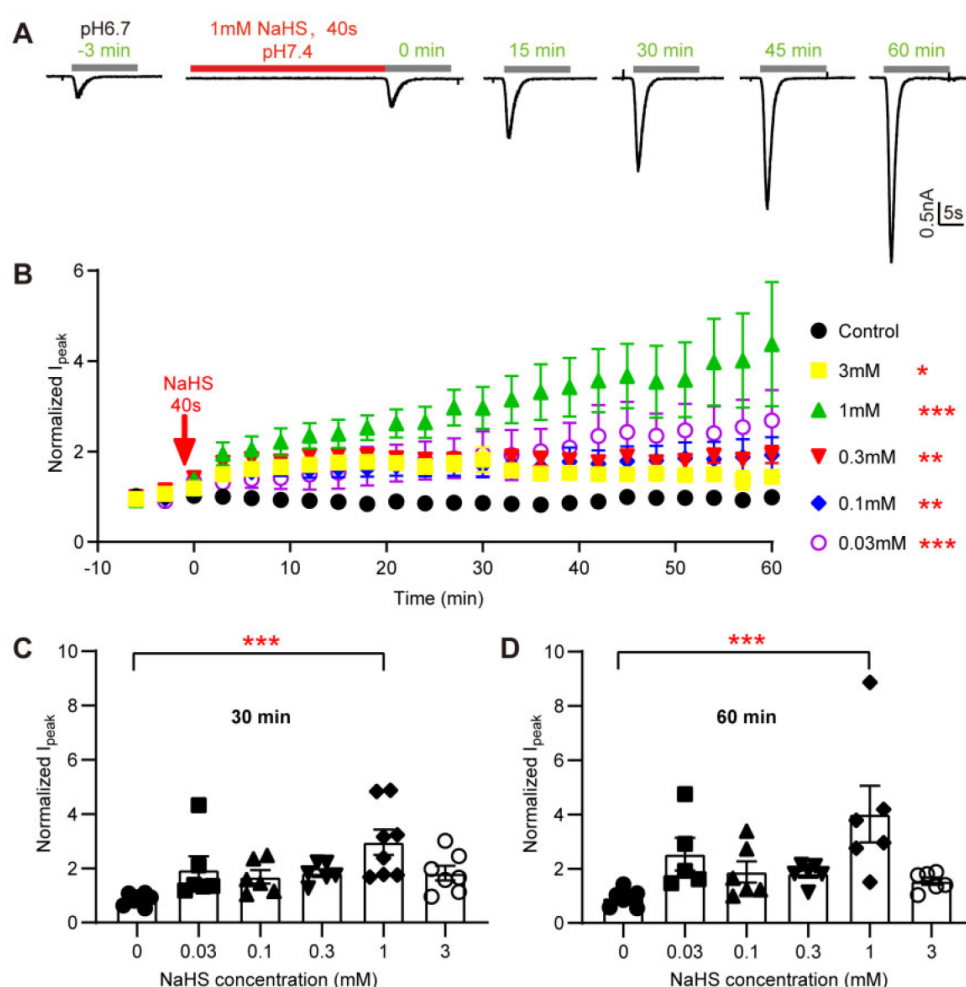


Figure 1. The H₂S Donor NaHS Potentiates ASIC1a Currents in a Concentration- and Time-Dependent Manner. (A) Representative current traces obtained with whole-cell patch-clamp of human ASIC1a-expressing CHO cells at -60 mV, induced by acidification to pH 6.7 at different time points as indicated. One millimolar NaHS was administered once in the experiment for 40 s (red horizontal line). (B) pH 6.7-induced ASIC1a peak current amplitudes (Mean \pm SEM) measured over a period of 60 min without NaHS (control, black symbols) or with a 40-s exposure to the indicated concentration just before the time point 0. The current amplitudes were normalized to the pH 6.7-induced currents measured before the NaHS exposure (at -3 and -6 min), $n=5-7$. * $P < 0.05$; ** $P < 0.01$; *** $P < 0.001$; compared with the control (black symbols) over the period 0-60 min by one-way ANOVA test and Dunnett's *post hoc* test. C, D, pH 6.7-induced peak current amplitudes of ASIC1a expressed in CHO cells at 30 min (C) and 60 min (D) after 40-s exposure to the indicated concentration of NaHS, from the experiments shown in (B), normalized to the pH 6.7-induced current amplitude before NaHS exposure, $n=5-6$. The bar and error bars indicate mean \pm SEM. *** $P < 0.001$, compared to control, by one-way ANOVA test and Dunnett's *post hoc* test.

current was significantly increased at 15 min by exposure to NaHS but not by exposure to control solution, and the ASIC1a current increase was significantly different between these two conditions (Supplementary Figure S2). This finding indicates that the potentiation of the ASIC currents by H₂S does not depend on an increase of the apparent affinity of ASICs to acid.

C-Terminal Cys Residues are Not Involved in the NaHS Modulation

Previous studies have suggested in various ion channels an involvement of Cys residues in H₂S modulation.^{60,61} According to the structural information,⁶² human ASIC1a contains only one unpaired extracellular Cys residue, Cys275. A recent study

observed a transient potentiation of ASIC currents by NaHS. In the cited study it was shown that extracellular pre-treatment with the hydrophilic sulfhydryl reagent sodium (2-sulfonatoethyl) methanethiosulfonate did not prevent this current modulation, and it was concluded that the effect is not mediated by extracellular Cys residues.⁶³ ASIC1a contains in addition Cys residues in the transmembrane and cytoplasmic parts. Since the intracellular C-terminus of ASIC1a contains many Cys residues that may affect ASIC function, NaHS modulation was examined on the mutant ASIC1a C466A/C471A/C497A/C528stop (ASIC1a- Δ CCt), in which the C-terminal Cys residues were eliminated by mutation and truncation.⁵¹ The functional properties of ASIC1a- Δ CCt had been shown to be very similar to those of WT.⁵¹ In ASIC1a- Δ CCt, NaHS also induced a robust, time-

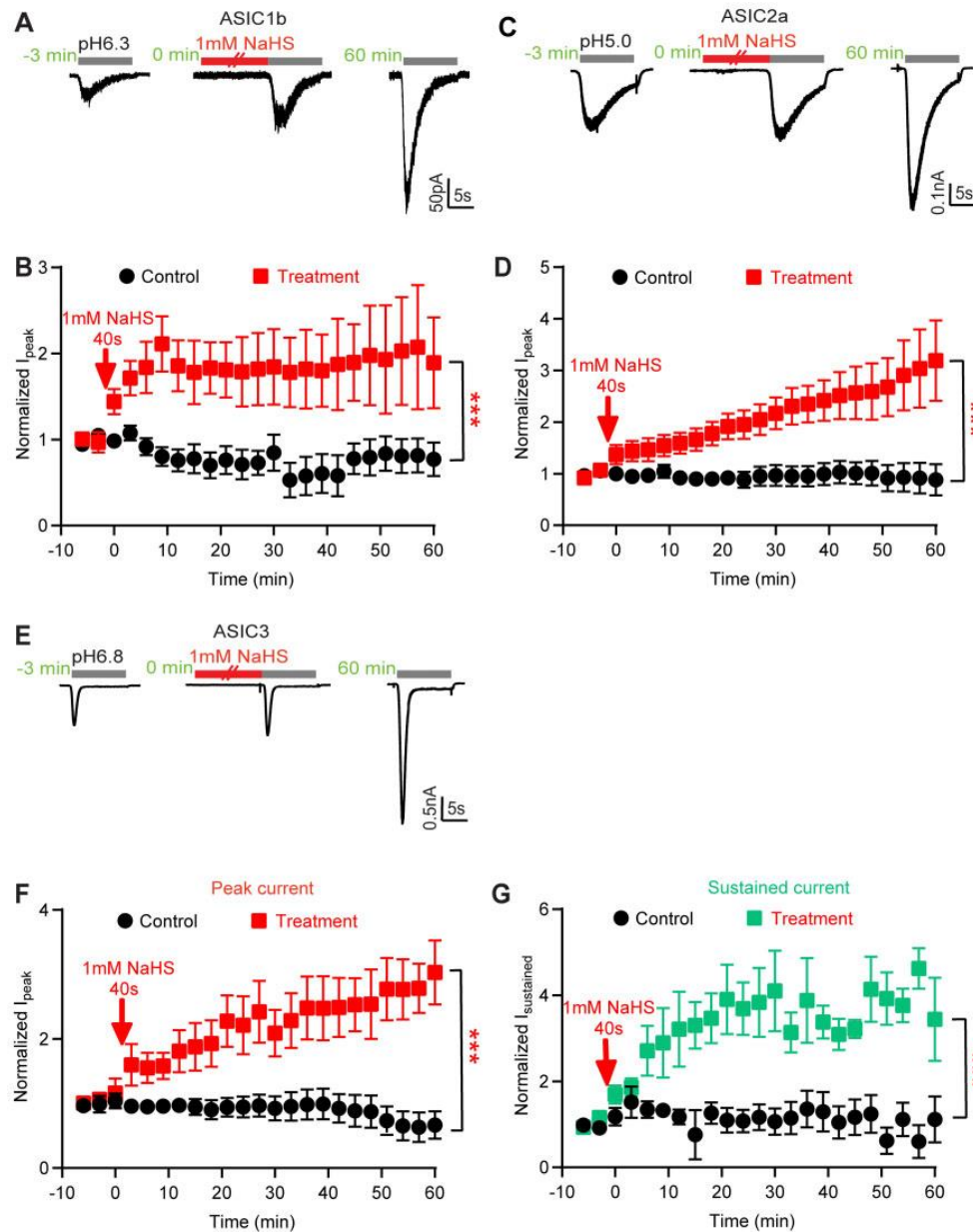


Figure 2. NaHS Potentiates the Current of All Tested ASIC Isoforms. Current traces and data were obtained by whole-cell patch-clamp at -60 mV of CHO cells transfected with the indicated ASIC isoforms. The indicated time points are relative to the 40-s application of 1 mM NaHS. All quantified currents had been normalized to that induced by acid before the NaHS treatment (at -3 and 60 min). The statistical significance in (B), (D), (F), and (G) is based in each case on a comparison between treatment and control over the period 0–60 min by one-way ANOVA test and Dunnett's post hoc test; $***P < 0.001$. (A) Representative rat ASIC1b current traces, induced by acidification to pH 6.3 at different time points, as indicated. (B) Time course of pH 6.3-induced peak ASIC1b current amplitudes measured without (control, black symbols) or with a 40-s exposure to 1 mM NaHS as indicated (treatment, red symbols), $n = 5$. (C) Representative human ASIC2a current traces, induced by acidification to pH 5.0. (D) Time course of pH 5.0-induced ASIC2a peak current amplitudes measured without (control, black symbols) or with a 40-s exposure to 1 mM NaHS as indicated (treatment, red symbols), $n = 5$. (E) Representative rat ASIC3 current traces, induced by acidification to pH 6.8 at different time points, as indicated. (F) Time course of pH 6.8-induced ASIC3 peak current amplitudes measured without (black symbols) or with a 40-s exposure to 1 mM NaHS as indicated (red symbols), $n = 5$. (G) Time course of pH 6.8-induced ASIC3 sustained current amplitudes measured without (black symbols) or with a 40-s exposure to 1 mM NaHS (green symbols) as indicated, $n = 5$.

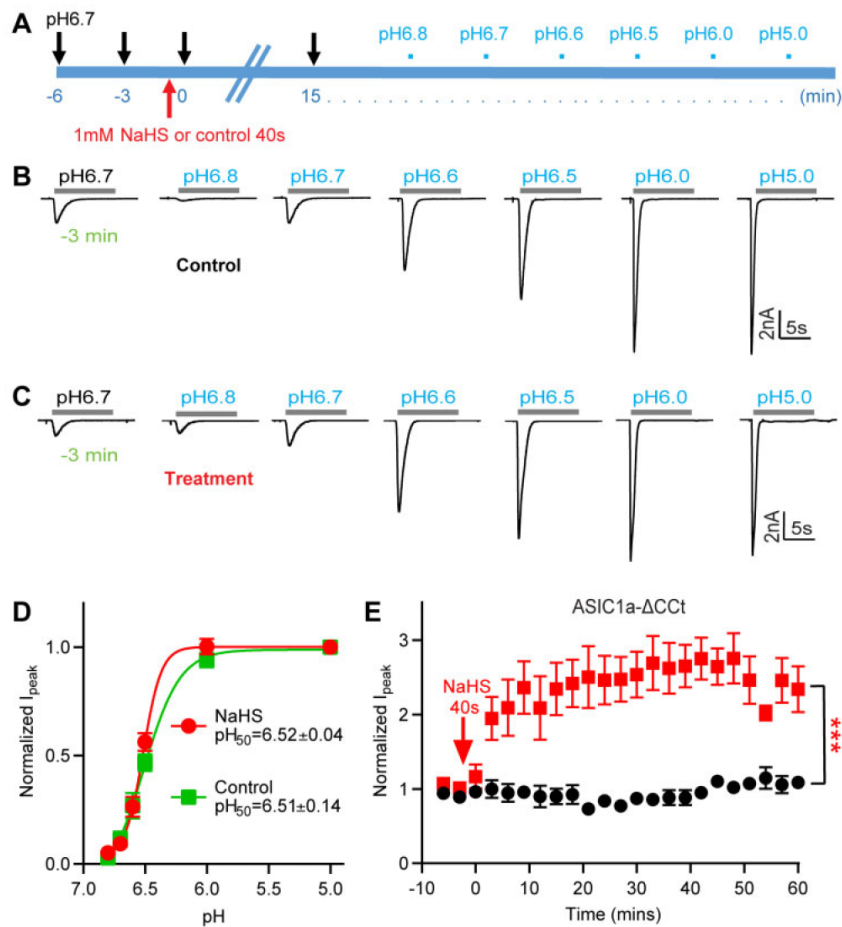


Figure 3. NaHS Potentiation of ASIC1a Currents Is Not Due to a Change in pH Dependence. **(A)** Schematic representation of the protocol used to test whether the exposure to 1 mM NaHS induces a shift in the pH dependence of ASIC1a expressed in CHO cells. **(B and C)** Representative ASIC1a current traces for the construction of a pH-response curve. Fifteen minutes before starting the recording of the pH-response curve, the cell was exposed during 40 s to a control solution **(B, "control")** or to a solution containing 1 mM NaHS **(C, "treatment")**. **(D)** ASIC1a peak current amplitudes, normalized to the peak amplitude induced by pH 5.0, for cells exposed to 1 mM NaHS (treatment, red) or not (control, green), $n = 5-9$. The solid lines represent a fit to the Hill equation. The pH_{50} values were not different between the two conditions (unpaired Student's *t*-test). **(E)** Time course of the pH 6.7-induced current of CHO cells expressing a mutant ASIC1a in which the intracellular C-terminal Cys residues were mutated or deleted (ASIC1a-C466A-C471A-C497A-C528stop, ASIC1a- Δ CCt), measured without (control, black symbols) or with a 40-s exposure to 1 mM NaHS at time point 0, as indicated (treatment, red symbols), $n = 4-6$. *** $P < 0.001$, comparison between treatment and control over the period 0-60 min by one-way ANOVA test and Dunnett's *post hoc* test. Current amplitudes were normalized to the pH 6.7-induced current amplitude measured before NaHS exposure (at -3 and -6 min).

dependent potentiation over time (Figure 3E). In the WT, the control response at the first stimulation after NaHS exposure was increased by $38 \pm 9\%$ (mean \pm SEM, relative to the average of the control responses at -6 and -3 min). This increase was different from that of the control experiments without NaHS ($P = 0.002$, unpaired Student's *t*-test) in the WT (Figure 1C, $n = 7$), while the increase of $12 \pm 13\%$ (mean \pm SEM) in the ASIC1a- Δ CCt mutant was statistically not different from the corresponding control ($P = 0.119$, $n = 5$). Although this shows an apparent difference directly after NaHS exposure between the mutant and WT ASIC1a, this difference was not statistically significant. When observed over the duration of the experiment, the potentiation of the ASIC1a- Δ CCt mutant by NaHS was indistinguishable from that of ASIC1a WT. This indicates that C-terminal Cys residues of ASIC1a are not involved in NaHS-induced

potentiation, and suggests together with the previous observations a possible indirect effect of H_2S on ASICs.

H_2S Donors Potentiate Endogenous Acid-Induced ASIC Currents in Cultured Hypothalamus Neurons

To gain insights into the regulation of neuronal ASICs by H_2S , the effect of NaHS on acid-induced currents in primary cultures of hypothalamus neurons was tested. ASIC currents in central neurons, activated by $pH \geq 6$ are due to ASIC1a homotrimers or heterotrimers involving ASIC1a, -2a, and -2b.^{10,64} Several studies have reported transient acidification-induced currents in rodent hypothalamus neurons that were identified as ASIC currents based on their biophysical and pharmacological properties.⁶⁵⁻⁶⁷ In our hands, exposure of cultured hypothalamus neurons to

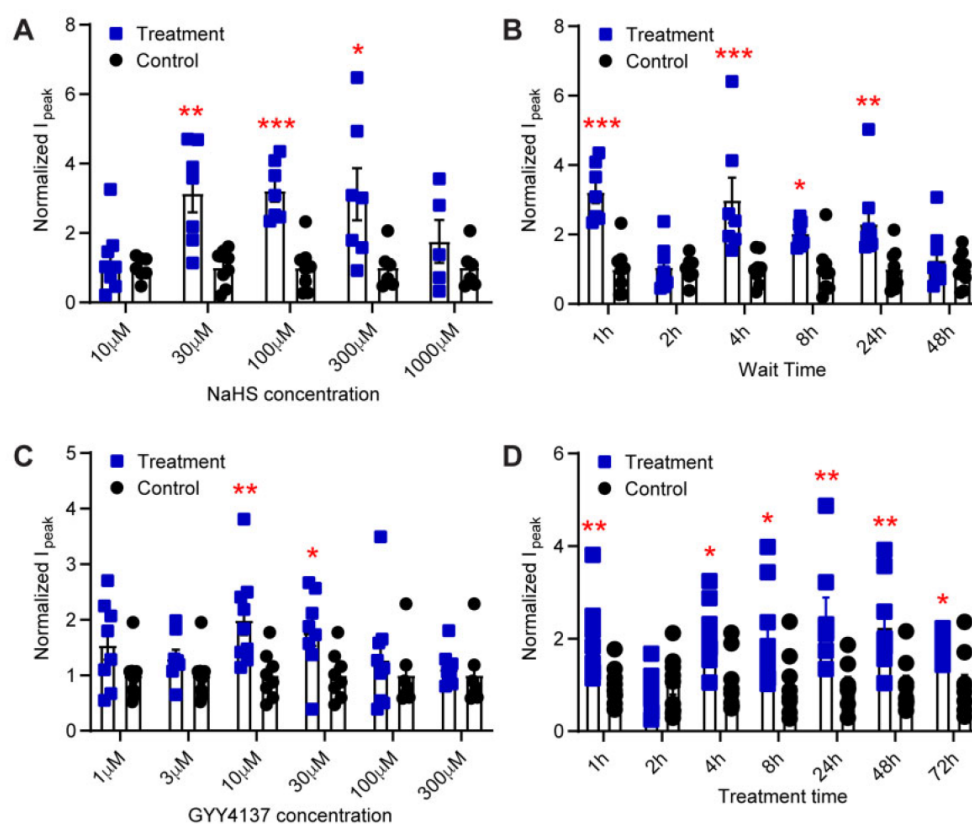


Figure 4. H₂S Donors Potentiate Endogenous ASIC Currents in Cultured Mouse Hypothalamus Neurons. The currents were measured by whole-cell voltage-clamp at -60 mV from cultured hypothalamus neurons of mice. The bars and error bars indicate mean \pm SEM. Together with each treatment condition, a number of control cells (ie, treatment protocol with solution lacking the H₂S donor) were measured, and the current amplitudes obtained for the treatment and for the respective control were normalized to the average of the control. (A and B) Cells were exposed for 1 min to NaHS and then put back into the incubator for a defined period before the current measurement. (A) pH 6.6-induced current amplitudes measured 1 h after exposure to the indicated NaHS concentration (treatment, blue) or to control solution without NaHS (control, black), $n = 5-8$. (B) pH 6.6-induced current amplitudes measured at the indicated time after a 1-min 100 μ M NaHS (blue symbols) or control exposure (black symbols), $n = 6-9$. (C and D) The H₂S donor GYY4137 at the indicated final concentrations was added to the culture medium, and cells were incubated in the cell incubator for the indicated period. (C) pH 6.6-induced current amplitudes measured after 1 h incubation with the indicated concentration of GYY4137 (treatment, blue) or with the addition of solution lacking GYY4137 (control, black), $n = 7-9$. (D) pH 6.6-induced current amplitudes measured after incubation for the indicated time with 10 μ M GYY4137 (treatment, blue) or with solution lacking GYY4137 (control, black), $n = 8-10$. * $P < 0.05$; ** $P < 0.01$; *** $P < 0.001$; **** $P < 0.0001$; comparison of each treatment condition with the corresponding control condition by unpaired multiple Mann-Whitney tests.

pH 6.6 induced rapid, desensitizing inward currents consistent with ASIC activity (Supplementary Figure S3). With the cultured neurons, stable recordings over 1 h, as done in Figure 1 with the transfected CHO cells, were not possible. Therefore, a different strategy was used. Dishes with cultured neurons were removed from the incubator and incubated for 1 min in the recording solution with or without NaHS, before this solution was replaced by culture medium and the cells were put back in the incubator. In the first set of experiments, cells were exposed to different concentrations of NaHS, and currents were measured after 1 h exposure in the incubator. NaHS potentiated the pH 6.6-induced ASIC currents in a concentration-dependent way (Figure 4A). Strikingly, the effect of NaHS (10 μ M–1 mM) was biphasic, with concentrations of 30–300 μ M increasing ASIC currents, whereas lower (10 μ M) or higher concentrations of NaHS (1 mM) did not increase the currents (Figure 4A). To determine the time dependence of ASIC modulation by NaHS in cultured hypothalamus neurons, acid-induced currents were recorded at different time points after a 1-min 100 μ M NaHS exposure. An increase of ASIC

currents was observed in the time span between 1 and 24 h, not however at 2 h after the NaHS treatment (Figure 4B). The NaHS modulation of pH 6.6-induced ASIC currents was lost 48 h after the NaHS incubation.

NaHS releases H₂S rapidly, and oxidation and reaction with other agents in the water reduce the actual concentration of H₂S in solution promptly.⁶⁸ In pathological conditions, the increase of endogenous H₂S levels can last a long time.⁶⁹ A different H₂S donor, GYY4137, has been shown to release H₂S slowly, over a period of hours to days, both in aqueous media and when administered to living animals.⁵⁶ To investigate the ASIC modulation by H₂S in cultured hypothalamus neurons over a longer time period and with a different H₂S donor, GYY4137 was added to the cultures in the incubator, and left until the time of current measurement. In the first series of experiments, the neurons were exposed to different GYY4137 concentrations for 1 h before the measurement of the current amplitude. As control, the same volume of culture medium, but without GYY4137, was added to the culture dish, and currents were measured after 1 h

of incubation. Similar to NaHS, GYY4137 potentiated the pH 6.6-induced currents in a concentration-dependent manner (Figure 4C). A statistically significant current increase was measured at 10 and 30 μM , whereas lower or higher concentrations (≤ 3 or ≥ 100 μM) did not increase the ASIC currents (Figure 4C). The time course of the GYY4137 effect, measured at a concentration of 10 μM , shows potentiation of the pH 6.6-induced currents by GYY4137 at all tested time points except after 2 h (Figure 4D).

H₂S Regulates the Expression of ASIC1a and Activates the Erk1/2 Signaling Pathway

To test whether the observed ASIC current increase upon exposure to GYY4137 is due to a changed ASIC expression, the effect of H₂S on total and plasma membrane expression of ASIC1a was measured. Since the hypothalamus is a small nucleus and many animals would be required to obtain enough cells for a biochemical analysis, ASIC expression was determined in cortical neurons, in which ASIC currents of relatively high amplitude have been measured.^{10,70} Primary cultures of cortical neurons were incubated for different time periods with 10 μM GYY4137. After extraction of total proteins and of plasma membrane-resident proteins by a centrifugation protocol,^{54,71,72} and separation by SDS-PAGE, total and plasma membrane expression of ASIC1a was determined by Western blot analysis (Figure 5A–C). Representative blots indicate an increased ASIC1a expression after GYY4137 exposure (Figure 5A). The increase in total ASIC1a expression appeared only at ≥ 8 h, but was maintained at the latest time point measured 24 h (Figure 5B). ASIC1a expression at the plasma membrane was significantly increased after GYY4137 treatment for 1 h, and then again at incubation times ≥ 4 h, not however after 2 h (Figure 5C).

A previous study reported H₂S regulation of ENaC expression, and demonstrated an implication of Erk1/2, an important member of the MAPK cascade, in the regulation of the ENaC expression by H₂S.⁷³ Activation of Erk1/2 (detected as phosphorylated Erk1/2, p-Erk1/2) can regulate the expression of ASIC1a.⁷⁴ It is therefore possible that H₂S may potentiate ASIC currents via the Erk1/2 kinase cascade. For this reason, the expression of Erk1/2 and p-Erk1/2 in cultured cortical neurons after exposure to 10 μM GYY4137 was examined by Western blot. GYY4137 did not significantly change the Erk1/2 expression (Figure 5A and D); it increased however the p-Erk1/2 signal indicating an activation of Erk1/2 (Figure 5E). This increase was statistically significant at all time points except at 2 h.

H₂S Does Not Activate the JNK and p38 Pathways in Cortical Neurons

MAPKs constitute a large family of protein kinases that respond to a wide range of extracellular stimuli, which lead to phosphorylation of their serine and threonine residues.⁷⁵ Besides Erk1/2, other MAPK subfamilies exist, such as the p38 and c-Jun amino-terminal kinases (JNK). p38 and JNK are activated at the MAPK level by similar types of stimuli. To test whether the upregulation of ASIC1a expression by H₂S may also depend on other MAPK cascades, expression of the total and of the activated forms of JNK and p38 was determined by Western blot (Figure 6). In cultured cortical neurons, 10 μM GYY4137 did not significantly change the expression of JNK and p-JNK (Figure 6A–C), nor of p38 and p-p38 (Figure 6A, D, and E).

H₂S Upregulates ASIC1a Expression via the MAPK Signaling Pathway

If the activation of the MAPK-Erk1/2 cascade is required for the H₂S-induced increase in ASIC activity, the inhibition of the pathway should prevent the ASIC1a modulation by H₂S. In a first experiment, the effect of the MAPK-Erk1/2 signaling pathway antagonist PD98059^{76,77} at 25 μM on H₂S regulation of ASIC1a expression was tested in cultured primary cortical neurons. Neuronal cultures were incubated for the indicated times with either 25 μM PD98059 alone or with 25 μM PD98059 and 10 μM GYY4137. The GYY4137-induced increase of the total and plasma membrane ASIC1a expression (Figure 5A–C) was abolished by PD98059 (Figure 7A–C). PD98059 did not change the expression of Erk1/2 and prevented the increase of the intensity of the p-Erk1/2 bands (Figure 7D and E). The potentiation of the pH 6.6-induced current by GYY4137 in cultured hypothalamus neurons (Figure 4C) was prevented by PD98059 at all time points tested (Figure 7F). The pH 6.6-induced current was also measured at the time point 24 h in control condition (no drug added), with GYY4137 alone and together with PD98059, and with PD98059 alone (Figure 7G), showing that PD98059 inhibited the GYY4137-induced current increase, but not the basal ASIC current. Taken together, our findings indicate that H₂S potentiates ASIC currents via the MAPK-Erk1/2 signaling pathway, by an increased total and plasma membrane expression.

Discussion

We show here that H₂S donors increase currents of recombinantly expressed ASICs and of endogenous ASICs in cultured brain neurons. The current increases over time and stays increased for many hours. The potentiation of the current amplitude is paralleled by an increased total and cell surface expression. We show that exposure to H₂S donors increases Erk1/2 signaling, and that pharmacological inhibition of the MAPK-Erk1/2 pathway prevents the H₂S-induced increase in ASIC expression and current amplitude.

Concentration Dependence of ASIC Regulation by H₂S Donors

Although there are some controversies regarding the determination of biological H₂S levels, it is generally estimated that in physiological conditions, mammalian cells and tissues are exposed to low micromolar H₂S concentrations.⁷⁸ The H₂S levels are dynamically regulated and can therefore change rapidly. In one study, a free H₂S concentration of ~ 0.03 $\mu\text{mol}\cdot\text{g}^{-1}$ protein (estimated to correspond to ~ 3 μM) was determined in brain tissue samples.⁷⁹ Kun Qu et al. measured the sulfide pool (both free H₂S and sulfane sulfur) concentration in brain tissue samples as ~ 12 μM in control and ~ 25 μM in an ischemic stroke mouse model.⁶⁹ In our experiments with recombinant ASICs, a unique, short (40 s) exposure of NaHS at 1 mM was tested, which is much higher than the physiological concentrations. On recombinant ASIC1a, different NaHS concentrations were tested. A potentiation occurred at ≥ 30 μM NaHS and was maximal at a concentration of 1 mM. It was however not possible to establish a clear concentration dependence. Exposure to 3 mM NaHS induced a maximal potentiation at ~ 12 –30 min after the exposure, which decreased subsequently with time. NaHS is a salt that dissociates rapidly to yield H₂S (as dissolved H₂S and dissociated HS⁻).⁷⁸ In our study, the NaHS concentration

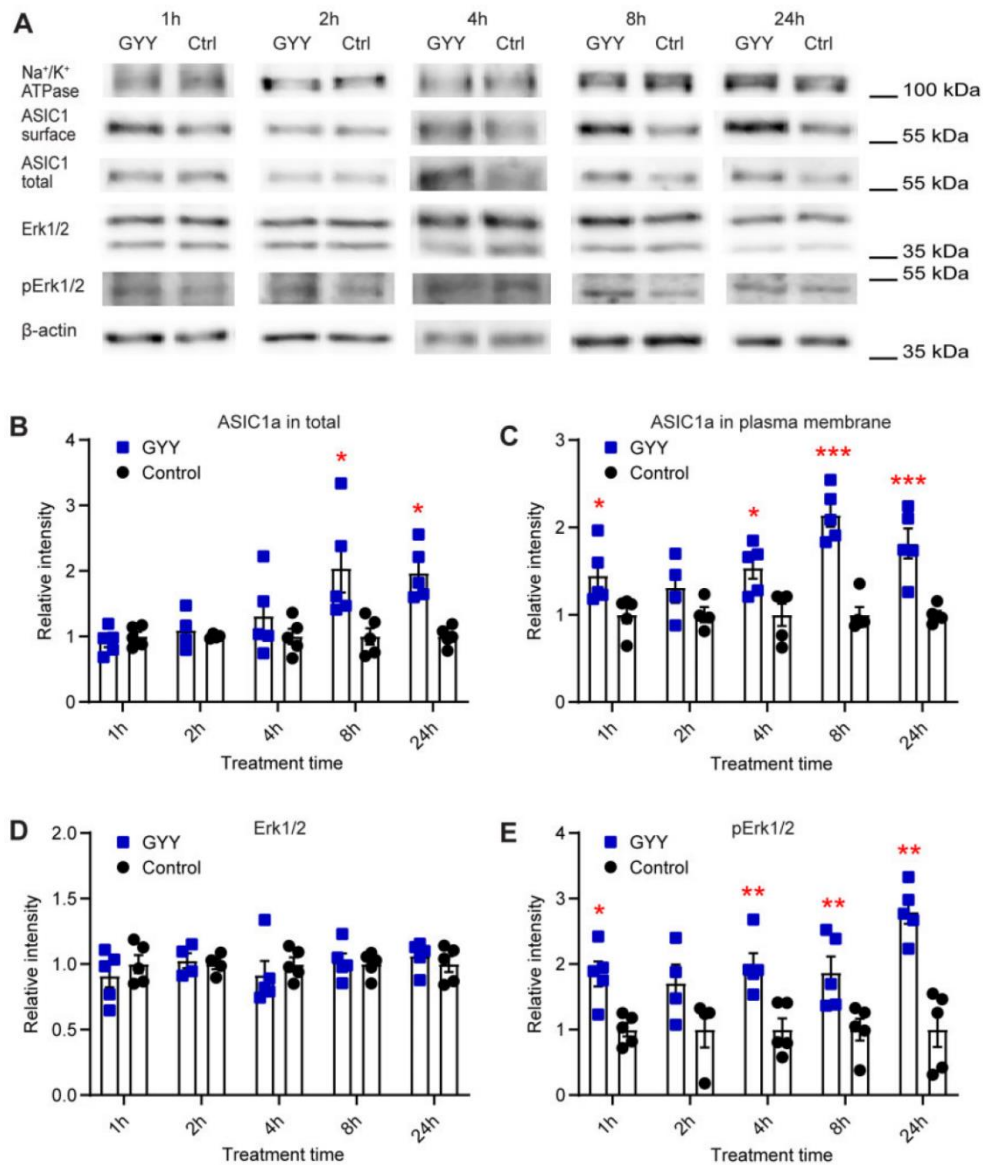


Figure 5. H₂S Donors Regulate the Expression of ASIC1a and the Activation of the Erk1/2 Signaling Pathway. The biochemical experiments were carried out in cultured mouse cortical neurons. Total and plasma membrane proteins were isolated, separated on SDS-PAGE, and specific proteins were visualized as described in the "Materials and Methods" section. (A) Representative Western blots of total and plasma membrane ASIC1a, and Erk1/2, p-Erk1/2, Na⁺/K⁺ATPase, and β -actin as indicated, after incubation with 10 μ M GYY4137 (GYY) or without (Ctrl) for the indicated time. β -actin was used as a control for the total protein, and Na⁺/K⁺ATPase α 1 as a control for plasma membrane proteins. The β -actin and Na⁺/K⁺ATPase bands shown in (A) were from the same sample, but not in all cases from the same lane on the gel, as the bands shown above or below. (B-E) Cells were exposed to 10 μ M GYY4137 (GYY, blue symbols) or to control medium (control, black symbols) for the indicated time. The measured intensities were normalized to the average intensity of the corresponding control. (B) Total expression of ASIC1a, n = 4-5. (C) Plasma membrane expression of ASIC1a, n = 4-5. (D) Expression of Erk1/2, n = 4-5. (E) Expression of p-Erk1/2, n = 4-5. *P < 0.05; **P < 0.01; comparison of each treatment condition with the corresponding control condition by multiple Mann-Whitney tests.

inducing a potentiation of ASIC currents was, with 30 μ M, higher than the physiological concentrations. With a prolonged or repeated administration of NaHS, lower concentrations might have induced potentiation of ASIC activity. We have measured the effects of a prolonged release of H₂S on ASIC function in experiments involving exposure of cultured hypothalamus neurons to the slow-releasing H₂S donor GYY4137, which induced

ASIC current potentiation at concentrations as low as 10 μ M. It has been shown that H₂S concentrations reached by GYY4137 are < 10% of the administered GYY4137 concentration,^{56,80} indicating that in these experiments, concentrations of < 1 μ M H₂S potentiated ASIC currents.

In cultured hypothalamus neurons, the potentiation occurred at concentrations of 30-300 μ M NaHS or 10-30 μ M

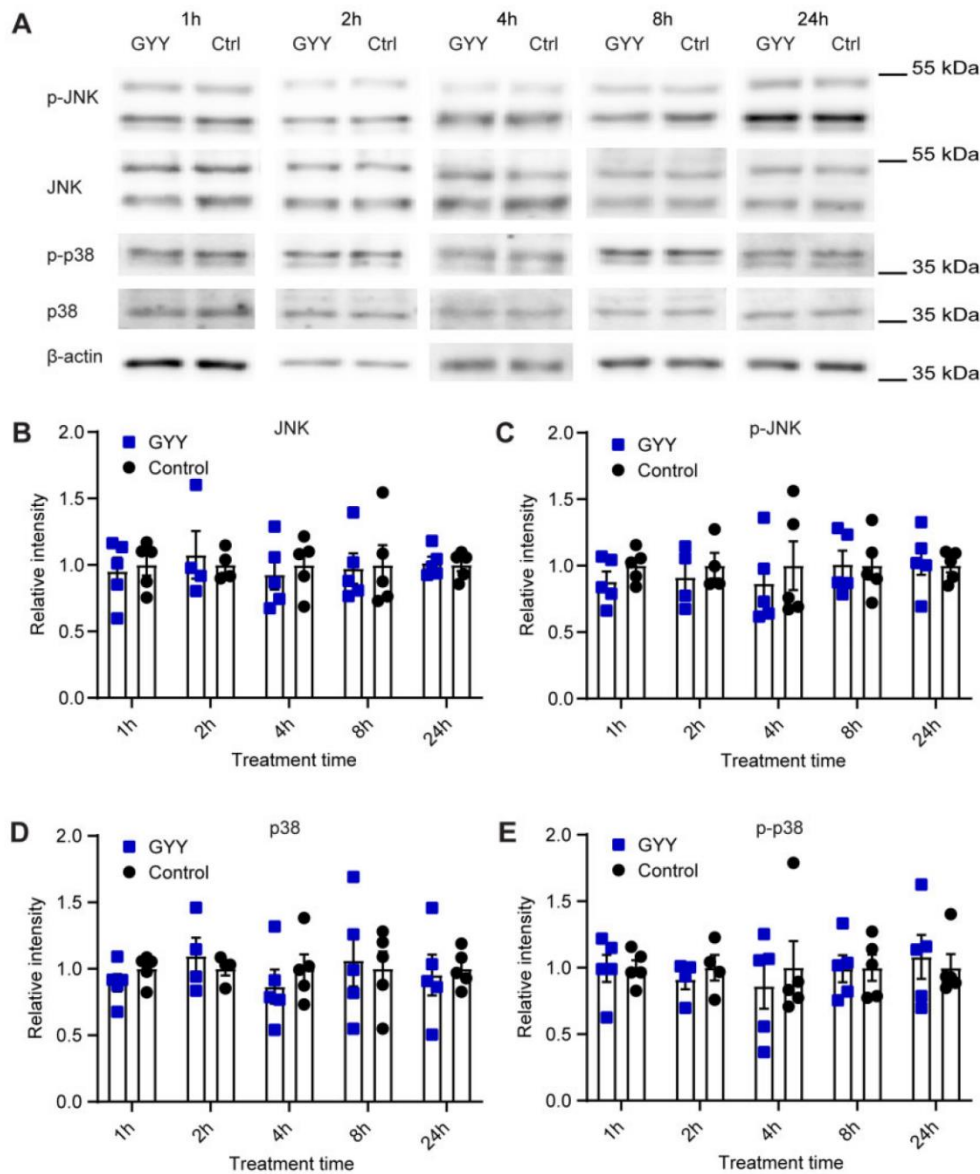


Figure 6. The p38 and JNK Signaling Pathways Are Not Involved in the Upregulation of ASIC1a Expression by H_2S Donors. The biochemical experiments were carried out in cultured mouse cortical neurons. Total proteins were isolated, separated on SDS-PAGE, and specific proteins were visualized as described in the “Materials and Methods” section. (A) Representative Western blots of total JNK, p-JNK, p38, p-p38, and β -actin as indicated, after incubation with 10 μ M GYY4137 (GYY) or without (Ctrl) for the indicated times. β -actin was used as control. The β -actin bands shown in (A) were from the same sample, but not in all cases from the same lane on the gel, as the bands shown above. (B-E) Cells were exposed to 10 μ M GYY4137 (GYY, blue symbols) or to control medium (control, black symbols) for the indicated time. The measured intensities were normalized to the average intensity of the corresponding control. (B) Expression of JNK, $n = 4-5$. (C) Expression of p-JNK, $n = 4-5$. (D) Expression of p38, $n = 4-5$. (E) Expression of p-p38, $n = 4-5$. Comparison of each treatment condition with the corresponding control condition by multiple Mann-Whitney tests indicated no significant differences

GYY4137, while in CHO cells, 1 mM NaHS also induced a potentiation of ASIC1a currents, and showed even a tendency towards an increased potentiation. This difference may be due to different ASIC subtypes in these cell systems, since CNS neurons express besides homotrimeric ASIC1a also heterotrimers containing ASIC1a together with ASIC2a or -2b, or it may be

influenced by differential expression of the signaling pathways involved in this regulation. Besides, the decreased ASIC current potentiation at high H_2S donor concentrations in neurons may be due to cell toxicity. While H_2S has a protective effect on neurons at low concentrations,⁸¹ H_2S donors have been shown to induce at higher concentrations cell death in a process that

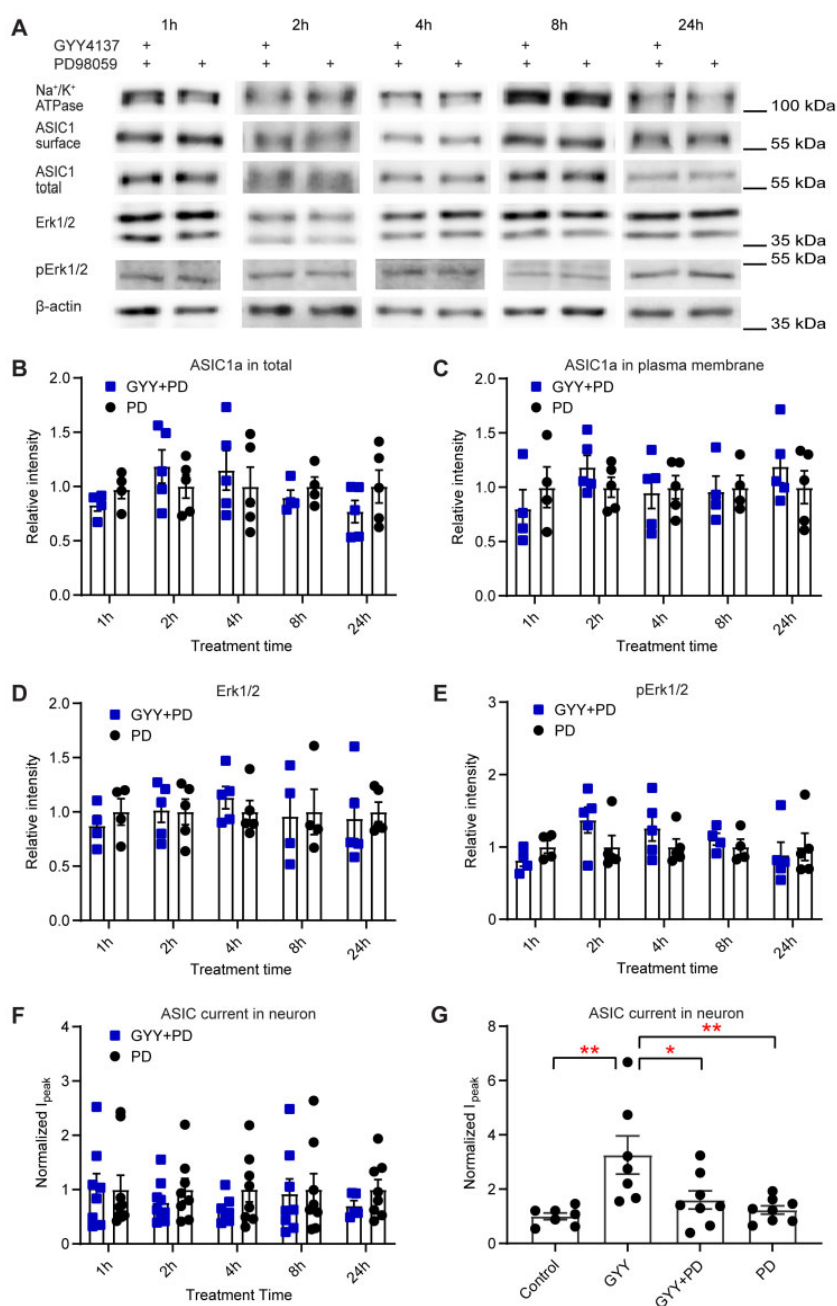


Figure 7. H₂S Donors Upregulate ASIC1a Expression via the MAPK Signaling Pathway. The biochemical experiments were carried out in cultured mouse cortical neurons. Total and plasma membrane proteins were isolated, separated on SDS-PAGE, and specific proteins were visualized as described in "Materials and Methods" section. (A) Representative Western blots of total and plasma membrane ASIC1a, and of Erk1/2, p-Erk1/2, Na⁺/K⁺ATPase, and β-actin after incubation for the indicated times with the MAPK pathway inhibitor PD98059 at a concentration of 25 μM, alone or together with the H₂S donor GYY4137 at 10 μM. β-actin was used as a control for the total protein, and Na⁺/K⁺ATPase α1 as a control for plasma membrane proteins. The β-actin and Na⁺/K⁺ATPase bands shown in (A) were from the same sample, but not in all cases from the same lane on the gel, as the bands shown above or below. (B-E) The quantification of the bands and normalization of the signals was carried out as described in the legend to Figure 5. (B-F) Cells were exposed during the indicated times with 25 μM PD98059 (PD, black symbols) or with 25 μM PD98059 and 10 μM GYY4137 (GYY+PD, blue symbols). Comparison of the conditions by multiple Mann-Whitney tests did not reveal any significant difference. (B) Total ASIC1a expression, n = 4-5. (C) Plasma membrane ASIC1a expression, n = 4-5. (D) Erk1/2 expression, n = 4-5. (E) p-Erk1/2 expression, n = 4-5. (F and G) The current measurements were carried out in cultured hypothalamus neurons, as described in the legend to Figure 4. (F) pH 6.6-induced current amplitudes measured at the indicated times after the start of incubation with 25 μM PD98059 (PD, black) or with 25 μM PD98059 and 10 μM GYY4137 (GYY+PD, blue), n = 5-9. Together with each treatment condition, a number of control cells (ie, treatment protocol with solution lacking the H₂S donor) were measured, and the current amplitudes obtained for the treatment and for the respective control were normalized to the average of the control. (G) pH 6.6-induced current amplitudes in cultured hypothalamus neurons obtained 24 h after the start of the incubation at the four following conditions: Control (culture medium), GYY (10 μM GYY4137), GYY+PD (25 μM PD98059 and 10 μM GYY4137), PD (25 μM PD98059), n = 7-8. *P < 0.05; **P < 0.01, between conditions, by one-way ANOVA test and Dunnett's post hoc test. The current amplitudes were normalized to the mean amplitude of the control condition.

involves glutamate receptors.^{82,83} This toxicity may prevent ASIC potentiation. CHO cells are more resistant to the H₂S toxicity because they do not express glutamate receptors.

H₂S Inhibition of ENaC and ASIC

As mentioned in the introduction, H₂S is known to regulate many different ion channels, among them the closely related ENaC. It was shown that ENaC activation by different means was prevented by NaHS in a distal nephron cell line,^{84,85} indicating that H₂S has an inhibitory effect on ENaC. A related study showed that dexamethasone inhibits H₂S-induced pulmonary edema in rats by preventing H₂S-induced downregulation of α -ENaC.⁸⁶ Very recently, NaHS-induced potentiation of ASIC1a, -2a, and -3, recombinantly expressed in CHO cells, was described.⁶³ These authors observed a potentiation of ASIC currents after a 3- to 5-min exposure to 200 μ M NaHS. In contrast to our data, the potentiation was rapidly reversible. It appears however that the authors did not continue the experiment for as long as we did in our study. This previous study was limited to recombinant ASICs. It did not provide any information on possibly involved signaling pathways or mechanisms, besides a conclusion that extracellular Cys residues on ASICs are not involved.⁶³

H₂S May Not Act Directly on ASIC1a

The molecular mechanism by which H₂S exerts its action involves the modification of Cys residues by S-sulfuration (or persulfidation), and this modification may cause functional changes in conformations, activities, and subcellular localization of the target proteins.⁸⁷ H₂S reacts with various molecules to create a mixture of biologically active species (polysulfides, persulfides).^{78,88} In addition, interactions between H₂S and NO generate several potential intermediates.^{78,89} These species induce S-sulfuration of Cys residues in the target proteins.^{78,90,91} Cysteine S-nitrosylation and S-sulfination are endogenously occurring post-translational modifications of proteins. Such S-nitrosylated or S-sulfinated Cys residues can be S-sulfurated by H₂S.^{92,93}

In the CNS, ASIC1a is the most prominently expressed ASIC subunit. According to the structural models, human ASIC1a has one extracellular unpaired Cys residue, Cys275, which is located in the palm.⁶² Besides, there are three Cys residues in the TM1 domain (Cys49, Cys59, and Cys61) and four in the intracellular C-terminus (Cys466, Cys471, Cys497, and Cys528). For the regulation of ASIC1a by redox reagents, it was concluded that Cys61 is involved in the effects of oxidizing reagents, whereas Lys133 appeared to be involved in the actions of reducing agents.³² This regulation of ASICs by redox reagents is transient, and affects only ASIC1a but not other ASICs,³² strongly suggesting that its mechanism is different from that of the regulation by H₂S. One study highlighted the importance of intracellular C-terminal Cys residues for the inhibition of ASIC1a currents by millimolar concentrations of the oxidant H₂O₂, showing that H₂O₂ induces the formation of intersubunit disulfide bonds.⁹⁴ By testing the mutant ASIC1a- Δ CCt in which the four C-terminal Cys residues are mutated or removed, we found no evidence for an involvement of these Cys residues in the modulation of ASIC1a by H₂S. Although directly after NaHS exposure, the current was increased in the WT but not in the mutant, this difference was not statistically significant. The cited study on ASIC modulation by NaHS concluded that H₂S does not modify extracellular Cys residues of ASIC1a.⁶³ Although the Cys residues of

the TM1 have not been tested, it appears likely that the H₂S donors do not induce a modification of ASIC1a Cys residues and may rather affect signaling pathways that affect ASIC function and expression.

Time Dependence of the ASIC Current Increase in Cultured Hypothalamus Neurons

Exposure of CHO cells expressing ASIC1a to 1 mM NaHS during 40 s induced an ASIC current potentiation that was measurable directly after the NaHS exposure and further increased during the \sim 1 h of the measurement. This suggests that there is a direct regulatory component of the H₂S effect, but that H₂S affects in addition the expression and/or the ASIC trafficking. The ASIC current modulation by H₂S donors was followed over a longer time period in cultured hypothalamus neurons. Both, NaHS and GYY4137 potentiated the ASIC currents 1 h after exposure, and at different time points, up to 24 h for NaHS and 72 h for GYY4137 after exposure, not however at 2 h after exposure. The biochemical analysis indicated a significant increase in total ASIC1a expression at \geq 8 h after GYY4137 exposure. The increase of ASIC1a expression at the plasma membrane was significant at 1 h, and at \geq 4 h after GYY4137 exposure. Many ion channels, such as AMPA receptors and ASIC1a, undergo both constitutive and regulated endocytosis, which act cooperatively to achieve homeostasis and/or plasticity in response to different environmental changes.^{95,96} Accumulation of ASIC1a in the plasma membrane can induce constitutive endocytosis in a clathrin- and dynamin-dependent manner in cortical neurons.⁹⁶ A possible underlying mechanism may be the following. The increase in cell surface expression and current amplitudes observed at 1 h after exposure to H₂S donors may be mostly induced by increased trafficking of ASIC1a to the plasma membrane. The net increase in cell surface expression may be transiently stopped by increased endocytosis (having the strongest effect at 2 h), which would then only be overcome after the increase in ASIC1a expression that takes more time to develop. This is consistent with the observation that H₂S regulates not only trafficking but also the expression of ASIC1a.

Several Signaling Pathways Are Involved in the Regulation of ASIC Expression

Although there is a small, immediate increase in ASIC currents after exposure to NaHS (Supplementary Figure S2), it appears that the large part of the current increase takes longer to develop. Several signaling pathways are known to participate in the regulation of ASIC trafficking and expression, such as protein kinase A (PKA),^{97,98} protein kinase C (PKC),⁹⁹ the phosphoinositide 3-kinase-protein kinase B (PI₃K-AKT), and extracellular signal-regulated kinase 1/2 (Erk1/2).⁷⁴ Erk1/2 belongs to the family of MAPKs, which are protein Ser/Thr kinases that respond to a wide range of extracellular stimuli.⁷⁵ Three major mammalian MAPKs, ERK1/2, JNK, and p38 kinase, are regulated by distinct signal transduction pathways that control many aspects of mammalian cellular physiology.

H₂O₂ at a concentration of 20 μ M was shown to upregulate ASIC1a expression through the MAPK-JNK signaling pathway in NS20Y cells and primary cultures of cortical neurons.¹⁰⁰ In cultured spinal dorsal horn neurons, activation of the PI₃K-AKT-Erk1/2 cascade enhanced ASIC1a currents via phosphorylation of the cytoplasmic residue Ser25 of ASIC1a, resulting in enhanced forward trafficking and increased surface expression.⁷⁴ Activation of PKC increased ASIC1a protein expression and

ASIC currents in cultured cortical neurons, and PKC regulation of ASIC1a protein expression involves the NF- κ B signaling pathway.^{99,101} p-Erk1/2 regulates not only the trafficking but also the expression of ASICs; activation of Erk1/2 enhanced forward trafficking in cultured spinal dorsal horn neurons.⁷⁴ p-Erk1/2 can lead to activation of NF- κ B, which in turn was shown to regulate the transcriptional expression of ASICs.^{99,102}

There is evidence that H₂S can activate several signaling pathways. NaHS was shown in transfected HEK-293 cells and in rat vascular smooth muscle cells to increase phosphorylation of Erk1/2 and of PKC.¹⁰³ In isolated rat hearts, H₂S stimulated both cardiac Akt and PKC activity.¹⁰⁴ In the context of ENaC inhibition in H₂S-induced pulmonary edema in rats, H₂S induced Erk1/2 expression and phosphorylation.⁸⁶ The mechanisms for H₂S-induced MAPK signaling activity are complex and likely depend on the cell type and on the concentrations used.¹⁰⁵

In the present study, exposure of cultured cortical neurons to 10 μ M GYY4137 did not change the expression of Erk1/2; however, it increased the phosphorylation of Erk1/2, indicating that it activated the pathway. In contrast, 10 μ M GYY4137 did not activate the JNK and p38 signaling pathways. The Erk1/2 pathway inhibitor PD98059 prevented the GYY4137-induced increase in ASIC1a expression in cultured cortical neurons and the GYY4137-induced increase in ASIC currents of cultured hypothalamus neurons, indicating that the activation of the Erk1/2 pathway is required for the H₂S-induced ASIC current increase.

It is known that H₂S, NO, and reactive oxygen species (ROS) interact with each other in their production, downstream signaling, and by direct chemical interaction, and this in different organs.^{78,106,107} In rat neonatal cardiomyocytes, H₂S inhibits mitochondrial complex IV and activates superoxide dismutase to decrease the levels of ROS in cardiomyocytes during ischemia/reperfusion.¹⁰⁸ H₂O₂, a major ROS, upregulates ASIC1a expression through the MAPK-JNK signaling pathway in NS20Y cells and primary cultures of cortical neurons.¹⁰⁰ In our study, we did however not detect an activation of JNK by GY4137. H₂S has been shown to increase NO levels in some tissues. Interestingly, NO potentiates ASIC currents, and there is evidence that this regulation involves direct oxidation of Cys residues.³³ Our study strongly suggests an indirect regulation of ASICs by H₂S, and currently, there is no evidence for an interplay between these gasotransmitters in the regulation of ASIC activity.

In this work, we have characterized the regulation of ASICs by exogenous H₂S. To examine whether endogenous H₂S can exert such a regulation, future experiments will use silencing or pharmacological inhibition of the enzymes that produce H₂S. Silencing of CSE with siRNA, or pharmacological inhibition of this enzyme both decreased the activation of Erk1/2,¹⁰⁹ while the overexpression of CSE increased the activation of Erk1/2.¹¹⁰ These observations are consistent with a possible effect of endogenous H₂S on ASICs.

Possible Physiological Importance of ASIC Regulation by H₂S

ASICs detect tissue acidosis occurring upon tissue injury, inflammation, ischemia, stroke, and tumors as well as fatiguing muscle, to activate pain-sensing nerves in the periphery and transmit pain signals to the brain. ASIC1a was shown to protect against seizures by shortening their duration,¹⁷ and ASIC1a activation is also involved in synaptic plasticity, learning, and memory.¹¹ Dysfunction of ASIC1a may contribute to the learning and memory deficit associated with Alzheimer's disease.^{111,112} ASIC2 is a negative modulator of rod

phototransduction, and functional ASIC2 channels are beneficial for the maintenance of retinal integrity.¹¹³ H₂S can improve the hippocampal damage induced by recurrent febrile seizures,¹¹⁴ and protect the retina in the context of retinal vascular diseases.¹¹⁵ H₂S is also involved in the regulation of neural synaptic plasticity and cognition¹¹⁶ and it attenuates spatial memory impairment and hippocampal neuroinflammation in the A β 1 rat model of Alzheimer's disease.¹¹⁷ The mechanism of the function of H₂S in these processes is still unclear, and it is possible that regulation of ASICs by H₂S may be involved.

Taken together, we found that H₂S potentiates ASIC currents in a time- and concentration-dependent way. This potentiation does not depend on the acid sensitivity of ASIC1a but is induced by an increased expression of ASIC1a at the plasma membrane. Our data suggest that this regulation, which is likely of importance in several physiological and pathological conditions, is mediated by the MAPK-Erk1/2 signaling pathway.

Acknowledgments

The authors thank Ophélie Molton, Anand Vaithia, and Olivier Bignucolo for comments on the manuscript.

Supplementary Material

Supplementary material is available at the APS Function online.

Funding

This research was supported by the Swiss National Science Foundation grant 31003A_172968 to S.K. Z.P. was supported by a scholarship grant from the Chinese Scholarship Council.

Conflict of Interest Statement

None declared.

References

1. Waldmann R, Champigny G, Bassilana F, Heurteaux C, Lazdunski M. A proton-gated cation channel involved in acid-sensing. *Nature* 1997;386 (6621):173–177.
2. Wemmie JA, Taugher RJ, Kreple CJ. Acid-sensing ion channels in pain and disease. *Nat Rev Neurosci* 2013;14(7):461–471.
3. Kellenberger S, Schild L. Epithelial sodium channel/degenerin family of ion channels: a variety of functions for a shared structure. *Physiol Rev* 2002;82 (3):735–767.
4. Yang L, Palmer LG. Ion conduction and selectivity in acid-sensing ion channel 1. *J Gen Physiol* 2014;144 (3):245–255.
5. Bassler EL, Ngo-Anh TJ, Geisler HS, Ruppertsberg JP, Grunder S. Molecular and functional characterization of acid-sensing ion channel (ASIC) 1b. *J Biol Chem* 2001;276(36):33782–33787.
6. Boillat A, Alijevic O, Kellenberger S. Calcium entry via TRPV1 but not ASICs induces neuropeptide release from sensory neurons. *Mol Cell Neurosci* 2014;61:13–22.
7. Deval E, Baron A, Lingueglia E, Mazarguil H, Zajac JM, Lazdunski M. Effects of neuropeptide SF and related peptides on acid sensing ion channel 3 and sensory neuron excitability. *Neuropharmacology* 2003;44(5):662–671.
8. Baron A, Waldmann R, Lazdunski M. ASIC-like, proton-activated currents in rat hippocampal neurons. *J Physiol* 2002;539(2):485–494.

9. Vukicevic M, Kellenberger S. Modulatory effects of acid-sensing ion channels on action potential generation in hippocampal neurons. *Am J Physiol Cell Physiol* 2004;287(3):C682–C690.
10. Wemmie JA, Chen J, Askwith CC, et al. The acid-activated ion channel ASIC contributes to synaptic plasticity, learning, and memory. *Neuron* 2002;34(3):463–477.
11. Wu PY, Huang YY, Chen CC, et al. Acid-sensing ion channel-1a is not required for normal hippocampal LTP and spatial memory. *J Neurosci* 2013;33(5):1828–1832.
12. Du J, Reznikov LR, Price MP, et al. Protons are a neurotransmitter that regulates synaptic plasticity in the lateral amygdala. *Proc Natl Acad Sci USA* 2014;111(24):8961–8966.
13. Gao J, Duan B, Wang DG, et al. Coupling between NMDA receptor and acid-sensing ion channel contributes to ischemic neuronal death. *Neuron* 2005;48(4):635–646.
14. Duan B, Wang YZ, Yang T, et al. Extracellular spermine exacerbates ischemic neuronal injury through sensitization of ASIC1a channels to extracellular acidosis. *J Neurosci* 2011;31(6):2101–2112.
15. Xiong ZG, Zhu XM, Chu XP, et al. Neuroprotection in ischemia: blocking calcium-permeable acid-sensing ion channels. *Cell* 2004;118(6):687–698.
16. Wang YZ, Xu TL. Acidosis, acid-sensing ion channels, and neuronal cell death. *Mol Neurobiol* 2011;44(3):350–358.
17. Ziemann AE, Schnizler MK, Albert GW, et al. Seizure termination by acidosis depends on ASIC1a. *Nat Neurosci* 2008;11(7):816–822.
18. Friese MA, Craner MJ, Etzensperger R, et al. Acid-sensing ion channel-1 contributes to axonal degeneration in autoimmune inflammation of the central nervous system. *Nat Med* 2007;13(12):1483–1489.
19. Vergo S, Craner MJ, Etzensperger R, et al. Acid-sensing ion channel 1 is involved in both axonal injury and demyelination in multiple sclerosis and its animal model. *Brain* 2011;134(Pt 2):571–584.
20. Li WG, Xu TL. ASIC3 channels in multimodal sensory perception. *ACS Chem Neurosci* 2011;2(1):26–37.
21. Chen CC, Zimmer A, Sun WH, Hall J, Brownstein MJ. A role for ASIC3 in the modulation of high-intensity pain stimuli. *Proc Natl Acad Sci USA* 2002;99(13):8992–8997.
22. Sluka KA, Price MP, Breese NM, Stucky CL, Wemmie JA, Welsh MJ. Chronic hyperalgesia induced by repeated acid injections in muscle is abolished by the loss of ASIC3, but not ASIC1. *Pain* 2003;106(3):229–239.
23. Deval E, Noel J, Lay N, et al. ASIC3, a sensor of acidic and primary inflammatory pain. *EMBO J* 2008;27(22):3047–3055.
24. Price MP, McIlwrath SL, Xie J, et al. The DRASIC cation channel contributes to the detection of cutaneous touch and acid stimuli in mice. *Neuron* 2001;32(6):1071–1083.
25. Sutherland SP, Benson CJ, Adelman JP, McCleskey EW. Acid-sensing ion channel 3 matches the acid-gated current in cardiac ischemia-sensing neurons. *Proc Natl Acad Sci USA* 2001;98(2):711–716.
26. Birdsong WT, Fierro L, Williams FG, et al. Sensing muscle ischemia: coincident detection of acid and ATP via interplay of two ion channels. *Neuron* 2010;68(4):739–749.
27. Bohlen CJ, Chesler AT, Sharif-Naeini R, et al. A heteromeric Texas coral snake toxin targets acid-sensing ion channels to produce pain. *Nature* 2011;479(7373):410–414.
28. Yu Y, Chen Z, Li W-G, et al. A nonproton ligand sensor in the acid-sensing ion channel. *Neuron* 2010;68(1):61–72.
29. Alijevic O, Kellenberger S. Subtype-specific modulation of acid-sensing ion channel (ASIC) function by 2-guanidine-4-methylquinazoline. *J Biol Chem* 2012;287(43):36059–36070.
30. Kellenberger S, Schild L. International Union of Basic and Clinical Pharmacology. XCI. Structure, function, and pharmacology of acid-sensing ion channels and the epithelial Na⁺ channel. *Pharmacol Rev* 2015;67(1):1–35.
31. Andrey F, Tsintsadze T, Volkova T, Lozovaya N, Krishtal O. Acid sensing ionic channels: modulation by redox reagents. *Biochim Biophys Acta* 2005;1745(1):1–6.
32. Chu XP, Close N, Saugstad JA, Xiong ZG. ASIC1a-specific modulation of acid-sensing ion channels in mouse cortical neurons by redox reagents. *J Neurosci* 2006;26(20):5329–5339.
33. Cadiou H, Studer M, Jones NG, et al. Modulation of acid-sensing ion channel activity by nitric oxide. *J Neurosci* 2007;27(48):13251–13260.
34. Warencya MW, Goodwin LR, Benishin CG, et al. Acute hydrogen sulfide poisoning: demonstration of selective uptake of sulfide by the brainstem by measurement of brain sulfide levels. *Biochem Pharmacol* 1989;38(6):973–981.
35. Powell MA, Arp AJ. Hydrogen sulfide oxidation by abundant nonhemoglobin heme compounds in marine invertebrates from sulfide-rich habitats. *J Exp Zool* 1989;249(2):121–132.
36. Jinshan C. Effects of carbon disulfide on some endocrine glands in male exposed workers. *Ind Health Occup Dis* 1989;15(6):330–334.
37. Stipanuk MH, Beck PW. Characterization of the enzymic capacity for cysteine desulphhydration in liver and kidney of the rat. *Biochem J* 1982;206(2):267.
38. Erickson P, Maxwell I, Su L, Baumann M, Glode L. Sequence of cDNA for rat cystathionine γ -lyase and comparison of deduced amino acid sequence with related *Escherichia coli* enzymes. *Biochem J* 1990;269(2):335.
39. Roper MD, Kraus JP. Rat cystathionine β -synthase: expression of four alternatively spliced isoforms in transfected cultured cells. *Arch Biochem Biophys* 1992;298(2):514–521.
40. Shibuya N, Mikami Y, Kimura Y, Nagahara N, Kimura H. Vascular endothelium expresses 3-mercaptopyruvate sulfoxidase and produces hydrogen sulfide. *J Biochem* 2009;146(5):623–626.
41. Sun Y, Tang C-s, Jin H-f, Du J-b. The vasorelaxing effect of hydrogen sulfide on isolated rat aortic rings versus pulmonary artery rings. *Acta Pharmacol Sin* 2011;32(4):456–464.
42. Yan H, Du J, Tang C. The possible role of hydrogen sulfide on the pathogenesis of spontaneous hypertension in rats. *Biochem Biophys Res Commun* 2004;313(1):22–27.
43. Fiorucci S, Antonelli E, Mencarelli A, et al. The third gas: H₂S regulates perfusion pressure in both the isolated and perfused normal rat liver and in cirrhosis. *Hepatology* 2005;42(3):539–548.
44. Zanardo RCO, Brancaleone V, Distrutti E, Fiorucci S, Cirino G, Wallace JL. Hydrogen sulfide is an endogenous modulator of leukocyte-mediated inflammation. *FASEB J* 2006;20(12):2118–2120.
45. Peng H, Cheng Y, Dai C, et al. A fluorescent probe for fast and quantitative detection of hydrogen sulfide in blood. *Angew Chem Int Ed* 2011;50(41):9672–9675.
46. Mustafa AK, Gadalla MM, Sen N, et al. H₂S signals through protein S-sulfhydration. *Sci Signal* 2009;2(96):ra72.
47. Kimura H. Hydrogen sulfide induces cyclic AMP and modulates the NMDA receptor. *Biochem Biophys Res Commun* 2000;267(1):129–133.
48. Zhang ZZZ, Huang HHH, Liu PLP, Tang CTC, Wang JWJ. Hydrogen sulfide contributes to cardioprotection during

- ischemia-reperfusion injury by opening K_{ATP} channels. *Can J Physiol Pharmacol* 2007;85(12):1248–1253.
49. Yang W, Yang G, Jia X, Wu L, Wang R. Activation of K_{ATP} channels by H_2S in rat insulin-secreting cells and the underlying mechanisms. *J Physiol (Lond)* 2005;569(2):519–531.
 50. Tang G, Zhang L, Yang G, Wu L, Wang R. Hydrogen sulfide-induced inhibition of L-type Ca^{2+} channels and insulin secretion in mouse pancreatic beta cells. *Diabetologia* 2013;56(3):533–541.
 51. van Bemmelen MX, Huser D, Gautschi I, Schild L. The human acid-sensing ion channel ASIC1a: evidence for a homotetrameric assembly state at the cell surface. *PLoS One* 2015;10(8):e0135191.
 52. Vaithia A, Vullo S, Peng Z, Alijevic O, Kellenberger S. Accelerated current decay kinetics of a rare human acid-sensing ion channel 1a variant that is used in many studies as wild type. *Front Mol Neurosci* 2019;12:133.
 53. Alijevic O, Bignucolo O, Hichri E, Peng Z, Kucera JP, Kellenberger S. Slowing of the time course of acidification decreases the acid-sensing ion channel 1a current amplitude and modulates action potential firing in neurons. *Front Cell Neurosci* 2020;14:41.
 54. Suski JM, Lebedzinska M, Wojtala A, et al. Isolation of plasma membrane-associated membranes from rat liver. *Nat Protoc* 2014;9(2):312.
 55. Bibert S, Roy S, Schaer D, Horisberger J-D, Geering K. Phosphorylation of phospholemman (FXD1) by protein kinases A and C modulates distinct Na, K-ATPase isozymes. *J Biol Chem* 2008;283(1):476–486.
 56. Lee ZW, Zhou J, Chen GS, et al. The slow-releasing hydrogen sulfide donor, GYY4137, exhibits novel anti-cancer effects in vitro and in vivo. *PLoS One* 2011;6(6):e21077.
 57. Li C, Ingrid S, Ding Y-g, et al. Imbalance of endogenous homocysteine and hydrogen sulfide metabolic pathway in essential hypertensive children. *Chinese Med J* 2007;120(5):389–393.
 58. Chang L, Geng B, Yu F, et al. Hydrogen sulfide inhibits myocardial injury induced by homocysteine in rats. *Amino Acids* 2008;34(4):573–585.
 59. Dombkowski RA, Russell MJ, Olson KR. Hydrogen sulfide as an endogenous regulator of vascular smooth muscle tone in trout. *Am J Physiol* 2004;286(4):R678–R685.
 60. Kimura H. Hydrogen sulfide as a neuromodulator. *Mol Neurobiol* 2002;26(1):13–19.
 61. Ji Y, Pang Q, Xu G, Wang L, Wang J, Zeng Y. Exogenous hydrogen sulfide postconditioning protects isolated rat hearts against ischemia-reperfusion injury. *Eur J Pharmacol* 2008;587(1):1–7.
 62. Jasti J, Furukawa H, Gonzales EB, Gouaux E. Structure of acid-sensing ion channel 1 at 1.9 resolution and low pH. *Nature* 2007;449(7160):316–323.
 63. Mukhopadhyay M, Bera AK. Modulation of acid-sensing ion channels by hydrogen sulfide. *Biochem Biophys Res Commun* 2020;527(1):71–75.
 64. Askwith CC, Wemmie JA, Price MP, Rokhlina T, Welsh MJ. ASIC2 modulates ASIC1 H^+ -activated currents in hippocampal neurons. *J Biol Chem* 2004;279(18):18296–18305.
 65. Ohbuchi T, Sato K, Suzuki H, et al. Acid-sensing ion channels in rat hypothalamic vasopressin neurons of the supraoptic nucleus. *J Physiol* 2010;588(Pt 12):2147–2162.
 66. Wang W, Yu Y, Xu TL. Modulation of acid-sensing ion channels by Cu^{2+} in cultured hypothalamic neurons of the rat. *Neuroscience* 2007;145(2):631–641.
 67. Chen GH, Hsu YT, Chen CC, Huang RC. Acid-sensing ion channels in neurons of the rat suprachiasmatic nucleus. *J Physiol* 2009;587(Pt 8):1727–1737.
 68. Zhao Y, Wang H, Xian M. Cysteine-activated hydrogen sulfide (H_2S) donors. *J Am Chem Soc* 2011;133(1):15–17.
 69. Qu K, Chen CP, Halliwell B, Moore PK, Wong PT-H. Hydrogen sulfide is a mediator of cerebral ischemic damage. *Stroke* 2006;37(3):889–893.
 70. Wemmie JA, Askwith CC, Lamani E, Cassell MD, Freeman JH Jr, Welsh MJ. Acid-sensing ion channel 1 is localized in brain regions with high synaptic density and contributes to fear conditioning. *J Neurosci* 2003;23(13):5496–5502.
 71. Kumar V, Prasad B, Patilea G, et al. Quantitative transporter proteomics by liquid chromatography with tandem mass spectrometry: addressing methodologic issues of plasma membrane isolation and expression-activity relationship. *Drug Metab Dispos* 2015;43(2):284–288.
 72. Bononi A, Pinton P. Study of PTEN subcellular localization. *Methods* 2015;77:92–103.
 73. Jiang L, Wang Y, Su C, et al. Epithelial sodium channel is involved in H_2S -induced acute pulmonary edema. *Inhal Toxicol* 2015;27(12):613–620.
 74. Duan B, Liu DS, Huang Y, et al. PI_3 -kinase/Akt pathway-regulated membrane insertion of acid-sensing ion channel 1a underlies BDNF-induced pain hypersensitivity. *J Neurosci* 2012;32(18):6351–6363.
 75. Widmann C, Gibson S, Jarpe MB, Johnson GL. Mitogen-activated protein kinase: conservation of a three-kinase module from yeast to human. *Physiol Rev* 1999;79(1):143–180.
 76. Chung HS, Park SR, Choi EK, et al. Role of sphingomyelin-MAPKs pathway in heat-induced apoptosis. *Exp Mol Med* 2003;35(3):181–188.
 77. Wu PK, Park JI. MEK1/2 inhibitors: molecular activity and resistance mechanisms. *Semin Oncol* 2015;42(6):849–862.
 78. Szabo C, Papapetropoulos A. International Union of Basic and Clinical Pharmacology. GII: pharmacological modulation of H_2S levels: H_2S donors and H_2S biosynthesis inhibitors. *Pharmacol Rev* 2017;69(4):497–564.
 79. Koike S, Kawamura K, Kimura Y, Shibuya N, Kimura H, Ogasawara Y. Analysis of endogenous H_2S and H_2S_n in mouse brain by high-performance liquid chromatography with fluorescence and tandem mass spectrometric detection. *Free Radic Biol Med* 2017;113:355–362.
 80. Li L, Whiteman M, Guan YY, et al. Characterization of a novel, water-soluble hydrogen sulfide-releasing molecule (GYY4137): new insights into the biology of hydrogen sulfide. *Circulation* 2008;117(18):2351–2360.
 81. Kimura Y, Kimura H. Hydrogen sulfide protects neurons from oxidative stress. *FASEB J* 2004;18(10):1165–1167.
 82. Whiteman M, Cheung NS, Zhu YZ, et al. Hydrogen sulphide: a novel inhibitor of hypochlorous acid-mediated oxidative damage in the brain? *Biochem Biophys Res Commun* 2005;326(4):794–798.
 83. Cheung NS, Peng ZF, Chen MJ, Moore PK, Whiteman M. Hydrogen sulfide induced neuronal death occurs via glutamate receptor and is associated with calpain activation and lysosomal rupture in mouse primary cortical neurons. *Neuropharmacology* 2007;53(4):505–514.
 84. Zhang J, Chen S, Liu H, et al. Hydrogen sulfide prevents hydrogen peroxide-induced activation of epithelial sodium channel through a PTEN/ $PI(3,4,5)P_3$ dependent pathway. *PLoS One* 2013;8(5):e64304.
 85. Wang Q, Song B, Jiang S, et al. Hydrogen sulfide prevents advanced glycation end-products induced activation of the

- epithelial sodium channel. *Oxid Med Cell Longev* 2015;2015:976848.
86. Jiang L, Wang J, Su C, et al. α -ENaC, a therapeutic target of dexamethasone on hydrogen sulfide induced acute pulmonary edema. *Environ Toxicol Pharmacol* 2014;38(2):616–624.
 87. Aroca A, Benito JM, Gotor C, Romero LC. Persulfidation proteome reveals the regulation of protein function by hydrogen sulfide in diverse biological processes in Arabidopsis. *J Exp Bot* 2017;68(17):4915–4927.
 88. Kimura H. Hydrogen sulfide and polysulfides as signaling molecules. *Proc Jpn Acad Ser B Phys Biol Sci* 2015;91(4):131–159.
 89. Whiteman M, Li L, Kostetski I, et al. Evidence for the formation of a novel nitrosothiol from the gaseous mediators nitric oxide and hydrogen sulphide. *Biochem Biophys Res Commun* 2006;343(1):303–310.
 90. Zhang D, Du J, Tang C, Huang Y, Jin H. H₂S-induced sulfhydrylation: biological function and detection methodology. *Front Pharmacol* 2017;8:608.
 91. Kimura Y, Mikami Y, Osumi K, Tsugane M, Oka J, Kimura H. Polysulfides are possible H₂S-derived signaling molecules in rat brain. *FASEB J* 2013;27(6):2451–2457.
 92. Kimura H. Hydrogen sulfide signalling in the CNS - comparison with NO. *Br J Pharmacol* 2020;177(22):5031–5045.
 93. Mishanina TV, Libiad M, Banerjee R. Biogenesis of reactive sulfur species for signaling by hydrogen sulfide oxidation pathways. *Nat Chem Biol* 2015;11(7):457–464.
 94. Zha X-m, Wang R, Collier DM, Snyder PM, Wemmie JA, Welsh M. Oxidant regulated inter-subunit disulfide bond formation between ASIC1a subunits. 2009;106(9):3573–3578.
 95. Beattie EC, Carroll RC, Yu X, et al. Regulation of AMPA receptor endocytosis by a signaling mechanism shared with LTD. *Nat Neurosci* 2000;3(12):1291–1300.
 96. Zeng W-Z, Liu D-S, Duan B, et al. Molecular mechanism of constitutive endocytosis of acid-sensing ion channel 1a and its protective function in acidosis-induced neuronal death. *J Neurosci* 2013;33(16):7066–7078.
 97. Zhou YM, Wu L, Wei S, et al. Enhancement of acid-sensing ion channel activity by prostaglandin E2 in rat dorsal root ganglion neurons. *Brain Res* 2019;1724:146442.
 98. Leonard AS, Yermolaieva O, Hruska-Hageman A, et al. cAMP-dependent protein kinase phosphorylation of the acid-sensing ion channel-1 regulates its binding to the protein interacting with C-kinase-1. *Proc Natl Acad Sci USA* 2003;100(4):2029–2034.
 99. Zhang L, Leng T-D, Yang T, Li J, Xiong Z-G. Protein kinase C regulates ASIC1a protein expression and channel function via NF- κ B signaling pathway. *Mol Neurobiol* 2020;57(11):4754–4766.
 100. Wu BM, Bargaineer J, Zhang L, Yang T, Xiong ZG, Leng TD. Upregulation of acid sensing ion channel 1a (ASIC1a) by hydrogen peroxide through the JNK pathway. *Acta Pharmacol Sin* 2020. doi: 10.1038/s41401-020-00559-3.
 101. Chen B, Liu J, Ho T, Ding X, Mo Y. ERK-mediated NF- κ B activation through ASIC1 in response to acidosis. *Oncogenesis* 2016;5(12):e279.
 102. Wang X, Chen Q, Xing D. Focal adhesion kinase activates NF- κ B via the ERK1/2 and p38 MAPK pathways in amyloid- β 25–35-induced apoptosis in PC12 cells. *J Alzheimer's Dis* 2012;32(1):77–94.
 103. Dai L, Qian Y, Zhou J, Zhu C, Jin L, Li S. Hydrogen sulfide inhibited L-type calcium channels (CaV1.2) via up-regulation of the channel sulfhydration in vascular smooth muscle cells. *Eur J Pharmacol* 2019;858:172455.
 104. Yong QC, Lee SW, Foo CS, Neo KL, Chen X, Bian JS. Endogenous hydrogen sulphide mediates cardioprotection induced by ischemic postconditioning. *Am J Physiol Heart Circ Physiol* 2008;295(3):H1330–H1340.
 105. Li L, Rose P, Moore PK. Hydrogen sulfide and cell signaling. *Annu Rev Pharmacol Toxicol* 2011;51(1):169–187.
 106. Andreadou I, Schulz R, Papapetropoulos A, et al. The role of mitochondrial reactive oxygen species, NO and H₂S in ischemia/reperfusion injury and cardioprotection. *J Cell Mol Med* 2020;24(12):6510–6522.
 107. Panthi S, Manandhar S, Gautam K. Hydrogen sulfide, nitric oxide, and neurodegenerative disorders. *Transl Neurodegener* 2018;7:3.
 108. Sun WH, Liu F, Chen Y, Zhu YC. Hydrogen sulfide decreases the levels of ROS by inhibiting mitochondrial complex IV and increasing SOD activities in cardiomyocytes under ischemia/reperfusion. *Biochem Biophys Res Commun* 2012;421(2):164–169.
 109. Papapetropoulos A, Pyriochou A, Altaany Z, et al. Hydrogen sulfide is an endogenous stimulator of angiogenesis. *Proc Natl Acad Sci USA* 2009;106(51):21972–21977.
 110. Yang G, Cao K, Wu L, Wang R. Cystathionine gamma-lyase overexpression inhibits cell proliferation via a H₂S-dependent modulation of ERK1/2 phosphorylation and p21Cip/WAK-1. *J Biol Chem* 2004;279(47):49199–49205.
 111. Mango D, Nisticò R. Role of ASIC1a in A β -induced synaptic alterations in the hippocampus. *Pharmacol Res* 2018;131:61–65.
 112. Gonzales EB, Sumien N. Acidity and acid-sensing ion channels in the normal and Alzheimer's disease brain. *J Alzheimer's Dis* 2017;57(4):1137–1144.
 113. Ettaiche M, Guy N, Hofman P, Lazdunski M, Waldmann R. Acid-sensing ion channel 2 is important for retinal function and protects against light-induced retinal degeneration. *J Neurosci* 2004;24(5):1005–1012.
 114. Han Y, Qin J, Chang X, Yang Z, Du J. Hydrogen sulfide and carbon monoxide are in synergy with each other in the pathogenesis of recurrent febrile seizures. *Cell Mol Neurobiol* 2006;26(1):101–107.
 115. Du J, Jin H, Yang L. Role of hydrogen sulfide in retinal diseases. *Front Pharmacol* 2017;8:588.
 116. Zhan J-Q, Zheng L-L, Chen H-B, et al. Hydrogen sulfide reverses aging-associated amygdalar synaptic plasticity and fear memory deficits in rats. *Front Neurosci* 2018;12:390.
 117. He F-Q, Qiu B-Y, Zhang X-H, et al. Tetrandrine attenuates spatial memory impairment and hippocampal neuroinflammation via inhibiting NF- κ B activation in a rat model of Alzheimer's disease induced by amyloid- β (1–42). *Brain Res* 2011;1384:89–96.

Supplementary Figures for "Hydrogen sulfide upregulates acid-sensing ion channels *via* the MAPK-Erk1/2 signaling pathway"

Zhong Peng, Stephan Kellenberger

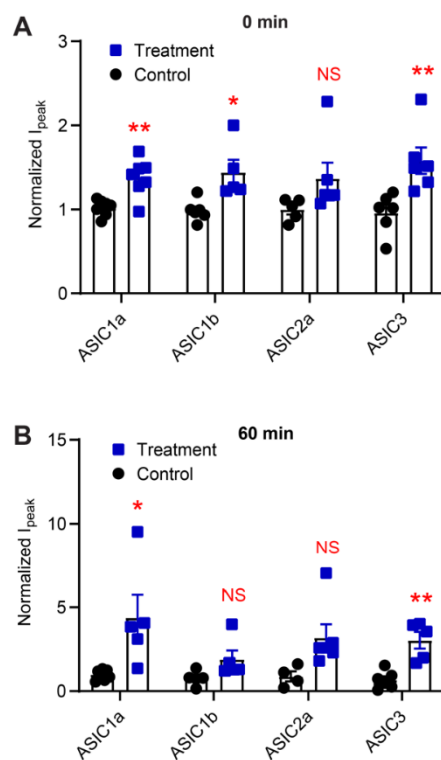


Figure S1. Peak current amplitudes of homomeric ASIC currents immediately after and 60 min after NaHS exposure. **A**, Normalized peak current amplitudes of different ASIC isoforms expressed in CHO cells immediately after a 40-s exposure to 1mM NaHS (Treatment, blue) or to a control solution (Control, black), $n=5-7$. **B**, Same experiment as in A, but at time point 60min after NaHS exposure. In all experiments, the currents were normalized to the amplitudes measured before NaHS (or control) exposure (at -3 and -6 min). *, $p<0.05$; **, $p<0.01$, comparison with the corresponding control experiments, Multiple Mann-Whitney tests.

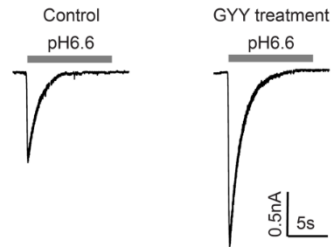


Figure S3. Typical acid-induced current traces in cultured hypothalamus neurons. Representative current traces in cultured hypothalamus neurons induced by pH6.6 with or without 10uM GYY4137 treatment as indicated, recorded with whole-cell patch-clamp at -60 mV.

3.2 Project 2: Circadian expression of ASIC1a in hypothalamus

Prepared manuscript for publication: Circadian expression of ASIC1a regulates TRH *via* the Akt-mTOR pathway in mouse hypothalamus and contributes to body temperature control

Authors: Zhong Peng, Panos G. Ziros, Tomaz Martini, Urs Albrecht, Gerasimos P. Sykiotis, Stephan Kellenberger

Abstract: The body temperature of mammals has a circadian rhythm, which is mainly regulated by the Hypothalamic-Pituitary-Thyroid (HPT) axis. Acid-sensing ion channels (ASICs) are neuronal voltage-insensitive Na⁺ channels activated by extracellular protons. ASICs are involved in many physiological and pathological processes, including fear conditioning, pain sensation and neurodegeneration. We characterize here the regulation of the body temperature by ASIC1a. We show that in WT mice under a normal light/dark cycle, the expression of ASIC1a in the hypothalamus has a circadian rhythm. Global deletion of ASIC1a changed the amplitude of the daily rhythm of body temperature. RNA sequencing indicated that the deletion of ASIC1a changed in the hypothalamus the expression of only nine functional genes at night, among them several components of the HPT axis, and of no functional genes during daytime. Activation of ASIC1a in cultured neurons upregulated the expression of thyrotropin-releasing hormone and Prolactin mRNA and activates the Akt-mTOR pathway. Our study demonstrates that ASIC1a regulates the expression of TRH to control body temperature, and it identifies the involved signaling mechanism. Since ASIC1a is abundantly expressed in the pituitary and hypothalamus, dysfunction of ASIC1a may be at the origin of other metabolic disorders.

My contribution to this manuscript:

The experiments of body temperature relative hormone genes expression in pituitary were carried out by Panos G. Ziros, technician in Dr. Gerasimos P. Sykiotis's laboratory, Lausanne University Hospital. The wheel-running behavior experiment was performed by Tomaz Martini, PhD student in Prof. Urs Albrecht's laboratory, University of Fribourg. I made most of the RT-PCR experiments, all of the patch-clamp and Western Blot experiments. I analyzed a large amount of experiments, made all the figures and wrote a first draft of the manuscript.

Circadian expression of ASIC1a regulates TRH via the Akt-mTOR pathway in mouse hypothalamus and contributes to body temperature control

Zhong Peng ¹, Panos G. Ziros ², Tomaz Martini ³, Urs Albrecht ³, Gerasimos P. Sykiotis ²,
Stephan Kellenberger ^{1,*}

¹ *Department of biomedical Sciences, University of Lausanne, Rue du Bugnon 27, 1011 Lausanne, Switzerland*

² *Service of Endocrinology, Diabetology and Metabolism, Lausanne University Hospital and University of Lausanne, CH-1011 Lausanne, Switzerland*

³ *Department of Biology/Unit of Biochemistry, Faculty of Sciences, University of Fribourg, Chemin du Musée 5, CH-1700, Fribourg, Switzerland*

** Corresponding author:*

Stephan Kellenberger, Department of biomedical Sciences, University of Lausanne, Rue du Bugnon 27, CH-1011 Lausanne, Switzerland, e-mail: stephan.kellenberger@unil.ch

ABSTRACT

The body temperature of mammals has a circadian rhythm, which is mainly regulated by the Hypothalamic-Pituitary-Thyroid (HPT) axis. Acid-sensing ion channels (ASICs) are neuronal voltage-insensitive Na⁺ channels activated by extracellular protons. ASICs are involved in many physiological and pathological processes, including fear conditioning, pain sensation and neurodegeneration. We characterize here the regulation of the body temperature by ASIC1a. We show that in WT mice under a normal light/dark cycle, the expression of ASIC1a in the hypothalamus has a circadian rhythm. Global deletion of ASIC1a changed the amplitude of the daily rhythm of body temperature. RNA sequencing indicated that the deletion of ASIC1a changed in the hypothalamus the expression of only nine functional genes at night, among them several components of the HPT axis, and of no functional genes during daytime. Activation of ASIC1a in cultured neurons upregulated the expression of thyrotropin-releasing hormone and Prolactin mRNA and activates the Akt-mTOR pathway. Our study demonstrates that ASIC1a regulates the expression of TRH to control body temperature, and it identifies the involved signaling mechanism. Since ASIC1a is abundantly expressed in the pituitary and hypothalamus, dysfunction of ASIC1a may be at the origin of other metabolic disorders.

Keywords: ASIC; Circadian rhythm; Hypothalamus; Body temperature

INTRODUCTION

Acid-sensing ion channels (ASICs) are non-voltage-gated Na^+ channels of the nervous system that are activated by extracellular acidification (Waldmann et al., 1997; Wemmie et al., 2013). Four genes encode at least six ASIC subunits (ASIC1a, -1b, -2a, -2b, -3 and -4), which form homotrimeric or heterotrimeric channel complexes (Wemmie et al., 2013). ASICs are Na^+ -selective (Yang and Palmer, 2014), and homomeric ASIC1a has in addition a small Ca^{2+} permeability (Bassler et al., 2001; Boillat et al., 2014; Waldmann et al., 1997). The activation of ASICs induces action potentials (APs) and leads to the excitation of neurons (Baron et al., 2002; Deval et al., 2003; Vukicevic and Kellenberger, 2004). ASIC1a, -2a and -2b are widely expressed in the nervous system. Highest levels in the brain are found in the main olfactory bulb, cerebral cortex, hippocampus, cerebellum, basolateral amygdaloid nuclei and the hypothalamus (Kellenberger and Schild, 2015; Waldmann et al., 1997; Wemmie et al., 2013). ASIC1a is distributed throughout the central and peripheral nervous systems, participating in synaptic transmission and plasticity (Du et al., 2014; Wemmie et al., 2002; Wu et al., 2013). Dysfunction of ASIC1a is associated with the development of diverse neurological diseases, including epileptic seizures (Ziemann et al., 2008), neurodegeneration after ischemic stroke (Duan et al., 2011; Gao et al., 2005; Wang and Xu, 2011; Xiong et al., 2004), and neurodegenerative diseases (Friese et al., 2007; Vergo et al., 2011). ASIC3 is widely expressed in peripheral sensory neurons and to some extent in non-neuronal tissues. It is implicated in multimodal sensory perception (Li and Xu, 2011; Wemmie et al., 2013), including nociception (Chen et al., 2002; Deval et al., 2008; Sluka et al., 2003), mechanosensation (Price et al., 2001), and chemosensation (Birdsong et al., 2010; Sutherland et al., 2001).

Activation of ASICs by extracellular acidification induces rapid channel opening, followed by desensitization. The Texas coral snake toxin Mit-Toxin- α/β (MitTx) induces a sustained activation of ASICs (Bohlen et al., 2011). Besides the excitation of neurons, ASICs also regulate intercellular signaling pathways. Activation of ASIC1a and the subsequent Ca^{2+} influx induces the activation (phosphorylation) of Ca^{2+} /calmodulin-dependent protein kinase II (CaMKII) and extracellular signal-regulated protein kinases (ERKs) (Yu et al., 2018). Acid stimulation recruits the serine/threonine kinase receptor interaction protein 1 (RIP1) to the ASIC1a C-terminus, causing RIP1 phosphorylation and subsequent neuronal death, and this effect is independent of the ion-conducting function of ASIC1a (Wang et al., 2015). Activation of ASICs also regulates ROS generation and activation of the Akt/NF- κ B associated signaling pathways leading to cell invasion and metastasis (Yang et al., 2019).

Circadian rhythms are internal manifestations of the solar day that permit adaptations to

predictable environmental temporal changes (Walker et al., 2020). The circadian timing system comprises peripheral oscillators located in most tissues of the body and a central pacemaker located in the suprachiasmatic nucleus (SCN) of the hypothalamus (Hastings et al., 2018; Rana and Mahmood, 2010). Various behaviors and physiological processes are regulated by the circadian clock, including body temperature (Filipski et al., 2002; Van Cauter et al., 1993), hormone secretion (Czeisler and Klerman, 1999), energy metabolism (Yang et al., 2006), sleep-wake cycles (Goichot et al., 1998) and blood pressure (Douma and Gumz, 2018). The circadian clock is constituted by three conceptual components, the intrinsic pacemaker, the input and the output pathways. The SCN acts as the circadian rhythm master pacemaker, transmits the generated rhythm signals to the periphery through the output system, and synchronizes the endogenous circadian rhythm of the peripheral organs (Astiz et al., 2019; Dibner et al., 2010; Schibler et al., 2003). Circadian rhythms are synchronized with the daily adjustments in the timing of the SCN, following the exposure to stimuli that signal the time of day; these stimuli are named *zeitgebers* (Zee et al., 2013). Light is the most important and potent *zeitgeber* for the SCN, and feeding cycles are the dominant *zeitgeber* for many peripheral clocks (Challet et al., 2003; Damiola et al., 2000). In mammals, the hypothalamus senses the temperature of blood flowing through it and controls the balance of heat production and of heat loss. Heat production depends on the Hypothalamic-Pituitary-Thyroid axis (HPT axis), which is under the control of the SCN (Brown et al., 2002). Disruption of the circadian rhythm of body temperature has been observed in many diseases of the endocrine system (Bargi-Souza et al., 2019).

Here, we found that the expression of ASIC1a has a circadian rhythm in the mouse hypothalamus, and that global deletion of ASIC1a changes amplitude of the circadian rhythm of body temperature. Activation of ASIC1a regulates the expression of thyrotropin-releasing hormone (TRH), by a mechanism that involves the Akt-mTOR pathway, to control the body temperature *via* the HPT axis.

MATERIALS AND METHODS

Ethical approval

All animal handling procedures were done in accordance with institutional and Swiss guidelines and approved by the authorities of the Canton of Vaud. All animal experiments respected the Swiss Animal Welfare legislation and were reviewed by the Veterinary service of the Canton de Vaud (SR 455 Animal Welfare Act; Project License N° 1750.4 licensed to Dr. Stephan Kellenberger).

All animal experiments were conducted in accordance with the regulations of the Norwegian

State Commission for Laboratory Animals and the Swiss Animal Protection Act, which are consistent with the European Convention for the Protection of Vertebrate Animals used for Experimental and Other Scientific Purposes and Council of Europe (ETS 123), and with approval from the AAALAC International accredited Animal Care and Use Program at University of Bergen and the Cantonal Veterinary Office of Canton de Vaud, Switzerland.

Analysis of wheel-running activity

WT and ASIC1a^{-/-} male mice were generated by breeding of heterozygous mice whose genetic background was C57BL/6. ASIC1a^{-/-} mice (Wemmie et al., 2002) were provided by Dr. John Wemmie, University of Iowa. At 2–3 months of age, the mice were housed in cages with unlimited access to a running wheel (Actimetrics, Wilmette, IL, USA) and entrained to a 12 h light (~ 200 lux), 12 h dark (LD 12:12) cycle in a light-proof ventilated cabinet for 10 days prior to the start of experiments. Their running activity under the LD 12:12 cycle was recorded over the next 7 days. Running-wheel activity was continuously recorded for each animal by using a digital system that registers wheel revolutions and stored at 5-min intervals for further analysis. Animals were then transferred in constant darkness (DD) and recordings under free-running conditions were used to define the internal period length, the circadian daily overall activity and the percentage of activity during subjective day.

The phase-response curve for light-induced phase shifts was defined for WT and ASIC1a^{-/-} mice, using an Aschoff type 2 procedure. Briefly, mice were entrained to a LD 12:12 cycle for 2 weeks before release in DD. On the first night after the end of LD or on the first subjective day in DD, a light pulse of 30 minutes was administered at *zeitgeber* time (ZT) 14 or 22 (ZT 0 is the beginning of subjective day and ZT12 is the beginning of the subjective night under DD) and the animal was then kept in DD for 10 days. Phase shifts are the difference, on the first day after the pulse, between regression lines fitted through activity onsets before and after the pulse. All data were analyzed using the Clocklab program (Actimetrics, Wilmette, IL, USA). Chi² periodogram analysis was used for measurement of the free-running period.

Telemetry device implantation

Telemetry device implantation was performed in the Cardiovascular Assessment Facility (Centre Hospitalier Universitaire Vaudois) on 12 mice per group. Electrodes (HD-S02, Data Sciences International) were placed in the heart axis of the anesthetized mice. About 20 minutes before anesthesia, buprenorphine chlorhydrate (0.1 mg/kg) was injected as analgesia. The mouse was anesthetized by isoflurane inhalation and placed on a warming pad (37–38°C) for

maintenance of body temperature and maintained under anesthesia *via* a nose cone (1.5-2% in O₂, 1L/min). Ocular gel was applied to hydrate the cornea during the surgical procedure. The skin of the mouse was shaved and disinfected with hydro-alcoholic solution at the level of the abdomen. A small incision was made in the skin and the peritoneal wall just large enough to allow the transmitter to enter the cavity. The flexible leads were tunneled under the skin towards the right pectoral muscle and the last ribs at about 1cm of the xiphoid appendix. The peritoneal and skin incisions were then sutured and disinfected. The supply of anesthetic gas was stopped and the animal was returned to its cage placed on a heating surface for complete wake. After surgery, mice received ibuprofen 20mg/mL in tap water for 4 days. After 10 days of recovery from surgery, the body temperature and the activity of the mice was measured in the cage in animal facility. The sensor contained a three-axis accelerometer used by the Ponemah software (Data Science International) to report activity measurements. The body temperature and activity were measured in 3 groups of mice (3-4 mice/group) per genotype for 4 days. Average values of the daily cycle were then calculated from the 4-day period.

Mouse neuron cultures

36 pregnant mice and 216 mouse embryos were used in these experiments to obtain cells for hippocampus, hypothalamus and cortical neuron culture; 40 postnatal day 2 mice were used in these experiments to obtain cells for suprachiasmatic nucleus (SCN) culture. Mice used in the experiments were kept in the departmental animal house and maintained on a 12 h light/dark cycle (7:00-19:00 light on, GMT+1). with food and water *ad libitum*. Hippocampus, hypothalamus and cortical neuron culture was performed as previously described (Alijevic et al., 2020a). Briefly, day 14-15 pregnant mice were sacrificed by exposure to CO₂, the embryos were killed, and the cortex and hypothalamus of the E14-15 embryos were dissected in ice-cold HBSS medium (ThermoFisher). The SCN neuron culture was performed as previously described (Ren and Miller, 2003). Briefly, postnatal day 2 mice were decapitated. Rapidly, the eyes were removed, the skull opened, and the optic nerve between the olfactory bulbs and the hemispheres was cut. The brain was placed into a dish filled with ice-cold HBSS, thicker sections (about 400µm) of the brain were cut off to allow isolation of the desired SCN section. Brain tissues were chopped into small pieces (~1 mm) and incubated at 37°C for 18 min in 0.05% Trypsin-EDTA (ThermoFisher), then washed three times in Neurobasal medium (ThermoFisher) containing 10 % FBS, and dissociated into single cells. After a 5-min centrifugation at 1000 rpm, neurons were re-suspended in Neurobasal/FBS medium. For hypothalamus neuron, neurons were seeded at 50'000 cells /dish on 35-mm Petri dishes (for

qRT-PCR assay) or containing five 10-mm diameter glass coverslips that were all previously coated with poly-L-lysine (functional analysis). For Western blot analysis, cortex neurons were seeded at 150'000 cells /dish on 35-mm Petri dishes previously coated with poly-L-lysine. The medium was replaced after 12h by Neurobasal Medium Electro (ThermoFisher) containing the B27 serum-free supplement, the GlutaMAX supplement (ThermoFisher) and Gentamicin (10 µg/ml final concentration, ThermoFisher). Neuronal cultures were maintained at 37°C in a humidified atmosphere of 5% (v/v) CO₂ in air, and every 2-3 days, half of the medium was replaced with fresh plating medium. Patch-clamp and biochemical assay experiments of neurons were carried out after at least 12 days after seeding.

Cultured neuron electrophysiological recording

Electrophysiological recordings were done using the whole-cell patch-clamp technique in voltage- and current-clamp mode with an EPC10 patch-clamp amplifier (HEKA Elektronik-Harvard Bioscience) as previously described (Alijevic et al., 2020a). Solution change were carried out using computer-controlled electrovalves (cF-8VS) and the MPRE8 perfusion head (Cell MicroControls, Norfolk, VA). Data were acquired with Patchmaster software and analysis of the currents was carried out with Fitmaster (HEKA Elektronik-Harvard Bioscience). The sampling interval and the low-pass filtering were set to 50 µs and to 3 kHz, respectively.

The pipette solution contained, in mM, 120 KCl, 30 NaCl, 10 HEPES, 5 EGTA, 2 MgATP, 1 MgCl₂ and 0.5 CaCl₂, adjusted to pH7.2 with Tris-base. The osmolarity of the pipette solution was 280–300 mOsm (Advanced Instrument Osmometer, Norwood, MA, USA). The extracellular Tyrode solution contained, in mM, 140 NaCl, 5 KCl, 10 glucose, 2 CaCl₂, and 1 MgCl₂, buffered to various pH values with either 10 mM HEPES (pH > 6.0) or 10 mM 2-(N-morpholino)-ethanesulfonic acid (MES; pH6.0). The osmolarity of the extracellular solution was 310–320 mOsm. The pH of the solutions was controlled on the day of the experiment and adjusted if necessary. All recordings were performed at room temperature (23 ± 2 °C).

Brain slice preparation and recording of spontaneous firing

9–10-week-old mice were deeply anesthetized at ZT1 or ZT13 with isoflurane. The mice were killed by decapitation, and the eyes were rapidly removed. The mouse brain was quickly removed and immediately placed in well-oxygenated (95% O₂/5% CO₂, v/v) ice-cold sucrose-based dissection solution containing (in mM): 110 sucrose, 60 NaCl, 3 KCl, 1.25 NaH₂PO₄, 28 NaHCO₃, 7 MgCl₂, 0.5 CaCl₂, 5 D-glucose. pH was adjusted to 7.4 using either NaOH or HCl. Three coronal hypothalamus slices (250 µm thick) containing the paraventricular nucleus (PVH)

were obtained using a 7000smz-2 Vibrotome (Campden Instruments). Brain slices were incubated at room temperature in oxygenated aCSF containing (in mM): 120 NaCl, 2.5 KCl, 1 NaH₂PO₄, 26.2 NaHCO₃, 1.3 MgCl₂, 2.5 CaCl₂, 11 D-glucose. pH was adjusted to 7.4 using either NaOH or HCl. Brain slices were incubated in oxygenated aCSF at room temperature for a least 1 h before being transferred to a recording chamber. The slices were bathed in oxygenated ACSF (32°C–34°C) at a flow rate of approximately 2 ml/min. The placement of brain slices was observed using an infrared–differential interference contrast video monitor. Loose patch-clamp recordings were obtained using borosilicate glass micropipettes (2–3 MΩ) containing aCSF as the pipette solution.

Seals were obtained with gentle or no suction to produce a loose patch seal with a resistance was 10–30 MΩ. Extracellular currents from spontaneous APs were recorded in voltage clamp mode at 0mV holding potential. Recordings lasted from 3min for cells firing regularly at high frequency up to 5min for cells that were silent or firing at low frequency. Currents were amplified using an Axon 200B amplifier and digitized at 250 kHz using a Digidata 1440A interface (Molecular Devices). Signals were filtered at 5 kHz and analyzed offline with pCLAMP programs (Axon Instruments).

Protein extraction and biochemical assay

374 mice were used in these experiments to collect the organs. Mice were sacrificed by cervical dislocation immediately before removal of the organs. Mouse tissues were lysed in cold RIPA buffer (20 mM Tris-HCl, 150 mM NaCl, 2 mM EDTA, 1% NP-40 (v/v), 1% sodium deoxycholate (w/v), pH7.5), containing 1:100 diluted protease and phosphatase inhibitor cocktail (Sigma Aldrich), with shaking for 20 minutes on ice. The mixture was then centrifuged at $\sim 14,000 \times g$ for 15 minutes at 4 °C, the supernatant was collected and the protein concentration was measured using the BCA Protein Assay Kit (23227, ThermoFisher), all samples were diluted to 1mg protein/mL. The samples in 1X sample loading buffer (0.3M Sucrose, 2% SDS, 2.5mM EDTA, 60mM Tris pH8.8, 0.05% (w/v) bromophenol blue, 25mM DTT) were heated at 95 °C for 10 min.

Western Blot analysis was carried out as previously described (Vaithia et al., 2019). Briefly, 10μl protein samples were separated on 10% SDS-PAGE gels at 100V, then transferred to 0.2μM nitrocellulose membranes (Amersham Biosciences) at 4°C, 100V for 2 h. After the transfer, the blot was blocked with 5% milk (in TBST buffer, Tris-buffered saline with 0.1% Tween 20 solution) for 1 h at room temperature, followed by 2% BSA in TBST buffer at room temperature. The blot was incubated at 4°C overnight with the primary antibodies, followed,

after washing, by the HRP-labeled secondary antibody for 2 h at room temperature. The signals were detected using the Fusion SOLO chemiluminescence system (Vilber Lourmat, Marne-la-Vallée, France) using SuperSignal™ West Femto Maximum Sensitivity Substrate (Thermo Scientific). The following antibodies were used: anti-ASIC1 (1:1000, rabbit, kindly provided by Dr. John Wemmie) (Wemmie et al., 2002), Anti-Actin (1:1000, rabbit; A2066, Sigma Aldrich) (Di Yorio et al., 2008), anti-Bmal1 (1:1000, rabbit) (Langmesser et al., 2008), anti-Akt (1:1000, rabbit; H-136, Santa Cruz) (Hu et al., 2012), anti-p-Akt (Ser473; 1:1000, mouse; 4051, Cell Signaling) (Yang et al., 2017), anti-mTOR (1:1000, rabbit; 2972, Cell Signaling) (Muta et al., 2015), anti-p-mTOR (Ser2448; 1:1000, rabbit; 5536, Cell Signaling) (Bravo-San Pedro et al., 2019), Goat anti-rabbit IgG (1:2000; B7401, Sigma). Donkey anti-rabbit IgG (1:2000; NA934VS, GE healthcare). Quantification was done using the ImageJ program. β -actin was used as the protein control, to which the signals were normalized.

RNA extraction and gene expression assay

Mouse tissues were lysed, and RNA was isolated according to the manufacturer's instructions from the RNeasy™ Total RNA Isolation Kit (AM1931, ThermoFisher) and stored at -80°C. Briefly, tissues were lysed in lysis solution and were then neutralized, and samples were loaded onto a silica filter for RNA binding on the filter. Samples were then washed thoroughly and eluted by DEPC-treated water. RNA was quantified by spectrophotometry and the purity was assessed by the absorbance ratios of 260:280 and 260:230 nm. A ratio of 260:280 \geq 1.8 and 260:230=1.9-2.2 was considered acceptable for quantitative real-time polymerase chain reaction (qRT-PCR). cDNA was synthesized using the PrimeScript™ RT Master Mix (RR036A, TaKaRa) kit. Real-time PCR analyses were carried out with triplicates of each sample cDNA on QuantStudio 12K Real-Time PCR System (Applied Biosystems, Inc.) with a SYBR Green Master Mix (4309155, ThermoFisher) under the following conditions: 3 min at 95°C, followed by 40 cycles of 10 s at 95°C and 25 s at 60°C. The primers used are shown in **Supplemental Table 1**. Gene-specific amplification was confirmed by melt curve analysis. Expression levels were calculated relative to *GAPDH* (brain tissue), *Ppia* (Peptidylprolyl isomerase A, pituitary) or *HPRT* (Hypoxanthine Guanine Phosphoribosyltransferase, thyroid gland) based on the efficiency- Δ Ct method.

Supplemental Table 1. Real-time PCR primers.

Gene	Forward primer	Reverse primer
<i>Fshb</i>	AGGGAGGAAAGGAAAGTGG	AGCCAGCTTCATCAGCATTT

<i>Gh</i>	ACGCGCTGCTCAAAA ACTAT	GCTAGAAGGCACAGCTGCTT
<i>Gpx2</i>	GTGCTGATTGAGAATGTGGC	AGGATGCTCGTTCTGCCCA
<i>Prl</i>	CTCAGGCCATCTTGGAGAAG	TCGGAGAGAAGTCTGGCAGT
<i>Tshb</i>	TCAACACCACCATCTGTGCT	TTGCCACACTTGCAGCTTAC
<i>ASIC1a</i>	CCTGCTCAACAACAGGTATG	CTCGTCCTGACTGTGGATCT
<i>mGAPDH</i>	AACGGGAAGCCCATCACC	CATACTCAGCACCGGCCTCA
<i>mBMAL1</i>	TGACCCTCATGGAAGGTTAGAA	GGACATTGCATTGCATGTTGG
<i>Ppia</i>	AGCACTGGGGAGAAAGGATT	CATGCCTTCTTTCACCTTCC
<i>Trh</i>	TCCTGGATCACAAAACGCCA	CTTGTCTTGGTTGGCACGTC
<i>Cers5</i>	GACTGCTTCCAAAGCCTTGAG	GCAGTTGGCACCATTGCTAG
<i>Sgk1</i>	GGG TGC CAA GGA TGA CTT TA	CTC GGT AAA CTC GGG ATC AA
<i>Ddit4</i>	CAAGGCAAGAGCTGCCATAG	CCGGTACTTAGCGTCAGGG
<i>Btg2</i>	CCCCCGGTGGCTGCCTCCTAT	GGGTCGGGTGGCTCCTATCTA
	G	
<i>Nr4a1</i>	TCTGGTCCTCATCACTGATCGA	AATGCGATTCTGCAGCTCTTC
<i>Nr4a3</i>	CAGTGTCGGGATGGTTAAGGAA	CAGACGACCTCTCCTCCCTTT
<i>Arl4d</i>	GCCTCGAGGGCTGAAGACACCC	CTGAATTCGCCTTGCTGATCCGG
	CAGCTT	TGTAA
<i>Egr1</i>	GAACAACCCTATGAGCACCTGA	CGAGTCGTTTGGCTGGGATA
	C	
<i>Egr2</i>	TCAATGTCACTGCCGCTGAT	AGAAATGATCTCTGCAACCAGA
		A
<i>Egr3</i>	GATCCACCTCAAGCAAAAGG	CGGTGTGAAAGGGTGGAAAT
<i>HPRT</i>	CAGTCCCAGCGTCGTGATTA	TGGCCTCCCATCTCCTTCAT
<i>TrhR</i>	CTTCTTAAACCCCATTCCTT	TTCCTGGAAGATACAGTGCT
<i>c-fos</i>	CGAAGGGAACGGAATAAGATG	GCTGCCAAAATAAACTCCAG
<i>Fosb</i>	ACAGATCGACTTCAGGCGGA	GTTTGTGGGCCACCAGGAC
<i>Junb</i>	ATCCTGCTGGGAGCGGGGA ACT	AGAGTCGTCGTGATAGAAAGGC
	GAGGGAAG	
<i>Mtor</i>	ATT CAA TCC ATA GCC CCG TC	TGC ATC ACT CGT TCA TCC TG
<i>Pomc</i>	CATAGATGTGTGGAGCTGGTG	CATCTCCGTTGCCAGGAAACAC
<i>TshR</i>	ATCGCGGATCCGAAGTAGCCCA	GATCAGAATTCCAAGGCTGTTT
	GAGGGTCCCTTGG	GCTTATACTCTTC

RNA sequencing

Genomic RNA was extracted from hypothalamus tissue samples using the Purelink RNA minikit (12183018A; Invitrogen, ThermoFisher Scientific) following a standard protocol. RNA was quantified by measuring the absorbance at 260 nm (A₂₆₀) with a NanoDrop 8000 spectrophotometer (ThermoFisher). Purity was assessed by the absorbance ratios of 260:280 and 260:230 nm (260:280 ≥ 1.8 and 260:230 = 1.9-2.2). RNA quantity was analyzed with the Agilent 5200 Fragment Analyzer System (Agilent Technologies, Inc), using RNA quality number (RQN) as a quality indicator; RQN ≥ 8 was considered acceptable for the RNA sequencing. Reverse transcribed RNA was used for sequencing performed at the Lausanne Genomic Technologies Facility (GTF, University of Lausanne). The sequencing library preparation was performed using the Nextera DNA Library Preparation Kit (Illumina, San Diego, CA, USA) for 100-bp paired-end sequencing runs on Illumina HiSeq 2500, aiming for a 100-fold coverage.

Purity-filtered reads were adapted and quality trimmed with Cutadapt (v. 1.8, Martin 2011). Reads matching to ribosomal RNA sequences were removed with fastq_screen (v. 0.11.1). Remaining reads were further filtered for low complexity with reaper (v. 15-065, Davis et al. 2013). Reads were aligned against *Mus musculus*.GRCm38.102 genome using STAR (v. 2.5.3a, Dobin et al. 2013). The number of read counts per gene locus was summarized with htseq-count (v. 0.9.1, Anders et al. 2014) using *Mus musculus*.GRCm38.102 gene annotation. Quality of the RNA-seq data alignment was assessed using RSeQC (v. 2.3.7, Wang et al. 2012). Reads were also aligned to the *Mus musculus*.GRCm38.102 transcriptome using STAR (v. 2.5.3a, Dobin et al. 2013) and the estimation of the isoforms abundance was computed using RSEM (v. 1.2.31, Li and Dewey 2011).

Statistical analysis was performed for genes in R (R version 4.0.2). Genes with low counts were filtered out according to the rule of 1 count per million (cpm) in at least 1 sample. Library sizes were scaled using TMM normalization and log-transformed into counts per million or CPM (EdgeR package version 3.32.1; Robinson et al. 2010).

Reagents

All drugs were purchased from Sigma-Aldrich (Buchs, Switzerland) unless otherwise mentioned.

Data Analysis and statistics

Results are expressed as the mean \pm S.E.M. Statistical comparisons were performed using Student's *t*-test for comparison between two groups or for paired comparisons, and one-way ANOVA followed by Dunnett's *post-hoc* test when more than two groups were involved. Statistical tests were carried out with Graphpad Prism8 (GraphPad, San Diego).

RESULTS

ASIC1a regulates the body temperature via the Hypothalamus-pituitary-thyroid axis

The body temperature in mammals exhibits a circadian rhythm and is higher in the active phase than in the inactive phase. This rhythm depends on the central pacemaker in the SCN. We implanted a body temperature sensor into the abdominal cavity of WT and ASIC1a^{-/-} mice, and the core body temperature and spontaneous activities were monitored continuously under 12 h light/dark cycle (LD) conditions. Both WT and ASIC1a^{-/-} mice showed circadian rhythms in the body temperature (**Figure 1A**). Interestingly, the body temperature was significantly higher in WT mice during the dark period, at *zeitgeber* time (ZT)17 and ZT18. The percentage of activity was however not significantly different between WT and ASIC1a^{-/-} mice (**Figure 1B**). These results suggested that ASIC1a may regulate the circadian rhythm of body temperature that depends on endocrine regulation.

The pituitary gland regulates various body functions and plays an important role in controlling hormone levels in the body. It secretes a number of hormones that control the balance of energy and body temperature. Three months old male WT and ASIC1a^{-/-} mice were sacrificed at ZT1 (light) or ZT13 (dark), and pituitary RNA was used for qRT-PCR analysis. mRNA levels of body temperature-related hormones, the genes thyroid-stimulating hormone beta subunit (*Tshb*), growth hormone (*GH*), glutathione peroxidase 2 (*GPX2*), follicle-stimulating hormone beta subunit (*Fshb*), prolactin (*Prl*) and pro-opiomelanocortin (*Pomc*) were tested (**Figure 1C**). Expression of *Tshb* significantly increased at ZT13 in the pituitary of WT but not ASIC1a^{-/-} mice and was significantly higher in WT than in ASIC1a^{-/-} at ZT13. The expression of *Prl* was significantly decreased at ZT13 in the pituitary of WT but not ASIC1a^{-/-} mice; *Prl* levels were not different between WT and ASIC1a^{-/-} at ZT13 and at ZT1. Thyroid stimulating hormone synthesis and secretion is controlled by the thyrotropin-releasing hormone (TRH) released from the hypothalamus (Harris et al., 1978). From the mice of which the expression levels in the pituitary had been determined, the mRNA expression level of *Trh* was also assayed with qRT-PCR in the hypothalamus. Expression of *Trh* was significantly increased at ZT13 in the hypothalamus of WT but not ASIC1a^{-/-} mice, and was significantly higher in WT than in

ASIC1a^{-/-} mice at ZT13 (**Figure 1D**). TRH is secreted from the hypothalamus and activates the thyrotropin-releasing hormone receptor (TRHR) in the pituitary to stimulate synthesis of TSH. The mRNA expression level of the TRHR can also affect the synthesis of TSH (Aninye et al., 2014). The expression of *TrhR* was significantly decreased at ZT13 in the pituitary of ASIC1a^{-/-} but not WT mice, but no difference was observed between WT and ASIC1a^{-/-} at ZT13 (**Figure 1E**). In the HPT axis, TSH activates the thyroid-stimulating hormone receptor (TSHR), which acts at the thyroid to stimulate all steps of TH biosynthesis and secretion (Aghajanova et al., 2011). Expression of *TshR* was significantly decreased at ZT13 in the thyroid gland of WT but not ASIC1a^{-/-} mice, and was significantly higher in WT than in ASIC1a^{-/-} at both time points (**Figure 1F**). These results suggest that the lower body temperature of ASIC1a^{-/-} mice relative to WT at ZT17 and ZT18 may be due to the downregulation of body temperature-related hormone expression of the HPT axis.

TRH is secreted from the hypothalamus to initiate the activation of the HPT axis. Although TRH can be found throughout the brain, the neurons involved in regulating thyroid function reside almost exclusively within the paraventricular nucleus of the hypothalamus (PVH) (Koller et al., 1987). In the PVH, the neurosecretory neurons are concentrated in the medial parvocellular division (mpd) of the PVH (Luther et al., 2002). Rhythmic activity of the hypothalamus is controlled by the SCN, and SCN neurons show a synchronous daily rhythm in spontaneous firing rate (SFR) in hypothalamic slices (Meredith et al., 2006). Acute coronal hypothalamus slices were prepared from the brains of WT and ASIC1a^{-/-} mice. Single-unit activity was recorded in the mpd with the loose patch technique to measure the SFR of neurosecretory neurons during day- and nighttime (**Figure 1G, H**), suggesting higher activity at night in both groups. No significant differences were seen between mice from the two genotypes in the average SFRs at the daytime (**Figure 1I**). mpd neurons from WT mice at night had significantly increased average SFRs compared to those at their respective daytime. The SFR of WT mice was significantly higher than that of ASIC1a^{-/-} mice at night, suggesting that the deletion of ASIC1a only affects the neurosecretory neurons activity in the PVH at night, not day time.

Expression of ASIC1a in the hypothalamus has a circadian rhythm

We have shown here that deletion of ASIC1a lowers the body temperature at night, by interacting with signaling of the HPT axis. It is currently not known whether ASIC1a expression in the brain follows a circadian rhythm. Hypothalamus, SCN and hippocampus were harvested at 4-hour intervals from 3-month-old WT male mice entrained in a standard LD cycle. After

extraction of total proteins and separation by SDS-PAGE, expression of ASIC1a was determined by Western blot analysis (**Figure 2A-C**). The expression of the ASIC1a protein was significantly increased at ZT12 in hypothalamus (**Figure 2A**), significantly decreased at ZT12 in SCN (**Figure 2B**) and no circadian changes were observed in hippocampus (**Figure 2C**). The mRNA level of *ASIC1a* in the hypothalamus at ZT12 and ZT16 was significantly higher than at ZT20 (**Figure 2D**), and the level in the SCN was significantly higher at ZT0 than that at ZT16 (**Figure 2E**). The expression of ASIC1a in the hypothalamus from which the SCN had been removed was still higher at ZT12 than at ZT0 (**Supplemental Figure 1D**). These results show that ASIC1a expression has a circadian rhythm in hypothalamus but not another tested brain region, and that the rhythm of ASIC1a expression in SCN is opposite to that of other hypothalamus divisions.

In the primary feedback loop, the circadian locomotor output cycle kaput (CLOCK) and brain and muscle ARNT-like protein 1 (BMAL1) proteins form heterodimers in the cytosol of SCN neurons. The CLOCK-BMAL1 complex translocates to the nucleus and activates expression of period (*Per1*, *Per2* and *Per3*) and cryptochrome (*Cry1* and *Cry2*) genes by binding to regulatory elements of the DNA containing E-boxes (Takahashi, 2017). In WT mice under a standard LD cycle, the expression of the BMAL1 protein was significantly increased at ZT8 in hypothalamus (**Supplemental Figure 1A**), significantly decreased at ZT8 in SCN (**Supplemental Figure 1B**) and significantly increased at ZT8 in hippocampus (**Supplemental Figure 1C**). The *Bmal1* mRNA level of the hypothalamus was significantly decreased at ZT16 as compared to ZT20 (**Supplemental Figure 1E**). In the SCN, these levels were significantly higher at ZT0 and ZT4 than at ZT12 (**Supplemental Figure 1F**). The circadian expression rhythm was synchronous between ASIC1a and BMAL1 in the SCN and hypothalamus.

Expression of ASIC1a in embryonic hypothalamus neurons has a circadian rhythm

ASIC1a is abundantly expressed in the embryonic and adult mouse brain (de la Rosa et al., 2003). Activation of ASICs induces APs in cultured neurons (Alijevic et al., 2020a; Baron et al., 2002; Vukicevic and Kellenberger, 2004). To determine whether there is a circadian cycle of ASIC activity, we recorded acid-induced currents and APs in cultured neurons. The amplitude of pH6.6-induced ASIC currents was significantly different between 12h and 18h p.m. on hypothalamus neurons, while no circadian changes were found in hippocampus and cortex neurons (**Figure 3A**). Since the hypothalamus contains different types of neurons, we classified various cell types in the hypothalamus, based on their different morphologies, as types 1-4 (**Supplemental Figure 2A**). The pH6.6-induced ASIC current density showed a

circadian rhythm in types 1-3, but not in type 4. The average acid-induced current density was in all types of hypothalamus neurons significantly higher than in cortex and hippocampal neurons (**Supplemental Figure 2B**).

TRH secretion and the circadian regulation of the HPT axis are controlled by neurosecretory neurons in the hypothalamus. To separate the measured neurons into neurosecretory and non-neurosecretory neurons, an electrophysiology protocol, developed by Tasker and colleagues (Luther et al., 2002; Tasker and Dudek, 1991), was applied. To this end, the current protocols described in **Supplemental Figure 2C** are applied to current-clamped neurons, and neurons are classified according to their voltage response. According to this analysis, 56% of type1 neurons are neurosecretory neurons, while this proportion is 14% in type2, and 25% in type3 neurons (**Figure 3B**). This analysis was not carried out for type4 neurons since these neurons had no circadian rhythm. Since the type1 neurons have the highest proportion of neurosecretory neurons, the circadian rhythm of acid-induced current was further tested on this neuron type. Since in cultured neurons, the circadian rhythm is shifted between cells, differences may be missed if the activity is measured as reported in Figure 3A. To synchronize the rhythm of the cells used for the experiments reported in **Figure 3C-E**, neurons at day 11 after seeding were exposed to 1 μ m dexamethasone for 30min. In order not to perturb the measurements by any short-term effect of dexamethasone, voltage- and current-clamp recordings were performed on the cultured neuron at 18, 24, 30 and 36 hours after synchronization treatment (ZT18, 0, 6, 12). The acid-induced ASIC current density had a circadian rhythm after synchronization treatment, with maximal amplitudes at ZT12 (**Figure 3C**). Exposure to pH6.6 induced APs in these current-clamped neurons (**Figure 3D**). The number of acid-induced APs showed a circadian rhythm in type1 neurons, with a maximum at ZT0 (**Figure 3E**). Thus, the maximal number of APs was found at a different ZT than the maximal ASIC current expression. The area under the curve (AUC) of the pH6.6-induced depolarization in these experiments, which is a measure of the pH6.6-induced ASIC activity, was maximal at ZT12 (**Figure 3F**), thus at the same ZT as maximal ASIC peak currents. It has previously been shown that very strong depolarizations limit the number of APs by a mechanism that resembles a depolarization block (Alijevic et al., 2020b; Vukicevic and Kellenberger, 2004). These observations confirm data obtained without synchronization treatment (**Supplemental Figure 2D-E**). These data show that the function of ASICs in embryonic neurosecretory neurons has a circadian rhythm, and ASIC currents affect the neuronal activity.

ASIC1a regulates the Akt-mTOR signaling pathway in the hypothalamus

To identify circadian rhythms in gene expression depending on ASIC1a in a genome-wide manner, we performed a global transcriptome deep sequencing of 3-month-old WT and ASIC1a^{-/-} mice that were kept under a standard LD cycle. The hypothalamus was harvested at ZT1 or ZT13. RNA levels were quantified by next-generation sequencing (RNA-seq; see Methods).

Surprisingly, only 18 genes had their expression changed in the hypothalamus of ASIC1a^{-/-} as compared to WT mice (**Figure 4A**). At ZT1, 1 gene (*Krt90*) was downregulated and 1 gene (*Cers5*) was upregulated in ASIC1a^{-/-} hypothalamus (**Figure 4B**). *Krt90* does not express a functional protein in the central nervous system. At ZT13, 3 genes (*Krt90*, *Prl* and *Gm49980*) were downregulated and 13 genes (*Cers5*, *1700016P03Rik*, *Arl4d*, *Btg2*, *Ddit4*, *Sgk1*, *Egr1*, *Egr2*, *Egr3*, *Nr4a1*, *Nr4a3*, *Fos*, *Fosb* and *Junb*) were upregulated in ASIC1a^{-/-} hypothalamus (**Figure 4B**). *Cers5* is an enzyme involved in the synthesis of ceramides from sphingoid bases and acyl-CoA substrates (Mullen et al., 2012); *Prl*, prolactin, is a pituitary hormone and has only been detected in the amygdala, the preoptic area of hypothalamus and the olfactory bulb (Cabrera-Reyes et al., 2017). *Arl4d*, *Ddit4* and *Sgk1* are kinases that affect diverse signaling pathways. *Arl4d* and *Sgk1* are both negatively regulated by the activation of Akt (Tolksdorf et al., 2018; Toska et al., 2019), while *Ddit4* is a potent inhibitor of mTOR (Nosedá et al., 2013). *Btg2*, *Egr1*, *Egr2*, *Egr3*, *Nr4a1* and *Nr4a3* are transcription factors which are inhibited by the activation of Akt or mTOR (Chien et al., 2017; Lau et al., 2011; Liu et al., 2020; Tsui et al., 2018; Yu et al., 2013). Both *c-fos*, *fosb* and *Junb* genes are early response genes (ERG) that are activated transiently and rapidly in response to a wide variety of cellular stimuli; *c-fos*, *fosb* and *Junb* are regulated by Akt or mTOR (Li et al., 2017; Ren et al., 2021). *1700016P03Rik* and *Gm49980* are non-coding genes.

The expression of all genes except for the non-coding genes and *Krt90* were tested by qRT-PCR in the same mouse hypothalamus RNA samples. The expression of *Prl* was significantly increased at ZT13 in the hypothalamus of WT but not ASIC1a^{-/-} mice and was significantly higher in the WT than in ASIC1a^{-/-} at ZT13. The indicated downregulation of *Cers5* in ASIC1a^{-/-} was not confirmed (**Figure 4C**). Regarding kinases and transcription factors, the qRT-PCR analysis showed that the expression in the hypothalamus of the following genes was increased at ZT13 relative to ZT1 in ASIC1a^{-/-}: *Arl4d*, *Btg2*, *Sgk1*, *Ddit4*, *Egr1*, *Egr3*, *Nr4a1* and *Nr4a3*. In WT hypothalamus, only *Btg2*, *Ddit4* and *Nr4a3* were increased at ZT13 relative to ZT1. The only significant difference between WT and ASIC1a^{-/-} at ZT1 was the higher expression of *Nr4a3* in WT hypothalamus. The higher expression in ASIC1a^{-/-} relative to WT at ZT13 was

confirmed for *Arl4d*, *Sgk1*, *Egr1*, *Egr3*, *Nr4a1* and *Nr4a3* (**Figure 4D-E**). Regarding the ERGs, the expression of *Fosb* was significantly increased at ZT13 over ZT1 in *ASIC1a^{-/-}* mice, and was significantly lower in *ASIC1a^{-/-}* than in WT mice at ZT1 and higher in *ASIC1a^{-/-}* than in WT at ZT13. A similar pattern was observed for *c-fos*, except for the fact that there was no difference between *ASIC1a^{-/-}* and WT mice at ZT1. The expression of *Junb* was significantly increased at ZT13 over ZT1 in WT but not in *ASIC1a^{-/-}* mice, and was significantly lower in *ASIC1a^{-/-}* than in WT mice at ZT13 (**Supplemental Figure 3A**). The expression of *ASIC1a* was significantly increased at ZT13 in WT mice, and was not detectable in *ASIC1a^{-/-}* mice (**Supplemental Figure 3B**). The expression of *Tshb* was not different between WT and *ASIC1a^{-/-}* mice, nor between the two time points (**Supplemental Figure 3C**). The expression of *Trh* was significantly increased at ZT13 in WT but not in *ASIC1a^{-/-}* mice, and was significantly higher in WT than in *ASIC1a^{-/-}* at ZT13, which had not been observed with the RNA-sequencing (**Supplemental Figure 3D**). Since all these genes are regulated by the Akt-mTOR signaling pathway, we measured the mRNA level of mTOR in WT and *ASIC1a^{-/-}* mouse hypothalamus at ZT1 and ZT13. The expression of *mTOR* was not different between WT and *ASIC1a^{-/-}* mice, nor between the two time points (**Figure 4F**).

Activation of ASIC1a regulates the expression of Trh and Prl via the Akt-mTOR signaling pathway

Global deletion of *ASIC1a* alters Akt-mTOR signaling pathway-relative gene expression in the hypothalamus at ZT13. The expression of *Trh* and *Prl* is also regulated by the Akt-mTOR pathway (McAninch and Bianco, 2014; Yan et al., 2017). It is currently not known whether the activity of the Akt-mTOR pathway in the hypothalamus follows a circadian rhythm. Hypothalami were harvested at 4-hour intervals from 3-month-old WT and *ASIC1a^{-/-}* male mice kept under a standard LD cycle. After extraction of total proteins and separation by SDS-PAGE, the expression of p-Akt, Akt, mTOR, p-mTOR and β -actin was determined by Western blot analysis (**Figure 5A** and **Supplemental Figure 4A**). The p-Akt/Akt expression ratio was decreased at ZT12 in *ASIC1a^{-/-}* and showed no circadian rhythm in WT hypothalamus; the p-mTOR/mTOR expression ratio showed a circadian rhythm in both WT and *ASIC1a^{-/-}* neurons with highest values at night in WT, and at ZT8 in *ASIC1a^{-/-}* hypothalamus. Overall, the p-mTOR/mTOR ratio was higher in WT than *ASIC1a^{-/-}* hypothalamus (**Figure 5A**). The expression of Akt and mTOR had no circadian rhythm in WT and *ASIC1a^{-/-}* mice, and no significant difference between the WT and *ASIC1a^{-/-}* mice (**Supplemental Figure 4A**). Expression of BMAL1 protein was significantly decreased at ZT8 and ZT12 in *ASIC1a^{-/-}*

hypothalamus (**Supplemental figure 4B**).

To test whether the observed activation of Akt and mTOR is due to a changed ASIC expression, the effect of an inhibitor of Akt (Triciribine) (Yang et al., 2004) or of mTOR (Rapamycin) (Raab-Graham et al., 2006), an ASIC agonist (MitTx) (Bohlen et al., 2011) and an ASIC inhibitor (PcTx1) (Escoubas et al., 2003) was measured on the activation of Akt and mTOR in cultured neurons. Since the hypothalamus is a small nucleus and many animals would be required to obtain enough cells for a Western-blot analysis, ASIC expression was determined in cortical neurons, in which ASIC currents of relatively high amplitude have been measured (Wemmie et al., 2003; Wemmie et al., 2002). Primary cultures of WT and ASIC1a^{-/-} cortical neurons were incubated with the indicated inhibitors or agonists for 2 hours. After extraction of total proteins and separation by SDS-PAGE, expression of ASIC1, p-Akt, Akt, mTOR, p-mTOR and β -actin was determined by Western blot analysis. Representative blots indicate no ASIC1a expression change after Triciribine, PcTx1, Rapamycin and MitTx treatment (**Supplemental Figure 4C**); the p-Akt/Akt ratio was decreased in WT and ASIC1a^{-/-} neurons after Triciribine treatment, and showed a tendency of upregulation in WT neurons after MitTx treatment (p=0.0579). The p-mTOR/mTOR expression ratio was decreased in WT and ASIC1a^{-/-} neurons after Triciribine and Rapamycin treatment, and significantly upregulated in WT neurons after MitTx treatment (**Supplemental Figure 4C**).

To test whether the activity of ASIC1a regulates the expression of *Prl* and *Trh*, the effects of Triciribine, PcTx1, Rapamycin and MitTx on the mRNA expression of *Prl* and *Trh* were measured. Primary cultures of WT and ASIC1a^{-/-} hypothalamus neurons were incubated with different inhibitors or agonists for 2 hours. After isolation of total mRNA, the expression of *Trh*, *Prl*, *Arl4d*, *Egr1*, *Egr3*, *Nr4a1* and *Sgk1* was determined by qRT-PCR analysis. The expression of both *Prl* and *Trh* was significantly decreased in WT and ASIC1a^{-/-} neurons after Triciribine and Rapamycin treatment, and significantly upregulated in WT but not ASIC1a^{-/-} neurons after MitTx treatment. PcTx1 decreased the expression of *Prl* and *Trh* in WT neurons (**Figure 5B-C**). Triciribine significantly increased the expression of *Arl4d*, *Egr1*, *Nr4a1* and *Sgk1* in WT and ASIC1a^{-/-} neuron, while PcTx1 significantly increased the expression of the same four transcripts only in WT neurons; *Egr3* was significantly upregulated in WT neurons after PcTx1 treatment, and significantly upregulated in ASIC1a^{-/-} neurons after Triciribine treatment; the expression of *Arl4d* and *Sgk1* was significantly upregulated in WT neurons after Rapamycin treatment, *Arl4d* and *Nr4a1* were significantly upregulated in ASIC1a^{-/-} neurons after Rapamycin treatment (**Supplemental Figure 4D**).

Activation of ASIC1a induces Ca²⁺ influx and activates the PI₃K, which activates the Akt-

mTOR pathway (Dou et al., 2019; Rommel et al., 2001). A previous study reported that the activation of cAMP response element-binding protein (CREB) potentiates the transcription of *Prl* and *Trh*; activation of CREB is also upregulated by the activation of Akt-mTOR pathway (Fu et al., 2015; Sotelo-Rivera et al., 2017). To test whether the expression of *Prl* and *Trh* is regulated by the activation of ASIC1a via the Akt-mTOR pathway, the effect of BAPTA-AM (a cell-permeable Ca²⁺ chelator) (Tymianski et al., 1994), KG-501 (an inhibitor of p-CREB) (Best et al., 2004), Triciribine, PcTx1 and Rapamycin on the MitTx induced expression increase of *Prl* and *Trh* was tested. Primary cultures of WT hypothalamus neurons were pre-incubated with different inhibitors for 30 min, then co-incubated with 2nM MitTx for 2 hours. After isolation of total mRNA, expression of *Trh* was determined by qRT-PCR analysis. The MitTx-induced expression of *Trh* in WT neurons was significantly decreased by each of these inhibitors (**Figure 5D**). These results indicate that the MitTx-induced expression level of *Trh* depends on intracellular Ca²⁺, the Akt-mTOR pathway and p-CREB.

ASIC1a regulates circadian rhythm behaviors

We have shown here that ASIC1a regulates the circadian rhythm of body temperature and the expression of *Trh* and *Prl*. To test whether ASIC1a also controls other circadian rhythms, the role of ASIC1a in the circadian system was first assessed by studying locomotor activity rhythms of WT and ASIC1a^{-/-} mice in wheel-running cages. Mice were first exposed to a 12 h light:12 h dark (LD) cycle followed by constant darkness (DD). Under LD conditions, the free-running period of locomotor activity (**Figure 6A-B**) was significantly different between WT and ASIC1a^{-/-} mice in the dark period. Under DD conditions, the free-running period was significantly different between WT and ASIC1a^{-/-} mice (**Figure 6C**), suggesting the involvement of ASIC1a in the molecular clockwork. Short light pulses at ZT14 or ZT22 before releasing the mice in the DD cycle shifted the cycle in the same way in WT and ASIC1a^{-/-} mice (**Figure 6D**).

DISCUSSION

We show here that the expression of ASIC1a has a circadian rhythm in the adult hypothalamus and in embryonic neurosecretory hypothalamus neurons. Global deletion of ASIC1a only affects the expression of 9 functional genes at ZT13, among them *Trh* and *Prl*, and none at ZT1 in hypothalamus. Our analysis in cultured neurons indicates that the activation of ASIC1a regulates the expression of *Trh* and *Prl* via the Akt-mTOR pathway. We conclude that the

circadian expression of ASIC1a in the hypothalamus modulates the daily rhythm of body temperature through the HPT axis.

The regulation of the circadian rhythm of the body temperature depends on the HPT axis

The HPT axis is part of the neuroendocrine system responsible for the regulation of metabolism and body temperature. Disruption of the HPT axis causes many diseases, such as hyperthyroidism, hypothyroidism, thyrotoxicosis, low-T3 syndrome and resistance to thyroid hormone (Ichiki, 2010; Qari, 2015; Schmidt-Ott and Ascheim, 2006). We observed here that the *Trh* and *Tsh* mRNA levels, which are maximal at night in hypothalamus and pituitary, respectively, lost their circadian rhythm in ASIC1a^{-/-} mice. In contrast, the *TrhR* mRNA adopted a circadian rhythm in the pituitary only after deletion of ASIC1a. Since ASIC1a is abundantly expressed in all secretory cell types of the pituitary (Wang et al., 2020), deletion of ASIC1a may alter the expression of the TRHR in the pituitary. The *TshR* expression in the thyroid gland was significantly lower in ASIC1a^{-/-} than WT at both ZT1 and ZT13, although the body temperature at ZT1 was not different. Together, these changes strongly suggest that the difference in body temperature of ASIC1a^{-/-} relative to WT mice at night was induced by the lowering of the expression of several components of the HPT axis at night.

Wheel-running activity was significantly decreased in ASIC1a^{-/-} compared to WT mice from ZT13 to ZT21 (**Figure 6A**). However, the body temperature was only significantly different at ZT17 and ZT18 (**Figure 1A**). Locomotion is the fastest and most influential factor in heat production. Because the presence of running wheels alters several aspects of energy balance, including body weight and composition, food intake, and energy expenditure of activity (Novak et al., 2012), the amplitude of the day-night difference may also be affected. The body temperature measurements were not influenced by the wheel running, since they were done in separate experiments. Therefore, the lower body temperature in ASIC^{-/-} mice was not due to less wheel running. We measured the body temperature and the spontaneous activity in the same mice, showing no difference between the WT and ASIC1a^{-/-} regarding the spontaneous activity (**Figure 1B**). The body temperature difference between WT and ASIC1a^{-/-} mice at ZT17 and ZT18 relies therefore likely on the neuroendocrine system of the HPT axis.

ASIC1a may regulate the expression of Prolactin to affect circadian behavior

Prolactin is a pituitary hormone. It is however also expressed in the dorsomedial, ventromedial, supraoptic nuclei and the PVH of the hypothalamus (Cabrera-Reyes et al., 2017), where it is

synthesized locally, independent of PRL synthesis in the pituitary gland (Freeman et al., 2000). In the brain, PRL receptors are expressed in cells of the PVH, medial preoptic nucleus, supraoptic nucleus, rostral arcuate nucleus and choroid plexus, but not in the cortex (Chiu and Wise, 1994). We found here that the expression of *Prl* was significantly increased at ZT13 in the hypothalamus of WT but not *ASIC1a*^{-/-} mice (**Figure 4C**), and significantly decreased at ZT13 in the pituitary of WT but not *ASIC1a*^{-/-} mice (**Figure 1C**). PRL stimulates dopamine release from discrete neuronal populations in the PVH dopaminergic neurons to maintain low levels of serum prolactin (DeMaria et al., 2000; Foord et al., 1983). Therefore, the observed upregulation of *Prl* at ZT13 in hypothalamus likely stimulates dopamine release from neuroendocrine neurons in hypothalamus to inhibit the synthesis of *Prl* in pituitary of WT mice. In *ASIC1a*^{-/-} mice, which have lost the circadian expression of *Prl* in the hypothalamus, the circadian rhythm of *Prl* expression in the pituitary is not maintained.

The major function of PRL is to stimulate milk production during lactation. In particular, prolactin plays a role in energy homeostasis (Ellacott et al., 2003), food intake (Lawrence et al., 2000) and wheel-running activity (Carter, 2019; Ladyman et al., 2020). Intraperitoneal injection of prolactin can acutely suppress wheel-running activity in virgin female mice, and specific deletion of the PRL receptor of the medial preoptic area was shown to completely abolish the early pregnancy-induced suppression of wheel-running activity (Ladyman et al., 2020). Male mice with a specific deletion of the PRL receptor in rat insulin promoter-positive hypothalamic neurons had lower body weights, increased oxygen consumption and increased running wheel activity than control mice (Ladyman et al., 2017). In our study, we found that wheel-running activity of WT mice was significantly higher than that of *ASIC1a*^{-/-} mice under dark condition (ZT13-ZT21, **Figure 6A**). Since pituitary and exogenous PRL inhibit the wheel-running activity, and the expression of *Prl* in pituitary was significantly decreased at ZT13 in the pituitary of WT but not *ASIC1a*^{-/-} mice (**Figure 1C**), the increase of wheel-running activity in WT under dark condition may be mediated by the decreased expression of *Prl* in the pituitary.

Activation of ASIC1a regulates Prl and Trh via the Ca²⁺/PI₃K/Akt/mTOR/CREB pathway

Our study indicates that the activation of *ASIC1a* regulates the Akt-mTOR signaling pathway. Activation of *ASIC1a* by the selective agonist MitTx led to a higher activity of Akt and mTOR, and inhibition of Akt decreased the expression of p-mTOR (**Supplemental Figure 5**). This indicates that the activation of *ASIC1a* upregulated Akt, which in turn upregulated mTOR. Phosphatidylinositol 3-kinase (PI₃K) acts upstream of Akt, the activated PI₃K bringing Akt into close proximity, and allowing the PI₃K to phosphorylate Akt at its kinase domain (Markman et

al., 2010). Intracellular Ca^{2+} and hypoxia activate PI₃K (Vergne et al., 2003). This activation is prevented in the absence of intra- or extracellular Ca^{2+} (Lee et al., 2008). Homomeric ASIC1a has a small but well documented Ca^{2+} permeability, and the effect of ASIC1a activation on *Prl* and *Trh* expression was inhibited by the Ca^{2+} chelator BAPTA-AM. This indicates that ASIC1a regulates *Prl* and *Trh* via the Ca^{2+} /PI₃K/Akt/mTOR pathway. In hypothalamus neurons, activation of ASICs induces a membrane depolarization which can activate voltage-gated Ca^{2+} channels and by this way increase the intracellular Ca^{2+} concentration. Part of the Ca^{2+} influx may therefore occur by this indirect entryway. The CREB is downstream of mTOR (Abd-Elrahman and Ferguson, 2019; Dai et al., 2017). In our study, the inhibitor of p-CREB decreased the level of ASIC1a-induced expression of *Prl* and *Trh*. Therefore, we conclude that the expression of *Prl* and *Trh* is induced by the activation of ASIC1a via Ca^{2+} /PI₃K/Akt/mTOR/CREB pathway.

The p-Akt/Akt expression ratio showed no circadian rhythm in WT hypothalamus (**Figure 5A**), whereas in cultured hypothalamus neurons, the activation of ASIC1a upregulated the p-Akt/Akt expression ratio. Deletion of ASIC1a significantly upregulated the p-Akt/Akt expression ratio in the hypothalamus (**Figure 5A**, $P=0.0283$, unpaired Student's *t*-test. $n=5-6$) and introduced a circadian rhythm in the p-Akt/Akt expression ratio. This suggests that the activity of Akt may be negatively regulated by ASIC1a by an unknown mechanism. The p-mTOR/mTOR expression ratio was significantly higher at night in WT and was overall higher in WT than ASIC1a^{-/-} hypothalamus (**Figure 5A**, $P=0.0002$, unpaired Student's *t*-test. $n=5-6$). Activation of ASIC1a induces activation of CaMKII and ERK1/2 by a mechanism that depends on Ca^{2+} influx (Yu et al., 2018), and Erk1/2 was shown to upregulate the activity of mTOR (Hsu et al., 2019). Thus, the activation of mTOR has a circadian rhythm that is likely synchronized with the expression of ASIC1a in the hypothalamus of WT mice. The decreased activation of mTOR in the absence of ASIC1a may be due to a missing regulation by both the CaMKII/ERK1/2 and the PI₃K/Akt pathway. The fact that the RNA sequencing did not identify any difference in expression of components of the CaMKII/ERK1/2 may however indicate that this pathway is less important.

Synchronous expression of ASIC1a and BMAL1 in the hypothalamus

In the SCN and the hypothalamus, the circadian rhythm of ASIC1a is synchronized with the expression of BMAL1 (**Figure 2 and Supplemental Figure 1**). After exposure to light, the expression of ASIC1a and BMAL1 increased in the hypothalamus and decreased in the SCN; it also increased in the hypothalamus without SCN. In line with other publications (Kohsaka et

al., 2007; Zhang et al., 2017), we find here the peak of *Bmal1* expression at ZT0 in the hypothalamus and the SCN. In our experiments, the daily rhythm was shifted between *Bmal1* mRNA and protein expression. The protein expression pattern of BMAL1 is affected by many factors, such as the age, diet, disease (Blancas-Velazquez et al., 2017; Cai et al., 2010; Yang et al., 2016). In the absence of *ASIC1a* in the hypothalamus, the expression of *Bmal1* did not lose its circadian rhythm. The relationship between *ASIC1a* and the clock genes is currently unclear, but our result suggests that the circadian expression of *ASIC1a* may be regulated by clock genes.

The SCN regulates the daily rhythm of the body temperature

We found no difference in the daytime firing rates of PVH mpd neurons between WT and *ASIC1a*^{-/-} mice (**Figure 1I**). In contrast, the SFR was significantly higher in WT than in *ASIC1a*^{-/-} at nighttime, and was increased at night relative to the day in WT but not in *ASIC1a*^{-/-} mpd neurons. The SCN sends inhibitory signals to the PVN, which may result in a lower metabolic heat production and a lower body temperature (Speed et al., 2018). In rats, vasopressin release during the light period inhibits the corticotropin-releasing hormone-containing neurons in the PVN (Kalsbeek et al., 2011). The SFR of mouse SCN neurons is significantly higher during the day than at night (Nygård et al., 2005; Paul et al., 2016). K⁺ channels, including a fast, delayed-rectifier current, contribute to the control of the circadian rhythm of SFR in the SCN (Itri et al., 2005). Our RNA sequencing analysis did not detect changes in the expression of K⁺ channels in hypothalamus. Thus, the activity of the mpd neurons may be regulated directly by the SCN, not via K⁺ channel expression changes. It is currently unclear how neuronal activity in the mpd is translated into body temperature rhythms. SFR and behavioral rhythms are phase-locked, and the changes of SFR rhythm could affect circadian activity (Yamazaki et al., 1998). The SCN may regulate the activity of mpd neurons and the expression of *Trh* to regulate the circadian rhythm of body temperature through the HPT axis.

Conclusion

Overall, we demonstrated that the expression of *ASIC1a* in the hypothalamus follows a circadian rhythm, and that deletion of *ASIC1a* partially prevents the increase in body temperature during the night. Analysis of the involved signaling suggests that *zeitgeber* light regulates through the SCN the activity of mpd neurons and the expression of *Prl* and *Trh* by a mechanism that depends on *ASIC1a*. *Trh* in turn regulates the circadian rhythm of body temperature via the HPT axis; *Prl* may be involved in the regulation of the wheel-running

activity.

Acknowledgements

We wish to thank Prof. Jeffrey G. Tasker (Tulane University) and Dr. Dmitri Firsov (University of Lausanne) for their advice on the project design and Prof. Ron Stoop (Lausanne University Hospital) for providing the equipment and the environment for the brain slice recording.

Funding

This research was supported by the Swiss National Science Foundation grant 31003A_172968 to SK. Zhong Peng was supported by a scholarship grant from the Chinese Scholarship Council.

Declaration of interests

The authors declare no conflicts of interest.

REFERENCES

- Abd-Elrahman, K.S., and Ferguson, S.S.G. (2019). Modulation of mTOR and CREB pathways following mGluR5 blockade contribute to improved Huntington's pathology in *zQ175* mice. *Molecular brain* *12*, 1-9.
- Aghajanova, L., Stavreus-Evers, A., Lindeberg, M., Landgren, B.-M., Sparre, L.S., and Hovatta, O. (2011). Thyroid-stimulating hormone receptor and thyroid hormone receptors are involved in human endometrial physiology. *Fertility and sterility* *95*, 230-237.
- Alijevic, O., Bignucolo, O., Hichri, E., Peng, Z., Kucera, J.P., and Kellenberger, S. (2020a). Slowing of the Time Course of Acidification Decreases the Acid-Sensing Ion Channel 1a Current Amplitude and Modulates Action Potential Firing in Neurons. *Frontiers in Cellular Neuroscience* *14*, 41.
- Alijevic, O., Bignucolo, O., Hichri, E., Peng, Z., Kucera, J.P., and Kellenberger, S. (2020b). Slowing of the Time Course of Acidification Decreases the Acid-Sensing Ion Channel 1a Current Amplitude and Modulates Action Potential Firing in Neurons. *Frontiers in cellular neuroscience* *14*, 41.
- Aninye, I.O., Matsumoto, S., Sidhaye, A.R., and Wondisford, F.E. (2014). Circadian regulation of *Tshb* gene expression by Rev-Erba (NR1D1) and nuclear corepressor 1 (NCOR1). *Journal of Biological Chemistry* *289*, 17070-17077.
- Astiz, M., Heyde, I., and Oster, H. (2019). Mechanisms of Communication in the Mammalian Circadian Timing System. *International journal of molecular sciences* *20*, 343.
- Bargi-Souza, P., Peliciari-Garcia, R.A., and Nunes, M.T. (2019). Disruption of the pituitary circadian clock induced by hypothyroidism and hyperthyroidism: consequences on daily pituitary hormone expression profiles. *Thyroid* *29*, 502-512.
- Baron, A., Waldmann, R., and Lazdunski, M. (2002). ASIC-like, proton-activated currents in rat hippocampal neurons. *J Physiol* *539*, 485-494.
- Bassler, E.L., Ngo-Anh, T.J., Geisler, H.S., Ruppertsberg, J.P., and Grunder, S. (2001). Molecular and functional characterization of acid-sensing ion channel (ASIC) 1b. *J Biol Chem* *276*, 33782-33787.

- Best, J.L., Amezcua, C.A., Mayr, B., Flechner, L., Murawsky, C.M., Emerson, B., Zor, T., Gardner, K.H., and Montminy, M. (2004). Identification of small-molecule antagonists that inhibit an activator: coactivator interaction. *Proceedings of the National Academy of Sciences* *101*, 17622-17627.
- Birdsong, W.T., Fierro, L., Williams, F.G., Spelta, V., Naves, L.A., Knowles, M., Marsh-Haffner, J., Adelman, J.P., Almers, W., Elde, R.P., *et al.* (2010). Sensing muscle ischemia: coincident detection of acid and ATP via interplay of two ion channels. *Neuron* *68*, 739-749.
- Blancas-Velazquez, A., la Fleur, S.E., and Mendoza, J. (2017). Effects of a free-choice high-fat high-sugar diet on brain PER2 and BMAL1 protein expression in mice. *Appetite* *117*, 263-269.
- Bohlen, C.J., Chesler, A.T., Sharif-Naeini, R., Medzihradzsky, K.F., Zhou, S., King, D., Sanchez, E.E., Burlingame, A.L., Basbaum, A.I., and Julius, D. (2011). A heteromeric Texas coral snake toxin targets acid-sensing ion channels to produce pain. *Nature* *479*, 410-414.
- Boillat, A., Alijevic, O., and Kellenberger, S. (2014). Calcium entry via TRPV1 but not ASICs induces neuropeptide release from sensory neurons. *Molecular and cellular neurosciences* *61*, 13-22.
- Bravo-San Pedro, J.M., Sica, V., Martins, I., Pol, J., Loos, F., Maiuri, M.C., Durand, S., Bossut, N., Aprahamian, F., and Anagnostopoulos, G. (2019). Acyl-CoA-binding protein is a lipogenic factor that triggers food intake and obesity. *Cell metabolism* *30*, 754-767.
- Brown, S.A., Zimbrunn, G., Fleury-Olela, F., Preitner, N., and Schibler, U. (2002). Rhythms of mammalian body temperature can sustain peripheral circadian clocks. *Current Biology* *12*, 1574-1583.
- Cabrera-Reyes, E.A., Limón-Morales, O., Rivero-Segura, N.A., Camacho-Arroyo, I., and Cerbón, M. (2017). Prolactin function and putative expression in the brain. *Endocrine* *57*, 199-213.
- Cai, Y., Liu, S., Sothorn, R.B., Xu, S., and Chan, P. (2010). Expression of clock genes *Per1* and *Bmal1* in total leukocytes in health and Parkinson's disease. *European journal of neurology* *17*, 550-554.
- Carter, K. (2019). Effect of Prolactin on Voluntary Running Behaviour and Locomotion.
- Challet, E., Caldelas, I., Graff, C., and Pevet, P. (2003). Synchronization of the molecular clockwork by light- and food-related cues in mammals. *Biol Chem* *384*, 711-719.
- Chen, C.C., Zimmer, A., Sun, W.H., Hall, J., Brownstein, M.J., and Zimmer, A. (2002). A role for ASIC3 in the modulation of high-intensity pain stimuli. *Proc Natl Acad Sci U S A* *99*, 8992-8997.
- Chien, M.-H., Lee, W.-J., Yang, Y.-C., Li, Y.-L., Chen, B.-R., Cheng, T.-Y., Yang, P.-W., Wang, M.-Y., Jan, Y.-H., and Lin, Y.-K. (2017). KSRP suppresses cell invasion and metastasis through miR-23a-mediated EGR3 mRNA degradation in non-small cell lung cancer. *Biochimica et Biophysica Acta (BBA)-Gene Regulatory Mechanisms* *1860*, 1013-1024.
- Chiu, S., and Wise, P.M. (1994). Prolactin receptor mRNA localization in the hypothalamus by in situ hybridization. *Journal of neuroendocrinology* *6*, 191-199.
- Czeisler, C.A., and Klerman, E.B. (1999). Circadian and sleep-dependent regulation of hormone release in humans. *Recent Prog Horm Res* *54*, 97-130; discussion 130-132.
- Dai, C., Ciccotosto, G.D., Cappai, R., Wang, Y., Tang, S., Hoyer, D., Schneider, E.K., Velkov, T., and Xiao, X. (2017). Rapamycin confers neuroprotection against colistin-induced oxidative stress, mitochondria dysfunction, and apoptosis through the activation of autophagy and mTOR/Akt/CREB signaling pathways. *ACS chemical neuroscience* *9*, 824-837.

- Damiola, F., Le Minh, N., Preitner, N., Kornmann, B., Fleury-Olela, F., and Schibler, U. (2000). Restricted feeding uncouples circadian oscillators in peripheral tissues from the central pacemaker in the suprachiasmatic nucleus. *Genes & development* *14*, 2950-2961.
- de la Rosa, D.A., Krueger, S.R., Kolar, A., Shao, D., Fitzsimonds, R.M., and Canessa, C.M. (2003). Distribution, subcellular localization and ontogeny of ASIC1 in the mammalian central nervous system. *The Journal of physiology* *546*, 77-87.
- DeMaria, J.E., Livingstone, J.D., and Freeman, M.E. (2000). Ovarian steroids influence the activity of neuroendocrine dopaminergic neurons. *Brain Res* *879*, 139-147.
- Deval, E., Baron, A., Lingueglia, E., Mazarguil, H., Zajac, J.M., and Lazdunski, M. (2003). Effects of neuropeptide SF and related peptides on acid sensing ion channel 3 and sensory neuron excitability. *Neuropharmacology* *44*, 662-671.
- Deval, E., Noel, J., Lay, N., Alloui, A., Diochot, S., Friend, V., Jodar, M., Lazdunski, M., and Lingueglia, E. (2008). ASIC3, a sensor of acidic and primary inflammatory pain. *EMBO J* *27*, 3047-3055.
- Di Yorio, M.P., Bilbao, M.G., Pustovrh, M.C., Prestifilippo, J.P., and Faletti, A.G. (2008). Leptin modulates the expression of its receptors in the hypothalamic-pituitary-ovarian axis in a differential way. *Journal of endocrinology* *198*, 355-366.
- Dibner, C., Schibler, U., and Albrecht, U. (2010). The mammalian circadian timing system: organization and coordination of central and peripheral clocks. *Annual review of physiology* *72*, 517-549.
- Dou, C., Zhou, Z., Xu, Q., Liu, Z., Zeng, Y., Wang, Y., Li, Q., Wang, L., Yang, W., Liu, Q., *et al.* (2019). Hypoxia-induced TUFT1 promotes the growth and metastasis of hepatocellular carcinoma by activating the Ca²⁺/PI3K/AKT pathway. *Oncogene* *38*, 1239-1255.
- Douma, L.G., and Gumz, M.L. (2018). Circadian clock-mediated regulation of blood pressure. *Free Radical Biology and Medicine* *119*, 108-114.
- Du, J., Reznikov, L.R., Price, M.P., Zha, X.M., Lu, Y., Moninger, T.O., Wemmie, J.A., and Welsh, M.J. (2014). Protons are a neurotransmitter that regulates synaptic plasticity in the lateral amygdala. *Proc Natl Acad Sci U S A* *111*, 8961-8966.
- Duan, B., Wang, Y.Z., Yang, T., Chu, X.P., Yu, Y., Huang, Y., Cao, H., Hansen, J., Simon, R.P., Zhu, M.X., *et al.* (2011). Extracellular spermine exacerbates ischemic neuronal injury through sensitization of ASIC1a channels to extracellular acidosis. *J Neurosci* *31*, 2101-2112.
- Ellacott, K.L.J., Lawrence, C.B., Pritchard, L.E., and Luckman, S.M. (2003). Repeated administration of the anorectic factor prolactin-releasing peptide leads to tolerance to its effects on energy homeostasis. *American Journal of Physiology-Regulatory, Integrative and Comparative Physiology* *285*, R1005-R1010.
- Escoubas, P., Bernard, C., Lambeau, G., Lazdunski, M., and Darbon, H. (2003). Recombinant production and solution structure of PcTx1, the specific peptide inhibitor of ASIC1a proton-gated cation channels. *Protein Science* *12*, 1332-1343.
- Filipski, E., King, V.M., Li, X., Granda, T.G., Mormont, M.-C., Liu, X., Claustrat, B., Hastings, M.H., and Lévi, F. (2002). Host Circadian Clock as a Control Point in Tumor Progression. *JNCI: Journal of the National Cancer Institute* *94*, 690-697.
- Foord, S.M., Peters, J.R., Dieguez, C., Scanlon, M.F., and Hall, R. (1983). Dopamine receptors on intact anterior pituitary cells in culture: functional association with the inhibition of prolactin and thyrotropin. *Endocrinology* *112*, 1567-1577.
- Freeman, M.E., Kanyicska, B., Lerant, A., and Nagy, G. (2000). Prolactin: structure, function, and regulation of secretion. *Physiol Rev.*

- Friese, M.A., Craner, M.J., Etzensperger, R., Vergo, S., Wemmie, J.A., Welsh, M.J., Vincent, A., and Fugger, L. (2007). Acid-sensing ion channel-1 contributes to axonal degeneration in autoimmune inflammation of the central nervous system. *Nat Med* *13*, 1483-1489.
- Fu, S.-P., Wang, W., Liu, B.-R., Yang, H.-M., Ji, H., Yang, Z.-Q., Guo, B., Liu, J.-X., and Wang, J.-F. (2015). β -Hydroxybutyric sodium salt inhibition of growth hormone and prolactin secretion via the cAMP/PKA/CREB and AMPK signaling pathways in dairy cow anterior pituitary cells. *International journal of molecular sciences* *16*, 4265-4280.
- Gao, J., Duan, B., Wang, D.G., Deng, X.H., Zhang, G.Y., Xu, L., and Xu, T.L. (2005). Coupling between NMDA receptor and acid-sensing ion channel contributes to ischemic neuronal death. *Neuron* *48*, 635-646.
- Goichot, B., Weibel, L., Chapotot, F., Gronfier, C., Piquard, F., and Brandenberger, G. (1998). Effect of the shift of the sleep-wake cycle on three robust endocrine markers of the circadian clock. *The American journal of physiology* *275*, E243-248.
- Harris, A.R.C., Christianson, D., Smith, M.S., Fang, S.-L., Braverman, L.E., and Vagenakis, A.G. (1978). The physiological role of thyrotropin-releasing hormone in the regulation of thyroid-stimulating hormone and prolactin secretion in the rat. *The Journal of clinical investigation* *61*, 441-448.
- Hastings, M.H., Maywood, E.S., and Brancaccio, M. (2018). Generation of circadian rhythms in the suprachiasmatic nucleus. *Nature Reviews Neuroscience* *19*, 453.
- Hsu, Y.-T., Li, J., Wu, D., Südhof, T.C., and Chen, L. (2019). Synaptic retinoic acid receptor signaling mediates mTOR-dependent metaplasticity that controls hippocampal learning. *Proceedings of the National Academy of Sciences* *116*, 7113-7122.
- Hu, J., Chai, Y., Wang, Y., Kheir, M.M., Li, H., Yuan, Z., Wan, H., Xing, D., Lei, F., and Du, L. (2012). PI3K p55 γ promoter activity enhancement is involved in the anti-apoptotic effect of berberine against cerebral ischemia–reperfusion. *European Journal of Pharmacology* *674*, 132-142.
- Ichiki, T. (2010). Thyroid hormone and atherosclerosis. *Vascular pharmacology* *52*, 151-156.
- Itri, J.N., Michel, S., Vansteensel, M.J., Meijer, J.H., and Colwell, C.S. (2005). Fast delayed rectifier potassium current is required for circadian neural activity. *Nat Neurosci* *8*, 650-656.
- Kalsbeek, A., Scheer, F.A., Perreau-Lenz, S., La Fleur, S.E., Yi, C.-X., Fliers, E., and Buijs, R.M. (2011). Circadian disruption and SCN control of energy metabolism. *FEBS letters* *585*, 1412-1426.
- Kellenberger, S., and Schild, L. (2015). *International Union of Basic and Clinical Pharmacology. XCI. Structure, Function, and Pharmacology of Acid-Sensing Ion Channels and the Epithelial Na⁺ Channel*. *Pharmacol Rev* *67*, 1-35.
- Kohsaka, A., Laposky, A.D., Ramsey, K.M., Estrada, C., Joshu, C., Kobayashi, Y., Turek, F.W., and Bass, J. (2007). High-fat diet disrupts behavioral and molecular circadian rhythms in mice. *Cell Metab* *6*, 414-421.
- Koller, K.J., Wolff, R.S., Warden, M.K., and Zoeller, R.T. (1987). Thyroid hormones regulate levels of thyrotropin-releasing-hormone mRNA in the paraventricular nucleus. *Proceedings of the National Academy of Sciences* *84*, 7329.
- Ladyman, S.R., Carter, K.M., Aung, Z.K., and Grattan, D.R. (2020). A reduction in voluntary physical activity during pregnancy in mice is mediated by prolactin. *bioRxiv*.
- Ladyman, S.R., MacLeod, M.A., Khant Aung, Z., Knowles, P., Phillipps, H.R., Brown, R.S.E., and Grattan, D.R. (2017). Prolactin receptors in Rip-cre cells, but not in Ag RP neurones, are involved in energy homeostasis. *Journal of neuroendocrinology* *29*, e12474.
- Langmesser, S., Tallone, T., Bordon, A., Rusconi, S., and Albrecht, U.J.B.m.b. (2008). Interaction of circadian clock proteins PER2 and CRY with BMAL1 and CLOCK. *9*, 1-16.

- Lau, M.T., Klausen, C., and Leung, P.C.K. (2011). E-cadherin inhibits tumor cell growth by suppressing PI3K/Akt signaling via β -catenin-Egr1-mediated PTEN expression. *Oncogene* *30*, 2753-2766.
- Lawrence, C.B., Celsi, F., Brennand, J., and Luckman, S.M. (2000). Alternative role for prolactin-releasing peptide in the regulation of food intake. *Nat Neurosci* *3*, 645-646.
- Lee, S.H., Lee, M.Y., Lee, J.H., and Han, H.J. (2008). A potential mechanism for short time exposure to hypoxia-induced DNA synthesis in primary cultured chicken hepatocytes: Correlation between Ca²⁺/PKC/MAPKs and PI3K/Akt/mTOR. *Journal of cellular biochemistry* *104*, 1598-1611.
- Li, B., Jia, S., Yue, T., Yang, L., Huang, C., Verkhatsky, A., and Peng, L. (2017). Biphasic regulation of Caveolin-1 gene expression by fluoxetine in astrocytes: opposite effects of PI3K/AKT and MAPK/ERK signaling pathways on c-fos. *Frontiers in cellular neuroscience* *11*, 335.
- Li, W.G., and Xu, T.L. (2011). ASIC3 channels in multimodal sensory perception. *ACS Chem Neurosci* *2*, 26-37.
- Liu, Y.-y., Zhang, W.-Y., Wang, C.-g., Huang, J.-A., Jiang, J.-h., and Zeng, D.-x. (2020). Resveratrol prevented experimental pulmonary vascular remodeling via miR-638 regulating NR4A3/cyclin D1 pathway. *Microvascular research* *130*, 103988.
- Luther, J., Daftary, S., Boudaba, C., Gould, G., Halmos, K.C., and Tasker, J. (2002). Neurosecretory and non-neurosecretory parvocellular neurones of the hypothalamic paraventricular nucleus express distinct electrophysiological properties. *Journal of neuroendocrinology* *14*, 929-932.
- Markman, B., Dienstmann, R., and Tabernero, J. (2010). Targeting the PI3K/Akt/mTOR pathway--beyond rapalogs. *Oncotarget* *1*, 530-543.
- McAninch, E.A., and Bianco, A.C. (2014). Thyroid hormone signaling in energy homeostasis and energy metabolism. *Annals of the New York Academy of Sciences* *1311*, 77.
- Meredith, A.L., Wiler, S.W., Miller, B.H., Takahashi, J.S., Fodor, A.A., Ruby, N.F., and Aldrich, R.W. (2006). BK calcium-activated potassium channels regulate circadian behavioral rhythms and pacemaker output. *Nat Neurosci* *9*, 1041.
- Mullen, T.D., Hannun, Y.A., and Obeid, L.M. (2012). Ceramide synthases at the centre of sphingolipid metabolism and biology. *Biochemical Journal* *441*, 789-802.
- Muta, K., Morgan, D.A., and Rahmouni, K. (2015). The role of hypothalamic mTORC1 signaling in insulin regulation of food intake, body weight, and sympathetic nerve activity in male mice. *Endocrinology* *156*, 1398-1407.
- Nosedá, R., Belin, S., Piguet, F., Vaccari, I., Scarlino, S., Brambilla, P., Boneschi, F.M., Feltri, M.L., Wrabetz, L., Quattrini, A., *et al.* (2013). DDIT4/REDD1/RTP801 Is a Novel Negative Regulator of Schwann Cell Myelination. *Journal of Neuroscience* *33*, 15295-15305.
- Novak, C.M., Burghardt, P.R., and Levine, J.A. (2012). The use of a running wheel to measure activity in rodents: Relationship to energy balance, general activity, and reward. *Neuroscience & Biobehavioral Reviews* *36*, 1001-1014.
- Nygård, M., Hill, R.H., Wikström, M.A., and Kristensson, K. (2005). Age-related changes in electrophysiological properties of the mouse suprachiasmatic nucleus in vitro. *Brain research bulletin* *65*, 149-154.
- Paul, J.R., DeWoskin, D., McMeekin, L.J., Cowell, R.M., Forger, D.B., and Gamble, K.L. (2016). Regulation of persistent sodium currents by glycogen synthase kinase 3 encodes daily rhythms of neuronal excitability. *Nature communications* *7*, 13470.
- Price, M.P., McIlwrath, S.L., Xie, J., Cheng, C., Qiao, J., Tarr, D.E., Sluka, K.A., Brennan, T.J., Lewin, G.R., and Welsh, M.J. (2001). The DRASIC cation channel contributes to the detection of cutaneous touch and acid stimuli in mice. *Neuron* *32*, 1071-1083.

- Qari, F.A. (2015). Thyroid hormone profile in patients with acute coronary syndrome. *Iranian Red Crescent Medical Journal* 17.
- Raab-Graham, K.F., Haddick, P.C.G., Jan, Y.N., and Jan, L.Y. (2006). Activity-and mTOR-dependent suppression of Kv1. 1 channel mRNA translation in dendrites. *Science* 314, 144-148.
- Rana, S., and Mahmood, S. (2010). Circadian rhythm and its role in malignancy. *Journal of Circadian Rhythms* 8, 3.
- Ren, D., and Miller, J.D. (2003). Primary cell culture of suprachiasmatic nucleus. *Brain research bulletin* 61, 547-553.
- Ren, J., Wang, X., Zhou, Y., Yue, X., Chen, S., Ding, X., Jiang, X., Liu, X., and Guo, Q. (2021). A novel SERPINE1-FOSB fusion gene in a case of pseudomyogenic hemangioendothelioma results in activation of intact FOSB and the PI3K-AKT-mTOR signaling pathway and responsiveness to sirolimus. *bioRxiv*.
- Rommel, C., Bodine, S.C., Clarke, B.A., Rossman, R., Nunez, L., Stitt, T.N., Yancopoulos, G.D., and Glass, D.J. (2001). Mediation of IGF-1-induced skeletal myotube hypertrophy by PI(3)K/Akt/mTOR and PI(3)K/Akt/GSK3 pathways. *Nature Cell Biology* 3, 1009-1013.
- Schibler, U., Ripperger, J., and Brown, S.A. (2003). Peripheral circadian oscillators in mammals: time and food. *J Biol Rhythms* 18, 250-260.
- Schmidt-Ott, U.M., and Ascheim, D.D. (2006). Thyroid hormone and heart failure. *Current Heart Failure Reports* 3, 114-119.
- Sluka, K.A., Price, M.P., Breese, N.M., Stucky, C.L., Wemmie, J.A., and Welsh, M.J. (2003). Chronic hyperalgesia induced by repeated acid injections in muscle is abolished by the loss of ASIC3, but not ASIC1. *Pain* 106, 229-239.
- Sotelo-Rivera, I., Cote-Vélez, A., Uribe, R.-M., Charli, J.-L., and Joseph-Bravo, P. (2017). Glucocorticoids curtail stimuli-induced CREB phosphorylation in TRH neurons through interaction of the glucocorticoid receptor with the catalytic subunit of protein kinase A. *Endocrine* 55, 861-871.
- Speed, J.S., Hyndman, K.A., Roth, K., Heimlich, J.B., Kasztan, M., Fox, B.M., Johnston, J.G., Becker, B.K., Jin, C., and Gamble, K.L. (2018). High dietary sodium causes dyssynchrony of the renal molecular clock in rats. *American Journal of Physiology-Renal Physiology* 314, F89-F98.
- Sutherland, S.P., Benson, C.J., Adelman, J.P., and McCleskey, E.W. (2001). Acid-sensing ion channel 3 matches the acid-gated current in cardiac ischemia-sensing neurons. *Proc Natl Acad Sci USA* 98, 711-716.
- Takahashi, J.S. (2017). Transcriptional architecture of the mammalian circadian clock. *Nature Reviews Genetics* 18, 164-179.
- Tasker, J.G., and Dudek, F.E. (1991). Electrophysiological properties of neurones in the region of the paraventricular nucleus in slices of rat hypothalamus. *J Physiol (Lond)* 434, 271-293.
- Tolksdorf, F., Mikulec, J., Geers, B., Endig, J., Sprezyna, P., Heukamp, L.C., Knolle, P.A., Kolanus, W., and Diehl, L. (2018). The PDL1-inducible GTPase Arl4d controls T effector function by limiting IL-2 production. *Sci Rep* 8, 1-9.
- Toska, E., Castel, P., Chhangawala, S., Arruabarrena-Aristorena, A., Chan, C., Hristidis, V.C., Cocco, E., Sallaku, M., Xu, G., and Park, J. (2019). PI3K inhibition activates SGK1 via a feedback loop to promote chromatin-based regulation of ER-dependent gene expression. *Cell reports* 27, 294-306.
- Tsui, K.H., Chiang, K.C., Lin, Y.H., Chang, K.S., Feng, T.H., and Juang, H.H. (2018). BTG2 is a tumor suppressor gene upregulated by p53 and PTEN in human bladder carcinoma cells. *Cancer medicine* 7, 184-195.

- Tymianski, M., Charlton, M.P., Carlen, P.L., and Tator, C.H. (1994). Properties of neuroprotective cell-permeant Ca^{2+} chelators: effects on $[\text{Ca}^{2+}]_i$ and glutamate neurotoxicity in vitro. *Journal of neurophysiology* 72, 1973-1992.
- Vaithia, A., Vullo, S., Peng, Z., Alijevic, O., and Kellenberger, S. (2019). Accelerated current decay kinetics of a rare human acid-sensing ion channel 1a variant that is used in many studies as wild type. *Frontiers in molecular neuroscience* 12, 133.
- Van Cauter, E., Sturis, J., Byrne, M.M., Blackman, J.D., Scherberg, N.H., Leproult, R., Refetoff, S., and Van Reeth, O. (1993). Preliminary studies on the immediate phase-shifting effects of light and exercise on the human circadian clock. *J Biol Rhythms* 8 *Suppl*, S99-108.
- Vergne, I., Chua, J., and Deretic, V. (2003). Tuberculosis toxin blocking phagosome maturation inhibits a novel Ca^{2+} /calmodulin-PI3K hVPS34 cascade. *The Journal of experimental medicine* 198, 653-659.
- Vergo, S., Craner, M.J., Etzensperger, R., Attfield, K., Friese, M.A., Newcombe, J., Esiri, M., and Fugger, L. (2011). Acid-sensing ion channel 1 is involved in both axonal injury and demyelination in multiple sclerosis and its animal model. *Brain : a journal of neurology* 134, 571-584.
- Vukicevic, M., and Kellenberger, S. (2004). Modulatory effects of acid-sensing ion channels on action potential generation in hippocampal neurons. *Am J Physiol Cell Physiol* 287, C682-690.
- Waldmann, R., Champigny, G., Bassilana, F., Heurteaux, C., and Lazdunski, M. (1997). A proton-gated cation channel involved in acid-sensing. *Nature* 386, 173-177.
- Walker, W.H., 2nd, Walton, J.C., DeVries, A.C., and Nelson, R.J. (2020). Circadian rhythm disruption and mental health. *Transl Psychiatry* 10, 28.
- Wang, K., Kretschmannova, K., Prévède, R.M., Smiljanic, K., Chen, Q., Fletcher, P.A., Sherman, A., and Stojilkovic, S.S. (2020). Cell-Type-Specific Expression Pattern of Proton-Sensing Receptors and Channels in Pituitary Gland. *Biophysical Journal* 119, 2335-2348.
- Wang, Y.Z., Wang, J.J., Huang, Y., Liu, F., Zeng, W.Z., Li, Y., Xiong, Z.G., Zhu, M.X., and Xu, T.L. (2015). Tissue acidosis induces neuronal necroptosis via ASIC1a channel independent of its ionic conduction. *Elife* 4.
- Wang, Y.Z., and Xu, T.L. (2011). Acidosis, acid-sensing ion channels, and neuronal cell death. *Molecular neurobiology* 44, 350-358.
- Wemmie, J.A., Askwith, C.C., Lamani, E., Cassell, M.D., Freeman, J.H., Jr., and Welsh, M.J. (2003). Acid-sensing ion channel 1 is localized in brain regions with high synaptic density and contributes to fear conditioning. *J Neurosci* 23, 5496-5502.
- Wemmie, J.A., Chen, J., Askwith, C.C., Hruska-Hageman, A.M., Price, M.P., Nolan, B.C., Yoder, P.G., Lamani, E., Hoshi, T., Freeman, J.H., Jr., *et al.* (2002). The acid-activated ion channel ASIC contributes to synaptic plasticity, learning, and memory. *Neuron* 34, 463-477.
- Wemmie, J.A., Tauger, R.J., and Kreple, C.J. (2013). Acid-sensing ion channels in pain and disease. *Nature reviews Neuroscience* 14, 461-471.
- Wu, P.Y., Huang, Y.Y., Chen, C.C., Hsu, T.T., Lin, Y.C., Weng, J.Y., Chien, T.C., Cheng, I.H., and Lien, C.C. (2013). Acid-sensing ion channel-1a is not required for normal hippocampal LTP and spatial memory. *J Neurosci* 33, 1828-1832.
- Xiong, Z.G., Zhu, X.M., Chu, X.P., Minami, M., Hey, J., Wei, W.L., MacDonald, J.F., Wemmie, J.A., Price, M.P., Welsh, M.J., *et al.* (2004). Neuroprotection in ischemia: blocking calcium-permeable acid-sensing ion channels. *Cell* 118, 687-698.

- Yamazaki, S., Kerbeshian, M.C., Hocker, C.G., Block, G.D., and Menaker, M. (1998). Rhythmic properties of the hamster suprachiasmatic nucleus *in vivo*. *Journal of Neuroscience* *18*, 10709-10723.
- Yan, A., Chen, Y., Chen, S., Li, S., Zhang, Y., Jia, J., Yu, H., Liu, L., Liu, F., and Hu, C. (2017). Leptin stimulates prolactin mRNA expression in the goldfish pituitary through a combination of the pi3k/akt/mTOR, mkk3/6/p38mapk and mek1/2/erk1/2 signalling pathways. *International journal of molecular sciences* *18*, 2781.
- Yang, G., Chen, L., Grant, G.R., Paschos, G., Song, W.-L., Musiek, E.S., Lee, V., McLoughlin, S.C., Grosser, T., and Cotsarelis, G. (2016). Timing of expression of the core clock gene *Bmal1* influences its effects on aging and survival. *Science translational medicine* *8*, 324ra316-324ra316.
- Yang, L., Dan, H.C., Sun, M., Liu, Q., Sun, X.-m., Feldman, R.I., Hamilton, A.D., Polokoff, M., Nicosia, S.V., and Herlyn, M. (2004). Akt/protein kinase B signaling inhibitor-2, a selective small molecule inhibitor of Akt signaling with antitumor activity in cancer cells overexpressing Akt. *Cancer research* *64*, 4394-4399.
- Yang, L., Hu, X., and Mo, Y.-Y. (2019). Acidosis promotes tumorigenesis by activating AKT/NF- κ B signaling. *Cancer and Metastasis Reviews* *38*, 179-188.
- Yang, L., and Palmer, L.G. (2014). Ion conduction and selectivity in acid-sensing ion channel 1. *J Gen Physiol* *144*, 245-255.
- Yang, S., Yang, H., Chang, R., Yin, P., Yang, Y., Yang, W., Huang, S., Gaertig, M.A., Li, S., and Li, X.-J. (2017). MANF regulates hypothalamic control of food intake and body weight. *Nature communications* *8*, 1-16.
- Yang, X., Downes, M., Yu, R.T., Bookout, A.L., He, W., Straume, M., Mangelsdorf, D.J., and Evans, R.M. (2006). Nuclear Receptor Expression Links the Circadian Clock to Metabolism. *Cell* *126*, 801-810.
- Yu, L., Su, Y.-s., Zhao, J., Wang, H., and Li, W. (2013). Repression of NR4A1 by a chromatin modifier promotes docetaxel resistance in PC-3 human prostate cancer cells. *FEBS letters* *587*, 2542-2551.
- Yu, Z., Wu, Y.J., Wang, Y.Z., Liu, D.S., Song, X.L., Jiang, Q., Li, Y., Zhang, S., Xu, N.J., Zhu, M.X., *et al.* (2018). The acid-sensing ion channel ASIC1a mediates striatal synapse remodeling and procedural motor learning. *Sci Signal* *11*.
- Zee, P.C., Attarian, H., and Videnovic, A. (2013). Circadian rhythm abnormalities. *Continuum (Minneapolis, Minn)* *19*, 132-147.
- Zhang, P., Li, G., Li, H., Tan, X., and Cheng, H.-Y.M. (2017). Environmental perturbation of the circadian clock during pregnancy leads to transgenerational mood disorder-like behaviors in mice. *Sci Rep* *7*, 1-14.
- Ziemann, A.E., Schnitzler, M.K., Albert, G.W., Severson, M.A., Howard, M.A., 3rd, Welsh, M.J., and Wemmie, J.A. (2008). Seizure termination by acidosis depends on ASIC1a. *Nat Neurosci* *11*, 816-822.

FIGURE LEGENDS

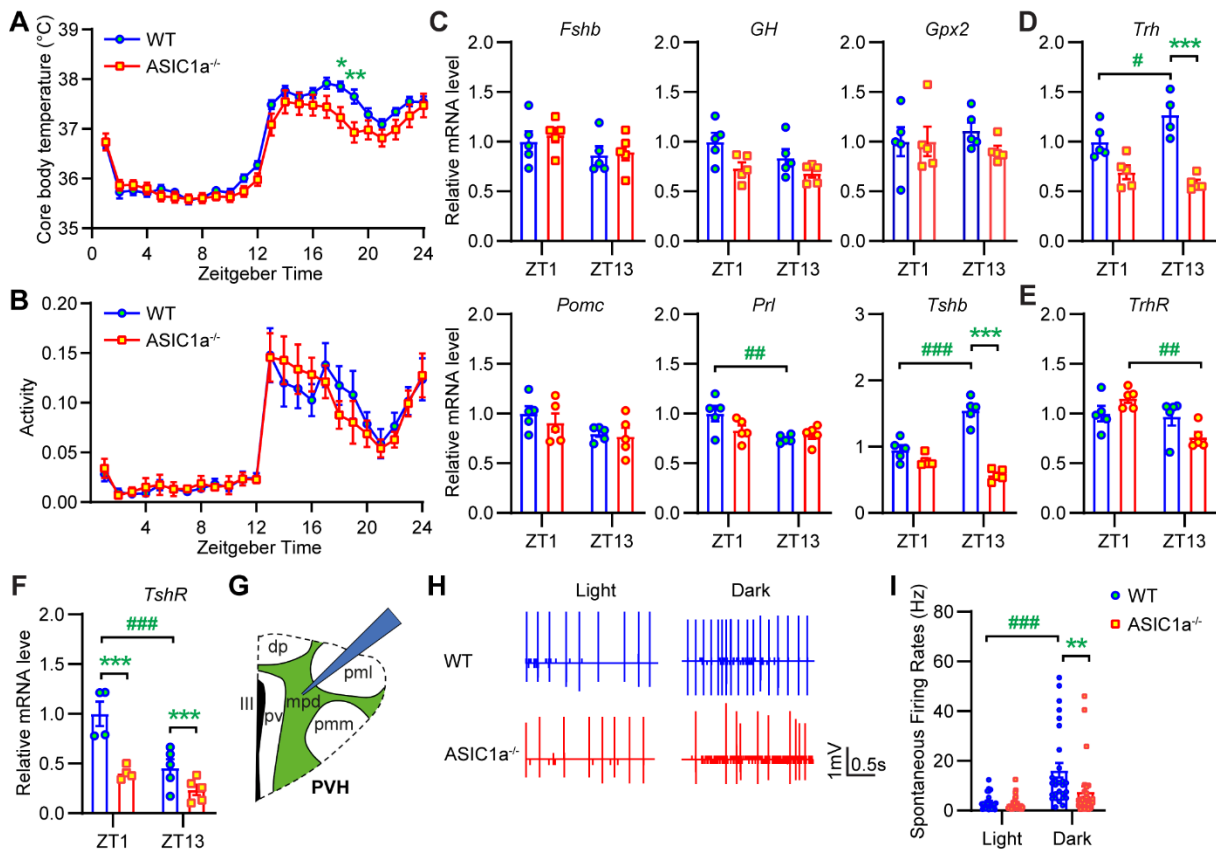


Figure 1. ASIC1a regulates the activity of hypothalamus neurosecretory neurons and controls body temperature *via* the hypothalamic–pituitary–thyroid axis. **A**, Core body temperature rhythm for 24 h under LD cycle, $n=11-12$. Data are presented as mean \pm SEM, compared to corresponding ZT time by one-way ANOVA test and Dunnett's *post-hoc* test, *, $p<0.05$; **, $p<0.01$. **B**, Daily profile of locomotor activity in LD cycle. Activity counts are expressed as percentage of daily total, $n=11-12$. **C-F**, *Fshb*, *Gh*, *Gpx2*, *Pomc*, *Prl* and *Tshb* mRNA levels in pituitary (**C**), *Trh* mRNA levels in hypothalamus (**D**), *TrhR* mRNA levels in pituitary (**E**), *TshR* mRNA levels in thyroid gland (**F**) were quantified by real-time qRT-PCR. The mean relative expression of each gene in WT mice at ZT1 was set to 1. Results for each mouse are presented as relative quantity over the mean of the WT at ZT1. Data are presented as mean \pm SEM, $n=4-5$. *, $p<0.05$; **, $p<0.01$; ***, $p<0.001$; compared WT to corresponding ZT ASIC1a^{-/-} by two-way ANOVA test and Holm-Sidak's *post-hoc* test. #, $p<0.05$; ##, $p<0.01$; ###, $p<0.001$; comparison of each ZT with the corresponding genotype by two-way ANOVA test and Holm-Sidak's *post-hoc* test. **G**, Experimental scheme of the coronal PVH slice map, recorded in loose-patch mode on mpd neurons. pv, periventricular parvocellular division; mpd, dorsal portion of the medial parvocellular division; dp, dorsal parvocellular division; pml, posterior magnocellular lateral division; pmm, posterior magnocellular medial division; III, third

ventricle. **H**, Representative traces recorded with the loose-patch technique during the day (left) and night (right) from WT (blue) and ASIC1a^{-/-} (red) mice brain slices. **I**, Dot plot of individual mpd neuron SFR from WT and ASIC1a^{-/-} mice during the day or night cycle. Cells not firing APs were not included in this analysis. Data are presented as mean ± SEM, *n*=26-30 cells from 4 mice in each condition. **, *p*<0.01; WT compared to ASIC1a^{-/-} in the same period, two-way ANOVA test and Holm-Sidak's *post-hoc* test ###, *p*<0.001; comparison between day and night with the corresponding genotype by two-way ANOVA test and Holm-Sidak's *post-hoc* test.

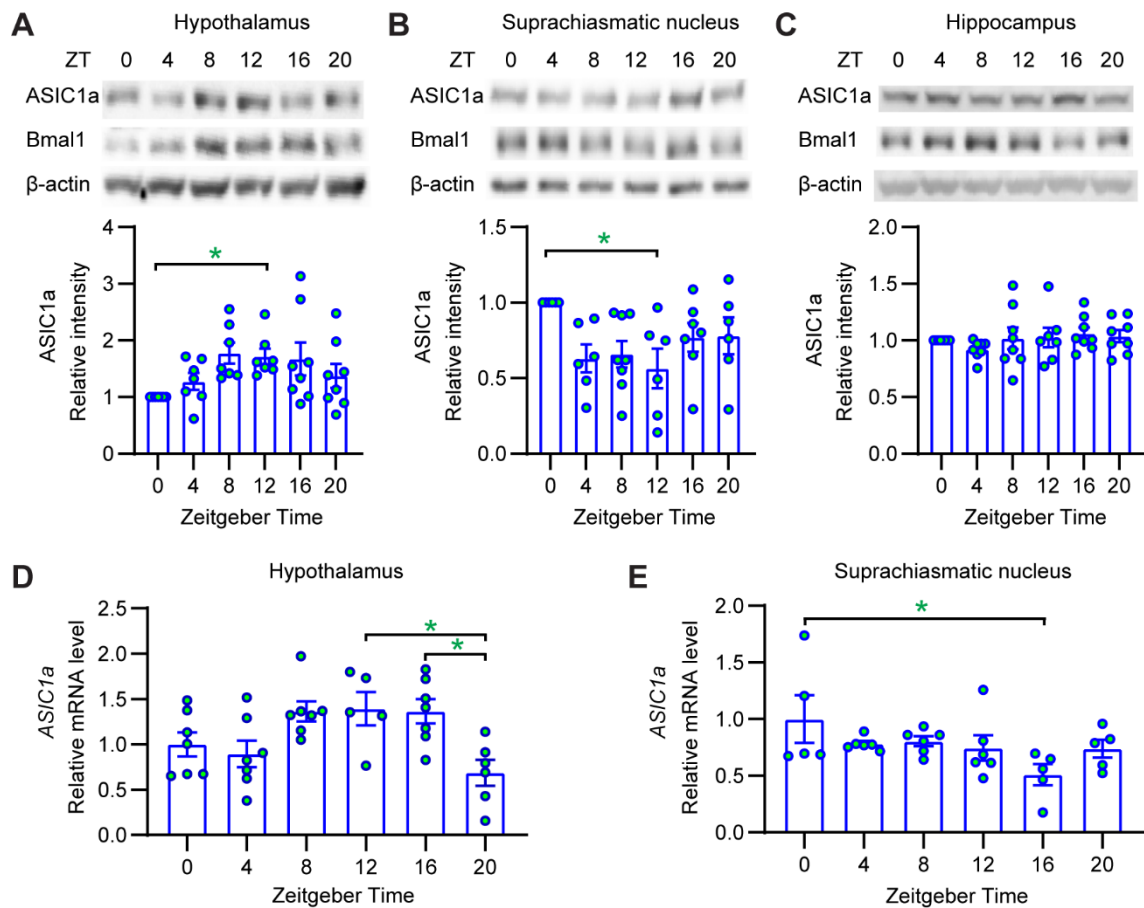


Figure 2. Circadian expression of ASIC1a in mouse brain. The biochemical experiments were carried out with the indicated tissues of male mice, and proteins were separated by SDS-PAGE. **A-C**, Representative Western blots of ASIC1a, Bmal1 and β-actin expression are shown for each protein across each ZT in hypothalamus (**A**), suprachiasmatic nucleus (**B**) and hippocampus (**C**). β-actin was used as a control for the total protein, and Bmal1 as the positive control. Quantification of ASIC1a expression from the independent experiments is shown in the lower panels. The mean relative expression of each mouse is normalized to ZT0 in each independent experiment, $n=6-7$. *, $p<0.05$; compared with each other by one-way ANOVA test and Dunnett's *post-hoc* test. **D-E**, Real-time qRT-PCR analysis of *ASIC1a* expression in mouse hypothalamus (**D**) and suprachiasmatic nucleus (**E**). The mean relative expression of *ASIC1a* at ZT0 was set to 1. Results for each mouse are presented as relative quantity over the mean of the ZT0 group. Data are presented as mean \pm SEM, $n=5-7$. *, $p<0.05$; compared with each other by one-way ANOVA test and Dunnett's *post-hoc* test.

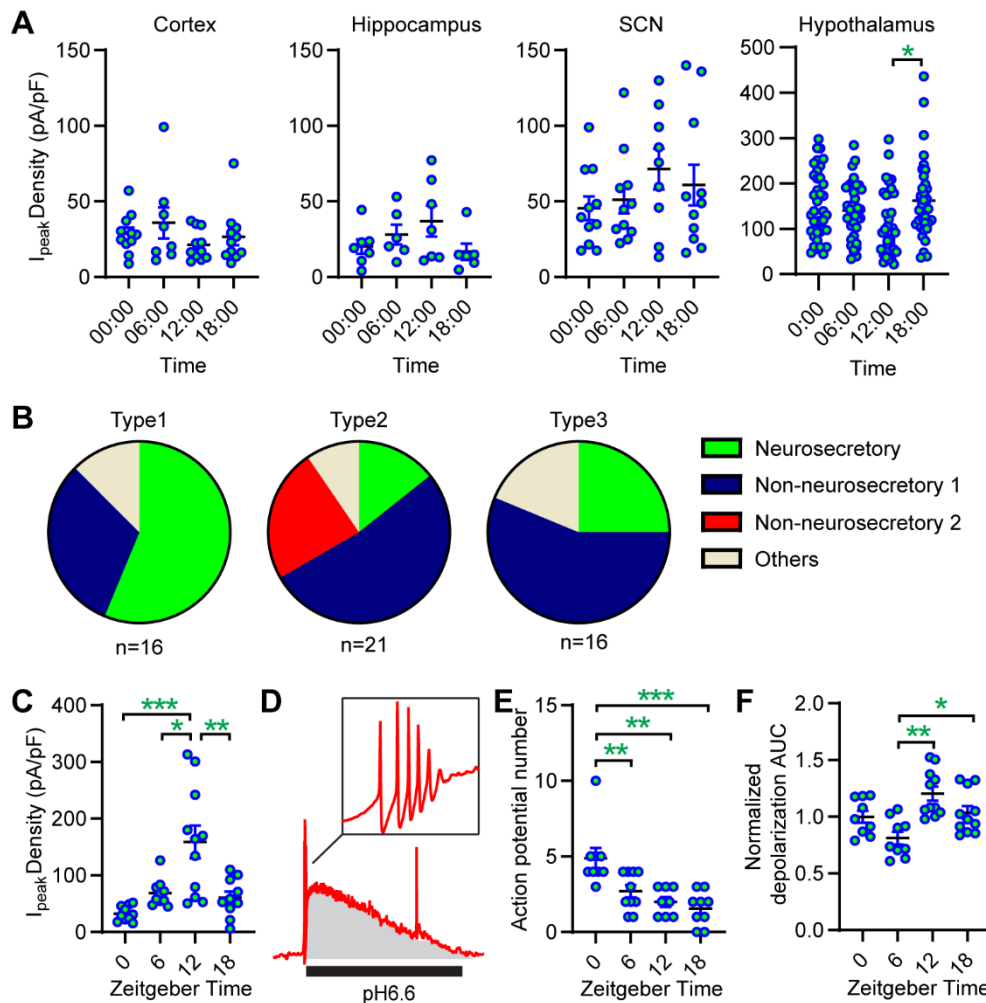


Figure 3. Circadian rhythm of acid-induced currents in cultured mouse brain neurons. **A**, Peak current densities of pH6.6-induced current at the indicated time in cultured mouse neurons. The currents were measured by whole-cell voltage-clamp at -60mV . In these experiments, the neurons were not synchronized by Dexamethasone treatment. Mean \pm SEM is also indicated, $n=6-39$. *, $p<0.05$; compared with each other by one-way ANOVA test and Dunnett's *post-hoc* test. **B**, Cultured hypothalamus neurons were classified into types 1-3 as indicated in supplemental Figure S2. Neurons were exposed to current protocols, indicated in supplemental Figure S2, to determine the proportion of secretory and non-secretory neurons. **C-E**, data were obtained after synchronization by $1\mu\text{M}$ Dexamethasone treatment of cultured mouse neurosecretory Type 1 hypothalamus neurons. **C**, Peak current densities of pH6.6-induced currents at the indicated ZT time. The currents were measured by whole-cell voltage-clamp at -60mV at the indicated ZT time. Data are presented as mean \pm SEM, $n=10-11$. *, $p<0.05$; **, $p<0.01$; ***, $p<0.001$; compared with each other by one-way ANOVA test and Dunnett's *post-hoc* test. **D**, Representative voltage traces obtained with whole-cell current-clamp of pH6.6-induced depolarization. **E**, Number of pH6.6-induced APs at the indicated ZT time, measured

by whole-cell current-clamp. **F**, Normalized AUC of the depolarization (voltage x time, grey area in **D**) of pH6.6-induced depolarization at the indicated ZT time, measured by whole-cell current-clamp. Data are presented as mean \pm SEM, $n=8-10$. *, $p<0.05$; **, $p<0.01$; ***, $p<0.001$; compared with each other by one-way ANOVA test and Dunnett's *post-hoc* test.

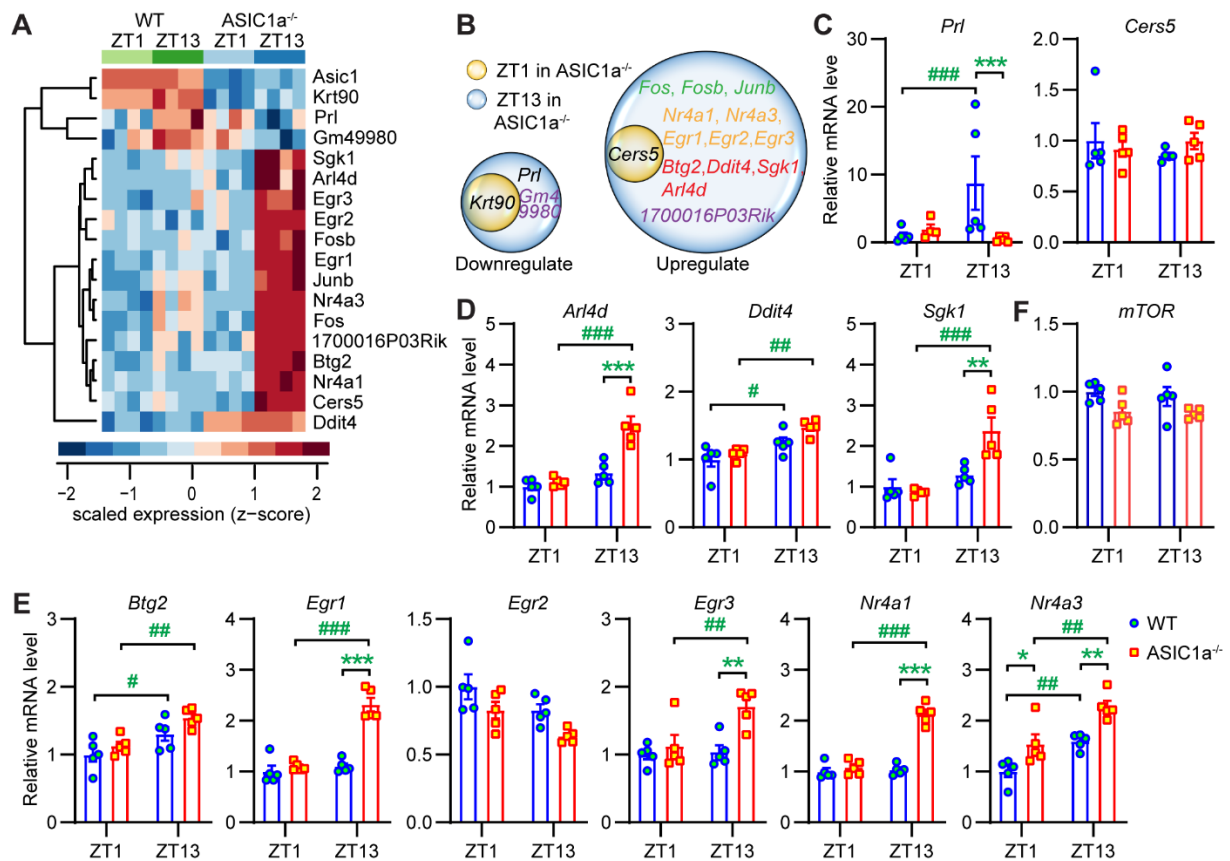


Figure 4. Effects of ASIC1a on the hypothalamus transcriptome. **A**, Heat map representing significantly altered transcripts ($P < 0.005$) in hypothalamus across the genotypes. Samples are in columns and genes are in rows. High expression is displayed in red (z -score > 1) while low expression in blue (z -score < 1). **B**, Venn diagrams comparing the expression-changed genes were drawn based on the RNA-seq data sets. **C-F**, Real-time qRT-PCR analysis to identify the gene expression change of functional (**C**), kinase (**D**) and transcription factor genes (**E**) and the mTOR gene (**F**). The mean relative expression of each gene in WT mice at ZT1 was set to 1. Results for each mouse are presented as relative quantity over the mean of the WT at ZT1 group. Data are presented as mean \pm SEM, $n=4-5$. *, $p < 0.05$; **, $p < 0.01$; ***, $p < 0.001$; WT compared to ASIC1a^{-/-} at the corresponding ZT, two-way ANOVA and Holm-Sidak's *post-hoc* test. #, $p < 0.05$; ##, $p < 0.01$; ###, $p < 0.001$; comparison for a given genotype between the ZT conditions, two-way ANOVA test and Holm-Sidak's *post-hoc* test.

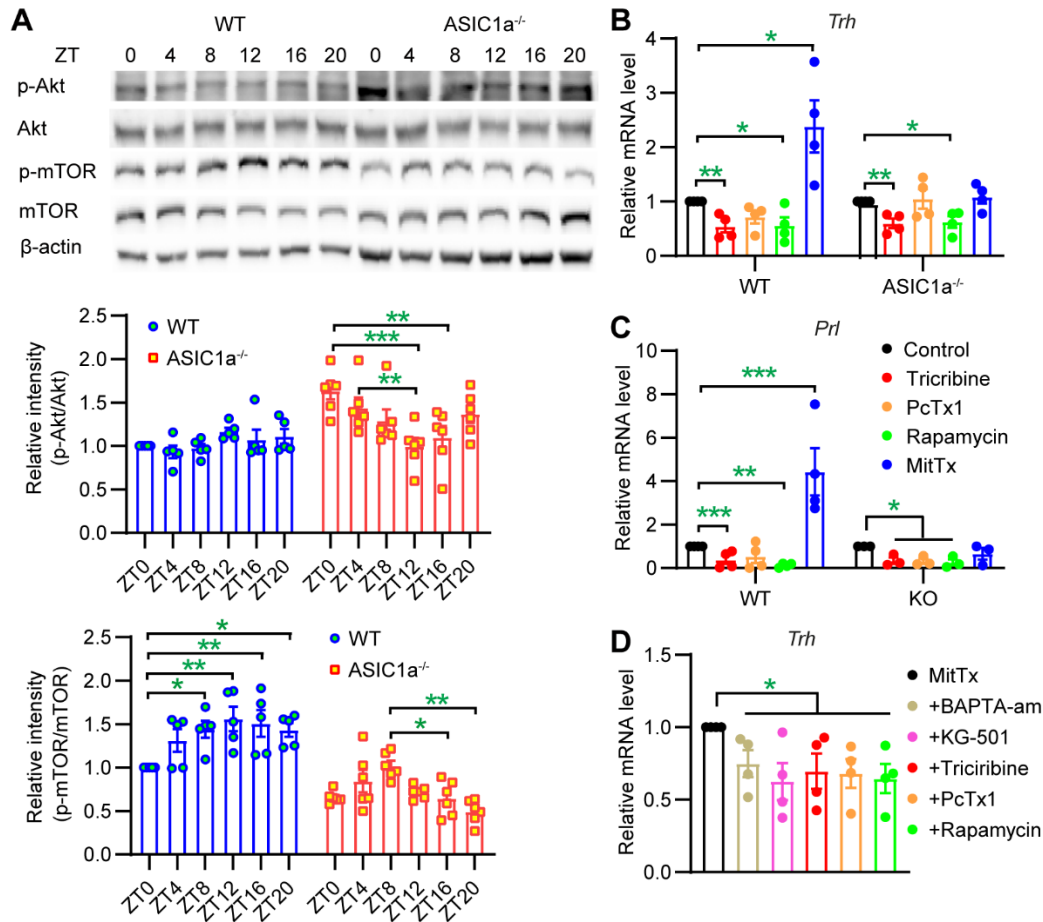


Figure 5. Activation of ASIC1a regulates the expression of *Trh* and *Prl* via the Akt-mTOR pathway. **A**, Representative Western blots of Akt, p-Akt, mTOR, p-mTOR and β -actin expression are shown for each protein across each ZT in WT and ASIC1a^{-/-} mouse hypothalamus as indicated (top panel). The biochemical experiments were carried out in male mice. Quantification of p-Akt/Akt (center panel) and p-mTOR/mTOR expression (bottom panel) from the independent experiments. The mean relative expression of each mouse was normalized to WT at ZT0 in each independent experiment, $n=5-6$. *, $p<0.05$; compared with each other by one-way ANOVA test and Dunnett's *post-hoc* test. **B-C**, Real-time qRT-PCR analysis of *Trh* (**B**) and *Prl* (**C**) expression in cultured hypothalamus neurons. Cultured neurons were exposed to Triciribine (10 μ m), PcTx1 (10nM), Rapamycin (200nM), MitTx (2nM) or vehicle (control) for 2 h. **D**, Real-time qRT-PCR analysis of *Trh* expression in cultured WT hypothalamus neurons exposed during 2h to 2 nM MitTx. Neurons were pretreated for 30min and then co-exposed for 2h with MitTx and the following inhibitors: BAPTA-AM (30 μ M), KG-501 (10 μ M), Triciribine (10 μ m), PcTx1 (10nM), Rapamycin (200nM). Results for each mouse are presented relative to the mean of the control (B-C) or MitTx-alone condition (**D**). Data are presented as mean \pm SEM, $n=4$. *, $p<0.05$; **, $p<0.01$; ***, $p<0.001$; compared with control (**B-C**) or MitTx (**D-E**) by one-way ANOVA test and Tukey honesty *post-hoc* test.

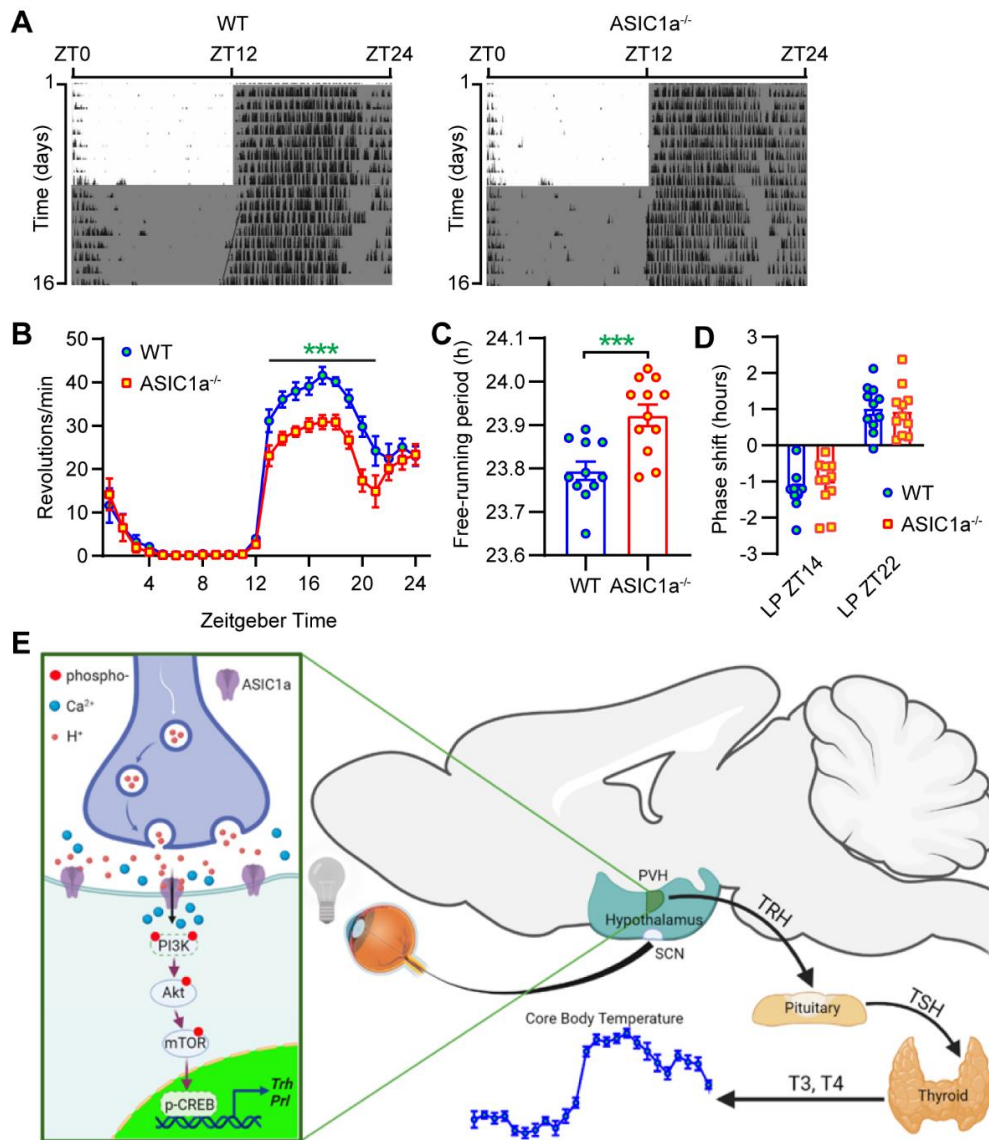


Figure 6. ASIC1a is necessary for the light adaptation of the circadian rhythm of wheel-running activity. **A**, Representative double-plotted actograms of wheel-running activity profile of a WT (left) and ASIC1a^{-/-} (right) mouse under 12 h light:12 h dark (LD) or constant dark (DD, lower half) are shown. Daily wheel-running activity profiles of mice were binned at 5 min intervals, and periods of darkness are shown by dark shading. **B**, WT and ASIC1a^{-/-} mice were entrained under LD cycle and their locomotor activity was recorded over 8 days. The average amounts of wheel revolutions over 24 h during these 8 days were calculated in 5 min time bins for both genotypes, $n=11-12$. **C**, WT and ASIC1a^{-/-} mice were transferred to DD cycle and locomotor activity recordings from days 9 to 16 in free-running conditions were used to assess their internal period length with the Chi2 periodogram analysis, $n=11-12$. The bar and error bars indicate mean \pm SEM. ***, $p<0.001$, compared to control, by unpaired Student's t -test. **D**, Phase-response curves of response to light of WT and ASIC1a^{-/-} mice. For each light pulse administered at different circadian times (ZT14 and ZT22), animals were entrained to a LD

cycle for 2 weeks before being released in constant darkness for 10 d. The pulse (200 lux, 1s) was administered on the first night after the end of LD or on the first subjective day in DD, and phase shifts were calculated, $n=11-12$. **E**, A diagram summarizing the findings of the current work (created with BioRender). Postsynaptic ASIC1a channels are activated by drops in the pH in the synaptic cleft in PVH under dark condition, leading to Ca^{2+} influx. The increase in intracellular Ca^{2+} activates the downstream PI3K/Akt/mTOR/CREB signaling pathway. The Akt-mTOR pathway presumably contributes to the expression of *Trh* to promote the release of TRH from the PVH of hypothalamus. TRH stimulates the release of TSH from pituitary and promote the secretion of T3 and T4 from the thyroid gland to regulate the body temperature. Together, the ASIC1a-Akt-mTOR signaling cascade represents a novel molecular mechanism that regulates the expression of *Trh* in the hypothalamus, which is important for the regulation of the daily cycle of the body temperature.

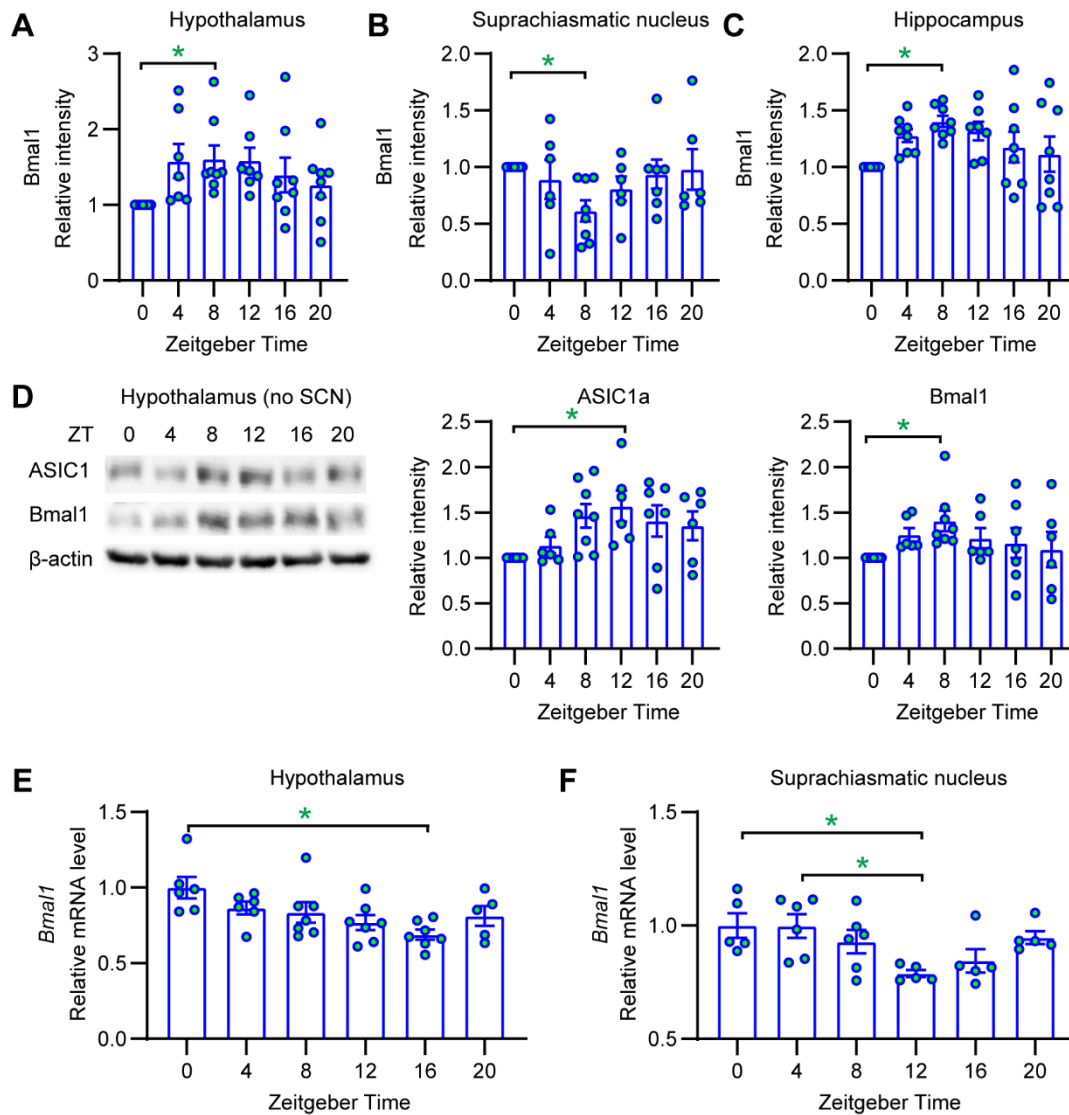


Figure S1. Circadian expression of ASIC1a and Bmal1 in mouse. **A-C**, Quantification of Bmal1 expression in hypothalamus (**A**), suprachiasmatic nucleus(**B**) and hippocampus (**C**). from the independent experiments illustrated in Figure 2A-C. The mean relative expression of each mouse is normalized to that at ZT0 in each corresponding experiment, $n=6-7$. *, $p<0.05$; compared with each other by one-way ANOVA test and Dunnett's *post-hoc* test. **D**, Representative Western blots of ASIC1a, Bmal1 and β -actin expression for the indicated proteins at the indicated ZT in hypothalamus without the suprachiasmatic nucleus (left). β -actin was used as a control for the total protein. Quantification of ASIC1a (center) and Bmal1 (right) expression from the independent experiments. The mean relative expression of each protein is normalized to ZT0 in each independent experiment, $n=6-7$. *, $p<0.05$; compared with each other by one-way ANOVA test and Dunnett's *post-hoc* test. **E-F**, Real-time qRT-PCR analysis of Bmal1 expression in mouse hypothalamus (**E**) and suprachiasmatic nucleus (**F**). The mean relative expression of Bmal1 at ZT0 was set to 1. Results for each mouse are presented as

relative quantity over the mean of the ZT0 group. Data are presented as mean \pm SEM, $n=5-7$.

*, $p<0.05$; compared with each other by one-way ANOVA test and Dunnett's *post-hoc* test.

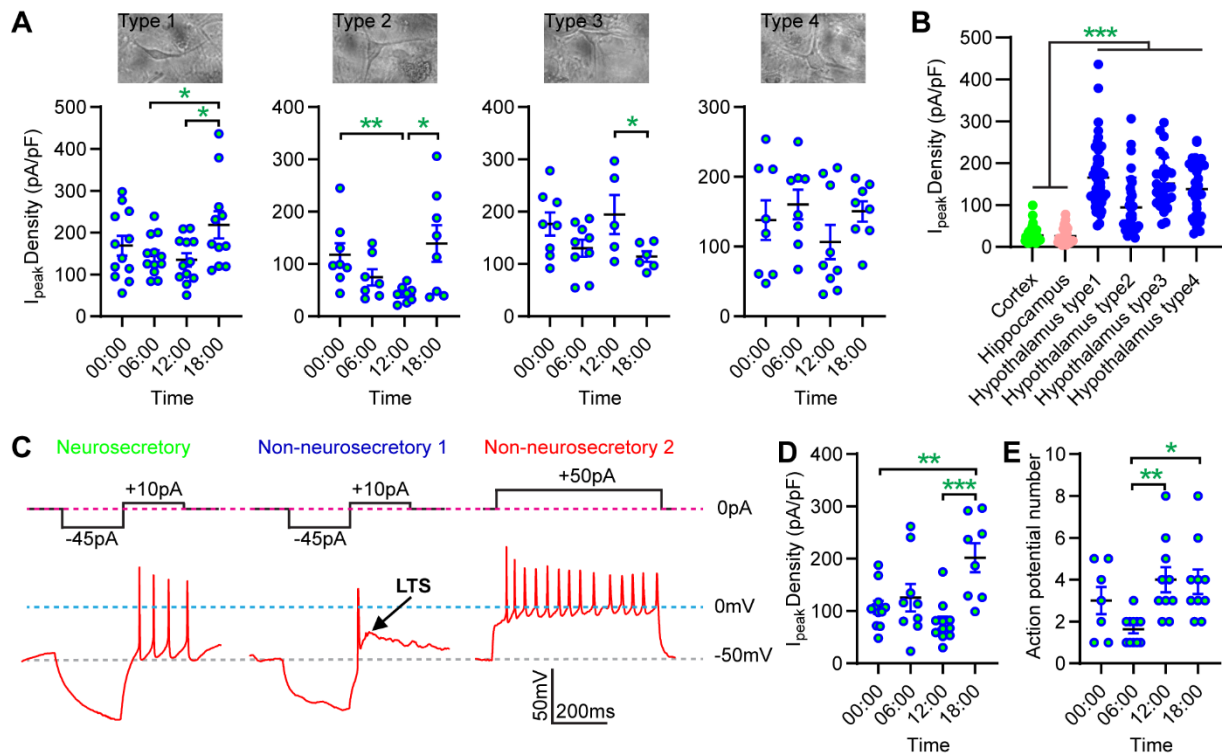


Figure S2. Circadian rhythm of ASIC currents in subtypes of cultured mouse hypothalamus neurons. **A**, Representative images of four typical morphology-based types of cultured hypothalamus neurons at day 12 (top panels). The peak current densities of pH6.6-induced current at the indicated time are indicated for each of the four types of hypothalamus neurons (bottom panels). **B**, Peak current densities of pH6.6-induced current in cultured mouse brain neurons, as indicated, over one circadian cycle. The data obtained at 4 different time points are pooled for presentation. **A-B**, The currents were measured by whole-cell voltage-clamp at -60mV from cultured neurons at the indicated time. Data are presented as mean \pm SEM, $n=6-39$. *, $p<0.05$; **, $p<0.01$; compared with each other by one-way ANOVA test and Dunnett's *post-hoc* test. **C**, Electrogenic properties of cultured hypothalamus neurons to classify them into neurosecretory and non-neurosecretory neurons (Luther et al., 2002; Tasker and Dudek, 1991). Current protocols were applied to cells under whole-cell current clamp. The protocol shown in the left and center panel was applied first, from the resting membrane potential. If the neuron responded with 1 or several APs as indicated in the left panel, but no low-threshold spike (LTS, see center panel), it was classified as a neurosecretory neuron. If it responded with an LTS and at least one AP, it was classified as non-neurosecretory neuron (center panel). If the protocol used in the left and center panel did not induce AP, the current protocol shown in the right panel was applied. If a burst of APs was induced, the neuron was classified as "non-neurosecretory", and if not as "others". **D**, Peak current densities of pH6.6-induced current at the indicated time

in cultured mouse neurosecretory Type 1 hypothalamus neurons. The currents were measured by whole-cell voltage-clamp at -60mV from cultured hypothalamus neurons. **E**, The pH6.6-induced AP at the indicated time in cultured mouse neurosecretory Type 1 hypothalamus neuron. The AP was measured by whole-cell current-clamp from cultured hypothalamus. **D-E**, Data are presented as mean \pm SEM, $n=7-11$. *, $p<0.05$; **, $p<0.01$; compared with each other by one-way ANOVA test and Dunnett's *post-hoc* test. Note that in the experiments of this figure the cultured cells had not been synchronized.

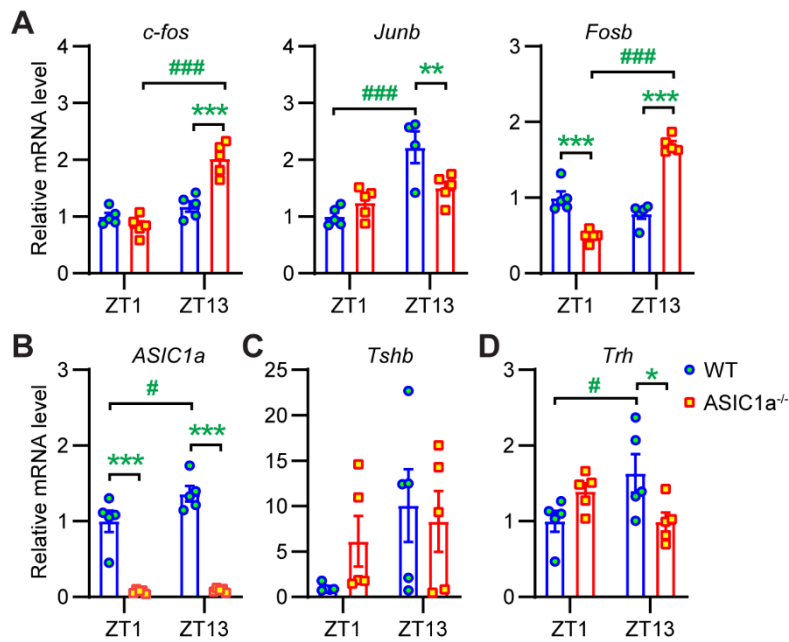


Figure S3. Circadian expression of hypothalamus genes. **A-D**, Real-time qRT-PCR analysis to identify the gene expression change of early response genes (**A**), *ASIC1a* (**B**), *Tshb* (**E**) and *Trh* (**F**). The mean relative expression of each gene in WT mice at ZT1 was set to 1. Results for each mouse are presented as relative quantity over the mean of the WT at ZT1 group. Data are presented as mean \pm SEM, $n=4-5$. *, $p<0.05$; **, $p<0.01$; ***, $p<0.001$; compared WT to corresponding ZT ASIC1a^{-/-} by two-way ANOVA test and Holm-Sidak's *post-hoc* test. #, $p<0.05$; ##, $p<0.01$; ###, $p<0.001$; comparison of each ZT with the corresponding genotype by two-way ANOVA test and Holm-Sidak's *post-hoc* test.

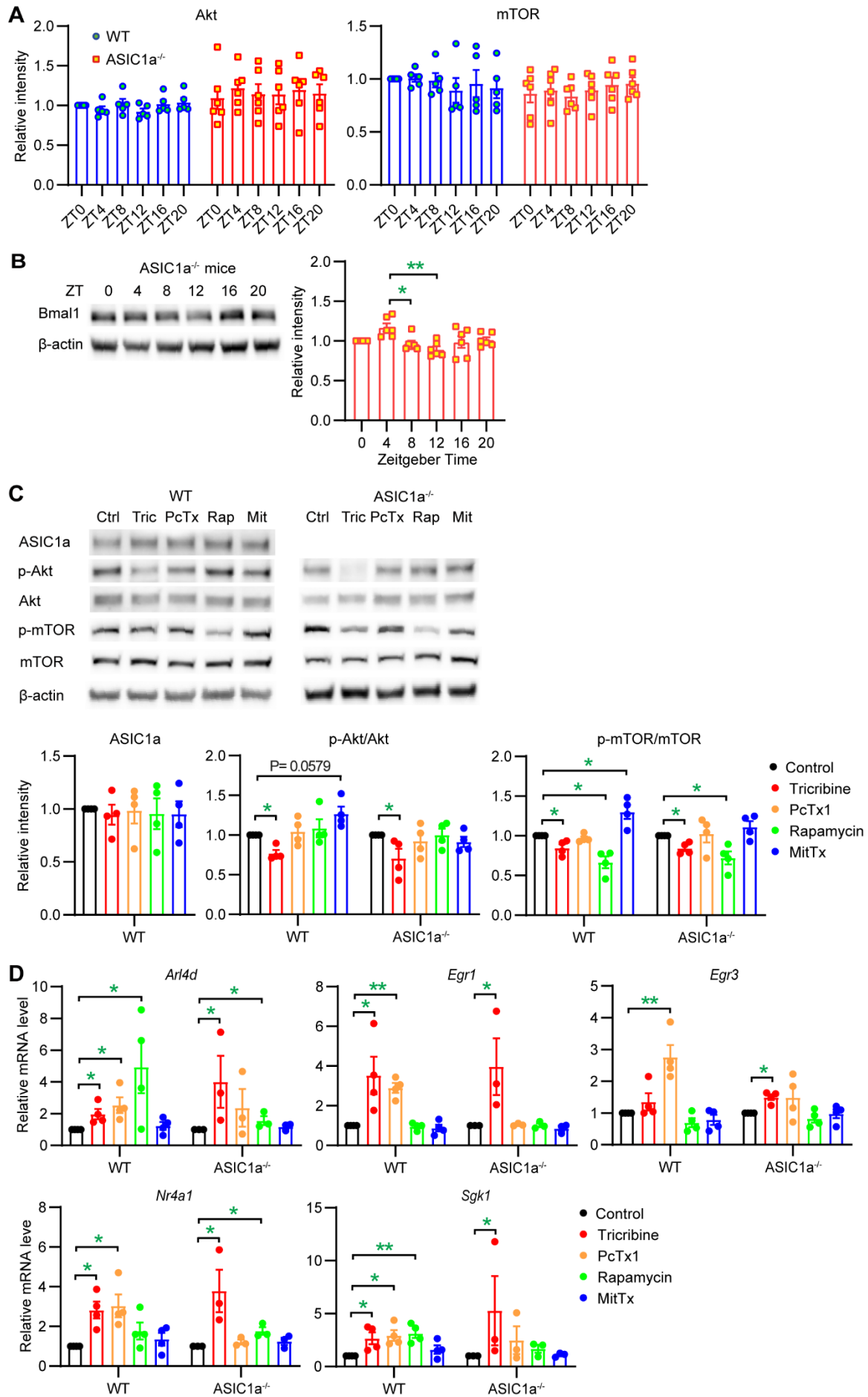


Figure S4. The regulation of the Akt-mTOR pathway. **A**, Quantification of Akt and mTOR expression from the independent experiments of hypothalamus tissue, as shown in figure 5A. β -actin was used as a control for the total protein. The mean relative expression of each mouse is normalized to WT at ZT0 in each independent experiment, $n=5-6$. **B**, Representative Western blots of Bmal1 and β -actin expression are shown for each protein across each ZT in ASIC1a^{-/-} mouse hypothalamus (left). β -actin was used as a control for the total protein. Right, Quantification of Bmal1 expression. The mean relative expression of each mouse was normalized to ZT0 in each independent experiment, $n=6$. *, $p<0.05$; **, $p<0.05$; compared to each other by one-way ANOVA test and Dunnett's *post-hoc* test. **C**, Representative Western blots of ASIC1a, Akt, p-Akt, mTOR, p-mTOR and β -actin expression are shown for each protein across each condition in WT and ASIC1a^{-/-} cultured cortical neurons treated with Triciribine (10 μ m), PcTx1 (10nM), Rapamycin (200nM), MitTx (2nM) or vehicle (control) for 2 hours as indicated (upper panels). Lower panels, quantification of ASIC1a (left), p-Akt/Akt ratio (center) and p-mTOR/mTOR ratio (right) expression. The mean relative expression of each mouse is normalized to control in each independent experiment, $n=4$. *, $p<0.05$; compared with control by one-way ANOVA test and Tukey honesty *post-hoc* test. **D**, Real-time qRT-PCR analysis of *Arl4d*, *Egr1*, *Nr4a1* and *Sgk1* expression in cultured hypothalamus neurons (from the same samples as those used in figure 5B-C). Cultured neurons were treated with Triciribine, PcTx1, Rapamycin, MitTx or vehicle (control) for 2 hours as indicated.

4. General Discussion

4.1 Mechanism and function of ASIC regulation by H₂S

4.1.1 H₂S potentiates ASIC currents in CHO cell

ASICs are gated by extracellular protons and induce ion influx. ASICs conduct cations, including Na⁺ and Ca²⁺, but their conductance of Na⁺ is the most physiologically relevant process¹³². The physiological functions of ASICs include fear conditioning, spine morphogenesis, acid-sensing²⁸⁴. Dysfunction of ASIC is associated with the development of diverse neurological diseases, including pain, itch, ischemic neuronal cell death, epileptic seizure, and neurodegenerative diseases²⁸⁵. In this study, we found that H₂S regulates the expression of ASICs *via* the MAPK-Erk1/2 signaling pathway. H₂S donors increased the acid-induced ASIC1a peak currents in a time- and concentration-dependent manner. H₂S donor GYY4137 increased the total and plasma membrane expression of ASIC1a, and GYY4137 also enhanced the activation of MAPK-Erk1/2 pathway. However, it was also shown that Erk1/2 can be activated by ASIC-mediated cell signaling. Inhibition of Erk1/2 suppressed the ASIC1a-induced increase of NF-κB activity²⁸⁶. Current rundown response to successive acid stimulations can be observed that is usual for ASIC1a^{287,288}. In this study, the peak current amplitude does not decrease after 1 hour of recording in CHO cells expressed ASIC1a without NaHS treatment (Figure 1B in project 1). It may be due to the slight acidic stimulation increasing the activation of Erk1/2 to potentiate the expression of ASIC1a in the plasma membrane and neutralize the rundown of ASIC peak current.

4.1.2 H₂S regulates ASICs in a biphasic manner

H₂S is a vital gaseous signaling molecule in the body and has an essential physiological role in regulating life activities²⁸⁹. H₂S is produced by three enzymes: CBS, CSE and 3MST¹¹¹⁻¹¹³. H₂S may be released from these enzymes and then immediately function as a signaling molecule, or it may be stored as a fixed form of thiane sulfur and then be released when the cell receives a physiological signal. H₂S sometimes has contrasting effects, with the same concentration of H₂S having different physiological effects on various tissues^{290,291}. Such as, H₂S increases Ca²⁺

influx in neurons and astrocytes by enhancing the activity of NMDA receptors. In contrast, Ca^{2+} influx is decreased in retinal neurons via the activation of V-ATPase²⁹². The effect of different concentrations of H_2S donors on ASICs was biphasic. The appropriate concentration of H_2S increasing ASIC currents, whereas lower or higher concentrations of H_2S donors do not increase the ASIC currents (Figure 4A and C in project 1). The time-dependence of H_2S on ASICs was also biphasic. ASICs currents were increased in the time span between 1 and 24h, not however at 2 hours after the H_2S treatment (Figure 4B and D in project1). The increase of acid-induced ASIC currents was lost 48h after the H_2S withdrawal.

4.1.3 H_2S may modulate ASICs directly

H_2S regulates the activity of some kinases through intracellular signals²⁹³⁻²⁹⁵. In addition to the adjustment of the signaling pathway activity, H_2S also regulates the direct activation of ion channels, receptors and some enzymes. Studies found that some effects induced by H_2S may be due to forms of sulfur-containing compounds^{296,297}. This study found that WT ASIC current increased continually over 1 hour after a short exposure to H_2S , and that the current was already significantly increased immediately after H_2S treatment (Supplementary Figure 1A in project 1). However, on ASIC1a- ΔCCt , in which the C-terminal Cys residues of ASIC1a were eliminated by mutation and truncation, the acid-induced current increase was not statistically significant increase immediately after H_2S treatment, although the latter increase in current was not different between mutant and WT (Figure 3E in project 1). The current increase was not significantly different at 0 min after 1mM NaHS treatment between the WT and ASIC1a- ΔCCt . Mutation of the intercellular Cys may attenuate the direct effect of H_2S bind on ASIC1a, but does not change the signaling pathway-dependent potentiation. So, H_2S may modulate the intracellular Cys residues of ASICs directly.

4.1.4 Physiological and pathological function of ASICs regulated by H_2S

Recent studies showed that H_2S has a cytoprotective effect in the mammalian brain, heart, and other tissues²⁹⁸.

It was also found that CSE can respond to hypoxia through transcriptional and post-

transcriptional regulation. To some extent, the expression of CSE genes can be regulated by hypoxia^{299,300}. Low body temperature can improve the outcome of ischemic stroke patient³⁰¹. Studies found that the endogenous level of H₂S in the brain was significantly increased after a stroke. And treatment with cysteine, a source for product H₂S, can increase the production of H₂S³⁰². After brain ischemic stroke, learning and memory impairments could be decreased by H₂S donor NaHS, and NaHS could reduce the hippocampal CA1 neuronal injury^{303,304}. Exposure to high concentration of H₂S induces a suspended animation-like state in mice and decreases the core body temperature³⁰⁵. The hypothalamus controls body temperature; the hypothalamus can regulate body temperature by releasing hormones. Our study found that ASIC1a is abundantly expressed in the hypothalamus, and circadian expression of ASIC1a regulates the body temperature. Therefore, H₂S may regulate the expression of ASIC1a in the hypothalamus under stroke conditions. The regulation of ASIC1a by H₂S may induce hypothermia to increase neuroprotective and improve the outcome of the stroke patient.

4.2 Circadian expression of ASIC1a regulates the body temperature.

4.2.1 Circadian rhythm of body temperature

Among the various circadian rhythms, the day and night rhythm of body temperature was found early has been well-studied. Body temperature has an important influence on various vital activities of the body, and many physiological and pathological processes can also affect body temperature and its rhythm^{306,307}. Compared with sleep-wake and other physiological rhythms, the period and phase of the circadian rhythm of body temperature are more stable. In this study, the phase shift under constant darkness conditions was significantly different between the WT and ASIC1a^{-/-} mice (Figure 6C in project 2). Therefore, the circadian rhythm of body temperature is often used as the chronobiological indicator of the body's status, and affects the therapeutic effects^{308,309}.

Under normal living conditions, body temperature exhibits a 24-hour rhythm. There are obvious circadian rhythms of body temperature in animals, but the amplitude, phase and diurnal

variation vary according to the animal species^{256,310}. Mice are nocturnal animals, and their feeding and drinking behaviors are mainly performed at night and rarely occur during the day; their activity level has a distinct circadian rhythm. This study revealed that there is a circadian rhythm of body temperature and regulated by the expression of ASIC1a. The main difference in body temperature between WT and ASIC1a^{-/-} occurred at the dark period, the body temperature of WT mice was significantly higher at ZT16 and ZT17. However, the activity was no different between WT and ASIC1a^{-/-} mice. Therefore, the body temperature difference between WT and ASIC1a^{-/-} mice not depend on the mice activity. The expression of the ASIC1a protein was significantly increased at ZT12 in hypothalamus. The expression of thyrotropin-releasing hormone gene (*Trh*) was also significantly increased at ZT13 in the hypothalamus of WT but not ASIC1a^{-/-} mice. These results indicate that the body temperature difference between WT and ASIC1a^{-/-} mice is depend on the expression of *Trh* in hypothalamus, and the expression of *Trh* was regulated by the circadian expression of ASIC1a.

4.2.2 Regulation of circadian rhythm by the pineal gland

Besides the SCN, the pineal gland can also regulate the circadian biological clocks in mammals. The pineal gland has lost its photosensitivity in mammals, but the destruction of the pineal gland has a significant effect on body temperature³¹¹⁻³¹³. In this study, we find that the expression of ASIC1a has a circadian rhythm in the hypothalamus and SCN, not in the hippocampus and cortex. ASIC1a is widely expressed in the pineal gland, but whether the expression of ASIC1a has a circadian rhythm in the pineal gland is still unclear. And the pineal gland regulates circadian rhythmic changes in body temperature and activity in mice has not been fully investigated. There is a link between the pineal gland and its hormone melatonin with the regulation of body temperature in animals, melatonin intervenes in generating seasonal rhythms and decreases the body temperature³¹⁴. We analyzed all body temperature relative-hormone gene expression in the pituitary, but the circadian expression change of melatonin in ASIC1a^{-/-} mice pineal gland still needs to test.

4.2.3 Circadian rhythm of hormone synthesis

The levels in blood of many hormones shown significant circadian rhythmic variations³¹⁵. The concentrations of the hormones are influenced by many factors (such as ingestion, exercise, emotions, drugs, *etc.*), and the influence of these factors modifies the pattern of their circadian rhythmic variation. In addition, hormone concentrations and their circadian rhythms are also related to species, sex, and age, with significant interspecies and individual differences. This study found that the expression of hormone gene *Tshb* has a circadian rhythm and significant difference between WT and *ASIC1a*^{-/-} mice in the pituitary. TSH synthesis and secretion is controlled by the TRH released from the hypothalamus³¹⁶. We also find that the expression of *Trh* in the hypothalamus has a circadian rhythm. Therefore, the body temperature regulated by *ASIC1a* may depend on the hypothalamic-pituitary-thyroid axis. Beside the hormone expression, the expression of TRH receptor was significantly decreased at ZT13 in the pituitary of *ASIC1a*^{-/-} but not WT mice, and the expression of TSH receptor was significantly decreased at ZT13 in the thyroid gland of WT but not *ASIC1a*^{-/-} mice (Figure 1 in project 2). Therefore, the expression of hormone receptors may regulate by the hormone release in the HPT axis.

4.2.4 Signalling pathway of *ASIC1a* regulates *Trh* and *Prl*

Both *c-fos*, *fosb* and *Junb* genes belong to early response genes (ERG). The FOS and JUN proteins form a heterodimer protein complex activator protein-1 (AP-1) in the nucleus³¹⁷. Studies have shown that the expression of prolactin gene (*Prl*) and *Trh* is mediated by AP-1 and depends on activating CREB³¹⁸. FOS expression in SCN under normal photoperiod had a circadian rhythm, and different studies have reported slightly different time points for its peak appearance³¹⁹. In this study, we found that the expression of *Junb*, not *c-fos* and *fosb*, was significantly increased at ZT13 in the hypothalamus of WT mice. *c-fos* and *fosb* were significantly increased in *ASIC1a*^{-/-} mice at ZT13, but the expression of *Prl* and *Trh* were increased in WT mice hypothalamus at ZT13. This indicates that the expression of *Trh* and *Prl* in hypothalamus were regulated by the activation of *ASIC1a*, and this regulation may depend on the Akt-mTOR-JUN-CREB pathway.

5. Perspectives

5.1 Regulation of ASICs by H₂S.

Recently, endogenous H₂S has been recognized as a new atypical neurotransmitter, and its physiological and pathological roles in the brain have been widely recognized and have attracted great attention. Studies suggest that physiological concentrations of H₂S play an important physiological role in enhancing long-term hippocampal-dependent memory and regulating neuroendocrine and cerebrovascular functions, while low or high concentrations are closely associated with the development of various central nervous system diseases, such as ischemic stroke and neuroinflammation.

This study found that H₂S regulates the expression of ASIC1a *via* the MAPK-Erk1/2 signaling pathway in culture cortex neurons. However, compared to the extensive biological studies in peripheral tissues, especially in the cardiovascular system, the role of H₂S in the CNS is still not fully understood. In the future, we need to investigate the physiological and pathological functions of H₂S regulation of ASICs in the CNS, which may provide more insight into the pathogenesis of certain CNS diseases and provide new diagnostic and therapeutic ideas and methods, with broad research prospects and applications.

We only used exogenous H₂S donors in this study. However, it is still unclear whether endogenous H₂S can regulate ASIC, so we need to study the ASIC regulation by the endogenous H₂S, such as exogenously expressed CBS, or by using siRNA or inhibitors to study the CBS regulates the ASIC expression.

To limit the use of experimental animals, we only studied the regulation of ASIC by H₂S on the cells, but the physiological function of ASICs regulated by H₂S is still unclear. So, we need more *in vivo* testing to study physiological functions of H₂S, such as study the neuroprotective effects of H₂S in ischemic stroke mice model and the potentiation effect of H₂S on ASIC1a dependent LTP on the hippocampus brain slice.

Further studies on the regulation of ASICs by endogenous H₂S in CNS may be the key to finding new functions of H₂S and polysulfides. And help us to better understanding the regulation of physiological and pathological processes and the inhibition of the disease progression.

5.2 Circadian expression of ASIC1a in hypothalamus.

As a fundamental physiological function in humans and other animals, body temperature follows a circadian rhythm. In this study, we found that the circadian rhythm of body temperature was regulated by the circadian expression of ASIC in the hypothalamus, and this issue was investigated. However, several open questions remain.

First, this project only studied the effect of ASIC on the body temperature of mice under the normal light cycle, and this effect depends on the HPT axis. However, there was a significant difference in the wheel-running behavior phase shift of mice under constant darkness. The phase shift of mice body temperature under constant darkness was not investigated, this issue should be examined in the future.

Second, about the mechanism study, this study found that the circadian rhythm of body temperature is related to hormone and neuronal activity circadian changes in the brain PVH. However, the neuronal type that regulates the hormone release in PVN is still unclear, and the circadian expression of neurotransmitter receptor/transporter is also unknown.

Third, other conditions on the circadian rhythm of body temperatures, such as feed cycle and ambient temperature change, should be applied to study the relationship between body temperature and circadian rhythm from different perspectives.

Fourth, hypothalamus mainly controls the regulation of body temperature, but the used mice in this study are whole-animal ASIC1a gene knockout mice. The circadian rhythm of hypothalamus neuronal activity was regulated by SCN and other brain nuclei. So, it is also necessary to specifically knock out ASIC1a in the mouse hypothalamus to study its function.

Fifth, although we found that ASIC expression in the hypothalamus has a circadian rhythm, it

is still unclear what kind of signaling pathway regulates the circadian expression of ASIC1a. Does SCN regulate the circadian expression of ASIC in the hypothalamus since SCN is the center of circadian rhythm regulation?

Future studies should investigate variability in a wide and representative range of ASIC1a expression and the regulation of circadian rhythm. These studies may be of high value for better knowledge of pathophysiology, diagnostic procedures and methods of treatment in circadian rhythm disruption.

6. References

- 1 Krishtal, O. A. & Pidoplichko, V. I. A receptor for protons in the nerve cell membrane. *Neuroscience* 5, 2325-2327, (1980).
- 2 Waldmann, R. *et al.* Molecular cloning of a non-inactivating proton-gated Na⁺ channel specific for sensory neurons. *J Biol Chem* 272, 20975-20978, (1997).
- 3 Gruol, D. L., Barker, J. L., Huang, L. Y. M., Macdonald, J. F. & Smith, T. G. Hydrogen-Ions Have Multiple Effects on the Excitability of Cultured Mammalian Neurons. *Brain Res* 183, 247-252, (1980).
- 4 Zha, X. M. Acid-sensing ion channels: trafficking and synaptic function. *Molecular brain* 6, 1, (2013).
- 5 Hesselager, M., Timmermann, D. B. & Ahring, P. K. pH Dependency and desensitization kinetics of heterologously expressed combinations of acid-sensing ion channel subunits. *J Biol Chem* 279, 11006-11015, (2004).
- 6 Benson, C. J. *et al.* Heteromultimers of DEG/ENaC subunits form H⁺-gated channels in mouse sensory neurons. *Proceedings of the National Academy of Sciences of the United States of America* 99, 2338-2343, (2002).
- 7 Alvarez de la Rosa, D. *et al.* Distribution, subcellular localization and ontogeny of ASIC1 in the mammalian central nervous system. *The Journal of physiology* 546, 77-87, (2003).
- 8 Price, M. P., Snyder, P. M. & Welsh, M. J. Cloning and expression of a novel human brain Na⁺ channel. *J Biol Chem* 271, 7879-7882, (1996).
- 9 Rosa, D., Zhang, P., Shao, D., White, F. & Canessa, C. Functional implications of the localization and activity of acid-sensitive channels in rat peripheral nervous system. *Proceedings of the National Academy of Sciences* 99, 2326-2331, (2002).
- 10 Price, M. P. *et al.* The mammalian sodium channel BNC1 is required for normal touch sensation. *Nature* 407, 1007-1011, (2000).
- 11 Wemmie, J. A. *et al.* The acid-activated ion channel ASIC contributes to synaptic plasticity, learning, and memory. *Neuron* 34, 463-477, (2002).
- 12 Wemmie, J. A. *et al.* Acid-sensing ion channel 1 is localized in brain regions with high synaptic density and contributes to fear conditioning. *The Journal of neuroscience : the official journal of the Society for Neuroscience* 23, 5496-5502, (2003).
- 13 Varming, T. Proton-gated ion channels in cultured mouse cortical neurons. *Neuropharmacology* 38, 1875-1881, (1999).
- 14 Askwith, C. C., Wemmie, J. A., Price, M. P., Rokhlina, T. & Welsh, M. J. Acid-sensing ion channel 2 (ASIC2) modulates ASIC1 H⁺-activated currents in hippocampal neurons. *J Biol Chem* 279, 18296-18305, (2004).
- 15 Baron, A., Waldmann, R. & Lazdunski, M. ASIC - like, proton - activated currents in rat hippocampal neurons. *The Journal of physiology* 539, 485-494, (2002).
- 16 Sontheimer, H. *et al.* Glial cells of the oligodendrocyte lineage express proton-activated Na⁺ channels. *Journal of neuroscience research* 24, 496-500, (1989).
- 17 Grifoni, S. C., Jernigan, N. L., Hamilton, G. & Drummond, H. A. ASIC proteins regulate smooth muscle cell migration. *Microvasc Res* 75, 202-210, (2008).

- 18 Kolker, S. J. *et al.* Acid-sensing ion channel 3 expressed in type B synoviocytes and chondrocytes modulates hyaluronan expression and release. *Ann Rheum Dis* 69, 903-909, (2010).
- 19 Jahr, H., van Driel, M., van Osch, G. J., Weinans, H. & van Leeuwen, J. P. Identification of acid-sensing ion channels in bone. *Biochem Biophys Res Commun* 337, 349-354, (2005).
- 20 Jasti, J., Furukawa, H., Gonzales, E. & Gouaux, E. Structure of acid-sensing ion channel 1 at 1.9 Å resolution and low pH. *Nature* 449, 316-323, (2007).
- 21 Coryell, M. W. *et al.* Targeting ASIC1a reduces innate fear and alters neuronal activity in the fear circuit. *Biol Psychiatry* 62, 1140-1148, (2007).
- 22 Sherwood, T. W. & Askwith, C. C. Dynorphin opioid peptides enhance acid-sensing ion channel 1a activity and acidosis-induced neuronal death. *The Journal of neuroscience : the official journal of the Society for Neuroscience* 29, 14371-14380, (2009).
- 23 Ziemann, A. E. *et al.* The Amygdala Is a Chemosensor that Detects Carbon Dioxide and Acidosis to Elicit Fear Behavior. *Cell* 139, 1012-1021, (2009).
- 24 de Weille, J. R., Bassilana, F., Lazdunski, M. & Waldmann, R. Identification, functional expression and chromosomal localisation of a sustained human proton-gated cation channel. *FEBS Lett* 433, 257-260, (1998).
- 25 Salinas, M., Lazdunski, M. & Lingueglia, E. Structural elements for the generation of sustained currents by the acid pain sensor ASIC3. *J Biol Chem* 284, 31851-31859, (2009).
- 26 Dube, G. R., Elagoz, A. & Mangat, H. Acid sensing ion channels and acid nociception. *Curr Pharm Des* 15, 1750-1766, (2009).
- 27 Dube, G. R. *et al.* Electrophysiological and in vivo characterization of A-317567, a novel blocker of acid sensing ion channels. *Pain* 117, 88-96, (2005).
- 28 Lai, C. C., Hong, K., Kinnell, M., Chalfie, M. & Driscoll, M. Sequence and transmembrane topology of MEC-4, an ion channel subunit required for mechanotransduction in *Caenorhabditis elegans*. *J Cell Biol* 133, 1071-1081, (1996).
- 29 Renard, S., Lingueglia, E., Voilley, N., Lazdunski, M. & Barbry, P. Biochemical analysis of the membrane topology of the amiloride-sensitive Na⁺ channel. *J Biol Chem* 269, 12981-12986, (1994).
- 30 Vullo, S. *et al.* Conformational dynamics and role of the acidic pocket in ASIC pH-dependent gating. *Proceedings of the National Academy of Sciences of the United States of America* 114, 3768-3773, (2017).
- 31 Gonzales, E. B., Kawate, T. & Gouaux, E. Pore architecture and ion sites in acid-sensing ion channels and P2X receptors. *Nature* 460, 599-604, (2009).
- 32 Bacongus, I. & Gouaux, E. Structural plasticity and dynamic selectivity of acid-sensing ion channel-spider toxin complexes. *Nature* 489, 400-405, (2012).
- 33 Coscoy, S., de Weille, J. R., Lingueglia, E. & Lazdunski, M. The pre-transmembrane 1 domain of acid-sensing ion channels participates in the ion pore. *J Biol Chem* 274, 10129-10132, (1999).
- 34 Pfister, Y. *et al.* A gating mutation in the internal pore of ASIC1a. *J Biol Chem* 281, 11787-11791, (2006).

- 35 Chen, X. & Grunder, S. Permeating protons contribute to tachyphylaxis of the acid-sensing ion channel (ASIC) 1a. *The Journal of physiology* 579, 657-670, (2007).
- 36 Wang, W. Z. *et al.* Modulation of acid-sensing ion channel currents, acid-induced increase of intracellular Ca²⁺, and acidosis-mediated neuronal injury by intracellular pH. *J Biol Chem* 281, 29369-29378, (2006).
- 37 Ugawa, S. *et al.* Amiloride-blockable acid-sensing ion channels are leading acid sensors expressed in human nociceptors. *J Clin Invest* 110, 1185-1190, (2002).
- 38 Jones, N. G., Slater, R., Cadiou, H., McNaughton, P. & McMahon, S. B. Acid-induced pain and its modulation in humans. *The Journal of neuroscience : the official journal of the Society for Neuroscience* 24, 10974-10979, (2004).
- 39 Escoubas, P. *et al.* Isolation of a tarantula toxin specific for a class of proton-gated Na⁺ channels. *J Biol Chem* 275, 25116-25121, (2000).
- 40 Diochot, S. *et al.* A new sea anemone peptide, APETx2, inhibits ASIC3, a major acid - sensitive channel in sensory neurons. *The EMBO Journal* 23, 1516-1525, (2004).
- 41 Cottrell, G. A., Green, K. A. & Davies, N. W. The Neuropeptide Phe-Met-Arg-Phe-NH₂ (Fmrfamide) Can Activate a Ligand-Gated Ion Channel in *Helix* Neurons. *Pflug Arch Eur J Phy* 416, 612-614, (1990).
- 42 Perry, S. J. *et al.* A human gene encoding morphine modulating peptides related to NPPF and FMRFamide. *FEBS Lett* 409, 426-430, (1997).
- 43 Vilim, F. S. *et al.* Gene for pain modulatory neuropeptide NPPF: induction in spinal cord by noxious stimuli. *Mol Pharmacol* 55, 804-811, (1999).
- 44 Hinuma, S. *et al.* New neuropeptides containing carboxy-terminal RFamide and their receptor in mammals. *Nat Cell Biol* 2, 703-708, (2000).
- 45 Aghajanova, L. *et al.* Thyroid-stimulating hormone receptor and thyroid hormone receptors are involved in human endometrial physiology. *Fertility and sterility* 95, 230-237, (2011).
- 46 Peng, Z. *et al.* ASIC3 Mediates Itch Sensation in Response to Coincident Stimulation by Acid and Nonproton Ligand. *Cell Rep* 13, 387-398, (2015).
- 47 García-Añoveros, J., Samad, T. A., Žuvela-Jelaska, L., Woolf, C. J. & Corey, D. P. Transport and localization of the DEG/ENaC ion channel BNaC1α to peripheral mechanosensory terminals of dorsal root ganglia neurons. *J Neurosci* 21, 2678-2686, (2001).
- 48 Lawson, S. Morphological and biochemical cell types of sensory neurons. *Sensory Neurons: Diversity, Development and Plasticity*. Oxford University Press, New York, 27-59, (1992).
- 49 Voilley, N., de Weille, J., Mamet, J. & Lazdunski, M. Nonsteroid anti-inflammatory drugs inhibit both the activity and the inflammation-induced expression of acid-sensing ion channels in nociceptors. *Journal of Neuroscience* 21, 8026-8033, (2001).
- 50 Mamet, J., Lazdunski, M. & Voilley, N. How nerve growth factor drives physiological and inflammatory expressions of acid-sensing ion channel 3 in sensory neurons. *Journal of Biological Chemistry* 278, 48907-48913, (2003).
- 51 Mamet, J., Baron, A., Lazdunski, M. & Voilley, N. Proinflammatory mediators, stimulators of sensory neuron excitability *via* the expression of acid-sensing ion channels. *The Journal*

- of neuroscience : the official journal of the Society for Neuroscience* 22, 10662-10670, (2002).
- 52 Yu, S. & Ouyang, A. TRPA1 in bradykinin-induced mechanical hypersensitivity of vagal C fibers in guinea pig esophagus. *Am J Physiol Gastrointest Liver Physiol* 296, G255-265, (2009).
 - 53 Duan, B. *et al.* PI₃-kinase/Akt pathway-regulated membrane insertion of acid-sensing ion channel 1a underlies BDNF-induced pain hypersensitivity. *The Journal of neuroscience : the official journal of the Society for Neuroscience* 32, 6351-6363, (2012).
 - 54 Duan, B. *et al.* Upregulation of acid-sensing ion channel ASIC1a in spinal dorsal horn neurons contributes to inflammatory pain hypersensitivity. *The Journal of neuroscience : the official journal of the Society for Neuroscience* 27, 11139-11148, (2007).
 - 55 McIlwrath, S. L., Hu, J., Anirudhan, G., Shin, J. B. & Lewin, G. R. The sensory mechanotransduction ion channel ASIC2 (acid sensitive ion channel 2) is regulated by neurotrophin availability. *Neuroscience* 131, 499-511, (2005).
 - 56 Benson, C. J., Eckert, S. P. & McCleskey, E. W. Acid-evoked currents in cardiac sensory neurons: A possible mediator of myocardial ischemic sensation. *Circulation research* 84, 921-928, (1999).
 - 57 Sutherland, S. P., Benson, C. J., Adelman, J. P. & McCleskey, E. W. Acid-sensing ion channel 3 matches the acid-gated current in cardiac ischemia-sensing neurons. *Proceedings of the National Academy of Sciences of the United States of America* 98, 711-716, (2001).
 - 58 Deval, E. *et al.* ASIC3, a sensor of acidic and primary inflammatory pain. *EMBO J* 27, 3047-3055, (2008).
 - 59 Yan, J. *et al.* Dural afferents express acid-sensing ion channels: a role for decreased meningeal pH in migraine headache. *Pain* 152, 106-113, (2011).
 - 60 Hattori, T. *et al.* ASIC2a and ASIC3 heteromultimerize to form pH-sensitive channels in mouse cardiac dorsal root ganglia neurons. *Circulation research* 105, 279-286, (2009).
 - 61 Xie, J., Price, M. P., Wemmie, J. A., Askwith, C. C. & Welsh, M. J. ASIC3 and ASIC1 mediate FMRFamide-related peptide enhancement of H⁺-gated currents in cultured dorsal root ganglion neurons. *J Neurophysiol* 89, 2459-2465, (2003).
 - 62 Cuzzocrea, S., Riley, D. P., Caputi, A. P. & Salvemini, D. Antioxidant therapy: a new pharmacological approach in shock, inflammation, and ischemia/reperfusion injury. *Pharmacol Rev* 53, 135-159, (2001).
 - 63 Revici, E., Stopen, E., Frenk, E. & Ravich, R. The painful focus. II. The relation of pain to local physiochemical changes. *Bulletin de l'Institut of Applied Biology* 1, 1, (1949).
 - 64 Pan, J. W., Hamm, J. R., Rothman, D. L. & Shulman, R. G. Intracellular pH in human skeletal muscle by ¹H NMR. *Proceedings of the National Academy of Sciences of the United States of America* 85, 7836-7839, (1988).
 - 65 Issberner, U., Reeh, P. & Steen, K. Pain due to tissue acidosis: a mechanism for inflammatory and ischemic myalgia? *Neuroscience Letters* 208, 191-194, (1996).
 - 66 Yu, Y. *et al.* A nonproton ligand sensor in the acid-sensing ion channel. *Neuron* 68, 61-72, (2010).

- 67 Walder, R. Y. *et al.* ASIC1 and ASIC3 play different roles in the development of Hyperalgesia after inflammatory muscle injury. *J Pain* 11, 210-218, (2010).
- 68 Blanchard, M. G., Rash, L. D. & Kellenberger, S. Inhibition of Voltage-Gated Na⁺ Currents in Sensory Neurons by the Sea Anemone Toxin APETx2. *Biophys J* 102, 324a-325a, (2012).
- 69 Yen, L. T., Hsu, Y. C., Lin, J. G., Hsieh, C. L. & Lin, Y. W. Role of ASIC3, Nav_v1.7 and Nav1.8 in electroacupuncture-induced analgesia in a mouse model of fibromyalgia pain. *Acupunct Med* 36, 110-116, (2018).
- 70 Jensen, J. E. *et al.* Understanding the molecular basis of toxin promiscuity: the analgesic sea anemone peptide APETx2 interacts with acid-sensing ion channel 3 and hERG channels via overlapping pharmacophores. *J Med Chem* 57, 9195-9203, (2014).
- 71 Payne, C. E. *et al.* A novel selective and orally bioavailable Nav 1.8 channel blocker, PF - 01247324, attenuates nociception and sensory neuron excitability. *British journal of pharmacology* 172, 2654-2670, (2015).
- 72 Chen, C. C. *et al.* A role for ASIC3 in the modulation of high-intensity pain stimuli. *Proceedings of the National Academy of Sciences of the United States of America* 99, 8992-8997, (2002).
- 73 Sluka, K. *et al.* Chronic hyperalgesia induced by repeated acid injections in muscle is abolished by the loss of ASIC3, but not ASIC1. *Pain* 106, 229-239, (2003).
- 74 Page, A. *et al.* The ion channel ASIC1 contributes to visceral but not cutaneous mechanoreceptor function. *Gastroenterology* 127, 1739-1747, (2004).
- 75 Page, A. J. *et al.* Different contributions of ASIC channels 1a, 2, and 3 in gastrointestinal mechanosensory function. *Gut* 54, 1408-1415, (2005).
- 76 Jones, R. C. W., Xu, L. J. & Gebhart, G. F. The mechanosensitivity of mouse colon afferent fibers and their sensitization by inflammatory mediators require transient receptor potential vanilloid 1 and acid-sensing ion channel 3. *Journal of Neuroscience* 25, 10981-10989, (2005).
- 77 Jones III, R. *et al.* Short-term sensitization of colon mechanoreceptors is associated with long-term hypersensitivity to colon distention in the mouse. *Gastroenterology* 133, 184-194, (2007).
- 78 Drew, L. *et al.* Acid - sensing ion channels ASIC2 and ASIC3 do not contribute to mechanically activated currents in mammalian sensory neurones. *The Journal of physiology* 556, 691-710, (2004).
- 79 Gao, J. *et al.* Coupling between NMDA receptor and acid-sensing ion channel contributes to ischemic neuronal death. *Neuron* 48, 635-646, (2005).
- 80 Xiong, Z. G. *et al.* Neuroprotection in ischemia: blocking calcium-permeable acid-sensing ion channels. *Cell* 118, 687-698, (2004).
- 81 Yermolaieva, O., Leonard, A. S., Schnizler, M. K., Abboud, F. M. & Welsh, M. J. Extracellular acidosis increases neuronal cell calcium by activating acid-sensing ion channel 1a. *Proceedings of the National Academy of Sciences of the United States of America* 101, 6752-6757, (2004).

- 82 González-Inchauspe, C., Urbano, F. J., Di Guilmi, M. N. & Uchitel, O. D. Acid-sensing ion channels activated by evoked released protons modulate synaptic transmission at the mouse calyx of held synapse. *Journal of Neuroscience* 37, 2589-2599, (2017).
- 83 Mango, D. & Nistico, R. Acid-sensing ion channel 1a is involved in N-methyl D-aspartate receptor-dependent long-term depression in the hippocampus. *Frontiers in pharmacology* 10, 555, (2019).
- 84 Chesler, M. & Kaila, K. Modulation of pH by neuronal activity. *Trends Neurosci* 15, 396-402, (1992).
- 85 Katsura, K., Kristian, T., Smith, M. L. & Siesjo, B. K. Acidosis induced by hypercapnia exaggerates ischemic brain damage. *J Cereb Blood Flow Metab* 14, 243-250, (1994).
- 86 Siesjo, B. K. & Siesjo, P. Mechanisms of secondary brain injury. *European journal of anaesthesiology* 13, 247-268, (1996).
- 87 Wu, P. Y. *et al.* Acid-sensing ion channel-1a is not required for normal hippocampal LTP and spatial memory. *The Journal of Neuroscience* 33, 1828-1832, (2013).
- 88 de Vries, S. Exocytosed protons feedback to suppress the Ca²⁺ current in mammalian cone photoreceptors. *Neuron* 32, 1107-1117, (2001).
- 89 Vessey, J. P. *et al.* Proton-mediated feedback inhibition of presynaptic calcium channels at the cone photoreceptor synapse. *Journal of Neuroscience* 25, 4108-4117, (2005).
- 90 Miesenbock, G., De Angelis, D. A. & Rothman, J. E. Visualizing secretion and synaptic transmission with pH-sensitive green fluorescent proteins. *Nature* 394, 192-195, (1998).
- 91 Olson, T. H., Riedl, M. S., Vulchanova, L., Ortiz-Gonzalez, X. R. & Elde, R. An acid sensing ion channel (ASIC) localizes to small primary afferent neurons in rats. *Neuroreport* 9, 1109-1113, (1998).
- 92 García-Añoveros, J., Derfler, B., Neville-Golden, J., Hyman, B. T. & Corey, D. P. BNaC1 and BNaC2 constitute a new family of human neuronal sodium channels related to degenerins and epithelial sodium channels. *Proceedings of the National Academy of Sciences* 94, 1459-1464, (1997).
- 93 Wemmie, J. A. *et al.* Overexpression of acid-sensing ion channel 1a in transgenic mice increases acquired fear-related behavior. *Proceedings of the National Academy of Sciences of the United States of America* 101, 3621-3626, (2004).
- 94 Zha, X. M., Wemmie, J. A., Green, S. H. & Welsh, M. J. Acid-sensing ion channel 1a is a postsynaptic proton receptor that affects the density of dendritic spines. *Proceedings of the National Academy of Sciences of the United States of America* 103, 16556-16561, (2006).
- 95 Cho, J. H. & Askwith, C. C. Presynaptic release probability is increased in hippocampal neurons from ASIC1 knockout mice. *Journal of Neurophysiology* 99, 426-441, (2008).
- 96 Vergo, S. *et al.* Acid-sensing ion channel 1 is involved in both axonal injury and demyelination in multiple sclerosis and its animal model. *Brain* 134, 571-584, (2011).
- 97 Pignataro, G., Simon, R. P. & Xiong, Z. G. Prolonged activation of ASIC1a and the time window for neuroprotection in cerebral ischaemia. *Brain* 130, 151-158, (2007).
- 98 Friese, M. A. *et al.* Acid-sensing ion channel-1 contributes to axonal degeneration in autoimmune inflammation of the central nervous system. *Nat Med* 13, 1483-1489, (2007).

- 99 Wong, H. K. *et al.* Blocking acid-sensing ion channel 1 alleviates Huntington's disease pathology via an ubiquitin-proteasome system-dependent mechanism. *Hum Mol Genet* 17, 3223-3235, (2008).
- 100 Arias, R. L. *et al.* Amiloride is neuroprotective in an MPTP model of Parkinson's disease. *Neurobiol Dis* 31, 334-341, (2008).
- 101 Hu, R. *et al.* Role of acid-sensing ion channel 1a in the secondary damage of traumatic spinal cord injury. *Ann Surg* 254, 353-362, (2011).
- 102 Mazzuca, M. *et al.* A tarantula peptide against pain via ASIC1a channels and opioid mechanisms. *Nat Neurosci* 10, 943-945, (2007).
- 103 Wu, L. J. *et al.* Characterization of acid-sensing ion channels in dorsal horn neurons of rat spinal cord. *J Biol Chem* 279, 43716-43724, (2004).
- 104 Zhou, Y. M. *et al.* Enhancement of acid-sensing ion channel activity by prostaglandin E2 in rat dorsal root ganglion neurons. *Brain Res* 1724, 146442, (2019).
- 105 Leonard, A. S. *et al.* cAMP-dependent protein kinase phosphorylation of the acid-sensing ion channel-1 regulates its binding to the protein interacting with C-kinase-1. *Proceedings of the National Academy of Sciences of the United States of America* 100, 2029-2034, (2003).
- 106 Zhang, L., Leng, T. D., Yang, T., Li, J. & Xiong, Z. G. Protein Kinase C Regulates ASIC1a Protein Expression and Channel Function via NF- κ B Signaling Pathway. *Mol Neurobiol* 57, 4754-4766, (2020).
- 107 Warenycia, M. W. *et al.* Acute hydrogen sulfide poisoning. Demonstration of selective uptake of sulfide by the brainstem by measurement of brain sulfide levels. *Biochem Pharmacol* 38, 973-981, (1989).
- 108 Powell, M. A. & Arp, A. J. Hydrogen-Sulfide Oxidation by Abundant Nonhemoglobin Heme Compounds in Marine-Invertebrates from Sulfide-Rich Habitats. *J Exp Zool* 249, 121-132, (1989).
- 109 Jinshan, C. Effects of carbon disulfide on some endocrine glands in male exposed workers. *Industrial Health and Occupational Diseases* 6, 003, (1989).
- 110 Mustafa, A. K. *et al.* H₂S Signals Through Protein S-Sulfhydration. *Sci Signal* 2, ra72, (2009).
- 111 Stipanuk, M. H. & Beck, P. W. Characterization of the enzymic capacity for cysteine desulphhydration in liver and kidney of the rat. *Biochem J* 206, 267-277, (1982).
- 112 Erickson, P., Maxwell, I., Su, L., Baumann, M. & Glode, L. Sequence of cDNA for rat cystathionine γ -lyase and comparison of deduced amino acid sequence with related *Escherichia coli* enzymes. *Biochemical Journal* 269, 335, (1990).
- 113 Roper, M. D. & Kraus, J. P. Rat cystathionine β -synthase: Expression of four alternatively spliced isoforms in transfected cultured cells. *Archives of biochemistry and biophysics* 298, 514-521, (1992).
- 114 Shibuya, N. *et al.* 3-Mercaptopyruvate sulfurtransferase produces hydrogen sulfide and bound sulfane sulfur in the brain. *Antioxid Redox Signal* 11, 703-714, (2009).

- 115 Shibuya, N., Mikami, Y., Kimura, Y., Nagahara, N. & Kimura, H. Vascular endothelium expresses 3-mercaptopyruvate sulfurtransferase and produces hydrogen sulfide. *J Biochem* 146, 623-626, (2009).
- 116 Sun, Y., Tang, C. S., Jin, H. F. & Du, J. B. The vasorelaxing effect of hydrogen sulfide on isolated rat aortic rings versus pulmonary artery rings. *Acta Pharmacol Sin* 32, 456-464, (2011).
- 117 Yan, H., Du, J. & Tang, C. The possible role of hydrogen sulfide on the pathogenesis of spontaneous hypertension in rats. *Biochem Biophys Res Commun* 313, 22-27, (2004).
- 118 Fiorucci, S. *et al.* The third gas: H₂S regulates perfusion pressure in both the isolated and perfused normal rat liver and in cirrhosis. *Hepatology* 42, 539-548, (2005).
- 119 Li, Q. *et al.* A crucial role for hydrogen sulfide in oxygen sensing *via* modulating large conductance calcium-activated potassium channels. *Antioxid Redox Signal* 12, 1179-1189, (2010).
- 120 Kimura, Y., Goto, Y. & Kimura, H. Hydrogen sulfide increases glutathione production and suppresses oxidative stress in mitochondria. *Antioxid Redox Signal* 12, 1-13, (2010).
- 121 Olson, K. R. H₂S and polysulfide metabolism: Conventional and unconventional pathways. *Biochem Pharmacol* 149, 77-90, (2018).
- 122 Staško, A., Brezová, V., Zalibera, M., Biskupič, S. & Ondriaš, K. Electron transfer: a primary step in the reactions of sodium hydrosulphide, an H₂S/HS⁻ donor. *Free radical research* 43, 581-593, (2009).
- 123 Whiteman, M. *et al.* Hydrogen sulphide: a novel inhibitor of hypochlorous acid-mediated oxidative damage in the brain? *Biochem Biophys Res Commun* 326, 794-798, (2005).
- 124 Cheung, N. S., Peng, Z. F., Chen, M. J., Moore, P. K. & Whiteman, M. Hydrogen sulfide induced neuronal death occurs via glutamate receptor and is associated with calpain activation and lysosomal rupture in mouse primary cortical neurons. *Neuropharmacology* 53, 505-514, (2007).
- 125 Li, L. *et al.* Characterization of a Novel, Water-Soluble Hydrogen Sulfide-Releasing Molecule (GYY4137). *Circulation* 117, 2351-2360, (2008).
- 126 Robinson, H. & Wray, S. A New Slow Releasing, H₂S Generating Compound, GYY4137 Relaxes Spontaneous and Oxytocin-Stimulated Contractions of Human and Rat Pregnant Myometrium. *Plos One* 7, e46278, (2012).
- 127 Kang, S. C., Sohn, E. H. & Lee, S. R. Hydrogen Sulfide as a Potential Alternative for the Treatment of Myocardial Fibrosis. *Oxid Med Cell Longev* 2020, (2020).
- 128 Sandage, C. *Tolerance Criteria for Continuous Inhalation Exposure to Toxic Material: I Effects on Animals of 90-day Exposure to Phenol, CCL4, and a Mixture of Indole, Skatole, H₂S, and Methyl Mercaptan.* (Biomedical Laboratory, Aerospace Medical Laboratory, Aeronautical Systems Division, Air Force Systems Command, United States Air Force, 1961).
- 129 Beauchamp, R. O., Jr., Bus, J. S., Popp, J. A., Boreiko, C. J. & Andjelkovich, D. A. A critical review of the literature on hydrogen sulfide toxicity. *Critical reviews in toxicology* 13, 25-97, (1984).

- 130 Dorman, D. C. *et al.* Cytochrome oxidase inhibition induced by acute hydrogen sulfide inhalation: correlation with tissue sulfide concentrations in the rat brain, liver, lung, and nasal epithelium. *Toxicol Sci* 65, 18-25, (2002).
- 131 Petersen, L. C. The effect of inhibitors on the oxygen kinetics of cytochrome *c* oxidase. *Biochimica et Biophysica Acta (BBA)-Bioenergetics* 460, 299-307, (1977).
- 132 Szabo, C. & Papapetropoulos, A. International Union of Basic and Clinical Pharmacology. CII: Pharmacological Modulation of H₂S Levels: H₂S Donors and H₂S Biosynthesis Inhibitors. *Pharmacol Rev* 69, 497-564, (2017).
- 133 Zanardo, R. C. O. *et al.* Hydrogen sulfide is an endogenous modulator of leukocyte-mediated inflammation. *Faseb J* 20, 2118-+, (2006).
- 134 Peng, H. *et al.* A fluorescent probe for fast and quantitative detection of hydrogen sulfide in blood. *Angew Chem Int Ed Engl* 50, 9672-9675, (2011).
- 135 Zaorska, E., Tomasova, L., Koszelewski, D., Ostaszewski, R. & Ufnal, M. Hydrogen Sulfide in Pharmacotherapy, Beyond the Hydrogen Sulfide-Donors. *Biomolecules* 10, 323, (2020).
- 136 Cline, J. D. Spectrophotometric determination of hydrogen sulfide in natural waters. *Limnol Oceanogr* 14, 454-458, (1969).
- 137 Steele, R. D. & Benevenga, N. J. The metabolism of 3-methylthiopropionate in rat liver homogenates. *J Biol Chem* 254, 8885-8890, (1979).
- 138 Hughes, M. N., Centelles, M. N. & Moore, K. P. Making and working with hydrogen sulfide: The chemistry and generation of hydrogen sulfide in vitro and its measurement *in vivo*: a review. *Free radical biology & medicine* 47, 1346-1353, (2009).
- 139 Olson, K. R. A Practical Look at the Chemistry and Biology of Hydrogen Sulfide. *Antioxid Redox Sign* 17, 32-44, (2012).
- 140 Shen, X., Peter, E. A., Bir, S., Wang, R. & Kevil, C. G. Analytical measurement of discrete hydrogen sulfide pools in biological specimens. *Free radical biology & medicine* 52, 2276-2283, (2012).
- 141 Shen, X. *et al.* Measurement of plasma hydrogen sulfide in vivo and in vitro. *Free radical biology & medicine* 50, 1021-1031, (2011).
- 142 Goodwin, L. R. *et al.* Determination of sulfide in brain tissue by gas dialysis/ion chromatography: postmortem studies and two case reports. *J Anal Toxicol* 13, 105-109, (1989).
- 143 Lamb, B., Westberg, H., Allwine, G., Bamesberger, L. & Guenther, A. Measurement of Biogenic Sulfur Emissions from Soils and Vegetation - Application of Dynamic Enclosure Methods with Natusch Filter and GC/FPD Analysis. *J Atmos Chem* 5, 469-491, (1987).
- 144 Kim, J. Y. *et al.* Development of dansyl based copper(II) complex to detect hydrogen sulfide in hypoxia. *Org Biomol Chem* 17, 7088-7094, (2019).
- 145 Zhong, K. *et al.* A colorimetric and near-infrared fluorescent probe for detection of hydrogen sulfide and its real multiple applications. *Spectrochim Acta A Mol Biomol Spectrosc* 221, 117135, (2019).
- 146 Doeller, J. E. *et al.* Polarographic measurement of hydrogen sulfide production and consumption by mammalian tissues. *Anal Biochem* 341, 40-51, (2005).

- 147 Liang, G. H. *et al.* Hydrogen sulfide dilates cerebral arterioles by activating smooth muscle cell plasma membrane K_{ATP} channels. *American journal of physiology. Heart and circulatory physiology* 300, H2088-2095, (2011).
- 148 Velazquez-Moyado, J. A. & Navarrete, A. The detection and quantification, *in vivo* and in real time, of hydrogen sulfide in ethanol-induced lesions in rat stomachs using an ion sensitive electrode. *J Pharmacol Tox Met* 89, 54-58, (2018).
- 149 Zhao, W., Zhang, J., Lu, Y. & Wang, R. The vasorelaxant effect of H_2S as a novel endogenous gaseous K_{ATP} channel opener. *EMBO J* 20, 6008-6016, (2001).
- 150 Jiang, B., Tang, G., Cao, K., Wu, L. & Wang, R. Molecular mechanism for H_2S -induced activation of K_{ATP} channels. *Antioxid Redox Signal* 12, 1167-1178, (2010).
- 151 Meera, P., Wallner, M. & Toro, L. A neuronal beta subunit (KCNMB4) makes the large conductance, voltage- and Ca^{2+} -activated K^+ channel resistant to charybdotoxin and iberiotoxin. *Proceedings of the National Academy of Sciences of the United States of America* 97, 5562-5567, (2000).
- 152 Wu, S. N. Large-conductance Ca^{2+} - activated K^+ channels:physiological role and pharmacology. *Current medicinal chemistry* 10, 649-661, (2003).
- 153 N'Gouemo, P. Targeting BK (big potassium) channels in epilepsy. *Expert opinion on therapeutic targets* 15, 1283-1295, (2011).
- 154 Sitdikova, G. F., Fuchs, R., Kainz, V., Weiger, T. M. & Hermann, A. Phosphorylation of BK channels modulates the sensitivity to hydrogen sulfide (H_2S). *Front Physiol* 5, 431-431, (2014).
- 155 Telezhkin, V. *et al.* Mechanism of inhibition by hydrogen sulfide of native and recombinant BK_{Ca} channels. *Respiratory physiology & neurobiology* 172, 169-178, (2010).
- 156 Sitdikova, G. F., Weiger, T. M. & Hermann, A. Hydrogen sulfide increases calcium-activated potassium (BK) channel activity of rat pituitary tumor cells. *Pflugers Archiv : European journal of physiology* 459, 389-397, (2010).
- 157 Buckler, K. J. Effects of exogenous hydrogen sulphide on calcium signalling, background (TASK) K channel activity and mitochondrial function in chemoreceptor cells. *Pflugers Archiv : European journal of physiology* 463, 743-754, (2012).
- 158 Tsubota-Matsunami, M., Noguchi, Y., Okawa, Y., Sekiguchi, F. & Kawabata, A. Colonic hydrogen sulfide-induced visceral pain and referred hyperalgesia involve activation of both $Ca_v3.2$ and TRPA1 channels in mice. *Journal of pharmacological sciences* 119, 293-296, (2012).
- 159 Matsunami, M., Kirishi, S., Okui, T. & Kawabata, A. Hydrogen sulfide-induced colonic mucosal cytoprotection involves T-type calcium channel-dependent neuronal excitation in rats. *Journal of physiology and pharmacology : an official journal of the Polish Physiological Society* 63, 61-68, (2012).
- 160 Zhang, R. *et al.* Hydrogen sulfide inhibits L-type calcium currents depending upon the protein sulfhydryl state in rat cardiomyocytes. *Plos One* 7, e37073, (2012).
- 161 Sun, Y. G. *et al.* Hydrogen sulphide is an inhibitor of L-type calcium channels and mechanical contraction in rat cardiomyocytes. *Cardiovascular research* 79, 632-641, (2008).

- 162 Ogawa, H. *et al.* H₂S functions as a nociceptive messenger through transient receptor potential ankyrin 1 (TRPA1) activation. *Neuroscience* 218, 335-343, (2012).
- 163 Streng, T. *et al.* Distribution and function of the hydrogen sulfide-sensitive TRPA1 ion channel in rat urinary bladder. *European urology* 53, 391-399, (2008).
- 164 Miyamoto, R., Otsuguro, K. & Ito, S. Time- and concentration-dependent activation of TRPA1 by hydrogen sulfide in rat DRG neurons. *Neurosci Lett* 499, 137-142, (2011).
- 165 Vernino, S., Amador, M., Luetje, C. W., Patrick, J. & Dani, J. A. Calcium modulation and high calcium permeability of neuronal nicotinic acetylcholine receptors. *Neuron* 8, 127-134, (1992).
- 166 Tang, G., Wu, L. & Wang, R. Interaction of hydrogen sulfide with ion channels. *Clinical and experimental pharmacology & physiology* 37, 753-763, (2010).
- 167 Yang, W., Yang, G., Jia, X., Wu, L. & Wang, R. Activation of K_{ATP} channels by H₂S in rat insulin-secreting cells and the underlying mechanisms. *The Journal of physiology* 569, 519-531, (2005).
- 168 Archer, S. & Michelakis, E. The mechanism(s) of hypoxic pulmonary vasoconstriction: potassium channels, redox O₂ sensors, and controversies. *News in physiological sciences : an international journal of physiology produced jointly by the International Union of Physiological Sciences and the American Physiological Society* 17, 131-137, (2002).
- 169 Buckler, K. J. A novel oxygen-sensitive potassium current in rat carotid body type I cells. *The Journal of physiology* 498 (Pt 3), 649-662, (1997).
- 170 Archer, S. L. *et al.* Preferential expression and function of voltage-gated, O₂-sensitive K⁺ channels in resistance pulmonary arteries explains regional heterogeneity in hypoxic pulmonary vasoconstriction: ionic diversity in smooth muscle cells. *Circulation research* 95, 308-318, (2004).
- 171 Kimura, H., Nagai, Y., Umemura, K. & Kimura, Y. Physiological roles of hydrogen sulfide: synaptic modulation, neuroprotection, and smooth muscle relaxation. *Antioxid Redox Signal* 7, 795-803, (2005).
- 172 Holland, M., Langton, P. D., Standen, N. B. & Boyle, J. P. Effects of the BK_{Ca} channel activator, NS1619, on rat cerebral artery smooth muscle. *Br J Pharmacol* 117, 119-129, (1996).
- 173 Xu, M., Wu, Y. M., Li, Q., Wang, F. W. & He, R. R. Electrophysiological effects of hydrogen sulfide on guinea pig papillary muscles *in vitro*. *Sheng li xue bao : [Acta physiologica Sinica]* 59, 215-220, (2007).
- 174 Johansen, D., Ytrehus, K. & Baxter, G. F. Exogenous hydrogen sulfide (H₂S) protects against regional myocardial ischemia-reperfusion injury-Evidence for a role of K_{ATP} channels. *Basic research in cardiology* 101, 53-60, (2006).
- 175 Zhang, Z., Huang, H., Liu, P., Tang, C. & Wang, J. Hydrogen sulfide contributes to cardioprotection during ischemia-reperfusion injury by opening K_{ATP} channels. *Canadian journal of physiology and pharmacology* 85, 1248-1253, (2007).
- 176 Hu, Y. *et al.* Cardioprotection induced by hydrogen sulfide preconditioning involves activation of ERK and PI₃K/Akt pathways. *Pflugers Archiv : European journal of physiology* 455, 607-616, (2008).

- 177 Liu, Y. *et al.* Hydrogen sulfide preconditioning or neutrophil depletion attenuates ischemia-reperfusion-induced mitochondrial dysfunction in rat small intestine. *Am J Physiol Gastrointest Liver Physiol* 302, G44-54, (2012).
- 178 Maeda, Y. *et al.* Hyperalgesia induced by spinal and peripheral hydrogen sulfide: evidence for involvement of Ca_v3.2 T-type calcium channels. *Pain* 142, 127-132, (2009).
- 179 Fukushima, O. *et al.* Phosphorylation of ERK in the spinal dorsal horn following pancreatic pronociceptive stimuli with proteinase-activated receptor-2 agonists and hydrogen sulfide in rats: evidence for involvement of distinct mechanisms. *Journal of neuroscience research* 88, 3198-3205, (2010).
- 180 Okubo, K. *et al.* Hydrogen sulfide-induced mechanical hyperalgesia and allodynia require activation of both Ca_v3.2 and TRPA1 channels in mice. *Br J Pharmacol* 166, 1738-1743, (2012).
- 181 Patacchini, R., Santicoli, P., Giuliani, S. & Maggi, C. A. Pharmacological investigation of hydrogen sulfide (H₂S) contractile activity in rat detrusor muscle. *European journal of pharmacology* 509, 171-177, (2005).
- 182 Nagasawa, K. *et al.* Hydrogen sulfide evokes neurite outgrowth and expression of high-voltage-activated Ca²⁺ currents in NG108-15 cells: involvement of T-type Ca²⁺ channels. *Journal of neurochemistry* 108, 676-684, (2009).
- 183 Tarui, T. *et al.* Involvement of Src kinase in T-type calcium channel-dependent neuronal differentiation of NG108-15 cells by hydrogen sulfide. *Journal of neurochemistry* 114, 512-519, (2010).
- 184 Kimura, Y. & Kimura, H. Hydrogen sulfide protects neurons from oxidative stress. *Faseb J* 18, 1165-1167, (2004).
- 185 Abe, K. & Kimura, H. The possible role of hydrogen sulfide as an endogenous neuromodulator. *Journal of Neuroscience* 16, 1066-1071, (1996).
- 186 Kimura, H. Hydrogen sulfide induces cyclic AMP and modulates the NMDA receptor. *Biochem Biophys Res Commun* 267, 129-133, (2000).
- 187 Abe, K. & Kimura, H. The possible role of hydrogen sulfide as an endogenous neuromodulator. *The Journal of neuroscience* 16, 1066-1071, (1996).
- 188 Kimura, H. Hydrogen sulfide as a neuromodulator. *Molecular Neurobiology* 26, 13-19, (2002).
- 189 Khattak, S. *et al.* The Role of Hydrogen Sulfide in Respiratory Diseases. *Biomolecules* 11, 682, (2021).
- 190 Potter, G. D. *et al.* Circadian Rhythm and Sleep Disruption: Causes, Metabolic Consequences, and Countermeasures. *Endocr Rev* 37, 584-608, (2016).
- 191 Panda, S., Hogenesch, J. B. & Kay, S. A. Circadian rhythms from flies to human. *Nature* 417, 329-335, (2002).
- 192 Morris, A. R., Stanton, D. L., Roman, D. & Liu, A. C. Systems Level Understanding of Circadian Integration with Cell Physiology. *J Mol Biol* 432, 3547-3564, (2020).
- 193 Ko, C. H. & Takahashi, J. S. Molecular components of the mammalian circadian clock. *Hum Mol Genet* 15 Spec No 2, R271-277, (2006).

- 194 Dibner, C., Schibler, U. & Albrecht, U. The mammalian circadian timing system: organization and coordination of central and peripheral clocks. *Annu Rev Physiol* 72, 517-549, (2010).
- 195 Astiz, M., Heyde, I. & Oster, H. Mechanisms of Communication in the Mammalian Circadian Timing System. *Int J Mol Sci* 20, 343, (2019).
- 196 Schibler, U., Ripperger, J. & Brown, S. A. Peripheral circadian oscillators in mammals: time and food. *J Biol Rhythms* 18, 250-260, (2003).
- 197 Duffy, J. F. *et al.* Sex difference in the near-24-hour intrinsic period of the human circadian timing system. *Proceedings of the National Academy of Sciences of the United States of America* 108 Suppl 3, 15602-15608, (2011).
- 198 Kelly, T. L. *et al.* Nonentrained circadian rhythms of melatonin in submariners scheduled to an 18-hour day. *J Biol Rhythms* 14, 190-196, (1999).
- 199 Leak, R. K. & Moore, R. Y. Topographic organization of suprachiasmatic nucleus projection neurons. *J Comp Neurol* 433, 312-334, (2001).
- 200 Fan, J. *et al.* Vasoactive intestinal polypeptide (VIP)-expressing neurons in the suprachiasmatic nucleus provide sparse GABAergic outputs to local neurons with circadian regulation occurring distal to the opening of postsynaptic GABAA ionotropic receptors. *The Journal of neuroscience : the official journal of the Society for Neuroscience* 35, 1905-1920, (2015).
- 201 Becquet, D., Girardet, C., Guillaumond, F., Francois-Bellan, A. M. & Bosler, O. Ultrastructural plasticity in the rat suprachiasmatic nucleus. Possible involvement in clock entrainment. *Glia* 56, 294-305, (2008).
- 202 Myung, J. *et al.* GABA-mediated repulsive coupling between circadian clock neurons in the SCN encodes seasonal time. *Proceedings of the National Academy of Sciences of the United States of America* 112, E3920-3929, (2015).
- 203 Hannibal, J., Hindersson, P., Knudsen, S. M., Georg, B. & Fahrenkrug, J. The photopigment melanopsin is exclusively present in pituitary adenylate cyclase-activating polypeptide-containing retinal ganglion cells of the retinohypothalamic tract. *Journal of Neuroscience* 22, RC191-RC191, (2002).
- 204 Husse, J., Eichele, G. & Oster, H. Synchronization of the mammalian circadian timing system: light can control peripheral clocks independently of the SCN clock: alternate routes of entrainment optimize the alignment of the body's circadian clock network with external time. 37, 1119-1128, (2015).
- 205 Honma, K. I. & Hiroshige, T. Internal Synchronization among Several Circadian-Rhythms in Rats under Constant Light. *Am J Physiol* 235, R243-R249, (1978).
- 206 Aton, S. J. & Herzog, E. D. Come together, right... now: synchronization of rhythms in a mammalian circadian clock. 48, 531-534, (2005).
- 207 Yamaguchi, S. *et al.* Synchronization of cellular clocks in the suprachiasmatic nucleus. *Science* 302, 1408-1412, (2003).
- 208 Bernard, S., Gonze, D., Cajavec, B., Herzog, H. & Kramer, A. Synchronization-induced rhythmicity of circadian oscillators in the suprachiasmatic nucleus. *PLoS Comput Biol* 3, e68, (2007).

- 209 Mohawk, J. A. & Takahashi, J. S. Cell autonomy and synchrony of suprachiasmatic nucleus circadian oscillators. *Trends Neurosci* 34, 349-358, (2011).
- 210 Kafka, M. S., Benedito, M. A., Blendy, J. A. & Tokola, N. S. Circadian rhythms in neurotransmitter receptors in discrete rat brain regions. *Chronobiol Int* 3, 91-100, (1986).
- 211 Granados-Fuentes, D., Tseng, A. & Herzog, E. D. A circadian clock in the olfactory bulb controls olfactory responsivity. *The Journal of neuroscience : the official journal of the Society for Neuroscience* 26, 12219-12225, (2006).
- 212 Eckel-Mahan, K. L. Circadian Oscillations within the Hippocampus Support Memory Formation and Persistence. *Front Mol Neurosci* 5, 46, (2012).
- 213 Harbour, V. L., Weigl, Y., Robinson, B. & Amir, S. Phase differences in expression of circadian clock genes in the central nucleus of the amygdala, dentate gyrus, and suprachiasmatic nucleus in the rat. *Plos One* 9, e103309, (2014).
- 214 Guo, H., Brewer, J. M., Lehman, M. N. & Bittman, E. L. Suprachiasmatic regulation of circadian rhythms of gene expression in hamster peripheral organs: effects of transplanting the pacemaker. *The Journal of neuroscience : the official journal of the Society for Neuroscience* 26, 6406-6412, (2006).
- 215 Liu, A. C., Lewis, W. G. & Kay, S. A. Mammalian circadian signaling networks and therapeutic targets. *Nat Chem Biol* 3, 630-639, (2007).
- 216 Moga, M. M. & Moore, R. Y. Organization of neural inputs to the suprachiasmatic nucleus in the rat. *J Comp Neurol* 389, 508-534, (1997).
- 217 Takahashi, J. S., Hong, H. K., Ko, C. H. & McDearmon, E. L. The genetics of mammalian circadian order and disorder: implications for physiology and disease. *Nat Rev Genet* 9, 764-775, (2008).
- 218 Abrahamson, E. E. & Moore, R. Y. Suprachiasmatic nucleus in the mouse: retinal innervation, intrinsic organization and efferent projections. *Brain Res* 916, 172-191, (2001).
- 219 Zhang, R., Lahens, N. F., Ballance, H. I., Hughes, M. E. & Hogenesch, J. B. A circadian gene expression atlas in mammals: implications for biology and medicine. *Proceedings of the National Academy of Sciences of the United States of America* 111, 16219-16224, (2014).
- 220 Ripperger, J. A. & Schibler, U. Rhythmic CLOCK-BMAL1 binding to multiple E-box motifs drives circadian *Dbp* transcription and chromatin transitions. *Nat Genet* 38, 369-374, (2006).
- 221 Ye, R. *et al.* Dual modes of CLOCK:BMAL1 inhibition mediated by Cryptochrome and Period proteins in the mammalian circadian clock. *Genes Dev* 28, 1989-1998, (2014).
- 222 Guillaumond, F., Dardente, H., Giguere, V. & Cermakian, N. Differential control of Bmal1 circadian transcription by REV-ERB and ROR nuclear receptors. *J Biol Rhythms* 20, 391-403, (2005).
- 223 Ding, J. M. *et al.* Resetting the biological clock: mediation of nocturnal circadian shifts by glutamate and NO. *Science* 266, 1713-1717, (1994).
- 224 Duffy, J. F., Kronauer, R. E. & Czeisler, C. A. Phase - shifting human circadian rhythms: influence of sleep timing, social contact and light exposure. 495, 289-297, (1996).

- 225 Shigeyoshi, Y. *et al.* Light-induced resetting of a mammalian circadian clock is associated with rapid induction of the *mPer1* transcript. *Cell* 91, 1043-1053, (1997).
- 226 Ishida, A. *et al.* Light activates the adrenal gland: timing of gene expression and glucocorticoid release. *Cell Metab* 2, 297-307, (2005).
- 227 Haus, E. & Smolensky, M. Biological clocks and shift work: circadian dysregulation and potential long-term effects. *Cancer Causes Control* 17, 489-500, (2006).
- 228 Logan, R. W. & McClung, C. A. Rhythms of life: circadian disruption and brain disorders across the lifespan. *Nat Rev Neurosci* 20, 49-65, (2019).
- 229 Stephan, F. K. The “other” circadian system: food as a Zeitgeber. 17, 284-292, (2002).
- 230 Oishi, K., Kasamatsu, M. & Ishida, N. Gene- and tissue-specific alterations of circadian clock gene expression in streptozotocin-induced diabetic mice under restricted feeding. *Biochem Biophys Res Commun* 317, 330-334, (2004).
- 231 Meier, U. & Gressner, A. M. Endocrine regulation of energy metabolism: review of pathobiochemical and clinical chemical aspects of leptin, ghrelin, adiponectin, and resistin. *Clin Chem* 50, 1511-1525, (2004).
- 232 Mohri, T. *et al.* Alterations of circadian expressions of clock genes in Dahl salt-sensitive rats fed a high-salt diet. *Hypertension* 42, 189-194, (2003).
- 233 Massey, L. K. Effect of dietary salt intake on circadian calcium metabolism, bone turnover, and calcium oxalate kidney stone risk in postmenopausal women. *Nutr Res* 25, 891-903, (2005).
- 234 Hasegawa, H. *et al.* Inhibition of the preoptic area and anterior hypothalamus by tetrodotoxin alters thermoregulatory functions in exercising rats. *J Appl Physiol (1985)* 98, 1458-1462, (2005).
- 235 Lazar, M. A. Thyroid hormone receptors: multiple forms, multiple possibilities. *Endocr Rev* 14, 184-193, (1993).
- 236 Zhang, Z., Boelen, A., Kalsbeek, A. & Fliers, E. TRH Neurons and Thyroid Hormone Coordinate the Hypothalamic Response to Cold. *Eur Thyroid J* 7, 279-288, (2018).
- 237 Lopez, M. *et al.* Hypothalamic AMPK and fatty acid metabolism mediate thyroid regulation of energy balance. *Nature Medicine* 16, 1001-U1097, (2010).
- 238 Whittle, A. J. *et al.* BMP8B Increases Brown Adipose Tissue Thermogenesis through Both Central and Peripheral Actions. *Cell* 149, 871-885, (2012).
- 239 Shimada, K. *et al.* Neuropeptide Y activates phosphorylation of ERK and STAT3 in stromal vascular cells from brown adipose tissue, but fails to affect thermogenic function of brown adipocytes. *Peptides* 34, 336-342, (2012).
- 240 Wang, B. *et al.* Activation of hypothalamic RIP - Cre neurons promotes beiging of WAT via sympathetic nervous system. *EMBO reports* 19, e44977, (2018).
- 241 Ambrosio, R., De Stefano, M. A., Di Girolamo, D. & Salvatore, D. Thyroid hormone signaling and deiodinase actions in muscle stem/progenitor cells. *Mol Cell Endocrinol* 459, 79-83, (2017).
- 242 Dentice, M. *et al.* Intracellular Inactivation of Thyroid Hormone Is a Survival Mechanism for Muscle Stem Cell Proliferation and Lineage Progression. *Cell Metabolism* 20, 1038-1048, (2014).

- 243 Perello, M. & Raingo, J. Leptin Activates Oxytocin Neurons of the Hypothalamic Paraventricular Nucleus in Both Control and Diet-Induced Obese Rodents. *Plos One* 8, e59625, (2013).
- 244 Kellogg Jr, D. L. In vivo mechanisms of cutaneous vasodilation and vasoconstriction in humans during thermoregulatory challenges. *Journal of applied physiology* 100, 1709-1718, (2006).
- 245 Kalsbeek, A., Fliers, E., Franke, A. N., Wortel, J. & Buijs, R. M. Functional connections between the suprachiasmatic nucleus and the thyroid gland as revealed by lesioning and viral tracing techniques in the rat. *Endocrinology* 141, 3832-3841, (2000).
- 246 Solberg, L. C., Olson, S. L., Turek, F. W. & Redei, E. Altered hormone levels and circadian rhythm of activity in the WKY rat, a putative animal model of depression. *Am J Physiol Regul Integr Comp Physiol* 281, R786-794, (2001).
- 247 Reinehr, T. Obesity and thyroid function. *Mol Cell Endocrinol* 316, 165-171, (2010).
- 248 Kuzmenko, N. V., Tsyrlin, V. A., Pliss, M. G. & Galagudza, M. M. Seasonal variations in levels of human thyroid-stimulating hormone and thyroid hormones: a meta-analysis. *Chronobiol Int*, 1-17, (2021).
- 249 Van Someren, E. J., Raymann, R. J., Scherder, E. J., Daanen, H. A. & Swaab, D. F. Circadian and age-related modulation of thermoreception and temperature regulation: mechanisms and functional implications. *Ageing Res Rev* 1, 721-778, (2002).
- 250 Brown, S. A., Zimbrunn, G., Fleury-Olela, F., Preitner, N. & Schibler, U. Rhythms of mammalian body temperature can sustain peripheral circadian clocks. *Curr Biol* 12, 1574-1583, (2002).
- 251 Challet, E. Minireview: Entrainment of the suprachiasmatic clockwork in diurnal and nocturnal mammals. *Endocrinology* 148, 5648-5655, (2007).
- 252 Saini, C., Morf, J., Stratmann, M., Gos, P. & Schibler, U. Simulated body temperature rhythms reveal the phase-shifting behavior and plasticity of mammalian circadian oscillators. *Genes Dev* 26, 567-580, (2012).
- 253 Ruoff, P. & Rensing, L. The temperature-compensated goodwin model simulates many circadian clock properties. *J Theor Biol* 179, 275-285, (1996).
- 254 Rensing, L. & Ruoff, P. Temperature effect on entrainment, phase shifting, and amplitude of circadian clocks and its molecular bases. *Chronobiol Int* 19, 807-864, (2002).
- 255 Vollmers, C. *et al.* Time of feeding and the intrinsic circadian clock drive rhythms in hepatic gene expression. *Proceedings of the National Academy of Sciences of the United States of America* 106, 21453-21458, (2009).
- 256 Benstaali, C., Mailloux, A., Bogdan, A., Auzéby, A. & Touitou, Y. Circadian rhythms of body temperature and motor activity in rodents - Their relationships with the light-dark cycle. *Life Sci* 68, 2645-2656, (2001).
- 257 Wright Jr, K. P., Hull, J. T. & Czeisler, C. A. Relationship between alertness, performance, and body temperature in humans. *American Journal of Physiology-Regulatory, Integrative Comparative Physiology*, (2002).
- 258 Volpato, G. P. *et al.* Inhaled hydrogen sulfide: a rapidly reversible inhibitor of cardiac and metabolic function in the mouse. *Anesthesiology* 108, 659-668, (2008).

- 259 Bennett, A. F. & Ruben, J. A. Endothermy and activity in vertebrates. *Science* 206, 649-654, (1979).
- 260 Nakamura, K. Central circuitries for body temperature regulation and fever. *Am J Physiol Regul Integr Comp Physiol* 301, R1207-1228, (2011).
- 261 Weinert, D. & Waterhouse, J. The circadian rhythm of core temperature: effects of physical activity and aging. *Physiol Behav* 90, 246-256, (2007).
- 262 Kelly, G. Body temperature variability (Part 1): A review of the history of body temperature and its variability due to site selection, biological rhythms, fitness, and aging. *Altern Med Rev* 11, 278-293, (2006).
- 263 Refinetti, R. The circadian rhythm of body temperature. *Front Biosci (Landmark Ed)* 15, 564-594, (2010).
- 264 Kohler, A. *et al.* Staying warm or moist? Operative temperature and thermal preferences of common frogs (*Rana temporaria*), and effects on locomotion. *Herpetol J* 21, 17-26, (2011).
- 265 Leng, Y., Musiek, E. S., Hu, K., Cappuccio, F. P. & Yaffe, K. Association between circadian rhythms and neurodegenerative diseases. *Lancet Neurol* 18, 307-318, (2019).
- 266 Musiek, E. S. Circadian clock disruption in neurodegenerative diseases: cause and effect? *Front Pharmacol* 6, 29, (2015).
- 267 Hossain, M. F. *et al.* Melatonin in Alzheimer's disease: a latent endogenous regulator of neurogenesis to mitigate Alzheimer's neuropathology. *Molecular neurobiology* 56, 8255-8276, (2019).
- 268 Parekh, P. K., Ozburn, A. R. & McClung, C. A. Circadian clock genes: effects on dopamine, reward and addiction. *Alcohol* 49, 341-349, (2015).
- 269 Staels, B. When the *Clock* stops ticking, metabolic syndrome explodes. *Nat Med* 12, 54-55; discussion 55, (2006).
- 270 Zimmet, P. *et al.* The Circadian Syndrome: is the Metabolic Syndrome and much more! *J Intern Med* 286, 181-191, (2019).
- 271 Bass, J. & Takahashi, J. S. Circadian integration of metabolism and energetics. *Science* 330, 1349-1354, (2010).
- 272 Lefebvre, P., Cariou, B., Lien, F., Kuipers, F. & Staels, B. Role of bile acids and bile acid receptors in metabolic regulation. *Physiol Rev* 89, 147-191, (2009).
- 273 Turek, F. W. *et al.* Obesity and metabolic syndrome in circadian *Clock* mutant mice. *Science* 308, 1043-1045, (2005).
- 274 Majdic, G. *et al.* Knockout mice lacking steroidogenic factor 1 are a novel genetic model of hypothalamic obesity. *Endocrinology* 143, 607-614, (2002).
- 275 Scott, E. M., Carter, A. M. & Grant, P. J. Association between polymorphisms in the *Clock* gene, obesity and the metabolic syndrome in man. *Int J Obesity* 32, 658-662, (2008).
- 276 Milagro, F. I. *et al.* CLOCK, PER2 and BMAL1 DNA methylation: association with obesity and metabolic syndrome characteristics and monounsaturated fat intake. *Chronobiol Int* 29, 1180-1194, (2012).

- 277 Kario, K. *et al.* Morning surge in blood pressure as a predictor of silent and clinical cerebrovascular disease in elderly hypertensives: a prospective study. *Circulation* 107, 1401-1406, (2003).
- 278 Zipes, D. P. & Wellens, H. J. J. Sudden cardiac death. *Professor Hein JJ Wellens*, 621-645, (2000).
- 279 Antoch, M. P. *et al.* Disruption of the circadian clock due to the *Clock* mutation has discrete effects on aging and carcinogenesis. *Cell Cycle* 7, 1197-1204, (2008).
- 280 Fu, L. & Lee, C. C. The circadian clock: pacemaker and tumour suppressor. *Nat Rev Cancer* 3, 350-361, (2003).
- 281 He, C., Anand, S. T., Ebell, M. H., Vena, J. E. & Robb, S. W. Circadian disrupting exposures and breast cancer risk: a meta-analysis. *Int Arch Occup Environ Health* 88, 533-547, (2015).
- 282 Chen, S. T. *et al.* Deregulated expression of the *PER1*, *PER2* and *PER3* genes in breast cancers. *Carcinogenesis* 26, 1241-1246, (2005).
- 283 Ohdo, S. Chronotherapeutic strategy: Rhythm monitoring, manipulation and disruption. *Adv Drug Deliv Rev* 62, 859-875, (2010).
- 284 Wemmie, J. A., Taugher, R. J. & Kreple, C. J. Acid-sensing ion channels in pain and disease. *Nature reviews. Neuroscience* 14, 461-471, (2013).
- 285 Kellenberger, S. & Schild, L. International Union of Basic and Clinical Pharmacology. XCI. structure, function, and pharmacology of acid-sensing ion channels and the epithelial Na⁺ channel. *Pharmacol Rev* 67, 1-35, (2015).
- 286 Chen, B., Liu, J., Ho, T. T., Ding, X. & Mo, Y. Y. ERK-mediated NF-κB activation through ASIC1 in response to acidosis. *Oncogenesis* 5, e279-e279, (2016).
- 287 Chen, X., Kalbacher, H. & Gründer, S. The tarantula toxin psalmotoxin 1 inhibits acid-sensing ion channel (ASIC) 1a by increasing its apparent H⁺ affinity. *Journal of General Physiology* 126, 71-79, (2005).
- 288 Paukert, M., Babini, E., Pusch, M. & Gründer, S. Identification of the Ca²⁺ blocking site of acid-sensing ion channel (ASIC) 1: implications for channel gating. *The Journal of general physiology* 124, 383-394, (2004).
- 289 Jin, Z., Chan, H., Ning, J., Lu, K. & Ma, D. The role of hydrogen sulfide in pathologies of the vital organs and its clinical application. *Journal of Physiology and Pharmacology* 66, 169-179, (2015).
- 290 Kimura, H. Production and physiological effects of hydrogen sulfide. *Antioxidants redox signaling* 20, 783-793, (2014).
- 291 Kimura, H. Hydrogen sulfide: its production, release and functions. *Amino Acids* 41, 113-121, (2011).
- 292 Kimura, H. Production and physiological effects of hydrogen sulfide. *Antioxid Redox Sign* 20, 783-793, (2014).
- 293 Kimura, H., Shibuya, N. & Kimura, Y. Hydrogen Sulfide Is a Signaling Molecule and a Cytoprotectant. *Antioxid Redox Sign* 17, 45-57, (2012).

- 294 Shefa, U., Kim, M. S., Jeong, N. Y. & Jung, J. Antioxidant and Cell-Signaling Functions of Hydrogen Sulfide in the Central Nervous System. *Oxid Med Cell Longev* 2018, 1873962, (2018).
- 295 Chen, Y., Zhang, F., Yin, J., Wu, S. & Zhou, X. Protective mechanisms of hydrogen sulfide in myocardial ischemia. *J Cell Physiol* 235, 9059-9070, (2020).
- 296 Blachier, F. *et al.* Production of hydrogen sulfide by the intestinal microbiota and epithelial cells and consequences for the colonic and rectal mucosa. *Am J Physiol Gastrointest Liver Physiol* 320, G125-G135, (2021).
- 297 Pacheco, A. *Sulfur-Containing Compounds as Hydrogen Sulfide Donors and Broad-Spectrum Antiviral Agents.* (Washington State University, 2017).
- 298 Shen, Y., Shen, Z., Luo, S., Guo, W. & Zhu, Y. Z. The Cardioprotective Effects of Hydrogen Sulfide in Heart Diseases: From Molecular Mechanisms to Therapeutic Potential. *Oxid Med Cell Longev* 2015, 925167, (2015).
- 299 Chunyu, Z. *et al.* The regulatory effect of hydrogen sulfide on hypoxic pulmonary hypertension in rats. *Biochem Biophys Res Commun* 302, 810-816, (2003).
- 300 Ratcliffe, P. J., O'Rourke, J. F., Maxwell, P. H. & Pugh, C. W. Oxygen sensing, hypoxia-inducible factor-1 and the regulation of mammalian gene expression. *J Exp Biol* 201, 1153-1162, (1998).
- 301 Tiainen, M. *et al.* Body temperature, blood infection parameters, and outcome of thrombolysis-treated ischemic stroke patients. *Int J Stroke* 8, 632-638, (2013).
- 302 Mani, S. *et al.* Decreased endogenous production of hydrogen sulfide accelerates atherosclerosis. *Circulation* 127, 2523-2534, (2013).
- 303 Song, Y.-J. *et al.* H₂S attenuates injury after ischemic stroke by diminishing the assembly of CaMKII with ASK1-MKK3-p38 signaling module. *Behavioural brain research* 384, 112520, (2020).
- 304 Wen, X. *et al.* H₂S attenuates cognitive deficits through Akt1/JNK3 signaling pathway in ischemic stroke. *Behavioural brain research* 269, 6-14, (2014).
- 305 Blackstone, E., Morrison, M. & Roth, M. B. H₂S induces a suspended animation-like state in mice. *Science* 308, 518-518, (2005).
- 306 Chen, W. Thermometry and interpretation of body temperature. *Biomedical Engineering Letters* 9, 3-17, (2019).
- 307 Obermeyer, Z., Samra, J. K. & Mullainathan, S. Individual differences in normal body temperature: longitudinal big data analysis of patient records. *BMJ* 359, j5468, (2017).
- 308 Mandal, A. S. *et al.* Drug delivery system based on chronobiology-A review. *Journal of Controlled Release* 147, 314-325, (2010).
- 309 Reinberg, A. & Ashkenazi, I. Internal desynchronization of circadian rhythms and tolerance to shift work. *Chronobiology international* 25, 625-643, (2008).
- 310 Mittleberger, R. E. & Skene, D. J. Social influences on mammalian circadian rhythms: animal and human studies. *Biological Reviews* 79, 533-556, (2004).
- 311 Reiter, R. J. The pineal and its hormones in the control of reproduction in mammals. *Endocrine reviews* 1, 109-131, (1980).
- 312 Schulz, P. & Steimer, T. Neurobiology of circadian systems. *CNS drugs* 23, 3-13, (2009).

- 313 Stehle, J. H. *et al.* A survey of molecular details in the human pineal gland in the light of phylogeny, structure, function and chronobiological diseases. *Journal of pineal research* 51, 17-43, (2011).
- 314 Wu, Y. H. & Swaab, D. F. The human pineal gland and melatonin in aging and Alzheimer's disease. *Journal of pineal research* 38, 145-152, (2005).
- 315 Portaluppi, F., Vergnani, L., Manfredini, R. & Fersini, C. Endocrine mechanisms of blood pressure rhythms. *Annals of the New York Academy of Sciences* 783, 113-131, (1996).
- 316 Harris, A. R. C. *et al.* The physiological role of thyrotropin-releasing hormone in the regulation of thyroid-stimulating hormone and prolactin secretion in the rat. *The Journal of clinical investigation* 61, 441-448, (1978).
- 317 Xanthoudakis, S. & Curran, T. Identification and characterization of Ref - 1, a nuclear protein that facilitates AP - 1 DNA - binding activity. *The EMBO journal* 11, 653-665, (1992).
- 318 Zanger, K., Cohen, L. E., Hashimoto, K., Radovick, S. & Wondisford, F. E. A novel mechanism for cyclic adenosine 3' , 5' -monophosphate regulation of gene expression by CREB-binding protein. *Molecular Endocrinology* 13, 268-275, (1999).
- 319 Aujard, F. *et al.* Artificially accelerated aging by shortened photoperiod alters early gene expression (Fos) in the suprachiasmatic nucleus and sulfatoxymelatonin excretion in a small primate, *Microcebus murinus*. *Neuroscience* 105, 403-412, (2001).